

CAPITAL UNIVERSITY OF SCIENCE AND
TECHNOLOGY, ISLAMABAD



**Effect of Nonlinear Thermal
Radiation and Variable Thermal
Conductivity on Heat and Mass
Transfer with Different Types of
Non-Newtonian Fluids**

by

Tanveer Sajid Mian

A thesis submitted in partial fulfillment for the
degree of Doctor of Philosophy

in the

**Faculty of Computing
Department of Mathematics**

2021

**Effect of Nonlinear Thermal Radiation and
Variable Thermal Conductivity on Heat and
Mass Transfer with Different Types of
Non-Newtonian Fluids**

By

Tanveer Sajid Mian
(PA141001)

Dr. Jae Dong Chung, Professor
Sejong University, Seoul, South Korea
(Foreign Evaluator 1)

Dr. Mohd Zuki Salleh, Professor
Universiti Malaysia Pahang, Pahang, Malaysia
(Foreign Evaluator 2)

Dr. Muhammad Sagheer
(Thesis supervisor)

Dr. Muhammad Sagheer
(Head, Department of Mathematics)

Dr. Muhammad Abdul Qadir
(Dean, Faculty of Computing)

DEPARTMENT OF MATHEMATICS
CAPITAL UNIVERSITY OF SCIENCE AND TECHNOLOGY
ISLAMABAD

2021

Copyright © 2021 by Tanveer Sajid Mian

All rights reserved. No part of this thesis may be reproduced, distributed, or transmitted in any form or by any means, including photocopying, recording, or other electronic or mechanical methods, by any information storage and retrieval system without the prior written permission of the author.

This work is dedicated to my parents, my sons, my wife, my brother and my teachers.



CAPITAL UNIVERSITY OF SCIENCE & TECHNOLOGY ISLAMABAD

Expressway, Kahuta Road, Zone-V, Islamabad
Phone: +92-51-111-555-666 Fax: +92-51-4486705
Email: info@cust.edu.pk Website: <https://www.cust.edu.pk>

CERTIFICATE OF APPROVAL

This is to certify that the research work presented in the thesis, entitled “**Effect of Nonlinear Thermal Radiation and Variable Thermal Conductivity on Different Types of Non-Newtonian Fluids**” was conducted under the supervision of **Dr. Muhammad Sagheer**. No part of this thesis has been submitted anywhere else for any other degree. This thesis is submitted to the **Department of Mathematics, Capital University of Science and Technology** in partial fulfillment of the requirements for the degree of Doctor in Philosophy in the field of **Mathematics**. The open defence of the thesis was conducted on **August 24, 2021**.

Student Name : Tanveer Sajid Mian (PA-141001)

The Examining Committee unanimously agrees to award PhD degree in the mentioned field.

Examination Committee :

(a) External Examiner 1: Dr. Mubashir Qayyum
Associate Professor
FAST-NUCES, Lahore

(b) External Examiner 2: Dr. Muhammad Kamran
Associate Professor
CUI, Wah Cantt Campus

(c) Internal Examiner : Dr. Rashid Ali
Associate Professor
CUST, Islamabad

Supervisor Name : Dr. Muhammad Sagheer
Professor
CUST, Islamabad

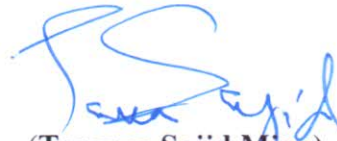
Name of HoD : Dr. Muhammad Sagheer
Professor
CUST, Islamabad

Name of Dean : Dr. Muhammad Abdul Qadir
Professor
CUST, Islamabad

AUTHOR'S DECLARATION

I, **Tanveer Sajid Mian (Registration No. PA-141001)**, hereby state that my PhD thesis entitled, '**Effect of Nonlinear Thermal Radiation and Variable Thermal Conductivity on Different Types of Non-Newtonian Fluids**' is my own work and has not been submitted previously by me for taking any degree from Capital University of Science and Technology, Islamabad or anywhere else in the country/ world.

At any time, if my statement is found to be incorrect even after my graduation, the University has the right to withdraw my PhD Degree.



(**Tanveer Sajid Mian**)

Dated: 24 August, 2021


Registration No : PA-141001

PLAGIARISM UNDERTAKING

I solemnly declare that research work presented in the thesis titled “**Effect of Nonlinear Thermal Radiation and Variable Thermal Conductivity on Different Types of Non-Newtonian Fluids**” is solely my research work with no significant contribution from any other person. Small contribution/ help wherever taken has been duly acknowledged and that complete thesis has been written by me.

I understand the zero tolerance policy of the HEC and Capital University of Science and Technology towards plagiarism. Therefore, I as an author of the above titled thesis declare that no portion of my thesis has been plagiarized and any material used as reference is properly referred/ cited.

I undertake that if I am found guilty of any formal plagiarism in the above titled thesis even after award of PhD Degree, the University reserves the right to withdraw/ revoke my PhD degree and that HEC and the University have the right to publish my name on the HEC/ University Website on which names of students are placed who submitted plagiarized thesis.


(Tanveer Sajid Mian)

Dated: 24 August, 2021

Registration No : PA-141001

List of Publications

It is certified that following publication(s) have been made out of the research work that has been carried out for this thesis:-

1. **T. Sajid**, M. Sagheer, and S. Hussain, “Darcy-Forcheimer flow of Maxwell nanofluid with nonlinear thermal radiation and activation energy,” *AIP Advances*, vol. 8, pp. 035102, 2018.
2. **T. Sajid**, M. Sagheer, and S. Hussain, “Impact of temperature-dependent heat source/sink and variable species diffusivity on radiative Reiner–Philippoff fluid,” *Mathematical Problems in Engineering*, vol. 2020, pp. 1-16, 2020.
3. **T. Sajid**, M. Sagheer, S. Hussain, and Faisal Shahzad “Impact of double-diffusive convection and motile gyrotactic microorganisms on magnetohydrodynamics bioconvection tangent hyperbolic nanofluid,” *Open Physics*, vol. 18, pp. 74-88, 2020.
4. **T. Sajid**, M. Sagheer, and S. Hussain, “Role of Maxwell velocity and Smoluchowski temperature jump slip boundary conditions on Carreau fluid flow along with nonlinear thermal radiation,” *Frontiers in Heat and Mass Transfer*, vol. 14, pp. 1-28, 2020.

Tanveer Sajid Mian
(PA141001.)

Acknowledgements

I would like to thank Almighty **Allah** for giving me the strength and courage to complete such a tedious task. I dedicate my research work to my father *Abdul Rashid Sajid* a role model for me and my mother *Nasreen Akhtar*, who supported me with their words of encouragement and specially with their prayers. I would further grateful to my dearest brother *Naveed Sajid*. His real motivation both morally and financially really helped me to complete this tedious task. I would like to thank my wife *Sumbul Tanveer* for anything good that has come to my life has been because of your patience and trust on me and my sons *Muhammad Zakariya* and *Muhammad Yahya* who are indeed a treasure from the Almighty Allah.

I would like to thank my supervisor, **Prof. Dr Muhammad Sagheer**, for the patient guidance, encouragement and advice he has provided throughout my time as his student. I have been extremely lucky to have a supervisor who cared so much about my work, and who responded to my questions and queries so promptly. I would also like to thank Dr Muhammad Shafqat, who helped me a lot during this project.

I would sincerely like to thank all my beloved friends Dr. Muhammad Yasir, Dr. Khalid Mehmood, Faisal Shahzad, Zulqurnain Sabir who were with me and support me through thick and thin. Most importantly I would like to thank *Dr. Muhammad Bilal* who really helps me during his stay at the university.

May God shower the above cited personalities with success and honour in their life.

Abstract

The motive behind current dissertation is to explore the heat and mass transfer analysis of incompressible laminar non-Newtonian fluids flow across a stretching sheet with the inclusion of distinguished physical parameters appear during the numerical simulation of the problem. Initially the Reiner-Philippoff fluid past a stretching sheet under the effects like variable thermal conductivity and nonlinear thermal radiation is analyzed. To amplify the thermophysical properties of the fluids specially in the case of hyperbolic tangent fluid and Maxwell fluid, the idea of nanofluid is employed. Nanofluids along with variable thermal conductivity and nonlinear thermal radiation increase the heat transfer rate of the fluids. Magnetic field is applied normal to the fluid and induced magnetic field is neglected by the assumption of small Reynold's number. Furthermore, the impact of viscous dissipation, Ohmic dissipation, heat generation/absorption, velocity slip, temperature slip, gyrotactic microorganisms and homogeneous/heterogenous reactions on non-Newtonian fluids are also scrutinized in detail. The governing nonlinear partial differential equations (PDEs) along with boundary conditions are first converted into the nonlinear ordinary differential equations (ODEs) by utilizing the similarity variables, and then the resulting nonlinear ODEs have been tackled numerically using nonlinear shooting method and finite difference method (Keller box). The numerical results are obtained with the utilization of MATLAB computational software. The physical quantities of interest such as skin friction coefficient, heat transfer analysis (Nusselt) and mass transfer analysis (Sherwood number) for sundry parameters appear during numerical simulation are computed numerically and discussed in the form of tables and figures. A comparison with previously available literature in limiting cases is also performed in order to check the reliability of the code.

Contents

Author's Declaration	v
Plagiarism Undertaking	vi
List of Publications	vii
Acknowledgement	viii
Abstract	ix
List of Figures	xiv
List of Tables	xvii
Abbreviations	xviii
Symbols	xix
1 Introduction	1
1.1 Research Background	1
1.1.1 Reiner-Philippoff Fluid	2
1.1.2 Tangent Hyperbolic Fluid	4
1.1.3 Maxwell Fluid	7
1.1.4 Carreau Fluid	10
1.2 Problem Statement	12
1.3 Research Objectives	13
1.4 Scope of Research	16
1.5 Research Methodology	17
1.6 Significance of the Study	17
1.7 Thesis Layout	18
2 Preliminaries	20
2.1 Fluid	20
2.2 Classification of Fluids	21
2.2.1 Newtonian Fluids	21

2.2.2	Non-Newtonian Fluids	21
2.3	Time-independent Fluid	22
2.3.1	Pseudoplastic Fluids	23
2.3.2	Dilatant Fluids	23
2.3.3	Bingham Plastic Fluids	23
2.4	Time-dependent fluids	24
2.4.1	Thixotropic Fluids	24
2.4.2	Rheopectic Fluids	24
2.5	Basic Definitions	24
2.5.1	Radiation	25
2.5.2	Specific Heat	25
2.5.3	Thermal Conductivity	26
2.5.4	Thermal Diffusivity	26
2.5.5	Activation Energy	26
2.6	Dimensionless Numbers	27
2.6.1	Reynold's Number	27
2.6.2	Biot Number	27
2.6.3	Schmidt Number	28
2.6.4	Weissenberg Number	28
2.6.5	Prandtl Number	28
2.6.6	Lewis Number	28
2.6.7	Peclet Number	29
2.6.8	Eckert Number	29
2.6.9	Grashof Number	29
2.6.10	Nusselt Number	30
2.6.11	Sherwood Number	30
2.7	Double Diffusive Convection	30
2.8	Bioconvection	31
2.8.1	Gyrotaxis	32
2.8.2	Gravitaxis	32
2.8.3	Phototaxis	32
2.8.4	Oxytaxis	32
2.9	Catalysis and Its Types	33
2.9.1	Homogeneous Catalysis	33
2.9.2	Biocatalysis	33
2.9.3	Heterogeneous Catalysis	34
2.10	Governing Laws Regarding Heat and Mass Transport in Fluids	34
2.10.1	Continuity Equation	34
2.10.2	Momentum Equation	35
2.10.3	Magnetohydrodynamics	36
2.10.4	Energy Transport	38
2.10.5	Mass Transport	38
2.11	Mass Transfer	39

3	Impact of Heat Source/ Sink and Variable Species Diffusivity on Radiative Reiner-Philippoff Fluid	40
3.1	Mathematical Formulation	41
3.2	Solution Methodology	55
3.3	Results and Discussion	60
3.3.1	Impact of γ and λ on velocity field $f'(\eta)$ and stress field $g'(\eta)$	60
3.3.2	Impact of A^* , B^* , Pr , ϵ_1 , Rd and θ_w on $\theta(\eta)$	63
3.3.3	Impact of ϵ_2 and Sc on Concentration Field $\phi(\eta)$	66
3.3.4	Impact of γ and λ on surface drag coefficient $Cf_x Re_x^{\frac{1}{2}}$	67
3.3.5	Impact of Rd and θ_w versus Pr , A^* and B^* versus θ_w , λ versus γ on heat transfer rate $Nu_x Re_x^{\frac{-1}{2}}$	68
3.3.6	Impact of Sc versus variable species diffusivity ϵ_2 on mass transfer rate $Sh_x Re_x^{\frac{-1}{2}}$	71
3.4	Concluding Remarks	75
4	Impact of Double-Diffusive Convection and Motile Gyrotactic Microorganisms on Bioconvection Tangent Hyperbolic Nanofluid	76
4.1	Mathematical Formulation	77
4.2	Solution Methodology	90
4.3	Results and Discussion	96
4.3.1	Impact of M , n and We on the Velocity Field $f'(\eta)$	96
4.3.2	Impact of M , Pr , Nb and Nt , Nd on $\theta(\eta)$	98
4.3.3	Impact of Nb , Nt , Ln on the Mass Fraction Field $\xi(\eta)$	101
4.3.4	Impact of Pe , Lb , Ω on $\chi(\eta)$	103
4.3.5	Impact of Ld and Le on the solute profile $\gamma(\eta)$	105
4.3.6	Impact of Ld , Nt versus Ln on $-\xi'$	107
4.3.7	Impact of Pe on the density of motile microorganisms profile $-\chi'(0)$	108
4.4	Concluding Remarks	111
5	Darcy-Forchheimer Flow of Maxwell Nanofluid Moving over a Stretching Sheet	112
5.1	Mathematical Formulation	113
5.2	Solution Methodology	126
5.3	Results and Discussion	127
5.3.1	Impact of β_2 , Fr , λ_2 and M on the velocity field $f'(\eta)$	127
5.3.2	Impact of β_2 , Fr , ϵ_1 , λ_2 , M , Nt , Pr , Rd , θ_w , γ_2 on $\theta(\eta)$	130
5.3.3	Impact of γ_2 , λ_2 , Le , Nt , σ_2 , β_2 and E on the concentration field $\phi(\eta)$	136
5.4	Concluding Remarks	144
6	Role of Maxwell Velocity and Smoluchowski Temperature Jump Slip Boundary Conditions on Carreau Fluid	145
6.1	Mathematical Formulation	146

6.2	Solution Methodology	163
6.3	Results and Discussion	165
6.3.1	Impact of $M, n, We_1, \gamma_3, We_2, \beta_3$ on the velocity fields f' and g'	166
6.3.2	Impact of $Pr, Ec_x, Ec_y, M, Rd, \theta_w$ on $\theta(\eta)$	170
6.3.3	Impact of Sc, K, K_1 on $h(\eta)$	174
6.4	Concluding Remarks	179
7	Conclusion and Future Work	180
7.1	Main Findings	180
7.2	Future Work	181
	Bibliography	183

List of Figures

2.1	(a) water (b) mineral oil (c) ethyl alcohol (d) gasoline	22
2.2	(a) corn starch (b) Ketchup (c) paint (d) honey (e) toothpaste (f) blood	22
2.3	Non-Newtonian Fluids	25
3.1	Flow model	41
3.2	Impact of γ on f'	61
3.3	Influence of λ on f'	61
3.4	Impact of γ on g'	62
3.5	Effect of λ on g'	62
3.6	Effect of A^* on θ	63
3.7	Impact of B^* on θ	64
3.8	Impact of Pr on θ	64
3.9	Effect of ϵ_1 on θ	65
3.10	Influence of Rd on θ	65
3.11	Effect of θ_w on θ	66
3.12	Impact of ϵ_2 on ϕ	66
3.13	Influence of Sc on ϕ	67
3.14	Impact of γ versus λ on $Cf_x Re_x^{\frac{1}{2}}$	67
3.15	λ versus γ on $Cf_x Re_x^{\frac{-1}{2}}$	68
3.16	Pr versus Rd on $Nu_x Re_x^{\frac{-1}{2}}$	69
3.17	Pr versus θ_w on $Nu_x Re_x^{\frac{-1}{2}}$	69
3.18	A^* versus θ_w on $Nu_x Re_x^{\frac{-1}{2}}$	70
3.19	B^* versus θ_w on $Nu_x Re_x^{\frac{-1}{2}}$	70
3.20	λ versus γ on $Nu_x Re_x^{\frac{-1}{2}}$	71
3.21	Impact of ϵ_2 and Sc on $Sh_x Re_x^{\frac{-1}{2}}$	72
4.1	Geometry of the problem.	78
4.2	Mechanism of the present technique	92
4.3	One-dimensional mesh for difference approximations.	93
4.4	Impact of M on $f'(\eta)$	97
4.5	Effect of n on $f'(\eta)$	97
4.6	Influence of We on $f'(\eta)$	98
4.7	Impact M on $\theta(\eta)$	99

4.8	Effect of Pr on $\theta(\eta)$.	99
4.9	Implication of Nb on $\theta(\eta)$.	100
4.10	Impact of Nt on $\theta(\eta)$.	100
4.11	Implication of Nd on $\theta(\eta)$.	101
4.12	Implication of Nb on $\xi(\eta)$.	102
4.13	Impact of Nt on $\xi(\eta)$.	102
4.14	Effect of Ln on $\xi(\eta)$.	103
4.15	Effect of Pe on $\chi(\eta)$.	104
4.16	Impact of Lb on $\chi(\eta)$.	104
4.17	Influence of Ω on $\chi(\eta)$.	105
4.18	Impact of Ld on $\gamma(\eta)$.	106
4.19	Effect of Le on $\gamma(\eta)$.	106
4.20	Effect of Nb on $\xi'(0)$.	107
4.21	Impact of Nt on $\xi'(0)$.	108
4.22	Effect of σ on $\chi'(0)$.	109
5.1	Flow geometry.	113
5.2	Impact of β_2 on f' .	128
5.3	Effect of Fr on f' .	128
5.4	Influence of λ_2 on f' .	129
5.5	Impact of M on f' .	129
5.6	Effect of β_2 on θ .	131
5.7	Influence of ϵ_1 on θ .	131
5.8	Impact of Fr on θ .	132
5.9	Effect of λ_2 on θ .	132
5.10	Influence of M on θ .	133
5.11	Influence of N_t on θ .	133
5.12	Impact of Pr on θ .	134
5.13	Effect of Rd on θ .	134
5.14	Influence of θ_w on θ .	135
5.15	Impact of γ_2 on θ .	135
5.16	Effect of γ_2 on ϕ .	137
5.17	Influence of λ_2 on ϕ .	137
5.18	Impact of Le on ϕ .	138
5.19	Effect of N_t on ϕ .	138
5.20	Influence of σ_2 on ϕ .	139
5.21	Impact of β_2 on ϕ .	139
5.22	Impact of E on ϕ .	140
6.1	Physical model of the problem.	146
6.2	Impact of M on f' and g' .	167
6.3	Effect of n on f' and g' .	167
6.4	Impact of We_1 on f' .	168
6.5	Effect of γ_3 on f' .	168
6.6	Impact of We_2 on g' .	169

6.7	Influence of γ_3 on g' .	169
6.8	Impact of β_3 on g' .	170
6.9	Impact of Pr on θ .	171
6.10	Effect of Ec_x on θ .	171
6.11	Effect of Ec_y on θ .	172
6.12	Impact of M on θ .	172
6.13	Influence of Rd on θ .	173
6.14	Impact of θ_w on θ .	173
6.15	Impact of Sc on h .	174
6.16	Effect of K on h .	175
6.17	Effect of K_1 on h .	175

List of Tables

3.1	Values of Nusselt number for various values of Pr	60
3.2	Numerical values of skin friction, Nusselt and Sherwood numbers for various physical parameters.	73
3.3	Effect of physical parameters on Nusselt number.	74
4.1	Numerical comparison of the obtained results with Khan et al. [37] for various values of Pr	96
4.2	Variation of $Nu_x Re_x^{-1/2}$, $Shu_x Re_x^{-1/2}$ and $Nn_x Re_x^{-1/2}$ for diverse parameters when $Nt=0.1$, $Pr=6.2$, $Le=0.5$, $Ld=0.1$ and $\Lambda=0.1$ are fixed.	110
5.1	Computation of $-\theta'(0)$ showing resemblance with Ref. [55]	141
5.2	Computation of Nusselt number against various values of embedded parameters.	142
5.3	Computation of Nusselt number for different embedded parameters.	143
6.1	Comparison of $f''(0)$	165
6.2	Comparison of $g''(0)$	165
6.3	Comparison of Nu_x	165
6.4	Impact of momentum and concentration equations parameters on surface drag coefficient and concentration profile.	177
6.5	Impact of various embedded parameters on Nu_x	178

Abbreviations

BVP	boundary value problem
IVP	initial value problem
MHD	magnetohydrodynamics
ODEs	ordinary differential equations
PDEs	partial differential equation
RK	Runge Kutta
w.r.t	with respect to

Symbols

κ^*	absorption coefficient
E_a	activation energy
$D_{B\infty}$	ambient Brownian diffusion coefficient
T_∞	ambient temperature
C_∞	ambient concentration
κ_∞	ambient fluid thermal conductivity
γ	Bingham number
Nb	Brownian motion
Lb	bioconvective Lewis number
N_B	Brownian Diffusion
N_c	bioconvective Rayleigh number
Nr	buoyancy ratio parameter
D_B	Brownian diffusion coefficient
C	concentration of fluid
a, c	constants
T_w	convective fluid temperature
$\dot{\gamma}$	deformation rate
β_2	Deborah number
Ld	Dufour Lewis number
μ	dynamic viscosity
σ_1	electric conductivity
Ec	Eckert number
ρ	fluid density

n	fitted rate constant
A^*	heat generation/absorption
B^*	heat generation/absorption
$(\rho c)_f$	heat capacity of fluid
h_f	heat transfer coefficient
$(\rho c)_p$	heat capacity of nanoparticles
F_r	inertia coefficient
ν	kinematic viscosity
μ_∞	limiting viscosity
Le	Lewis number
j_w	mass flux
B_0	magnetic field strength
σ	microorganism concentration difference
M	magnetic parameter
Nd	modified Dufour parameter
γ_3	momentum slip parameter
σ_v	momentum accommodation coefficient
λ_0	molecular mean free path
M	magnetic parameter
Nu_x	Nusselt number
Ln	nanofluid Lewis number
Pe	Peclet number
λ_2	porosity parameter
Pr	Prandtl number
n	power law index
λ	Reiner-Philippoff fluid parameter
q_r	radiative heat flux
Rd	radiation parameter
τ_s	reference shear stress
Re	Reynolds number
φ	ratio of diffusion coefficients

λ_1	relaxation time
σ_2	reaction rate constant
$U(x)$	stretching velocity
Sc	Schmidt number
q_w	surface heat flux
Sh_x	Sherwood number
τ	shear stress
σ^*	Stefan-Boltzman constant
μ_0	shear viscosity
C_p	specific heat
C_f	skin friction coefficient
a	stretching rate
β_3	stretching rate
τ_w	shear stress at the wall
V_w	stretching velocity along y -axis
K_1	strength of heterogeneous reaction
r	specific heat ratio
K	strength of homogeneous reaction
q_w	surface heat flux
θ_w	temperature ratio parameter
D_T	thermophoresis diffusion
Nt	thermophoresis parameter
α	thermal diffusivity
k	thermal conductivity
δ_3	temperature jump parameter
D_A	thermal diffusion coefficient
σ_T	temperature accomodation coefficient
θ_w	temperature ratio parameter
δ_2	temperature difference parameter
T_f	temperature of hot fluid
ϵ_2	variable molecular diffusivity parameter

ϵ_1	variable thermal conductivity parameter
u, v	velocity components
ϕ	volume fraction of nanoparticles
q_m	wall mass flux
T_w	wall temperature
We	Weissenberg number

Chapter 1

Introduction

The present chapter presents the brief theoretical background of different types of non-Newtonian fluids past a stretching sheet. Moreover literature regarding different effects like thermal radiation, thermal conductivity, Joules heating, magnetohydrodynamics (MHD) and boundary layer flow over stretching sheet has also been presented and discussed in detail. At the end, motivation behind the current study and thesis layout has been given.

1.1 Research Background

The fundamental and historical achievements in the field of fluid mechanics took place in eighteenth and nineteenth centuries. Sir Isaac Newton (1642-1727) presented his law of viscosity termed as Newton's law of viscosity for frictionless /perfect fluid. Later on different scientists like Bernoulli, Leonard Euler and Pierre Simon Laplace achieved many beautiful results regarding frictionless fluids. The Swiss mathematician and physicist Daniel Bernoulli (1700-1782) in 1738 presented a principle called Bernoulli principle stated that a decremental change in potential energy amplifies the fluid speed. Leonard Euler (1707-1783) derived Bernoulli's equation in 1752. Later on an additional equation, termed as adiabatic condition,

was supplied by Pierre Simon Laplace (1749-1827) in 1816. William Fourde (1810-1879) and his son Robert (1864-1924) developed laws regarding resistance offered by water to ships. In 1870 James Clark Maxwell introduced a viscoelastic type model called the Maxwell fluid model. Claude Navier (1785-1836) and Gabriel Stokes (1819-1903) provided tremendous contribution to viscous flow theory by the addition of Newtonian viscous terms to the governing equations of motion. Later on Osborne Reynold (1842-1912) in 1883 published his famous work on fluid flow through a pipe which demonstrated the Reynold's number after him. Ludwig Prandtl (1875-1953) in 1904 delivered a lecture on boundary layer flow theory. Prandtl introduced two sub-regions of a flow based on the fluids viscosity: a region inside the boundary layer where viscosity has the substantial effect but effect is ignorable outside the boundary layer region.

1.1.1 Reiner-Philippoff Fluid

Reiner and Philippoff in 1962 proposed a model called Reiner-Philippoff model which was basically a viscoelastic type model. The behaviour of Reiner-Philippoff fluid past a channel was deliberated by Kapur and Gupta [1]. Ghosal [2] investigated the dispersion of solutes in non-Newtonian Ellis and Reiner-Philippoff fluid flow through a circular tube. Na et al. [3] studied the impact of Reiner-Philippoff fluid past an expandable surface. Yam et al. [4] deliberated Reiner-Philippoff fluid past a wedge and observed that the velocity field depreciates by the virtue of an incremental change in the fluid parameter. The behaviour of Reiner-Philippoff fluid flow across a riga plate was deliberated by Ahmad [5]. Reddy et al. [6] explored the influence of thermal radiation on magneto Reiner-Philippoff fluid and observed that a positive variation in magnetic number lessens the velocity field. Kumar et al. [7] pondered the consequences of Cattaneo-Christov heat flux on Reiner-Philippoff fluid moving along an extendible elastic surface. Reddy et al. [8] contemplated Darcy-Forchheimer flow of radiative Reiner-Philippoff fluid flow across a porous elastic sheet and found that the heat transfer rate amplifies as a result of an augmentation in the thermal radiation parameter. Ullah et al. [9]

comprehended Reiner-Phillipof fluid flow over an unstable stretching using Buongiorno nanofluid model and observed that temperature field escalates owing to a magnification in the Brownian parameter. Ishaq et al. [10] numerically studied the stability analysis of the Reiner-Philippoff fluid past an expandable surface. The dilatant and pseudoplastic impact of peristaltic flow of Reiner-Phillipoff fluid were discussed by Tahir and Ahmad [11] and found that the velocity of the dilatant fluid diminishes as a result of an amplification in the shear stress phenomenon. The entropy generation analysis of Darcy-Forcheimer flow of Reiner-Philippoff fluid were deeply scrutinized by Xiong et al. [12]. The influence of heat source/sink, Ohmic dissipations, thermal radiation and Fourier heat flux on Reiner-Philippoff flow moving over an extendable surface were deliberated by Khan et al. [13]

Thermal conductivity is defined as the capability of any material to conduct heat. Thermal conductivity is very vital in heat transport phenomenon due to its immense utilization in industry such as electrolytes, steam generators, concrete heating, laminating, catalysis, molding blow etc. The frequent collision of molecules inside the liquid drives to an improvement in the energy exchange between the molecules and as a result more heat energy is transported through the medium. When the molecules collide randomly, it causes the transfer of heat energy in a specific direction. Researchers across the world investigated thermal conductivity phenomenon in terms of heat transmission through various materials. Megahed [14] discussed the conduct of thermal conductivity on Powell-Eyring fluid impinging on porous stretching sheet. Reddy et al. [15] modeled the Williamson fluid past a stretchable surface accompanied with MHD and nanoparticles. Ramzan et al. [16] investigated the Eyring-Powell nanofluid moving along a stretchable surface accompanied with thermal conductivity and chemical reaction. Shah et al. [17] examined the performance of Carreau fluid along with temperature varying conductivity moving across an expandable surface. Shokouhmand et al. [18] investigated thermal conductivity impact on two dimensional porous fin. Kumar et al. [19] examined the behaviour of incompressible nanofluid over a horizontally expandable surface embedded with thermal conductivity and molecular diffusivity.

Marinca and Marinca [20] achieved the exact solution of magneto radiative second grade fluid along with thermal conductivity moving across a stretching surface. Ferdows and Bangalee [21] studied the performance of thermal conductivity on an electrically conducting fluid. Lahmar et al. [22] utilized the differential transform scheme to achieve the numerical solution of squeezed magneto nanofluid flow over an inclined stretching medium and observed that the velocity field lessens by the virtue of a magnification in Lorentz force.

1.1.2 Tangent Hyperbolic Fluid

The idea of hyperbolic tangent fluid was introduced by Pop and Ingham [23] in 2001. The stress tensor expression of tangent hyperbolic nanofluid is deduced from the well known kinetic theory of liquids. This model describes shear thinning/thickening phenomenon. Blood is the perfect example of tangent hyperbolic model. Nadeem and Akram [24] numerically achieved the solution of tangent hyperbolic model based fluid past an axisymmetric channel with the utilization of perturbation technique and observed that the pressure gradient depreciates owing to a magnification in the Weissenberg number. Akbar et al. [25] numerically obtained the solution of tangent hyperbolic fluid past an expandable surface under the effect of Lorentz force and noted that the velocity field diminishes by the virtue of a magnification in the magnetic parameter. Akram and Nadeem [26] deliberated magnetic field impact on the tangent hyperbolic fluid moving across an asymmetric channel. Prbhakar et al. [27] investigated inclined magnetic field impact on tangent hyperbolic nanofluid moving over an elastic surface and found that the velocity field debacles owing to an abatement in magnetic number. Saidulu et al. [28] scrutinized thermal radiation effect on tangent hyperbolic fluid moving towards an elastic medium and found that the temperature field augments as a result of a magnification in thermal radiation parameter. Al-Khaled et al. [29] inspected the effect of microorganisms and nonlinear thermal radiation on tangent hyperbolic nanofluid moving towards a stretchable surface and observed that temperature amplifies as a result of magnification in the nonlinear phenomenon.

Double-diffusion phenomena explain the convection phenomenon lead by two different density gradients having different diffusion rates. Double-diffusive convection has distinguished utilization in various disciplines like oceanography, biology, astrophysics, geology, crystal growth and chemical reactions etc. Gaikwad et al. [30] analyzed the effect of double-diffusive convection on fluid flow towards an expandable surface and noted that Nusselt number amplifies by the virtue of an augmentation in the Dufour parameter. Nield and Kuznetsov [31] implemented double-diffusive convection phenomenon on fluid moving across a porous expandable surface. The influence of double-diffusion convection on fluid moving across a square cavity is investigated in detail by Mahapatra et al. [32]. Rana and Chand [33] explored viscoelastic fluid past an expandable surface under the effect of double-diffusive convection. Kumar et al. [34] investigated nanoparticles and double diffusion impact on viscoelastic fluid and found that a magnification in velocity field occurs by amplifying the Dufour Lewis parameter. Gireesha et al. [35] pondered the influence of double-diffusive convection and nanoparticles on Casson fluid past an elastic surface under the effect of Lorentz force and found that the velocity depreciates by amplifies Lorentz force.

The idea of nanofluid was introduced by Choi in 1995. The addition of nanoparticles in the base fluid enhances thermal conductivity as well as heat transfer rate of the fluid having distinguished applications in the biomedical, electronics, drug delivery, food products, ceramic industry, computer chips etc. Nonlinear thermal radiation is effective where temperature difference is large. Nonlinear thermal radiation has extensive application in industry especially in nuclear and combustion reactors, polymer production, space crafts, nuclear fusions etc. The influence of nonlinear radiative heat flux along with internal heat generation on tangent hyperbolic fluid moving towards an elastic medium was scrutinized in detail by Mahanthesh et al. [36]. Khan et al. [37] investigated nanoparticles and MHD effect on tangent hyperbolic fluid moving subjected to an expandable medium. The impact of MHD and on tangent hyperbolic nanofluid fluid flow subjected to an elastic sheet was observed by Qayyum et al. [38]. Nagendramma et al. [39]

pondered the effect of nanoparticles and double stratification on fluid past a cylinder and noted that an amplification in power law index reduces the fluid flow. Khan et al. [40] scrutinized tangent hyperbolic nanofluid past a stretchable surface under the effect of nonlinear thermal radiation as well as activation energy and observed that the temperature field amplifies by the virtue of an amplification in thermal radiation parameter. Ali et al. [41] investigated MHD and temperature varying conductivity impact on tangent hyperbolic fluid confined by an expandable medium. Ullah et al. [42] studied Lorentz force impact on tangent hyperbolic nanofluid past an extendable sheet.

Bioconvection phenomenon takes place when microorganisms having density greater than water, swim upwards. The direction in which gyrotactic microorganisms swim totally rely on the balance between gravitational and viscous torques [43, 44]. Oyelakin et al. [45] pondered the impact of bioconvection and motile gyrotactic microorganisms on the Casson fluid and noted that the microorganism profile depreciates owing to an escalation in Peclet number. Wang et al. [46] explored the effects of bioconvection and gyrotactic microorganisms on tangent hyperbolic nanofluid past a slippery expandable surface. Al-Khaled et al. [47] investigated the influence of gyrotactic microorganisms and nonlinear temperature based radiation on chemically reactive bioconvective tangent hyperbolic fluid flow over an expandable surface. Shafiq et al. [48] numerically investigated the tangent hyperbolic nanofluid accompanied with gyrotactic microorganisms.

Magnetohydrodynamics (MHD) is actually the study of fluid passing through a magnetic field in the presence of electric current. Magnetohydrodynamics is a subcategory of fluids in which the behaviour of electrically conducting fluids is discussed. Hannes Alfvén [49] was the first who introduced the concept of MHD fluid and later on received Noble prize for his revolutionary work on MHD in 1970. In the last few decades, researchers have worked on various aspects of MHD due to its tremendous involvement in processes like plasmas, X-ray radiation, electrolysis, planetary science and etc. Tian et al. [50] pondered the performance of MHD on non-Newtonian nanofluid moving over a convectively heated surface.

Fagbade et al. [51] scrutinized the electrically conducting viscoelastic fluid moving towards a stretching sheet embedded with thermal radiation. Jafarimoghaddam [52] found the analytical and numerical solutions of electrically conducting Eyring-Powell fluid embedded with thermal radiation and found that a positive variation in radiation parameter amplifies the temperature field. Jaffer et al. [53] studied viscoelastic fluid moving along a stretchable surface under the effect of MHD. Rabbi et al. [54] scrutinized the impact of chemical reaction and MHD on Casson nanofluid and observed that a positive variation in Brownian motion parameter amplifies the temperature field.

1.1.3 Maxwell Fluid

Maxwell fluid belongs to a category of viscoelastic fluid having the properties of both elasticity and viscosity. This model is capable of predicting relaxation time characteristics. Relaxation time is the time taken by the to return from the deformed state to its initial equilibrium state. Examples of Maxwell fluid are paints, polymers, glycerine, dashpot.

Darcy's law is not effective at higher flow rate. Forchheimer removed the shortcoming occurred in Darcy's law by introducing a velocity expression of order two in Darcian velocity expression in order to study the impact of inertia at higher flow rate. Darcy-Forchheimer expression [55] is very effective in the case of high Reynold's number. Muhammad et al. [55] studied the Darcy-Frchheimer Maxwell fluid flow towards an expandable medium. The impact of stratification and convective heat transfer on Darcy-Forchheimer Maxwell nanofluid were deeply investigated by Hayat et al. [56]. Waqas et al. [57] contemplated Maxwell fluid flow towards an expandable surface accompanied with effects like multiple convective boundary conditions, thermal radiation and nonlinear Forchheimer velocity expression. The impact of multiple convective boundary conditions and nonlinear Darcy-Forchheimer velocity expression on Maxwell fluid were scrutinized by Sadiq et al. [58]. Thermal radiation is used where high temperature difference is required having immense utilization in nuclear reactors, space aircrafts, combustion

reactors, polymer production etc. Hsiao [59] studied both MHD and viscous dissipation on radiative Maxwell fluid flow subjected to an elastic medium. Ibrahim et al. [60] examined the impact of thermal radiation, chemical reaction and slip boundary condition on Maxwell fluid flow towards an elastic surface. The impact of nonlinear temperature based radiation on Maxwell fluid flow subjected to an expandable surface was studied in detail by Ghaffari et al. [61].

The suspension of metallic nanoparticles like aluminium, silver and copper in the base fluid like engine oil and ethylene glycol amplifies temperature of the fluid. The idea of nanofluid was coined by Choi [62] with enormous utilizations in medical, polymer production, ceramic industry, refrigerator, chiller and engine cooling. It is well established that the insertion of nanometer sized particles in the base fluid amplifies heat transfer phenomenon. Convective transport in nanofluids was coined by Buongiorno [63] and it was proposed that the nanofluids possess a high thermal conductivity in contrast to simple fluids. He presented the seven slip mechanisms comprising of inertia, thermophoresis, magnus impact, gravity, fluid drainage, Brownian diffusion and diffusiophoresis to generate a base fluid velocity and relative velocity. Murshed et al. [64] pondered the impact of nanoparticles on a fluid past a stretching sheet and found that both viscosity and thermal conductivity escalate owing to an amplification in nanoparticle volume fraction. Usri et al. [65] observed that an insertion of nanoparticles in the base fluid enhances the ability of fluid to conduct heat. The impact of nanoparticles, chemical reaction and MHD on Maxwell fluid moving along a stretching sheet was discussed in detail by Afify and Algazery [66] with a conclusion that the temperature field escalates by virtue of an increment in thermophoresis parameter. Macha and Kishan [67] pondered the effect of buoyancy forces on viscoelastic nanofluid past a stretching wedge and came up with the conclusion that the temperature field improves because of an enhancement in Brownian diffusion coefficient. Eid and Mahny [68] studied Sisko nanofluid accompanied with heat generation/absorption past a stretchable surface and found that the temperature field improves owing to an augmentation in the Brownian motion parameter. The influence of nanoparticles

along with buoyancy effects on Carreau fluid was discussed in detail by Koriko et al. [69]. Shaw et al. [70] discussed the performance of nonlinear convection on Sisko nanofluid moving across an inclined permeable medium accompanied with MHD.

Swante Arrhenius in 1889 introduced the concept of activation energy. The minimum energy that must be provided for compounds to undergo a chemical reaction can be termed as activation energy having immense utilizations in various areas like oil reservoir engineering, water and oil emulsions etc. Shafique et al. [71] contemplated the influence of activation energy on rotating Maxwell fluid flow across an elastic surface. The impact of chemical reaction and activation energy on magneto viscoelastic fluid moving subjected to an expandable surface were debated in detail by Mustafa et al. [72]. Gulzar et al. [73] adopted the OHAM scheme to achieved the numerical solution of Maxwell fluid embedded with viscous dissipation, activation energy and entropy generation. Ramiah et al. [74] scrutinized the impact of Fourier heat flux and activation energy on rotating Maxwell fluid moving towards an extendable surface under the effect of Lorentz force. The effect of activation energy and thermal radiation on Maxwell past a stretching sheet were debated in detail by Rafiq et al. [75].

Stretching sheet has achieved the attention of researchers because of its distinguished applications in industry like polymers, glass blowing, paper, hot rolling, extraction of polymer sheet from a die, crystal growing, manufacturing foods, drawing of plastic films etc. The boundary layer flow phenomenon over continuously solid surface was coined by Sakiadis [76] and furthermore Crane [77] extended the work of Sakiadis by presenting the idea of viscous fluid flow across a smooth stretching medium. Wang [78] found the asymptotic as well as numerical solution of viscous fluid film moving over a stretchable surface. Cortell [79] developed a model regarding power-law fluid moving across an extendable surface under the application of magnetic field and noted that a positive change in power-law index guides to an abatement in the velocity field. Shaker et al. [80] pondered Maxwell

fluid moving along a flat sheet accompanied with variable thermal conductivity. Bai et al. [81] studied Maxwell fluid accompanied with thermophoresis effect past an elastic surface and observed that the heat transfer rate amplifies by the virtue of an amplification in the Brownian motion parameter. Boundary layer impact on Maxwell fluid past an extendable medium having variable thickness were scrutinized by Liu and Liu [82]. Maxwell nanofluid flow subjected to an elastic surface under the effect of boundary layer theory were investigated by Xu and Xu [83].

1.1.4 Carreau Fluid

Carreau fluid is the combination of both Newtonian and power law models. This model has the ability to describe both shear thinning, shear thickening and Newtonian phenomena as a result of a variation in power law index. Blood flow through small and large arteries is the example of Carreau fluid. In some diseased conditions, blood exhibits non-Newtonian properties. Researchers across the world have been interested in Carreau fluid in terms of heat and mass transfer analysis with the inclusion of various effects.

Slip condition occurs when the velocity of the fluid at its boundary is not equal to the one of the boundary. Azam [84] contemplated the impact of partial slip conditions on magneto Carreau fluid flow subjected to a radially expandable sheet. Masood and Hashim [85] studied the effect of multiple slips and chemically reactive species on magneto Carreau fluid past a wedge. Raju et al. [86] studied the performance of Carreau fluid moving towards a slendeing sheet accompanied with slip effects and gyrotactic microorganisms and noted that a positive deviation in slip parameter depreciates the velocity profile. Kumar et al. [87] scrutinized the impact of slip conditions and nonlinear thermal radiation on magneto Carreau fluid flow towards an elastic surface. A numerical solution of a Carreau fluid model along with slip conditions, Cattaneo-Christov heat flux and microorganisms was obtained by Parsad et al. [88]. Carreau fluid moving over an elastic surface

embedded with slip boundary conditions, chemical reaction and activation energy was studied in detail by Khan et al. [89]. Muhammad et al. [90] elucidated the effect of slip conditions and gyrotactic microorganisms on Carreau fluid moving over a stretching wedge.

In certain objects when electron jumps from higher to lower orbit, it emits energy in the form of radiation. The expression regarding linear thermal radiation was achieved by linearizing the Rosseland radiative heat flux having unique Prandtl number [91] by means of Taylor's series in the case when temperature difference is small enough. Nonlinear thermal radiation is applicable where high temperature is required like utilization in nuclear reactors, thermal furnaces, space crafts, polymer preparation etc. Pantokratoras scrutinized the behaviour of linear and nonlinear Rosseland approximation on fluid past a vertical isothermal plate [92]. Carreau fluid accompanied with nonlinear thermal radiation and MHD was debated in detail by Babu et al. [93]. Mahanthesha et al. [94] studied radiative nanofluid moving along a stretchable surface and canvassed that the temperature field amplifies under the effect of nonlinear thermal radiation rather than linear thermal radiation. Kho et al. [95] deliberated Williamson nanofluid moving towards an stretchable medium embedded with radiation effect. Zaib et al. [96] numerically achieved the solution of a Carreau fluid model along with chemical reaction and thermal radiation past an extendable surface and found that the temperature profile enhances by virtue of an augmentation in the radiation parameter. Koriko et al. [97] scrutinized three dimensional stratified Eyring-Powell nanofluid accompanied with nonlinear thermal radiation. Hosseinzadeh et al. [98] studied Maxwell fluid moving over a permeable extendable surface under the effect of nonlinear radiative heat flux. Mondal et al. [99] scrutinized viscous fluid past an expandable surface under the effect of internal heat generation and nonlinear thermal radiation.

The procedure where the work done by a fluid on the adjoining layer under the activity of shear forces is changed into heat is called viscous dissipation. Joule

heating occurs when conducting electrons transfer energy to conductor atoms through the collision procedure. In the occurrence of Ohmic dissipation, excessive heat is generated within the fluid either via direct current or magnetic field. Viscous-Ohmic dissipation has extensive applications in industry like making of industrial electric ovens, induction stoves, incandescent light bulbs, polymerization, food processing, chemical reactors etc. The viscous dissipation has many applications: cooling of reactors, polymer processing, condensation procedure of metallic plate, aerodynamic extrusion of plastic sheets. Pal and Mondal [100] studied the effect of viscous-Ohmic dissipation, double diffusive convection, thermal radiation and MHD on incompressible fluid past a nonlinear stretching surface. Daniel et al. [101] deliberated nanofluid flow accompanied with viscous-Ohmic dissipation. Anjali and Kumari [102] studied viscous-Ohmic dissipation effect on the fluid moving over an expandable medium and observed that the temperature amplifies by amplifying Brownian number. The consequences of viscous and Ohmic dissipation along with heat source/sink on magneto nanofluid was scrutinized in detail by Upreti et al. [103]. Pal [104] analyzed the influence of viscous and Ohmic dissipations on unsteady ferromagnetic fluid and found that the temperature field amplifies as a result of an augmentation in the Eckert parameter. Impact of viscous dissipation on Casson fluid flow over an extendable surface was discussed by Gireesha et al. [105] and it was noted that temperature field escalates owing to an amplification in the Eckert number. Srinivasacharya and Jagadeeshwar [106] pondered the effect of slip boundary condition and Ohmic dissipation on magneto fluid past a stretching sheet and found that the slip phenomenon produces a decremental change in fluid velocity.

1.2 Problem Statement

In the light of literature mentioned above there is still a room available for the study of various types of non-Newtonian fluids with the inclusion of various effects for the study of heat and mass transfer analysis. The detail of different problems presented in this thesis has been given below.

1. Two dimensional Reiner-Philippoff fluid comprising of both dilatant and viscoelastic nature past a stretching sheet is to be studied. Heat transfer aspect of the modeled problem is analyzed with the inclusion of various effects like heat source/sink, nonlinear thermal radiation and variable conductivity whereas mass transfer profile is investigated by considering variable molecular diffusivity.
2. Impact of diffusive convection on the tangent hyperbolic nanofluid moving subjected to an elastic surface is studied. The fluid behaviour is scrutinized in the case of Lorentz force and mixed convection effects. Heat transfer aspect is studied in the case of Buongiorno nanofluid and moreover mass transfer analysis is carried out by including gyrotactic microorganisms suspended in the base fluid.
3. Maxwell fluid flow under the effect of Darcy-Forchheimer flow past a convectively heated porous stretching medium is studied extensively. The behaviour of Darcy-Forchheimer phenomenon on the fluid velocity is studied in the modeled problem. Heat transfer phenomenon is studied deeply by considering the effects like nonlinear based thermal radiation, thermal conductivity and nanofluid respectively whereas mass transport analysis is carried out by considering activation energy in the mass transport equation.
4. The Carreau fluid moving over a bi-directional expandable sheet under the effect of Lorentz force is investigated in detail. The energy as well as concentration aspects of the fluid is investigated with the addition of effects like nonlinear based thermal radiation, viscous dissipation and homogeneous/heterogeneous reactions. The Maxwell velocity and Smoluchowski temperature slip boundary conditions are imposed on the non-Newtonian Carreau fluid moving towards an expandable surface..

1.3 Research Objectives

Research objectives of the present thesis have been given below.

1. Researchers across the world have tried to investigate Reiner-Philippoff past an elastic surface with the inclusion of various effects. Reddy et al. [6] studied transverse magnetic field effect on radiative Reiner-Philippoff fluid past an expandable sheet.

Kumar et al. [7] investigated Cattaneo-Christov heat flux impact on Reiner-Philippoff model moving towards an elastic surface. Reddy et al. [8] contemplated Darcy-Forchheimer flow of radiative Reiner-Philippoff fluid flow across a porous elastic sheet. Ullah et al. [9] comprehended Reiner-Phillipof fluid flow over an unstable stretching using Buongriono nanofluid model. Ishaq et al. [10] numerically studied the stability analysis of the Reiner-Philippoff fluid past an expandable surface. In available literature no attention has been paid to study the mass transfer aspect of the Reiner-Philippoff fluid. The present model aims to fill such gap by considering variable molecular diffusivity in order to analyze the mass transfer aspect. The heat transfer analysis is aimed to be carried out by considering the effects like heat source/sink and variable thermal not addressed before.

2. Tangent hyperbolic model is a viscoelastic model which is investigated in the last few decades by considering various physical effects. Qayyum et al. [38] pondered the influence of heat generation/absorption and Lorentz force on tangent hyperbolic nanofluid fluid flow subjected to an elastic sheet. Nagendramma et al. [39] studied tangent hyperbolic nanofluid past a cylinder by considering the effects like inclined magnetic field and double stratification. Khan et al. [40] scrutinized tangent hyperbolic nanofluid flow towards an extendable medium accompanied with nonlinear based thermal radiation and activation energy effect. Ali et al. [41] studied tangent hyperbolic fluid moving over an expandable sheet accompanied with MHD and temperature varying conductivity. The impact of Lorentz force on tangent hyperbolic nanofluid past an extendable sheet was studied by Ullah et al. [42]. There is still a room in literature to study the tangent hyperbolic fluid by considering the double diffusive convection, motile microorganisms, homogeneous/heterogeneous reactions past an expandable sheet.

3. The behaviour of Maxwell fluid past an expandable sheet has been investigated by researchers across the world for the purpose of heat and mass transfer analysis with the inclusion of various effects like nanoparticles, thermal radiation, MHD etc. Muhammad et al. [55] elucidated the influence of nonlinear Darcy-Forchheimer velocity effect on Maxwell fluid flow subjected to an expandable surface. The impact of stratification, convective heat transfer and Darcy-Forchheimer effects on Maxwell nanofluid were deeply investigated by Hayat et al. [56]. Waqas et al. [57] contemplated Maxwell fluid flow across an expandable medium accompanied with quadratic Forchheimer velocity and heat generation. Sadiq et al. [58] studied the Darcy-Forchheimer flow of Maxwell nanofluid by considering the effect like mixed convection. Hsiao [59] studied the impact of both MHD and thermal radiation on Maxwell fluid flow towards a stretchable surface. Plenty of room is available in the existing literature for the study of Maxwell fluid flow subjected to an expandable sheet accompanied with various effects for the purpose of heat and mass transfer analysis. In the light of available literature mathematical model is developed for Maxwell fluid flow towards a convectively heated stretching sheet accompanied with activation energy for the purpose of mass transfer analysis and moreover nonlinear thermal radiation and variable thermal conductivity for the purpose of heat transfer analysis. Sheet surface is convectively heated and zero mass flux boundary condition will be considered at the surface.
4. Carreau fluid has been studied by the number of researchers in order to study its limitations at minimum and maximum shear rates with the inclusion of various effects for heat and mass transfer analysis. Masood and Hashim [85] pondered chemically reactive species impact on the magneto Carreau fluid flow subjected to a slippery expandable wedge. Raju et al. [86] pondered Carreau fluid moving towards a slandering sheet by taking slip effects and gyrotactic microorganisms. The impact of slip conditions and nonlinear based thermal radiation on magneto Carreau fluid flow across an elastic surface were scrutinized by Kumar et al. [87]. Carreau fluid accompanied with

nonlinear thermal radiation and MHD was debated in detail by Babu et al. [93]. Zaib et al. [96] numerically achieved the solution of a Carreau fluid model accompanied with chemical reaction and thermal radiation past an extendable surface. There is still a space available in the existing literature regarding Carreau fluid by considering various types of slip conditions like Wu's slip, Navier slip and mass transfer by considering various effects like activation energy, catalytic chemical reactions, motile microorganisms etc. In the light of deficiencies available in the literature a mathematical model is designed regarding Carreau fluid past an extendable surface by considering slip boundary conditions at the sheet surface. Maxwell velocity slip and Smoluchowski temperature jump boundary conditions are never utilized before as slip boundary conditions. Heat and mass transfer analysis will be carried out by considering nonlinear thermal radiation, viscous and Ohmic dissipations, homogeneous/heterogeneous chemical reactions.

1.4 Scope of Research

The motive behind the present research is to investigate non-Newtonian fluids like Reiner-Philippoff fluid, tangent hyperbolic fluid, Maxwell fluid, Carreau fluid past a stretching sheet with the consideration of various effects for the analysis of heat and mass transfer. The work presented in Chapter 3 can be extended in terms of Reiner-Philippoff fluid flow over different geometries like wedge, cylinder, sphere, cone etc. The literature mentioned in Chapter 4 can be extended in the direction of hyperbolic tangent fluid flow through parallel stretching disks, converging/diverging channels, inclined stretching sheet with the inclusion of effects like hybrid nanoparticles, carbon nanotubes, activation energy etc. This study presented in Chapter 5 can be extended in the direction of Maxwell nanofluid past an oscillatory stretching sheet, needle, peristaltic flow, sensor surface, nonlinear stretching sheet etc with the inclusion of effects like gyrotactic microorganisms, melting surface, convective heat and mass transfers, variable molecular diffusivity etc. The momentum and temperature slip boundary conditions presented in Chapter 6 for

the case of Carreau fluid can be further utilized in other viscoelastic type non-Newtonian fluids flow over different geometries like channel, sphere, cone, wedge, pipe etc.

1.5 Research Methodology

The modeled partial differential equations of the proposed models are converted into ordinary differential equation with the utilization of similarity transformations and furthermore tackled these equations numerically with the help of non-linear shooting method and Keller-box scheme. Shooting method is the ability to integrate the differential equations as an initial value problem with guesses for the unknown initial values. This ability is not required with the finite difference method, for the unknowns are considered to be the values of the true solution at the number of interior mesh points. The keller-box method is an implicit numerical scheme which is second order accurate in both space and time for the standard diffusion equations. All the simulations of the modeled problems has been done in Matlab 2016a software [107]. Matlab is a programming and numeric computing platform used by millions of engineering and researchers working in fluid dynamics area to analyze data, develop algorithms, and create models.

1.6 Significance of the Study

In this thesis heat and mass transfer analysis of various non-Newtonian fluids has been carried out. Heat transfer of the fluid increases in the presence of nanoparticles, thermal radiation, Joule heating and variable thermal conductivity. From the present study, it is observed that the temperature of the fluid escalates owing to an amplification in the thermal radiation, variable thermal conductivity and nanoparticles. Nanoparticles enhance heat transfer rate having applications in biomedical, optical, electronics, ceramic industry, computer chips, car engines, nuclear reactors etc. Thermal radiation and variable thermal conductivity is used

where high temperature difference is required like fusion reactors, combustion reactors, polymer production, jet engine, gas turbines etc. Mass transfer analysis has been carried out with the consideration of activation energy, thermal diffusivity, motile gyrotactic microorganisms and homogeneous-heterogenous reactions. Microorganisms present in the fluids have different applications in the industry like production of ethanol, lactic acid, butanol, alcoholic beverages, vinegar, yogurt, bio-fuels etc. Homogeneous-heterogenous reactions have immense applications like cooling towers, fog dispersion, polymer production and hydrometallurgical industry. The present research opens a pathway for the researchers to analyze the heat and mass transfer analysis of the non-Newtonian fluids by considering various effects that amplifies the heat and mass transfer analysis of the fluid.

Today's era is about the study of different procedures to enhance the heat transfer rate. Solar energy is the great source of heat and utilized in solar collectors present in solar aircrafts, solar ships, solar panels present in the homes. Solar collector is a device that collects solar radiation from the sun. Nanoparticles based direct solar collectors are solar thermal collectors where nanoparticles in a liquid medium can scatter and absorb solar radiation. Researches across the world have tried to enhance the performance of solar collectors by considering various types of nanoparticles, hybrid nanoparticles etc. This dissertation provides a platform for the researchers to study and enhance heat transfer analysis of solar thermal collectors with the consideration of nanofluids, thermal radiation, viscous dissipation, nonlinear thermal radiation and Joule heating.

1.7 Thesis Layout

The layout of the rest of the thesis has been presented below

Chapter 2 comprises of derivations of some governing laws regarding continuity, mass, momentum, energy, concentration. The idea of fluids and dimensionless numbers are also given in this chapter.

Chapter 3 discusses two dimensional radiative Reiner-Philippoff fluid flow towards

a stretchable surface accompanied with thermal conductivity, molecular diffusivity and heat source/sink has been studied extensively. The governing modelled equations are handled numerically with the help of nonlinear shooting technique.

Chapter 4 discusses the flow of mixed convective tangent hyperbolic nanofluid moving over a stretching sheet under the effect of double diffusive convection, MHD and motile gyrotactic microorganisms. The numerical solution is achieved by Keller box method.

Chapter 5 scrutinizes the Maxwell nanofluid moving across a porous convectively heated stretchable surface under the effect of thermal radiation, thermal conductivity and magnetohydrodynamics. To achieve the solution of the modelled equations numerically, shooting scheme has been employed.

Chapter 6 is all about the study of 3D Carreau fluid past a bidirectional slippery stretching medium accompanied with magnetohydrodynamics, viscous dissipation, Ohmic dissipation and nonlinear thermal radiation.

Chapter 7 comprises of the conclusion and the future work.

Chapter 2

Preliminaries

The primary goal of this chapter is to study the concept of fluid and its categorization based on shear stress behaviour. The relevant definitions and concepts regarding the next chapters have been incorporated in this chapter. The governing equations of motion regarding mass, momentum, temperature and concentration of fluid flow over stretching sheet accompanied with healthy discussion on bioconvection, catalysis and double diffusive convection are included within. A description of the relevant dimensionless parameters emerges during numerical simulation of the modeled problems is also given.

2.1 Fluid

Fluids typically comprises of liquids, gases and plasmas. In fluids, the applied stress is directly related to strain. In the case of a constant applied shear force, a solid ultimately stops flowing at certain fixed strain angle. A fluid is keep flowing and continuously deforming and reaches a constant rate of strain. Fluids can be organized into various types on the basis of properties like viscosity, conductivity and compressibility. The Navier–Stokes equations may be used to describe the behaviour of fluids. Further classification of fluids has been presented underneath.[\[108\]](#)

2.2 Classification of Fluids

Fluids on the basis of their physical properties like viscosity, shear stress, strain can be divided into main categories presented below:

2.2.1 Newtonian Fluids

Fluids for which the applied shear stress and the rate of deformation are linearly proportional to each other termed as Newtonian fluids.

Fig. 2.1 represents various examples of Newtonian fluids that are utilized in everyday life, such as water, mineral oil, ethyl alcohol and gasoline. In the case of Newtonian fluids, mathematical expression of τ_{xy} is given by expression enumerated underneath

$$\tau_{xy} = \mu \frac{du}{dy}, \quad (2.1)$$

where μ represents dynamic viscosity and $\frac{du}{dy}$ is the rate of deformation. The SI unit of shear stress τ_{xy} is $\text{N}\cdot\text{s}\cdot\text{m}^{-2}$. [108]

2.2.2 Non-Newtonian Fluids

In the case of non-Newtonian fluids, the deformation rate $\dot{\gamma}$ and the shear stress σ are not linearly related. [109]

Indeed, under certain conditions, the ratio of applied shear stress and shear rate is not dependent only on flow conditions but dependent on the kinematic history of the fluid element also. Due to the complexity between shear stress and strain, it is difficult to predict the exact nature of non-Newtonian fluids. Various mathematical models have been developed in order to study the rheological behaviour of non-Newtonian fluids.

Fig. 2.2 represents various products behaving like non-Newtonian fluids. Depending on how viscosity changes over time, non-Newtonian fluids can be divided into two different categories

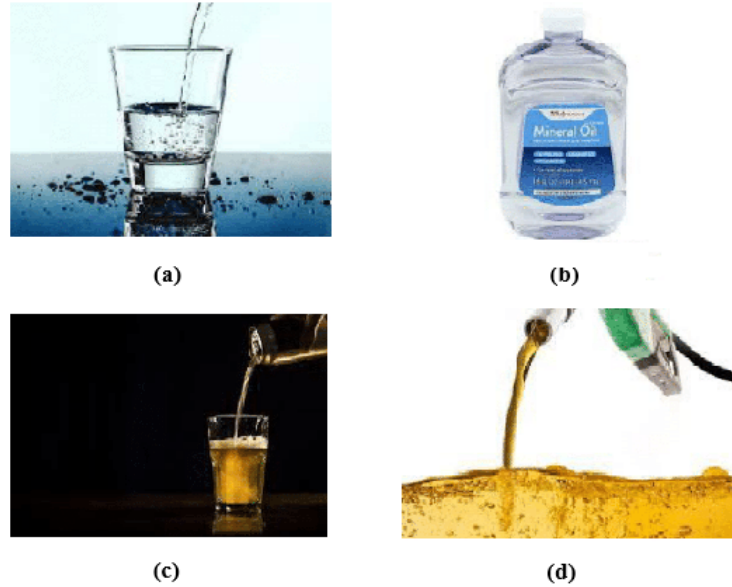


FIGURE 2.1: (a) water (b) mineral oil (c) ethyl alcohol (d) gasoline

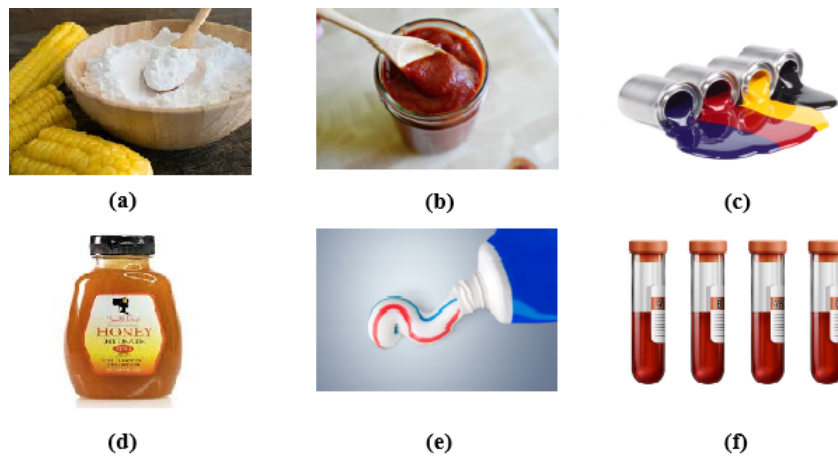


FIGURE 2.2: (a) corn starch (b) Ketchup (c) paint (d) honey (e) toothpaste
(f) blood

2.3 Time-independent Fluid

Time-independent fluids are those in which the deformation rate $\dot{\gamma}$ is assessed only by the present value of σ at that instant.[109].Mathematically,

$$\mu \times \dot{\gamma}_{yx} = f(\tau_{yx}). \quad (2.2)$$

The many types of non-Newtonian fluids are depicted in Fig. 2.3. There are three types of fluids that are time-independent.

2.3.1 Pseudoplastic Fluids

Pseudoplastic fluids is the ratio of shear stress by shear rate mathematically written as $(\frac{\sigma_{yx}}{\dot{\gamma}_{yx}})$. The apparent viscosity diminishes gradually a result of an amplification in the shear rate.

The shear stress by shear rate termed as apparent viscosity approaches a Newtonian behaviour and moreover viscosity of the fluid is independent of zero shear rate.

$$\lim_{\dot{\gamma} \rightarrow 0} \frac{\sigma_{yx}}{\dot{\gamma}_{yx}} = \eta_0. \quad (2.3)$$

Fluid behaviour is non-Newtonian and moreover viscosity of the fluid is dependent at high shear rate.

$$\lim_{\dot{\gamma} \rightarrow \infty} \frac{\sigma_{yx}}{\dot{\gamma}_{yx}} = \eta_\infty. \quad (2.4)$$

Examples are milk, human blood, clay and paints.[109]

2.3.2 Dilatant Fluids

Yield stress is the amount of stress necessary for any material to be permanently deformed. Although dilatant fluids do not exhibit yield stress, their apparent viscosity escalates by virtue of a magnification in the shear rate. Mixture of corn starch suspension in the water is the best example of dilatant type fluids.[109]

2.3.3 Bingham Plastic Fluids

This type of fluid relies on the yield stress phenomenon σ_0 . If the value of σ_0 is greater than the yield stress, the fluid start moving. The fluid is not moving if the value of σ_0 is less than the yield stress. Bingham polymers require a specific amount of force to flow. A viscoplastic substance called a Bingham plastic acts like a stiff body at low inertial forces but flows like a viscous fluid in the presence of high inertial forces. Daily life examples of this sort of fluids are toothpaste, mayonnaise, drilling mud.[109]

2.4 Time-dependent fluids

Many products, particularly in the food, pharmaceutical, cosmetics comprising of flow characteristics that are not easily represented by a straight forward mathematical formula like Eq. (2.1). In the case of fluids rely on time, the viscosity of fluid deformation ($\dot{\gamma}$) not depend only on stress (σ) but also on the function of time. It is common to split time-dependent fluid behaviour into two kinds, thixotropy and rheopectic, based on a material's response under the application of applied force and time as well.[109]

2.4.1 Thixotropic Fluids

Thixotropy is a phenomena that occurs throughout time. The apparent viscosity $\eta = \frac{\sigma}{\dot{\gamma}}$ decreases under the application of applied stress over any defined period of time. Rheopectic fluids behave differently from thixotropic fluids. Examples are Cytoplasm, synovial fluid, gelatine, cream, castor oil, tire rubber.[109]

2.4.2 Rheopectic Fluids

The viscosity of the fluid escalates with time under the effect of applied shear stress is termed as rheopectic fluids also known as shear thinning fluids. When these fluids are agitated, their viscosity increases. This implies that when the fluid is jolted, it thickens or even solidifies. Gypsum pastes and printer inks are rheopectic in nature.[109]

2.5 Basic Definitions

This section comprises of the some basic definitions regarding the various effects used in momentum, temperature and mass transport equations in order to study heat as well as mass transport phenomenons.

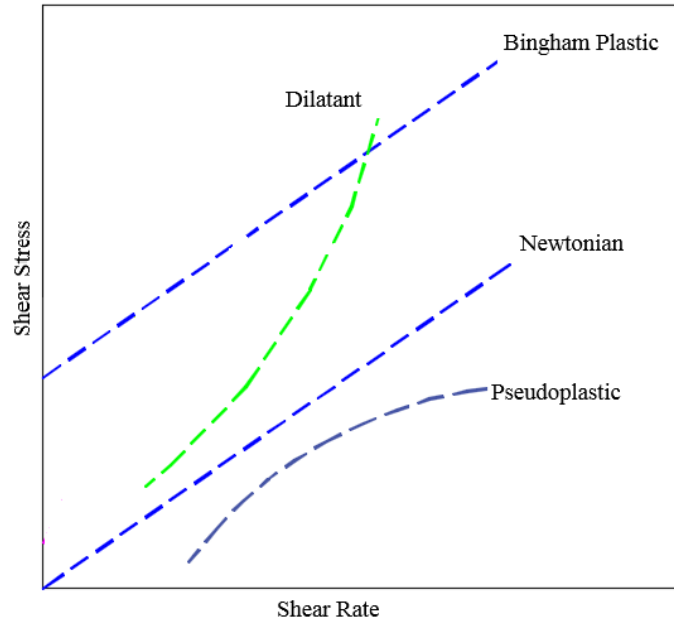


FIGURE 2.3: Non-Newtonian Fluids

2.5.1 Radiation

Thermal radiation is electromagnetic waves produced as a result of thermal movement of the molecules. The transmission of energy via radiation, unlike conduction and convection, does not need the existence of an intervening medium. Thermal radiation, which is the type of radiation released by substances as a result of their temperature, is of particular importance in heat transfer research. Thermal radiation is emitted by the objects having temperature greater than absolute zero. The radiation discharge from a surface having temperature at zero T_s conveyed by Stefan–Boltzmann law given below

$$\dot{Q}_{\text{emit,max}} = \sigma A_s T_s^4, \quad (2.5)$$

where $\sigma = 5.67 \times 10^{-8}$ is the Stefan–Boltzmann constant having unit $\text{W m}^{-2} \text{K}^4$. [110]

2.5.2 Specific Heat

Energy required to raise the temperature of a unit mass of a substance by one degree is called specific heat.

Mathematically,

$$C = \frac{Q}{m\Delta T}, \quad (2.6)$$

here Q indicates heat energy, m is mass and ΔT represents temperature difference.

The SI unit is $\text{J kg}^{-1} \text{K}^{-1}$.[\[110\]](#)

2.5.3 Thermal Conductivity

The rate of heat transfer through a unit thickness of the material per unit area per unit temperature difference is termed as thermal conductivity which actually measures the capacity of the material to transmit heat. Thermal conductivity of a substance with a high value implies that it is a good heat conductor. Thermal conduction phenomenon follows the Fourier's law of thermal conduction.

Mathematically,

$$\dot{Q} = -\kappa A \frac{\Delta T}{\Delta x}, \quad (2.7)$$

where κ , A , ΔT , Δx represents thermal conductivity, area, temperature difference and thickness of the material respectively. The SI unit of thermal conductivity is $\text{W m}^{-1} \text{K}^{-1}$.[\[110\]](#)

2.5.4 Thermal Diffusivity

Thermal Diffusivity represents how fast heat diffuses through a material. Mathematically,

$$\alpha = \frac{\text{Heat conducted}}{\text{Heat stored}} = \frac{\kappa}{\rho C_p}. \quad (2.8)$$

where κ indicates the capacity of any material to transmit heat, and ρC_p symbolizes the tendency of the material to store heat per unit volume.[\[110\]](#)

2.5.5 Activation Energy

The minimum energy necessary to initiate a chemical reaction is known as activation energy.

Mathematically,

$$k = A \exp\left(\frac{-E_a}{RT}\right), \quad (2.9)$$

where k , T , R and E_a are pre-exponential factor, temperature, gas constant and activation energy. The SI unit of activation energy is J mol^{-1} . Swante Arrhenius presented the idea of activation energy in 1889.[111]

2.6 Dimensionless Numbers

Basic definitions regarding dimensionless numbers appear during numerical simulation of the problems are given below.

2.6.1 Reynold's Number

Reynold's number is the ratio of inertial forces to the viscous forces.[111]

This is given by

$$Re = \frac{w\delta}{\nu}, \quad (2.10)$$

symbols w , δ and ν are the velocity, layer thickness and kinematic viscosity respectively. Reynold's number describe the behaviour of viscous fluid flow. Reynold's number also explains the fluid behaviour is laminar or turbulent.

2.6.2 Biot Number

The ratio of the heat transferred by convection to the heat flow by conduction is termed as Biot number. Biot number emerges from Fourier's-Biot law.

Mathematically, Biot number is represented by

$$Bi = \frac{hL}{\kappa}, \quad (2.11)$$

where h , L and κ denotes the heat transmission, length and heat transfer by conduction respectively having units $\text{W m}^{-2}\text{K}^{-1}$, m and $\text{W m}^{-1}\text{K}^{-1}$.[111]

2.6.3 Schmidt Number

It is the ratio of momentum diffusivity to the mass diffusivity. It provides the information of velocity and molecular concentration. Mathematically,

$$Sc = \frac{\text{kinematic viscosity}}{\text{mass diffusivity}} = \frac{\nu}{D}. \quad (2.12)$$

The units of ν and D are $\text{m}^2 \text{s}^{-1}$ and $\text{m}^2 \text{s}^{-1}$. [111]

2.6.4 Weissenberg Number

It expresses the ratio of relaxation time to the shear velocity. Mathematically,

$$We = \frac{\lambda \mu \dot{\gamma}^2}{\mu \dot{\gamma}} = \lambda \dot{\gamma} \quad (2.13)$$

where $\dot{\gamma}$ and λ are the shear rate and the relaxation time having units s^{-1} and s . [111]

2.6.5 Prandtl Number

It is the ratio of the momentum diffusivity to the thermal diffusivity. In the case of $Pr < 1$, thermal diffusivity dominates the momentum diffusivity but situation is opposite in the case of $Pr > 1$. Mathematically,

$$Pr = \frac{\text{Kinematic viscosity}}{\text{Thermal diffusivity}} = \frac{\nu}{\alpha}. \quad (2.14)$$

The units of ν and α are $\text{m}^2 \text{s}^{-1}$ and $\text{m}^2 \text{s}^{-1}$. [111]

2.6.6 Lewis Number

It is the ratio of thermal diffusivity to the mass diffusivity. Mathematically,

$$Le = \frac{\alpha}{D}, \quad (2.15)$$

where α and D are thermal and molecular diffusivities having same units m^2s^{-1} . [111]

2.6.7 Peclet Number

Peclet number is the ratio of advection versus diffusion.

Large Peclet number indicates the advection flow and a small number indicates a diffuse flow. Mathematically,

$$Pe = \frac{Lu}{D}, \quad (2.16)$$

where L , u and D depicts the reference length, velocity and diffusion coefficient having SI, units m , ms^{-1} and m^2s^{-1} respectively. [111]

2.6.8 Eckert Number

The Eckert number provides a measure of the kinetic energy of the flow relative to the enthalpy difference across the thermal boundary layer.

Mathematically, it can be expressed as

$$Ec = \frac{u^2}{C_p \Delta T}, \quad (2.17)$$

where u , C_p , ΔT denotes fluid flow velocity, specific heat, temperature difference having units ms^{-1} , $\text{m}^2 \text{s}^2 \text{K}^{-1}$ and K . [111]

2.6.9 Grashof Number

Grashof number represents the ratio between the buoyancy force and the viscous forces. Gravity is the main factor of the buoyancy force which is responsible for the natural convection phenomenon.

Grashof number is analogous to the Reynold's number. The free convection occurred due to the buoyancy force and the motion is restricted by the viscous force.

Mathematically,

$$Gr = \frac{g\beta(T_w - T_\infty)L^3}{\nu^2}, \quad (2.18)$$

where g , β , $(T_w - T_\infty)$, L , ν indicates gravity, volumetric thermal expansion coefficient, temperature difference, characteristic length, kinematic viscosity having units K^{-1} , K , m and $\text{m}^2 \text{s}^{-1}$. [111]

2.6.10 Nusselt Number

It is the ratio of the convective heat transfer to conductive heat transmission.

Mathematically,

$$Nu = \frac{q_{\text{conv}}}{q_{\text{cond}}} = \frac{h\Delta T}{\kappa \frac{\Delta T}{L}} = \frac{hL}{\kappa}, \quad (2.19)$$

where h , L and κ are the heat transmission parameter, medium length and heat conduction respectively having SI, units $\text{W m}^{-2} \text{K}^{-1}$, m and $\text{W m}^{-1} \text{K}^{-1}$ respectively. [111]

2.6.11 Sherwood Number

It represents the ratio of convective to the diffusive mass transfer. This number perform same role in terms of mass transmission like Nusselt number in the case of transmission. Mathematically,

$$Sh = \frac{h_m L}{D}, \quad (2.20)$$

where h_m , L and D are the mass transfer coefficient, reference length and molecular diffusivity having SI, m s^{-1} , m and $\text{m}^2 \text{s}^{-1}$. [111]

2.7 Double Diffusive Convection

Double diffusive convection is a phenomenon that describes convection induced by two distinct density gradients with different diffusion speeds. Convection is caused by density variations within fluids acting under the influence of gravity. Because the concentrations of heat and salt have independent gradients and diffusing rates,

oceanography provides a good example of double diffusion convection. Cold water coming from glacier as a result of melting phenomenon has a high density and low temperature as compared to salty and high-temperature sea water having low density. Both of these factors are affected by the input of cold freshwater from an iceberg. Variables may cause these density changes. Thermal as well as compositional gradients can disperse with time, diminishing their ability to drive convection and necessitating the presence of gradients in other areas of the flow to keep convection going. The conservation Eqs. (2.21)-(2.25) for continuity, momentum, heat, salinity and buoyancy effect (under Boussinesq's approximation) are given by

$$\nabla \cdot \mathbf{u} = 0, \quad (2.21)$$

$$\frac{\partial \mathbf{u}}{\partial t} + \mathbf{u} \cdot \nabla \mathbf{u} = -\frac{1}{\rho_0} \nabla p - g \frac{\rho}{\rho_0} \mathbf{k} + \nu \nabla^2 \mathbf{u}, \quad (2.22)$$

$$\frac{\partial T}{\partial t} + \mathbf{u} \cdot \nabla T = \kappa_T \nabla^2 T, \quad (2.23)$$

$$\frac{\partial S}{\partial t} + \mathbf{u} \cdot \nabla S = \kappa_S \nabla^2 S, \quad (2.24)$$

$$\frac{\rho - \rho_0}{\rho_0} = \beta(S - S_0) - \alpha(T - T_0). \quad (2.25)$$

Symbols, κ_T and κ_S are thermal conductivity of heat and salt, ν is the kinematic viscosity and (ρ_0, p_0, T_0, S_0) denote the (constant) reference values of density, pressure, temperature and salinity.[112]

For more details on double diffusive convection phenomenon, see references [112–114].

2.8 Bioconvection

Bioconvection patterns are actually the joint phenomenon appear as a result of swimming of microorganisms having denser than water in suspensions. The microorganisms gathering at the upper surface for the purpose of oxygen and light. The upper surface of the fluid becomes too dense and becomes unstable as a result of the gathering of microorganisms. The microorganisms fall down generate the

bioconvection phenomenon.[115]

Taxes is actually the swimming of microorganisms in certain direction in response to the certain stimuli. Different types of taxes are given below.

2.8.1 Gyrotaxis

Gyrotaxis phenomenon is obtained by the balancing the two torques. The first one is termed as viscous torque that works on a body situated in a shear flow direction. The second one is termed as the gravitational torque which is generated by the gravity effect because the microorganism centre of mass is dislocated from its center of buoyancy in a negative direction.[115]

2.8.2 Gravitaxis

In the case of Gravitaxis microorganisms swimming in the direction opposite to the gravity effect. Algae cells like Chlamydomonas, ciliated protozoan exhibits gravitactic behaviour. [115]

2.8.3 Phototaxis

Phototaxis is the phenomenon in which microorganisms move towards or away from the light source. In the case of positive Phototaxis, microorganisms move straight in the direction of light source and negative phototaxis directed the movement of microorganisms away from the light source.[115]

2.8.4 Oxytaxis

The level of oxygen is not sufficient in the lower region of the fluid, the bacteria present in lower region of the fluid consume all oxygen very quickly, as the result the deficiency of the oxygen occur in the lower region of the fluid causing the bacteria inactive. The lively bacteria move toward the upper region having sufficient

oxygen and causing the upper layer of the fluid unsettled due the abundance of microorganisms which give rise to the process of bioconvection.[115]

For more details on bioconvection phenomenon, see reference [115].

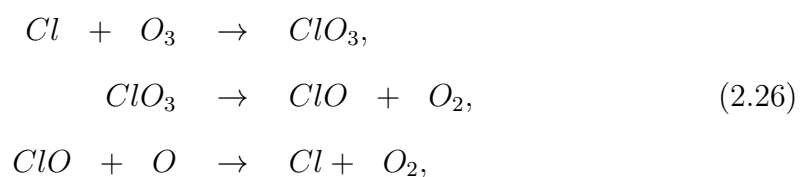
2.9 Catalysis and Its Types

A catalyst speed up a chemical reaction. It is doing so by making bonds with the molecules reacting with each other, and by permitting these molecules to react with each other in order to create a product, which detaches from the catalyst, and left it unchanged in such a way that it is accessible for the next reaction.[116]

There are three types of catalysis

2.9.1 Homogeneous Catalysis

In the case of homogeneous catalysis, both the catalyst and the reactants are situated in the same phase, i.e. catalyst and the reactants are in the gas phase, or, in the liquid phase. Ozone is the simple example of homogeneous catalysis given by [116]



or over all



2.9.2 Biocatalysis

Enzymes are nature's catalysts. Enzyme catalysis the decomposition of hydrogen peroxide taken as reactant in order to form the product comprising of water and

oxygen given by



Enzymes are type of chemical reaction permit biological reactions to occur at the rates mandatory to attain life cycle, in particular the formation of proteins and DNA.[116]

2.9.3 Heterogeneous Catalysis

In the process of heterogeneous catalysis, catalyst are in solid form reacts with molecules of a solution to form a product. As solids are usually porous in nature and impenetrable, catalytic reactions happen at the solid surface. To utilize the commonly used metal like platinum in an economical way to achieve the desired chemical reaction, catalysts are 1-100 nanometer in size, supported on an inert, porous structure.[117]

Different types of heterogenous reactions are



For more details on catalysis, see references [116] and [117].

2.10 Governing Laws Regarding Heat and Mass Transport in Fluids

2.10.1 Continuity Equation

The expression regarding law of conservation of mass conservation is given by

$$\frac{\partial \rho}{\partial t} + \nabla \cdot (\rho \mathbf{V}) = 0. \quad (2.31)$$

The symbols ρ and \mathbf{V} expresses the density and the fluid velocity. The expression Eq. (2.31) in the case of incompressible fluid is given by

$$\nabla \cdot \mathbf{V} = 0. \quad (2.32)$$

In term of cartesian coordinates

$$\frac{\partial u}{\partial x} + \frac{\partial v}{\partial y} + \frac{\partial w}{\partial z} = 0, \quad (2.33)$$

whereas the symbols u , v and w denotes the elements of velocity components in x , y and z direction. [118]

2.10.2 Momentum Equation

The mathematical form of momentum equation is conveyed by

$$\frac{\partial(\rho\mathbf{V})}{\partial t} + \nabla \cdot [(\rho\mathbf{V})\mathbf{V}] - \nabla \cdot \tau_1 - \rho g = 0. \quad (2.34)$$

Expression regarding the internal forces appears in the body is premeditated by

$$\tau_1 = -p\mathbf{I} + \mathbf{S}. \quad (2.35)$$

Now the momentum expression takes the form

$$\rho \left(\frac{\partial \mathbf{V}}{\partial t} + \mathbf{V} \cdot (\nabla \mathbf{V}) \right) = \nabla \cdot (-p\mathbf{I} + \mathbf{S}) + \rho g. \quad (2.36)$$

The symbols g , p and \mathbf{S} indicates the body force, pressure and extra stress tensor. Cauchy stress tensor express in the following form

$$\tau = \begin{pmatrix} \sigma_{xx} & \tau_{xy} & \tau_{xz} \\ \tau_{yx} & \sigma_{yy} & \tau_{yz} \\ \tau_{zx} & \tau_{zy} & \sigma_{zz} \end{pmatrix}. \quad (2.37)$$

The Eq. (2.36) can be further transformed into by taking scalar product with basis vectors and further take $\mathbf{g} = -g\nabla z$ where z is distance from an arbitrary reference elevation in the direction of gravity. Now the Eq. (2.34) is

$$\rho \left(\frac{D\mathbf{V}}{Dt} \right) = \rho \left(\frac{\partial \mathbf{V}}{\partial t} + \mathbf{V} \cdot (\nabla \mathbf{V}) \right) = \nabla \cdot (-p\mathbf{I} + \mathbf{S}) + \nabla(-\rho g z). \quad (2.38)$$

Cartesian coordinates of the velocity are $\mathbf{V} = [u(x, y, z, t), v(x, y, z, t), w(x, y, z, t)]$. The steady state incompressible momentum equation in components form is manifested by

$$\rho \left(\frac{\partial u}{\partial t} + u \frac{\partial u}{\partial x} + v \frac{\partial u}{\partial y} + w \frac{\partial u}{\partial z} \right) = \frac{\partial \sigma_{xx}}{\partial x} + \frac{\partial \tau_{xy}}{\partial y} + \frac{\partial \tau_{xz}}{\partial z} + \rho g_x. \quad (2.39)$$

$$\rho \left(\frac{\partial v}{\partial t} + u \frac{\partial v}{\partial x} + v \frac{\partial v}{\partial y} + w \frac{\partial v}{\partial z} \right) = \frac{\partial \tau_{yx}}{\partial x} + \frac{\partial \sigma_{yy}}{\partial y} + \frac{\partial \tau_{yz}}{\partial z} + \rho g_y. \quad (2.40)$$

$$\rho \left(\frac{\partial w}{\partial t} + u \frac{\partial w}{\partial x} + v \frac{\partial w}{\partial y} + w \frac{\partial w}{\partial z} \right) = \frac{\partial \tau_{zx}}{\partial x} + \frac{\partial \tau_{zy}}{\partial y} + \frac{\partial \sigma_{zz}}{\partial z} + \rho g_z. \quad (2.41)$$

Components of Cauchy stress tensor are $\tau_{xx}, \tau_{xy}, \tau_{xz}, \tau_{yx}, \tau_{yy}, \tau_{yz}, \tau_{zx}, \tau_{zy}$ and τ_{zz} and the body force comprises of g_x, g_y and g_z . [118]

2.10.3 Magnetohydrodynamics

Magnetohydrodynamics (MHD) is derived from *magneto*-mean magnetic field, *hydro*-mean water, *dynamics*-mean motion. Magnetohydrodynamics analyze the performance of electrically conducting fluids like salt water, electrolytes and plasmas. Hannes Alfvén presented the idea of MHD in 1889. The expression for momentum equation together with the magnetic field is given by

$$\rho \left(\frac{\partial \mathbf{u}}{\partial t} + (\mathbf{V} \cdot \nabla) \mathbf{V} \right) = -\nabla P + \mathbf{j} \times \mathbf{B}, \quad (2.42)$$

where P , \mathbf{B} , \mathbf{V} and \mathbf{j} expresses kinetic pressure, magnetic field, velocity and current density. The expression of current density in the light of Ohm's law is given by

$$\mathbf{j} = \sigma \mathbf{E}', \quad (2.43)$$

whereas the symbols σ and E' represents the electric conductivity and electric field. The motion of plasma with velocity \mathbf{V} in the occurrence of external magnetic field as well as Lorentz transformation is given by

$$\mathbf{E}' = E + \mathbf{V} \times \mathbf{B}, \quad (2.44)$$

now Eq. (2.43) takes the form

$$\frac{1}{\sigma} \mathbf{j} = E + \mathbf{V} \times \mathbf{B}, \quad (2.45)$$

after assuming $\sigma \rightarrow \infty$, we get

$$\mathbf{E} = -\mathbf{V} \times \mathbf{B}, \quad (2.46)$$

mathematical expression for Faraday's law is mentioned below

$$\nabla \times \mathbf{E} = -\frac{\partial \mathbf{B}}{\partial t}, \quad (2.47)$$

after omitting electric field, the MHD equation is represented by

$$\frac{\partial \mathbf{B}}{\partial t} = \nabla \times (\mathbf{V} \times \mathbf{B}). \quad (2.48)$$

still the MHD expression incomplete, we implement fourth Maxwell's law which is actually the generalization of the Ampere circuital law.

The mathematical equation of fourth Maxwell's law is denoted by

$$\nabla \times \mathbf{B} = \mu_0 \mathbf{j} + \frac{1}{c^2} \frac{\partial \mathbf{E}}{\partial t}, \quad (2.49)$$

neglecting $\frac{\partial \mathbf{E}}{\partial t}$ in the equation mentioned above we get

$$\nabla \times \mathbf{B} = \mu_0 \mathbf{j}, \quad (2.50)$$

the magnetic field \mathbf{B} should fulfil the condition $\nabla \cdot \mathbf{B} = 0$. The expressions for MHD in closed form are mentioned below:

$$\rho \left(\frac{\partial V}{\partial t} + (\mathbf{V} \nabla) \mathbf{V} \right) = -\nabla P + \frac{1}{\mu_0} (\nabla \times \mathbf{B}) \times \mathbf{B}, \quad (2.51)$$

and

$$\frac{\partial \mathbf{B}}{\partial t} = \nabla \times (\mathbf{V} \times \mathbf{B}). \quad (2.52)$$

The expressions \mathbf{V} and \mathbf{B} indicates the fluid velocity and magnetic field.[119]

2.10.4 Energy Transport

According to the energy conservation theory (Total energy remains constant). [118] The mathematical expression regarding the conservation of energy is denoted by

$$\rho \left[\frac{\partial \mathbf{U}}{\partial t} + \mathbf{V} \cdot \nabla \mathbf{U} \right] = [\tau_1 : \nabla \mathbf{V} + p \nabla \cdot \mathbf{V}] + \nabla (\kappa \nabla T) \pm \hat{H}r. \quad (2.53)$$

The symbols \mathbf{U} and $\hat{H}r$ used in the above expression represents internal energy and internal heat respectively. Introducing the expression of constant volume process $d\mathbf{U} \equiv C_v dt$ in the expression given above provides

$$\rho C_v \left[\frac{\partial T}{\partial t} + \mathbf{V} \cdot \nabla T \right] = [\tau_1 : \nabla \mathbf{V} + p \nabla \cdot \mathbf{V}] + \nabla (\kappa \nabla T) \pm \hat{H}r. \quad (2.54)$$

If the fluid is incompressible then $\mathbf{V} = 0$, $\nabla \cdot \mathbf{V} = 0$ and furthermore take $C_v = C$, then the final form of energy equation become

$$\rho C \frac{\partial T}{\partial t} = \nabla (\kappa \nabla T) \pm \hat{H}r. \quad (2.55)$$

2.10.5 Mass Transport

The mathematical expression regarding Fick's second law is given by

$$\frac{dC}{dt} = -\nabla \cdot \mathbf{j}. \quad (2.56)$$

According to Fick's first law, molar flux j and the diffusivity phenomenon D and

directly linked with each other and mathematically written as

$$\mathbf{j} = -\mathbf{D}\nabla C. \quad (2.57)$$

Taking derivative of Eq. (2.57) and using in Eq. (2.56) provides the mass transport equation mentioned underneath

$$\frac{dC}{dt} = \mathbf{D}\nabla^2 C. \quad (2.58)$$

The symbols C , \mathbf{D} and j expresses the mass concentration, diffusion and flux.

2.11 Mass Transfer

Mass transfer is actually the transport of net mass from region of having high concentration of the molecules towards the area having lower concentration of the molecules and moreover concentration difference occur in the two objects is the leading force responsible for net transport of the mass from one place to another different place. The process of mass transport rely on two factors termed as convection and diffusion. Mass transfer has distinguished utilizations in different areas like purification of kidneys and liver, reactor engineering, absorbers, distillation of alcohol, cooling towers etc. Fick's first and second law of diffusion describes the mass transport process very precisely. The mass transport phenomenon with the inclusion of effects like chemical reaction, activation energy, homogeneous/heterogenous reaction, double diffusion convection and motile gyrotatic microorganisms have been discussed theoretically and experimentally in next chapters.

Chapter 3

Impact of Heat Source/ Sink and Variable Species Diffusivity on Radiative Reiner-Philippoff Fluid

The impact of distinguished effects like variable thermal conductivity and molecular diffusivity on radiative Reiner-Philippoff fluid moving over a stretchable surface accompanied with heat source/sink has been investigated in detail. Temperature inside the fluid is controlled with the implementation of nonlinear based thermal radiation and variable change in thermal conduction phenomenons. Variable change in fluid concentration can be examined under the effect of variable molecular diffusion. The PDEs are converted into ODEs with the help of suitable self similarity variables. Furthermore, the dimensionless model is numerically handled with the utilization of well established shooting technique. The influence of dimensionless essential parameters on mass fraction field, Nusselt number, velocity field are examined through tables and graphs. It is noteworthy that a magnification in species diffusivity parameter guides to an incremental change in the concentration field. An amplification in the Reiner-Philippoff fluid effect promotes shear thickening behaviour inside the fluid which reduces the fluid speed and magnifies the temperature field. Reliability of the numerical outcomes is judged by comparing the obtained outcomes with the already available literature.

3.1 Mathematical Formulation

The stress-deformation relation of Reiner–Philippoff fluid [8] is:

$$\frac{\partial u}{\partial y} = \frac{\tau_{ij}}{\mu_\infty + \frac{\mu_0 - \mu_\infty}{1 + \left(\frac{\tau}{\tau_s}\right)^2}}. \quad (3.1)$$

The distinguished symbols such as τ , τ_s , μ_0 and μ_∞ indicate the shear stress, reference shear stress, zero shear viscosity and limiting viscosity. Reiner–Philippoff fluid belongs to a class of non-Newtonian fluids which exhibits all three, dilatant, Newtonian and pseudo-plastic type behaviours. The depicted flow function [9] is defined as

$$f(\zeta) = \frac{\zeta}{\lambda - 1 + \frac{1}{1 + \zeta^2}}, \quad (3.2)$$

where $\zeta = \frac{\tau}{\tau_s}$ and $\lambda = \frac{\mu_0}{\mu_\infty}$. The behaviour of the fluid varies with change in λ . Fluid behaves like Newtonian in case of $\lambda = 1$, dilatant for $\lambda < 1$ and pseudo-plastic for $\lambda > 1$. Figure 3.1 reflects the geometrical behaviour of two dimensional non-

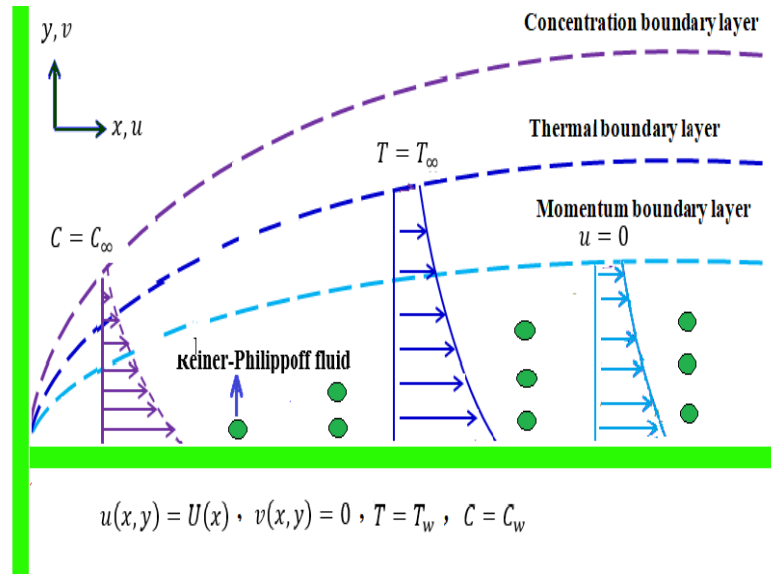


FIGURE 3.1: Flow model

Newtonian Reiner-Philippoff fluid moving over a stretched sheet with stretching velocity $u_w = U_0 x^{1/3}$ acting along x -axis. At the surface of the sheet, the terms

T_w and C_w indicates temperature as well as concentration whereas T_∞ and C_∞ depicts free stream temperature as well as concentration. The effects like thermal radiation, thermal conductivity and heat source have been taken to study the heat transfer phenomena in energy equation while the variable molecular diffusivity is assumed to affect the mass transfer phenomenon. For the Reiner-Philippoff fluid the relation between stress τ_{ij} as well as strain-rate e_{ij} is given by [1]

$$\tau_{ij} = \left[\mu_0 + \frac{\mu_\infty - \mu_0}{\frac{1}{2\tau_0^2} \left(\sum_{p=1}^3 \sum_{q=1}^3 \tau_{pq} \tau_{qp} \right)} \right] e_{ij}. \quad (3.3)$$

This model has the ability to transform Newtonian models of the viscosity having coefficients μ_0 and μ_∞ as well as the shear rate τ_0 approaches to zero or infinity. The fluid flow phenomenon of these types of fluid models are quite interesting in terms of it applications. It is quite interesting that an increment or decrement in τ_0 changes the fluid properties to the Newtonian, while for the intermediate values in the case of τ_0 , the behaviour is markedly non-Newtonian. The mathematical expression of Navier Stoke's equation is given by

$$\rho \left(\frac{\partial u}{\partial t} + u \frac{\partial u}{\partial x} + v \frac{\partial u}{\partial y} \right) + \frac{\partial p}{\partial x} = \frac{\partial \tau_{xx}}{\partial x} + \frac{\partial \tau_{xy}}{\partial y}, \quad (3.4)$$

$$\rho \left(\frac{\partial v}{\partial t} + u \frac{\partial v}{\partial x} + v \frac{\partial v}{\partial y} \right) + \frac{\partial p}{\partial y} = \frac{\partial \tau_{xy}}{\partial x} + \frac{\partial \tau_{yy}}{\partial y}, \quad (3.5)$$

$$\frac{\partial u}{\partial x} + \frac{\partial v}{\partial y} = 0. \quad (3.6)$$

It is not easy to obtain the explicit values for the case of stress components relating to the velocity components by considering the assumption given below

1. In the case of smaller value of τ_0 , the shear rate having order fourth or greater is negligible, the mathematical of stress behaviour is given below

$$\tau_{xx} = \tau_{xx}^0 + \tau_0^2 \tau'_{xx}, \quad (3.7)$$

where τ_{xx}^0 indicates the stress element in terms of Newtonian fluid having viscosity coefficient μ_0 and moreover τ'_{xx} represents remaining contribution

in the case of Reiner-Philippoff fluid in terms of stress component. The mathematical expression of τ_{ij}^0 is premeditated by

$$\tau_{xx}^0 = \mu_0 \left(2 \frac{\partial u}{\partial x} \right), \quad \tau_{yy}^0 = \mu_0 \left(2 \frac{\partial v}{\partial y} \right), \quad \tau_{xy}^0 = \mu_0 \left(\frac{\partial u}{\partial y} + \frac{\partial v}{\partial x} \right), \quad (3.8)$$

subsisting from Eq. (3.7) and Eq. (3.8) in Eq. (3.3), we get

$$\tau_{ij} = \left[\mu_0 + \frac{\mu_\infty - \mu_0}{\frac{1}{2\tau_0^2}(\tau_{xx}^{02} + 2\tau_{xy}^{02} + \tau_{yy}^{02} + \dots)} \right] e_{ij}. \quad (3.9)$$

Ignoring higher powers of τ_0 , the expression of stress component is given by

$$\tau_{ij} = \left[\mu_0 + \frac{2(\mu_\infty - \mu_0)}{\tau_{xx}^{02} + 2\tau_{xy}^{02} + \tau_{yy}^{02}} \right] e_{ij}. \quad (3.10)$$

2. when τ_0 is large such that fourth and higher powers of $\frac{1}{\tau_0}$ can be neglected, the stress components are given by

$$\tau_{xx} = \tau_{xx}^\infty + \frac{\tau_{xx}''}{\tau_0^2}, \quad (3.11)$$

where τ_{xx}^∞ is the stress component for the Newtonian fluid of viscosity coefficient μ_∞ and τ_{xx}'' is the remaining contribution of the Reiner-Philippoff fluid to the stress components.

The mathematical expressions of τ_{ij}^0 are premeditated by

$$\tau_{xx}^0 = \mu_\infty \left(2 \frac{\partial u}{\partial x} \right), \quad \tau_{yy}^\infty = \mu_\infty \left(2 \frac{\partial v}{\partial y} \right), \quad \tau_{xy}^\infty = \mu_\infty \left(\frac{\partial u}{\partial y} + \frac{\partial v}{\partial x} \right), \quad (3.12)$$

substituting from Eq. (3.10) in Eq. (3.3) we get

$$\tau_{ij} = \left[\mu_\infty + \frac{(\mu_0 - \mu_\infty)(\tau_{xx}^\infty + 2\tau_{xy}^\infty + \tau_{yy}^\infty)}{2\tau_0^2} \right] e_{ij}, \quad (3.13)$$

In Eq. (3.7) and Eq. (3.11), the expressions mentioned in square brackets can be expressed as λ_0 as well as λ_∞ . The symbols λ_0 and λ_∞ expresses the zero fluid shear rate and infinite fluid shear rate. The term e_{ij} represents the rate at which the fluid deforms. Substituting the values of stress component

from Eq. (3.7) and Eq. (3.11) in Eq. (3.4) and Eq. (3.5), we get

$$\rho \left(\frac{\partial u}{\partial t} + u \frac{\partial u}{\partial x} + v \frac{\partial u}{\partial y} \right) = -\frac{\partial p}{\partial x} + \frac{\partial}{\partial x} \left[2\lambda \frac{\partial u}{\partial x} \right] + \frac{\partial}{\partial y} \left[\lambda \left(\frac{\partial u}{\partial y} + \frac{\partial v}{\partial x} \right) \right]. \quad (3.14)$$

$$\rho \left(\frac{\partial v}{\partial t} + u \frac{\partial v}{\partial x} + v \frac{\partial v}{\partial y} \right) = -\frac{\partial p}{\partial y} + \frac{\partial}{\partial x} \left[\lambda \left(\frac{\partial u}{\partial y} + \frac{\partial v}{\partial x} \right) \right] + \frac{\partial}{\partial y} \left[\lambda \cdot 2 \frac{\partial v}{\partial y} \right]. \quad (3.15)$$

The order of t , x and u are unity and y having order δ . In eq. (3.14), the symbols v and λ are represented by orders δ and δ^2 . It is not a difficult task to evaluate the orders of various expressions included in Eq. (3.14) and Eq. (3.15). Under the application of boundary layer assumptions, the steady state incompressible fluid in the light of Eq. (3.14) and Eq. (3.15) are

$$\rho \left(\frac{\partial u}{\partial t} + u \frac{\partial u}{\partial x} + v \frac{\partial u}{\partial y} \right) = -\frac{\partial p}{\partial x} + \left[\frac{\partial}{\partial y} \lambda \frac{\partial u}{\partial y} \right], \quad (3.16)$$

Pressure gradient is constant along the vertical direction y -axis

$$0 = -\frac{\partial p}{\partial y}. \quad (3.17)$$

The PDEs after the utilization of boundary layer theory approximations are given by

$$\frac{\partial u}{\partial t} + u \frac{\partial u}{\partial x} + v \frac{\partial u}{\partial y} = \frac{\partial U}{\partial t} + U \frac{\partial U}{\partial x} + \frac{1}{\rho} \left[\frac{\partial}{\partial y} \lambda \frac{\partial u}{\partial y} \right], \quad (3.18)$$

$$\frac{\partial u}{\partial x} + \frac{\partial v}{\partial y} = 0. \quad (3.19)$$

$$\rho \left(\frac{\partial u}{\partial t} + u \frac{\partial u}{\partial x} + v \frac{\partial u}{\partial y} \right) = \frac{1}{\rho} \left[\frac{\partial}{\partial y} \lambda \frac{\partial u}{\partial y} \right], \quad (3.20)$$

whereas

$$\frac{\partial u}{\partial y} = \frac{\tau_{ij}}{\mu_{\infty} + \frac{(\mu_0 - \mu_{\infty})}{1 + \left(\frac{\tau_{ij}}{\tau_s} \right)^2}}. \quad (3.21)$$

The governing equations [8], are enumerated underneath:

$$\frac{\partial u}{\partial x} + \frac{\partial v}{\partial y} = 0, \quad (3.22)$$

$$u \frac{\partial u}{\partial x} + v \frac{\partial u}{\partial y} = \frac{1}{\rho_f} \frac{\partial \tau}{\partial y}, \quad (3.23)$$

$$\frac{1}{\rho C_p} \left(u \frac{\partial T}{\partial x} + v \frac{\partial T}{\partial y} \right) = \frac{\partial}{\partial y} \left(\kappa(T) \frac{\partial T}{\partial y} \right) + \frac{\kappa_\infty U_w(x)}{xv} \left[A^*(T_0 - T_\infty) e^{-\eta} + B^*(T - T_\infty) \right] - \frac{\partial q_r}{\partial y}, \quad (3.24)$$

$$u \frac{\partial C}{\partial x} + v \frac{\partial C}{\partial y} = \frac{\partial}{\partial y} \left(D_B(C) \frac{\partial C}{\partial y} \right). \quad (3.25)$$

The boundary conditions associated with the above Reiner-Philippoff model are premeditated by

$$\left. \begin{aligned} y = 0 : u(x, y) = U(x), v = 0, T = T_w, C = C_w, \\ y \rightarrow \infty : u \rightarrow 0, T \rightarrow T_\infty, C \rightarrow C_\infty. \end{aligned} \right\} \quad (3.26)$$

The variable thermal conductivity and variable molecular diffusivity [7] are given by

$$\kappa(T) = \kappa_\infty \left(1 + \epsilon_1 \left(\frac{T - T_\infty}{T_w - T_\infty} \right) \right), \quad (3.27)$$

$$D_B(C) = D_{B_\infty} \left(1 + \epsilon_2 \left(\frac{C - C_\infty}{C_w - C_\infty} \right) \right). \quad (3.28)$$

The last expression mentioned in the governing modeled energy equation (3.52) is termed as thermal radiation heat flux based on the Rosseland approximation. Rosseland approximation relies on the hypotheses that the participating medium (fluid) is an optically thick in which the radiation cover a smaller distance before it encounter with scattering or absorption phenomenon. The penetration length of radiation is small compare to the characteristic length and moreover photon mean free length is very small. The Rosseland Radiative heat flux [94] applies to optically thick boundary layer flow mentioned in (3.52) is premeditated by

$$q_r = -\frac{4\sigma^*}{3\kappa^*} \frac{\partial T^4}{\partial y} = -\frac{16\sigma^*}{3\kappa^*} T^3 \frac{\partial T}{\partial y}. \quad (3.29)$$

The symbols σ^* signifies the constant worth of Stefan-Boltzmann and κ^* symbols the rate. The mathematical expressions for stream functions $u = \frac{\partial \psi}{\partial y}$ and $v = -\frac{\partial \psi}{\partial x}$.

A similarity transformation [6] under the effect of the stretching velocity $u_w = U(x) = U_0 x^{1/3}$ is given below:

$$\left. \begin{aligned} \psi &= \sqrt{U(x)x\nu}f(\eta), \quad \eta = \sqrt{\frac{U(x)}{\nu x}}y, \quad \tau = \rho\sqrt{U_0^3\nu}g(\eta), \\ \phi(\eta) &= \frac{C - C_\infty}{C_w - C_\infty}, \quad \theta(\eta) = \frac{T - T_\infty}{T_w - T_\infty}. \end{aligned} \right\} \quad (3.30)$$

The detailed procedure for the conversion of Eqs. (3.50)-(3.53) are given below.

$$\begin{aligned} \bullet \quad \psi &= \sqrt{U(x)x\nu}f \\ &= \sqrt{U_0\nu}x^{2/3}f \\ u &= \frac{\partial\psi}{\partial y} \\ &= \sqrt{U_0\nu}x^{2/3}\frac{\partial f}{\partial\eta}\frac{\partial\eta}{\partial y} \\ &= U_0x^{1/3}f'. \end{aligned} \quad (3.31)$$

$$\begin{aligned} \bullet \quad v &= -\frac{\partial\psi}{\partial x} \\ &= -\frac{\partial}{\partial x}\sqrt{U(x)\nu}x^{2/3}f \\ &= -\left(\frac{2}{3}\sqrt{\frac{U_0}{\nu}}x^{-1/3}f + \sqrt{\frac{U_0}{\nu}}x^{2/3}f'\left(-\frac{1}{3}\sqrt{\frac{U_0}{\nu}}x^{-4/3}y\right)\right) \\ &= -\left(\frac{2}{3}\sqrt{\frac{U_0}{\nu}}x^{-1/3}f - \frac{1}{3}\sqrt{\frac{U_0}{\nu}}x^{2/3}f'x^{-1}\left(\sqrt{\frac{U_0}{\nu}}x^{-1/3}y\right)\right) \\ &= -\frac{2}{3}\sqrt{\frac{U_0}{\nu}}x^{-1/3}f + \frac{1}{3}\eta\sqrt{\frac{U_0}{\nu}}x^{-1/3}f'. \end{aligned} \quad (3.32)$$

$$\begin{aligned} \bullet \quad \frac{\partial u}{\partial x} &= \frac{\partial}{\partial x}(U_0x^{1/3}f') \\ &= \frac{1}{3}U_0x^{-2/3}f' + U_0x^{1/3}f''\left(\frac{-1}{3}x^{-4/3}y\right) \\ &= \frac{1}{3}U_0x^{-2/3}(f' - \eta f'') \end{aligned} \quad (3.33)$$

$$\begin{aligned} \bullet \quad \frac{\partial u}{\partial y} &= U_0x^{1/3}\frac{\partial f'}{\partial\eta}\frac{\partial\eta}{\partial y} \\ &= U_0x^{1/3}f''\sqrt{\frac{U_0}{\nu}}x^{-1/3} \\ &= U_0\sqrt{\frac{U_0}{\nu}}f''. \end{aligned} \quad (3.34)$$

$$\begin{aligned}
\bullet \quad \frac{\partial v}{\partial y} &= \frac{\partial}{\partial y} \left(-\frac{2}{3} \sqrt{U_0 \nu} x^{-1/3} f + \frac{1}{3} \eta \sqrt{U_0 \nu} x^{-1/3} f' \right) \\
&= -\frac{1}{3} U_0 x^{-2/3} f' + \frac{1}{3} \eta U_0 x^{-2/3} f'' \\
&= \frac{1}{3} U_0 x^{-2/3} (-f' + \eta f'') \\
&= \frac{1}{3} U_0 x^{-2/3} (-f' + \eta f''). \tag{3.35}
\end{aligned}$$

$$\begin{aligned}
\bullet \quad u \frac{\partial u}{\partial x} &= U_0 x^{1/3} f'(\eta) \left(\frac{1}{3} U_0 x^{-2/3} f' - \frac{1}{3} \eta U_0 x^{-2/3} f'' \right) \\
&= \frac{1}{3} U_0^2 x^{-1/3} f'^2 - \frac{1}{3} \eta U_0^2 x^{-1/3} f' f''. \tag{3.36}
\end{aligned}$$

$$\begin{aligned}
\bullet \quad v \frac{\partial u}{\partial y} &= \left(-\frac{2}{3} \sqrt{U_0 \nu} x^{-1/3} f + \frac{1}{3} \eta \sqrt{U_0 \nu} x^{-1/3} f' \right) \cdot \sqrt{\frac{U_0}{\nu}} U_0 f'' \\
&= -\frac{2}{3} U_0^2 x^{-1/3} f f'' + \frac{1}{3} \eta U_0^2 x^{-1/3} f' f''. \tag{3.37}
\end{aligned}$$

$$\begin{aligned}
\bullet \quad \tau &= \rho \sqrt{U_0^3 \nu} g \\
\frac{\partial \tau}{\partial y} &= \sqrt{\frac{U_0}{\nu}} x^{-1/3} \rho \sqrt{U_0^3 \nu} g' \\
&= \rho U_0^2 x^{-1/3} g'. \tag{3.38}
\end{aligned}$$

$$\begin{aligned}
\bullet \quad \frac{\partial T}{\partial x} &= (T_w - T_\infty) \frac{\partial \theta}{\partial \eta} \cdot \frac{\partial \eta}{\partial x} \\
&= (T_w - T_\infty) \theta' \left(-\frac{1}{3} \sqrt{\frac{U_0}{\nu}} x^{-4/3} y \right). \tag{3.39}
\end{aligned}$$

$$\begin{aligned}
\bullet \quad u \frac{\partial T}{\partial x} &= U_0 x^{1/3} f' \cdot \left(-\frac{1}{3} x^{-1} \left(\sqrt{\frac{U_0}{\nu}} x^{-4/3} y \right) (T_w - T_\infty) \theta' \right) \\
&= -\frac{1}{3} \eta U_0 x^{-2/3} (T_w - T_\infty) f' \theta'. \tag{3.40}
\end{aligned}$$

$$\begin{aligned}
\bullet \quad \frac{\partial T}{\partial y} &= \frac{\partial}{\partial y} ((T_w - T_\infty) \theta + T_\infty) \\
&= \frac{\partial \theta}{\partial \eta} \frac{\partial \eta}{\partial y} \\
&= (T_w - T_\infty) \sqrt{\frac{U_0}{\nu}} x^{-1/3} \theta'. \tag{3.41}
\end{aligned}$$

$$\begin{aligned}
\bullet \quad v \frac{\partial T}{\partial y} &= \left(-\frac{2}{3} \sqrt{U_0 \nu} x^{-1/3} f + \frac{1}{3} \eta \sqrt{U_0 \nu} x^{-1/3} f' \right) \cdot (T_w - T_\infty) \sqrt{\frac{U_0}{\nu}} x^{-1/3} \theta'(\eta) \\
&= U_0 x^{-2/3} (T_w - T_\infty) \left(-\frac{2}{3} f \theta' + \frac{1}{3} \eta f' \theta' \right). \tag{3.42}
\end{aligned}$$

$$\begin{aligned}
\bullet \quad \kappa(T) &= \kappa_\infty \left(1 + \epsilon_1 \left(\frac{T - T_\infty}{T_w - T_\infty} \right) \right) \\
&= \kappa_\infty (1 + \epsilon_1 \theta).
\end{aligned} \tag{3.43}$$

$$\begin{aligned}
\bullet \quad \frac{\partial \kappa(T)}{\partial y} &= \frac{\epsilon_1 \kappa_\infty}{(T_w - T_\infty)} \cdot \frac{\partial \theta}{\partial \eta} \frac{\partial \eta}{\partial y} \\
&= \frac{\epsilon_1 \kappa_\infty}{(T_w - T_\infty)} \cdot (T_w - T_\infty) \sqrt{\frac{U_0}{\nu}} x^{-1/3} \theta' \\
&= \kappa_\infty \epsilon_1 \sqrt{\frac{U_0}{\nu}} x^{-1/3} \theta'.
\end{aligned} \tag{3.44}$$

$$\begin{aligned}
\bullet \quad \frac{\partial T}{\partial y} \cdot \frac{\partial \kappa(T)}{\partial y} &= \kappa_\infty \epsilon_1 \sqrt{\frac{U_0}{\nu}} x^{-1/3} \theta' \cdot (T_w - T_\infty) \sqrt{\frac{U_0}{\nu}} x^{-1/3} \theta' \\
&= (T_w - T_\infty) \kappa_\infty \epsilon_1 \left(\frac{U_0}{\nu} \right) x^{-2/3} \theta'^2.
\end{aligned} \tag{3.45}$$

$$\begin{aligned}
\bullet \quad \frac{\partial^2 T}{\partial y^2} &= \frac{\partial}{\partial y} \left(\frac{\partial T}{\partial y} \right) \\
&= \frac{\partial}{\partial y} \left((T_w - T_\infty) \sqrt{\frac{U_0}{\nu}} x^{-1/3} \theta' \right) \\
&= (T_w - T_\infty) \sqrt{\frac{U_0}{\nu}} x^{-1/3} \cdot \frac{\partial \theta'}{\partial \eta} \cdot \frac{\partial \eta}{\partial y} \\
&= \sqrt{\frac{U_0}{\nu}} x^{-\frac{1}{3}} \cdot \sqrt{\frac{U_0}{\nu}} x^{-1/3} (T_w - T_\infty) \theta'' \\
&= \left(\frac{U_0}{\nu} \right) x^{-2/3} (T_w - T_\infty) \theta''.
\end{aligned} \tag{3.46}$$

$$\bullet \quad \kappa(T) \frac{\partial^2 T}{\partial y^2} = \kappa_\infty \sqrt{\frac{U_0}{\nu}} x^{-2/3} (T_w - T_\infty) (1 + \epsilon_1 \theta) \theta''. \tag{3.47}$$

$$\begin{aligned}
\bullet \quad \frac{1}{\rho C_p} \frac{\partial}{\partial y} \left(\kappa(T) \frac{\partial T}{\partial y} \right) &= \frac{1}{\rho C_p} \left(\frac{\partial \kappa(T)}{\partial y} \frac{\partial T}{\partial y} + \kappa(T) \frac{\partial^2 T}{\partial y^2} \right) \\
&= \frac{\kappa_\infty U_0}{\rho C_p \nu} x^{-2/3} (T_w - T_\infty) (\epsilon_1 \theta'^2 + (1 + \epsilon_1 \theta) \theta'') \\
&= \frac{(T_w - T_\infty) U_0 x^{-2/3} (\epsilon_1 \theta'^2 + (1 + \epsilon_1 \theta) \theta'')}{\left(\frac{\mu C_p}{\kappa_\infty} \right)}.
\end{aligned} \tag{3.48}$$

$$\begin{aligned}
\bullet \quad T^3 \frac{\partial^2 T}{\partial y^2} &= ((T_w - T_\infty) \theta + T_\infty)^3 \cdot \left(\frac{U_0}{\nu} \right) x^{-2/3} (T_w - T_\infty) \theta'' \\
&= T_\infty^3 \left(1 + \frac{(T_w - T_\infty)}{T_\infty} \theta \right)^3 \cdot \left(\frac{U_0}{\nu} \right) x^{-2/3} (T_w - T_\infty) \theta'' \\
&= T_\infty^3 (1 + (\theta_w - 1) \theta)^3 \left(\frac{U_0}{\nu} \right) x^{-2/3} (T_w - T_\infty) \theta''.
\end{aligned} \tag{3.49}$$

$$\begin{aligned}
\bullet \quad T^2 \left(\frac{\partial T}{\partial y} \right)^2 &= ((T_w - T_\infty)\theta + T_\infty)^2 \cdot \left((T_w - T_\infty) \sqrt{\frac{U_0}{\nu}} x^{-1/3} \theta' \right)^2 \\
&= ((T_w - T_\infty)\theta + T_\infty)^2 \cdot \left((T_w - T_\infty)^2 \left(\frac{U_0}{\nu} \right) x^{-2/3} \theta'^2 \right) \\
&= T_\infty^3 \left(1 + \frac{(T_w - T_\infty)}{T_\infty} \theta \right)^2 \left((T_w - T_\infty) \left(\frac{T_w}{T_\infty} - 1 \right) \left(\frac{U_0}{\nu} \right) x^{-2/3} \theta'^2 \right) \\
&= T_\infty^3 (1 + (\theta_w - 1)\theta)^2 \left((T_w - T_\infty)(\theta_w - 1) \left(\frac{U_0}{\nu} \right) x^{-2/3} \theta'^2 \right). \quad (3.50)
\end{aligned}$$

$$\begin{aligned}
\bullet \quad q_r &= -\frac{16\sigma^*}{3\kappa^*} T^3 \frac{\partial T}{\partial y} \\
\frac{1}{\rho C_p} \frac{\partial q_r}{\partial y} &= -\frac{16\sigma^*}{3\kappa^*} \frac{1}{\rho C_p} \left(\left(T^3 \frac{\partial^2 T}{\partial y^2} \right) + 3T^2 \left(\frac{\partial T}{\partial y} \right)^2 \right) \\
&= -\frac{16\sigma^* T_\infty^3}{3\kappa^*} \frac{1}{\rho C_p} \left(\frac{U_0}{\nu} \right) x^{-2/3} \left((1 + (\theta_w - 1)\theta)^3 (T_w - T_\infty) \theta'' \right. \\
&\quad \left. + 3(1 + (\theta_w - 1)\theta)^2 (\theta_w - 1) (T_w - T_\infty) \theta'^2 \right). \quad (3.51)
\end{aligned}$$

$$\begin{aligned}
\bullet \quad \frac{\kappa_\infty U_w(x)}{x\nu\rho C_p} (A^*(T_w - T_\infty)e^{-\eta} + B^*(T - T_\infty)) \\
&= \frac{\kappa_\infty U_0 x^{1/3} (T_w - T_\infty)}{x\nu\rho C_p} (A^*e^{-\eta} + B^*\theta) \\
&= \frac{U_0 x^{-2/3} (T_w - T_\infty)}{\left(\frac{\mu C_p}{\kappa_\infty} \right)} (A^*e^{-\eta} + B^*\theta). \quad (3.52)
\end{aligned}$$

$$\begin{aligned}
\bullet \quad \frac{\partial C}{\partial x} &= \frac{\partial}{\partial x} ((C_w - C_\infty) + C_\infty) \\
&= (C_w - C_\infty) \frac{\partial \phi}{\partial \eta} \left(-\frac{1}{3} \sqrt{\frac{U_0}{\nu}} x^{-4/3} y \right) \\
&= (C_w - C_\infty) \phi' \left(-\frac{1}{3} x^{-1} \left(\sqrt{\frac{U_0}{\nu}} x^{-1/3} y \right) \right) \\
&= (C_w - C_\infty) \phi' \left(-\frac{1}{3} \eta x^{-1} \right) \\
&= -\frac{1}{3} \eta x^{-1} (C_w - C_\infty) \phi'. \quad (3.53)
\end{aligned}$$

$$\begin{aligned}
\bullet \quad u \frac{\partial C}{\partial x} &= U_0 x^{1/3} f'(\eta) \cdot \left(-\frac{1}{3} \eta x^{-1} (C_w - C_\infty) \phi' \right) \\
&= (C_w - C_\infty) \left(-\frac{1}{3} \eta U_0 x^{-2/3} \right) f' \phi' \\
&= -\frac{1}{3} \eta U_0 x^{-2/3} (C_w - C_\infty) f' \phi'. \quad (3.54)
\end{aligned}$$

$$\begin{aligned}
\bullet \frac{\partial C}{\partial y} &= \frac{\partial C}{\partial \eta} \frac{\partial \eta}{\partial y} \\
&= (C_w - C_\infty) \phi' \cdot \sqrt{\frac{U_0}{\nu}} x^{-1/3}.
\end{aligned} \tag{3.55}$$

$$\begin{aligned}
\bullet v \frac{\partial C}{\partial y} &= U_0 (C_w - C_\infty) x^{-\frac{1}{3}} \left(-\frac{2}{3} x^{-1/3} f + \frac{1}{3} \eta x^{-1/3} f' \right) \phi' \\
&= (C_w - C_\infty) U_0 x^{-2/3} \left(-\frac{2}{3} f \phi' + \frac{1}{3} \eta f' \phi' \right).
\end{aligned} \tag{3.56}$$

$$\bullet D_B(C) = D_{B\infty} \left(1 + \epsilon_2 \left(\frac{C - C_\infty}{C_w - C_\infty} \right) \right). \tag{3.57}$$

$$\begin{aligned}
\bullet \frac{\partial D_B(C)}{\partial y} &= D_{B\infty} \epsilon_2 \left(\frac{1}{C_w - C_\infty} \right) \frac{\partial C}{\partial y} \\
&= \frac{D_{B\infty} \epsilon_2}{(C_w - C_\infty)} (C_w - C_\infty) \sqrt{\frac{U_0}{\nu}} x^{-1/3} \phi'(\eta) \\
&= D_{B\infty} \epsilon_2 \sqrt{\frac{U_0}{\nu}} x^{-1/3} \phi'(\eta).
\end{aligned} \tag{3.58}$$

$$\bullet \frac{\partial D_B(C)}{\partial y} \cdot \frac{\partial C}{\partial y} = D_{B\infty} \epsilon_2 (C_w - C_\infty) \left(\frac{U_0}{\nu} \right) x^{-2/3} \phi'^2(\eta). \tag{3.59}$$

$$\begin{aligned}
\bullet \frac{\partial^2 C}{\partial y^2} &= (C_w - C_\infty) \sqrt{\frac{U_0}{\nu}} x^{-1/3} \frac{\partial \phi'}{\partial \eta} \cdot \frac{\partial \eta}{\partial y} \\
&= (C_w - C_\infty) \left(\frac{U_0}{\nu} \right) x^{-2/3} \phi''.
\end{aligned} \tag{3.60}$$

$$\begin{aligned}
\bullet D_B(C) \frac{\partial^2 C}{\partial y^2} &= D_{B\infty} \left(1 + \epsilon_2 \left(\frac{C - C_\infty}{C_w - C_\infty} \right) \right) \cdot (C_w - C_\infty) \left(\frac{U_0}{\nu} \right) x^{-2/3} \phi'' \\
&= D_{B\infty} (C_w - C_\infty) \left(\frac{U_0}{\nu} \right) x^{-2/3} (1 + \epsilon_2) \phi''.
\end{aligned} \tag{3.61}$$

$$\begin{aligned}
\bullet \frac{\partial}{\partial y} \left(D_B(C) \frac{\partial C}{\partial y} \right) &= \left(\frac{\partial D_B(C)}{\partial y} \frac{\partial C}{\partial y} + D_B(C) \frac{\partial^2 C}{\partial y^2} \right) \\
&= D_{B\infty} (C_w - C_\infty) \left(\frac{U_0}{\nu} \right) x^{-\frac{2}{3}} (\epsilon_2 \phi'^2(\eta) + (1 + \epsilon_2) \phi'').
\end{aligned} \tag{3.62}$$

The dimensionless form of stress deformation equation mentioned in (3.1) is given by

$$\bullet \frac{\partial u}{\partial y} = \frac{\tau}{\mu_\infty + \frac{\mu_0 - \mu_\infty}{1 + \left(\frac{\tau}{\tau_s} \right)^2}}$$

$$\begin{aligned}
&= \frac{\tau}{\mu_\infty + \frac{\tau_s^2(\mu_0 - \mu_\infty)}{\tau^2 + \tau_s^2}} \\
&= \frac{\tau(\tau^2 + \tau_s^2)}{\mu_\infty\tau_s^2 + \mu_\infty\tau^2 + \mu_0\tau_s^2 - \mu_\infty\tau_s^2} \\
&= \frac{\mu_\infty\tau^2 + \mu_0\tau_s^2}{\tau(\tau^2 + \tau_s^2)}. \\
\Rightarrow \frac{U_0^{3/2}}{\sqrt{\nu}} f'' &= \frac{\rho\sqrt{U_0^3\nu}g(\tau_s^2 + (\rho\sqrt{U_0^3\nu}g)^2)}{\mu_\infty(\rho\sqrt{U_0^3\nu}g)^2 + \mu_0\tau_s^2} \\
&= \frac{\rho\sqrt{U_0^3\nu}g \cdot \rho^2 U_0^3 \nu \left(\frac{\tau_s^2}{\rho^2 U_0^3 \nu} + g^2 \right)}{\mu_\infty \rho^2 U_0^3 \nu \left(\frac{\mu_0}{\mu_\infty} \frac{\tau_s^2}{\rho^2 U_0^3 \nu} + g^2 \right)} \\
&= \frac{\rho\sqrt{U_0^3\nu}g}{\mu_\infty} \frac{g^2 + \gamma^2}{g^2 + \lambda\gamma^2}. \\
\Rightarrow \frac{U_0^{3/2}}{\rho\sqrt{\nu}} \cdot \frac{\mu_\infty}{U_0^{3/2}\sqrt{\nu}} f'' &= g \frac{g^2 + \gamma^2}{g^2 + \lambda\gamma^2} \\
\Rightarrow g &= f'' \frac{g^2 + \lambda\gamma^2}{g^2 + \gamma^2}. \tag{3.63}
\end{aligned}$$

Using (3.33) and (3.34) in the continuity equation (3.22), we get

$$\frac{\partial u}{\partial x} + \frac{\partial v}{\partial y} = \frac{1}{3}U_0x^{-2/3}(f'(\eta) - \eta f''(\eta) - f'(\eta) + \eta f''(\eta)) = 0. \tag{3.64}$$

Using (3.36)-(3.38) in (3.23), the dimensionless momentum equation is

$$\begin{aligned}
\rho_f \left(\frac{1}{\rho_f} U_0^2 x^{-1/3} g' \right) &= \frac{1}{3} U_0^2 x^{-1/3} f'^2 - \frac{2}{3} U_0^2 x^{-1/3} f f'' \\
U_0^2 x^{-1/3} g' &= \frac{1}{3} U_0^2 x^{-1/3} f'^2 - \frac{2}{3} U_0^2 x^{-1/3} f f'' \\
g' &= \frac{1}{3} f'^2 - \frac{2}{3} f f''. \tag{3.65}
\end{aligned}$$

The dimensionless temperature equation (3.24) after using (3.39)-(3.52) is

$$\begin{aligned}
& - \frac{2}{3} U_0 x^{-2/3} (T_w - T_\infty) f \theta' \\
&= (T_w - T_\infty) U_0 x^{-2/3} \left(\frac{(\epsilon_1 \theta'^2 + (1 + \epsilon_1 \theta) \theta'')}{\frac{\mu C_p}{\kappa_\infty}} \right. \\
&\quad + \frac{16\sigma^* T_{\infty 3}}{3\kappa^* (\rho C_p) (\mu C_p)} \left((1 + (\theta_w - 1)\theta)^3 \theta'' \right. \\
&\quad \left. \left. + 3(1 + (\theta_w - 1)\theta)^2 (\theta_w - 1)\theta'^2 \right) + \frac{(A^* e^{-\eta} + B^* \theta)}{\frac{\mu C_p}{\kappa_\infty}} \right).
\end{aligned}$$

$$\begin{aligned}
&\Rightarrow (\epsilon_1 \theta'^2 + (1 + \epsilon_1 \theta) \theta'') + \frac{16\sigma^* T_\infty^3}{3\kappa^* \kappa_\infty} \left((1 + (\theta_w - 1)\theta)^3 \theta'' \right. \\
&\quad \left. + 3(1 + (\theta_w - 1)\theta)^2 (\theta_w - 1)\theta'^2 \right) + (A^* e^{-\eta} + B^* \theta) \\
&\quad + \frac{2}{3} \left(\frac{\mu C_p}{\kappa_\infty} \right) f \theta' = 0 \\
&\Rightarrow (\epsilon_1 \theta'^2 + (1 + \epsilon_1 \theta) \theta'') + \frac{2}{3} Pr f \theta' + \frac{4}{3} Rd \left((1 + (\theta_w - 1)\theta)^3 \theta'' \right. \\
&\quad \left. + 3(1 + (\theta_w - 1)\theta)^2 (\theta_w - 1)\theta'^2 \right) + (A^* e^{-\eta} + B^* \theta) = 0 \\
&\Rightarrow \left((1 + \epsilon_1 \theta) + \frac{4}{3} Rd (1 + (\theta_w - 1)\theta)^3 \right) \theta'' \\
&\quad + (\epsilon_1 + 4Rd(1 + (\theta_w - 1)\theta)^2 (\theta_w - 1)) \theta'^2 \\
&\quad + \frac{2}{3} Pr f \theta' + (A^* e^{-\eta} + B^* \theta) = 0, \tag{3.66}
\end{aligned}$$

where ϵ_1 and ϵ_2 are parameters depending on nature of the fluid, Rd denotes thermal radiation, A^* and B^* are space and temperature dependent heat source and sink

Using (3.53)-(3.62) in the concentration equation (3.25) gives

$$\begin{aligned}
&-\frac{2}{3} U_0 (C_w - C_\infty) x^{-2/3} f \phi' = D_{B\infty} (C_w - C_\infty) \left(\frac{U_0}{\nu} \right) x^{-2/3} ((1 + \epsilon_2) \phi'' + \phi'^2) \\
&\Rightarrow -\frac{2}{3} f \phi' = \frac{D_{B\infty}}{\nu} (((1 + \epsilon_2) \phi) \phi'' + \epsilon_2 \phi'^2) \\
&\Rightarrow -\frac{2}{3} f \phi' = \frac{1}{\nu} (((1 + \epsilon_2) \phi) \phi'' + \epsilon_2 \phi'^2) \\
&\quad \frac{D_{B\infty}}{Sc} \\
&\Rightarrow -\frac{2}{3} f \phi' = \frac{1}{Sc} (((1 + \epsilon_2) \phi) \phi'' + \epsilon_2 \phi'^2) \\
&\Rightarrow (1 + \epsilon_2 \phi) \phi'' + \epsilon_2 \phi'^2 + \frac{2}{3} Sc f \phi' = 0. \tag{3.67}
\end{aligned}$$

The distinguished parameters appearing in the above equations are given by

$$\left. \begin{aligned}
\gamma &= \left(\frac{\rho_s}{\rho \sqrt{U_0^3 \nu}} \right), \quad \lambda = \frac{\mu_0}{\mu_\infty}, \quad Pr = \frac{\mu C_p}{k_\infty}, \quad Sc = \frac{\nu}{D_{B\infty}}, \quad Rd = \frac{4\sigma T_\infty^3}{k^* k_\infty}, \\
\theta_w &= \frac{T_w}{T_\infty}.
\end{aligned} \right\} \tag{3.68}$$

where γ and λ are Bingham number and Reiner-Philippoff fluid parameter.

The dimensionless boundary conditions is achieved through the procedure

$$\begin{aligned}
\bullet \quad u &= U(x) && \text{at } y = 0 \\
&\Rightarrow U(x) = U_0 x^{\frac{1}{3}} f'(\eta) && \text{at } \eta = 0 \\
&\Rightarrow U_0 x^{\frac{1}{3}} = U_0 x^{\frac{1}{3}} f'(\eta) && \text{at } \eta = 0 \\
&\Rightarrow f'(\eta) = 1 && \text{at } \eta = 0.
\end{aligned} \tag{3.69}$$

$$\begin{aligned}
\bullet \quad v &= 0 && \text{at } y = 0 \\
&\Rightarrow \frac{\sqrt{U_0 \nu} x^{-\frac{2}{3}}}{3} (-2f(\eta) + \eta f'(\eta)) = 0 && \text{at } \eta = 0 \\
&\Rightarrow \frac{-2}{3} \sqrt{U_0 \nu} x^{-\frac{2}{3}} f(\eta) + 0 = 0 && \text{at } \eta = 0 \\
&\Rightarrow \frac{-2}{3} \sqrt{U_0 \nu} x^{-\frac{2}{3}} f(\eta) = 0 && \text{at } \eta = 0 \\
&\Rightarrow f(\eta) = 0 && \text{at } \eta = 0.
\end{aligned} \tag{3.70}$$

$$\begin{aligned}
\bullet \quad T(x, y) &= T_w && \text{at } y = 0 \\
&\Rightarrow (T_w - T_\infty)\theta(\eta) + T_\infty = T_w && \text{at } \eta = 0 \\
&\Rightarrow (T_w - T_\infty)\theta(\eta) = T_w - T_\infty && \text{at } \eta = 0 \\
&\Rightarrow \theta = 1. && \text{at } \eta = 0.
\end{aligned} \tag{3.71}$$

$$\begin{aligned}
\bullet \quad C(x, y) &= C_w && \text{at } y = 0 \\
&\Rightarrow (C_w - C_\infty)\phi(\eta) + C_\infty = C_w && \text{at } \eta = 0 \\
&\Rightarrow (C_w - C_\infty)\phi(\eta) = C_w - C_\infty && \text{at } \eta = 0 \\
&\Rightarrow \phi = 1. && \text{at } \eta = 0.
\end{aligned} \tag{3.72}$$

$$\begin{aligned}
\bullet \quad U(x) &\rightarrow 0 && \text{as } y \rightarrow \infty \\
&\Rightarrow U_0 x^{\frac{1}{3}} f'(\eta) \rightarrow 0 && \text{as } \eta \rightarrow \infty \\
&\Rightarrow f' \rightarrow 0. && \text{as } \eta \rightarrow \infty
\end{aligned} \tag{3.73}$$

$$\begin{aligned}
\bullet \quad T(x, y) &\rightarrow T_\infty && \text{as } y \rightarrow \infty \\
&\Rightarrow (T_w - T_\infty)\theta(\eta) + T_\infty \rightarrow T_\infty && \text{as } \eta \rightarrow \infty \\
&\Rightarrow (T_w - T_\infty)\theta(\eta) \rightarrow T_\infty - T_\infty && \text{as } \eta \rightarrow \infty \\
&\Rightarrow \theta \rightarrow 0 && \text{as } \eta \rightarrow \infty.
\end{aligned} \tag{3.74}$$

$$\begin{aligned}
\bullet \quad & C(x, y) \rightarrow C_\infty && \text{as } y \rightarrow \infty \\
& \Rightarrow (C_w - C_\infty)\phi(\eta) + C_\infty \rightarrow C_\infty && \text{as } \eta \rightarrow \infty \\
& \Rightarrow (C_w - C_\infty)\phi(\eta) \rightarrow C_\infty - C_\infty && \text{as } \eta \rightarrow \infty \\
& \Rightarrow \phi \rightarrow 0 && \text{as } \eta \rightarrow \infty.
\end{aligned} \tag{3.75}$$

The surface drag coefficient, C_{fx} is given by

$$\begin{aligned}
C_{fx} &= \frac{\tau}{\left(\frac{\rho U_w^2}{2}\right)} \\
&= \frac{2\rho\sqrt{U_0^3\nu}g}{\rho U_0^2 x^{2/3}} \\
&= \frac{2U_0^{3/2}\sqrt{\nu}g}{U_0^2 x^{2/3}} \\
&= \frac{2\sqrt{\nu}g}{U_0^{1/2} x^{2/3}} \\
\Rightarrow \frac{C_{fx}}{2}\sqrt{Re_x} &= g.
\end{aligned} \tag{3.76}$$

The Nusselt number is formulated as

$$\begin{aligned}
Nu_x &= \frac{xq_w}{\kappa_\infty(T_w - T_\infty)}, \text{ where} \\
q_r &= -\frac{16\sigma^*}{3\kappa^*} \left(T^3 \frac{\partial T}{\partial y}\right), \\
&= -\frac{16\sigma^*}{3\kappa^*} ((T_w - T_\infty)\theta + T_\infty)^3 (T_w - T_\infty) \sqrt{\frac{U_0}{\nu}} x^{-1/3} \theta', \\
&= -\frac{16\sigma^*}{3\kappa^*} T_\infty^3 (1 + (\theta_w - 1)\theta)^3 (T_w - T_\infty) \sqrt{\frac{U_0}{\nu}} x^{-1/3} \theta',
\end{aligned} \tag{3.77}$$

$$\begin{aligned}
q_w &= -\kappa_\infty \left(\frac{\partial T}{\partial y}\right) + q_r, \\
&= (T_w - T_\infty) \sqrt{\frac{U_0}{\nu}} x^{-1/3} \left(-\kappa_\infty \theta' - \frac{16\sigma^*}{3\kappa^*} T_\infty^3 ((1 + (\theta_w - 1)\theta)^3 \theta')\right), \\
&= -\kappa_\infty (T_w - T_\infty) \sqrt{\frac{U_0}{\nu}} x^{-1/3} \left(\theta' + \frac{4}{3} Rd(1 + (\theta_w - 1)\theta)^3 \theta'\right).
\end{aligned} \tag{3.78}$$

therefore,

$$\begin{aligned}
Nu_x &= \frac{-x\kappa_\infty (T_w - T_\infty) \sqrt{\frac{U_0}{\nu}} x^{-1/3} \left(1 + \frac{4}{3} Rd(1 + (\theta_w - 1)\theta)^3\right) \theta'}{\kappa_\infty (T_w - T_\infty)}, \\
&= -\sqrt{\frac{U_0}{\nu}} x^{2/3} \left(1 + \frac{4}{3} Rd(1 + (\theta_w - 1)\theta)^3\right) \theta', \\
&= -\sqrt{Re_x} \left(1 + \frac{4}{3} Rd(1 + (\theta_w - 1)\theta)^3\right) \theta'.
\end{aligned} \tag{3.79}$$

Mass transfer rate is manifested by

$$Sh_x = \frac{xq_m}{D_B(C_w - C_\infty)}, \text{ where} \quad (3.80)$$

$$q_m = -D_B \frac{\partial C}{\partial y},$$

$$= -D_B(C_w - C_\infty) \sqrt{\frac{U_0}{\nu}} x^{-1/3} \phi'(\eta). \quad (3.82)$$

Therefore,

$$Sh_x = \frac{-xD_B(C_w - C_\infty) \sqrt{\frac{U_0}{\nu}} x^{-1/3} \phi'(\eta)}{D_B(C_w - C_\infty)},$$

$$= -\sqrt{\frac{U_0}{\nu}} x^{2/3} \phi',$$

$$= -\sqrt{Re_x} \phi'. \quad (3.83)$$

3.2 Solution Methodology

The solution of the modeled problem has been achieved numerically with the assistance of shooting scheme [120].

Some key points regarding the shooting method for the solution of problems are given below

- Reduce the higher order nonlinear ODEs to first order ODEs by using a suitable notation.
- Assign values to the missing initial conditions
- Differential equations are numerically treated with RK4 scheme.
- If the solution at the terminal point is achieved with the help of suitable values of the missing initial conditions then stop the process.
- If the solution is not obtained within the specified range of accuracy then update the initial guesses again and again with the help of Newton's method.
- Sometimes the method diverges because of bad choice of initial guesses, several occasions this technique diverges as a result of singular Jacobian matrix .

- No specific rule hinder behind the suitable choice of initial guesses to achieve the convergence criterion of the modelled problems.

In the light of above mentioned points. The detailed procedure of modeled problem with the assistance of shooting scheme. For numerical solution, the unbounded domain $[0, \infty)$ has been replaced by $[0, \eta_\infty]$ where η_∞ is a real number selected in such a manner that the obtained solution does not show any significant variations for $\eta > \eta_\infty$. It is noteworthy that $\eta_\infty = 7$ assures the expected level of convergence for all the numerical outcomes. The stress deformation and momentum equations (3.63) and (3.65) will be tackled collectively by the assistance of shooting method and then the temperature and concentration equations by using f as a known function. Denoting f by y_1 , f' by y_2 , g by y_3 and the missing initial condition by c_1 , the momentum and stress deformations equations have been converted into first order ODEs mentioned below:

$$\left. \begin{aligned} y_1' &= y_2, & y_1(0) &= 0, \\ y_2' &= \frac{y_3(y_3^2 + \gamma^2)}{(y_2^2 + \lambda\gamma^2)}, & y_2(0) &= 1, \\ y_3' &= \frac{1}{3}y_2^2 - \frac{2}{3}y_1y_2', & y_3(0) &= c_1. \end{aligned} \right\} \quad (3.84)$$

Now solve the momentum equation with the help numerical scheme called RK4 method along with choosing value of initial guess $c_1^{(0)}=0.1$. There is no hard and fast rule for the choice of initial guess $c_1^{(0)}$. If system of equations satisfy the approximate solution $y_1(\eta_\infty, c_1^{(0)}) = 1$ then stop the process. Generally it is not possible. If this condition cannot be achieved then solve the above system with help of the iterative scheme called Newton's method.

$$c_1^{(n+1)} = c_1^{(n)} - \frac{y_2(\eta_\infty, c_1^{(n)})}{\left. \frac{\partial y_2}{\partial c_1}(\eta_\infty, c_1) \right|_{c_1=c_1^{(n)}}}, \quad \text{where } n=0, 1, 2, 3, .. \quad (3.85)$$

where n in $c_1^{(n)}$ represent the iteration n . After adopting the following notations.

$$\frac{\partial y_1}{\partial c_1} = y_4, \quad \frac{\partial y_2}{\partial c_1} = y_5, \quad \frac{\partial y_3}{\partial c_1} = y_6. \quad (3.86)$$

Newton's method take the form given below

$$c_1^{(n+1)} = c_1^{(n)} - \frac{y_2(\eta_\infty, c_1^{(n)})}{y_5(\eta_\infty, c_1^{(n)})}. \quad (3.87)$$

The differential form of Eq. (84) with respect to c_1 are given underneath

$$\left. \begin{aligned} y_4' &= y_5, & y_4(0) &= 0, \\ y_5' &= \frac{(3y_3^2 y_6 + y_6 \gamma^2) - 2y_3 y_6 y_2'}{(y_3^2 + \lambda \gamma^2)}, & y_5(0) &= 0, \\ y_6' &= \frac{2}{3} y_2 y_5 - \frac{2}{3} (y_1 y_5' + y_4 y_2'), & y_6(0) &= 1. \end{aligned} \right\} \quad (3.88)$$

The Eqs. (3.88) have been handled numerically with the assistance of the RK-4 method. Furthermore the missing initial conditions are updated with the help of Newton's scheme until the criteria stated below is met.

$$|y_2(\eta_\infty) - 0| < \epsilon. \quad (3.89)$$

Here the symbol ϵ is a positive number having value $\epsilon = 10^{-6}$.

The symbol ϵ is the desired efficiency. The solution $y_2(\eta_\infty)$ approaches 0 within the desired efficiency criteria and the value of $\eta_\infty = 7$.

In order to solve the temperature equation (3.66), it is converted into the following system comprising of the first order differential expressions mentioned in Eqs. (3.66) signifying θ by u_1 , θ' by u_2 and using f as a known function. The following system of ODEs together with the initial conditions is achieved.

$$\left. \begin{aligned} u_1' &= u_2, & u_1(0) &= 1, \\ u_2' &= - \frac{\left[(\epsilon_1 + 4Rd(\theta_w - 1)(1 + (\theta_w - 1)u_1)^2)u_2^2 \right.}{\left. \left((1 + \epsilon_1 u_1) + \frac{4}{3} Rd(1 + (\theta_w - 1)u_1)^3 \right) \right.} + \frac{2}{3} Pr f u_2 + (A^* \exp^{-\eta} + B^* u_1)}{\left. \right]}, & u_2(0) &= c_2. \end{aligned} \right\} \quad (3.90)$$

Now solve the energy equation with the utilization of numerical scheme called RK4 method along with choosing value of initial guess $c_2^{(0)}=0.1$. If solution at the

boundary $u_1(\eta_\infty, c_2^{(0)}) = 0$ is achieved then terminate the process otherwise, refine the initial guess with the utilization of iterative scheme called Newton's method.

Mathematical form of Newton's method is given by

$$c_2^{(n+1)} = c_2^{(n)} - \frac{u_1(\eta_\infty, c_2^{(n)})}{\left. \frac{\partial u_1}{\partial c_2}(\eta_\infty, c_2) \right|_{c_2=c_2^{(n)}}}. \quad (3.91)$$

After adopting the following notations.

$$\frac{\partial u_1}{\partial c_2} = u_3, \quad \frac{\partial u_2}{\partial c_2} = u_4. \quad (3.92)$$

Newton's method take the form given below

$$c_2^{(n+1)} = c_2^{(n)} - \frac{u_1(\eta_\infty, c_2^{(n)})}{u_3(\eta_\infty, c_2^{(n)})}. \quad (3.93)$$

The differential form of eq. (90) with respect to c_2 are given underneath

$$\left. \begin{aligned} u_3' &= u_4, & u_3(0) &= 0, \\ u_4' &= - \frac{\left[\begin{aligned} &(8Rd(\theta_w - 1)^2\Psi u_3 u_2^2) + \\ &(\epsilon + 4Rd(\theta_w - 1)\Psi^2(2u_2 u_4)) + \\ &((\epsilon_1 u_3) + 4Rd\Psi^2(\theta_w - 1)u_3 u_2') + \\ &(\frac{2}{3}Pr f u_4 + B^* u_3) \end{aligned} \right]}{\left((1 + \epsilon_1 u_1) + \frac{4}{3}Rd\Psi^3 \right)}, & u_4(0) &= 1, \end{aligned} \right\} \quad (3.94)$$

where $(1 + (\theta_w - 1)u_1) = \Psi$.

Now Eq. (94) can solve numerically with the help of RK4 method and refined initial guess c_2 by Newton's method until the criteria given below is achieved.

$$|u_1(\eta_\infty) - 0| < \epsilon. \quad (3.95)$$

The concentration equation (3.67) is transformed into the first order ODEs by denoting ϕ by z_1 , ϕ' by z_2 and taking f as a known function.

The following resulting system of equations is achieved.

$$\left. \begin{aligned} z_1' &= z_2, & z_1(0) &= 1, \\ z_2' &= -\frac{\left(\epsilon_2 z_2^2 + \frac{2}{3} Scf z_2\right)}{1 + \epsilon_2 z_1}, & z_2(0) &= c_3. \end{aligned} \right\} \quad (3.96)$$

Now solve the concentration equation with the help of numerical scheme called RK4 method along with choosing value of initial guess $c_3^{(0)}=0.1$ until the solution at the boundary is achieved. Generally it is not possible in the first attempt.

Now refine the initial guess of Eq. (3.96) with the help of Newton's iterative method given below

$$c_3^{(n+1)} = c_3^{(n)} - \frac{z_1\left(\eta_\infty, c_3^{(n)}\right)}{\left.\frac{\partial z_1}{\partial c_3}(\eta_\infty, c_3)\right|_{c_3=c_3^{(n)}}}. \quad (3.97)$$

After adopting the following notations.

$$\frac{\partial z_1}{\partial c_3} = z_3, \quad \frac{\partial z_2}{\partial c_3} = z_4. \quad (3.98)$$

Newton's method take the form given below

$$c_3^{(n+1)} = c_3^{(n)} - \frac{z_1\left(\eta_\infty, c_3^{(n)}\right)}{z_3\left(\eta_\infty, c_3^{(n)}\right)}. \quad (3.99)$$

The differential form of Eq. (98) with respect to c_3 are given underneath

$$\left. \begin{aligned} z_3' &= z_4, & z_3(0) &= 0, \\ z_4' &= -\frac{\left(2\epsilon_2 z_2 z_4 + \frac{2}{3} Scf z_4\right)}{1 + \epsilon_2 z_1}, & z_4(0) &= 1. \end{aligned} \right\} \quad (3.100)$$

Now eq. (100) can solves numerically with the help of RK4 method with refined initial guess with as far as the criteria mentioned below is not fulfilled.

$$\max\{|z_1(\eta_\infty) - 0|\} < \epsilon. \quad (3.101)$$

A symbol $\varepsilon > 0$ depicts a positive number.

Table 3.1 is designed to display the comparison analysis of heat transport phenomenon for present outcomes with those of Reddy et al. [8] by changing γ and λ and keeping the other parameters fixed.

TABLE 3.1: Values of Nusselt number for various values of Pr .

$Nu_x Re_x^{-\frac{1}{2}}$		
$\lambda = 1$		
Pr	Present	Reddy et al. [8]
1	0.556065	0.559879
1.5	0.727928	0.727497
2	0.873992	0.886106

3.3 Results and Discussion

The current section displays the impact of sundry dimensionless quantities against velocity, temperature, mass fraction field, surface drag coefficient, heat as well as mass transfer rates are debated in the form of tables and figures.

3.3.1 Impact of γ and λ on velocity field $f'(\eta)$ and stress field $g'(\eta)$

Figure 3.2 exhibits the response of the velocity field to variation in γ . It is quite interesting that the viscosity of the fluid amplifies owing to an amplification in the shear rate which amplifies the velocity field. Figure 3.3 shows the effectiveness of λ on $f'(\eta)$. A magnification in λ brings about an amplification in the fluid viscosity and depreciates the velocity field. Figure 3.4 shows that the viscosity of the fluid diminishes on the behalf of an improvement in the γ eases the fluid motion and enhances the shear stress field. Figure 3.5 reveals that the shear stress field abates owing to an increment in λ . A magnification in viscosity of fluid lessens shear stress field.

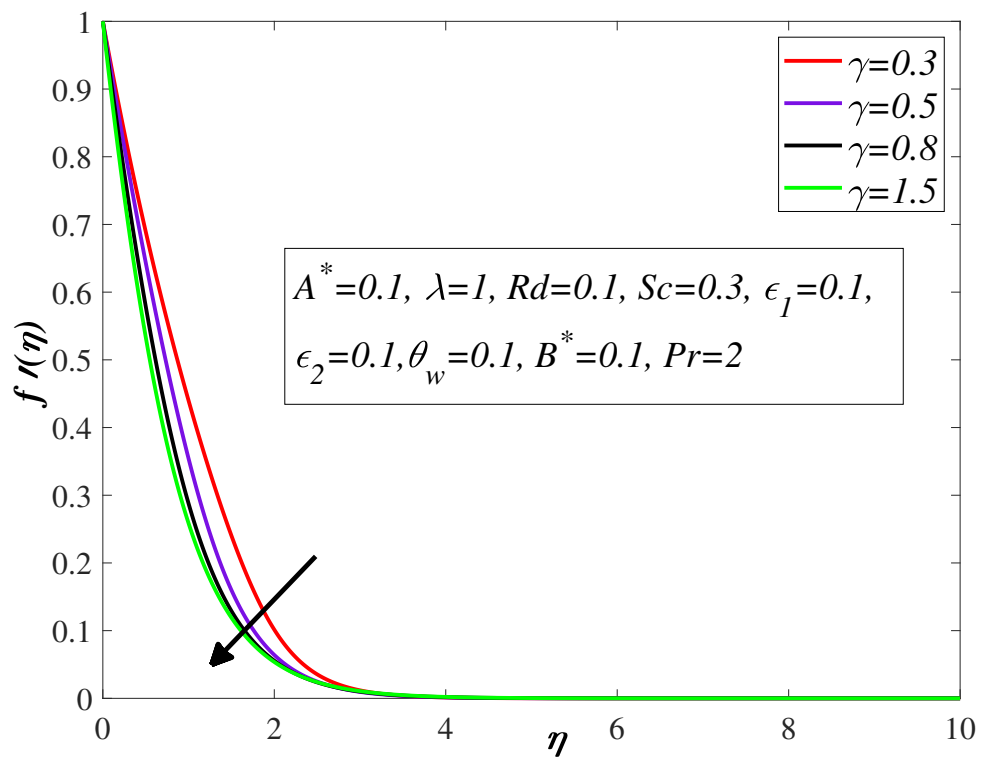


FIGURE 3.2: Impact of γ on f' .

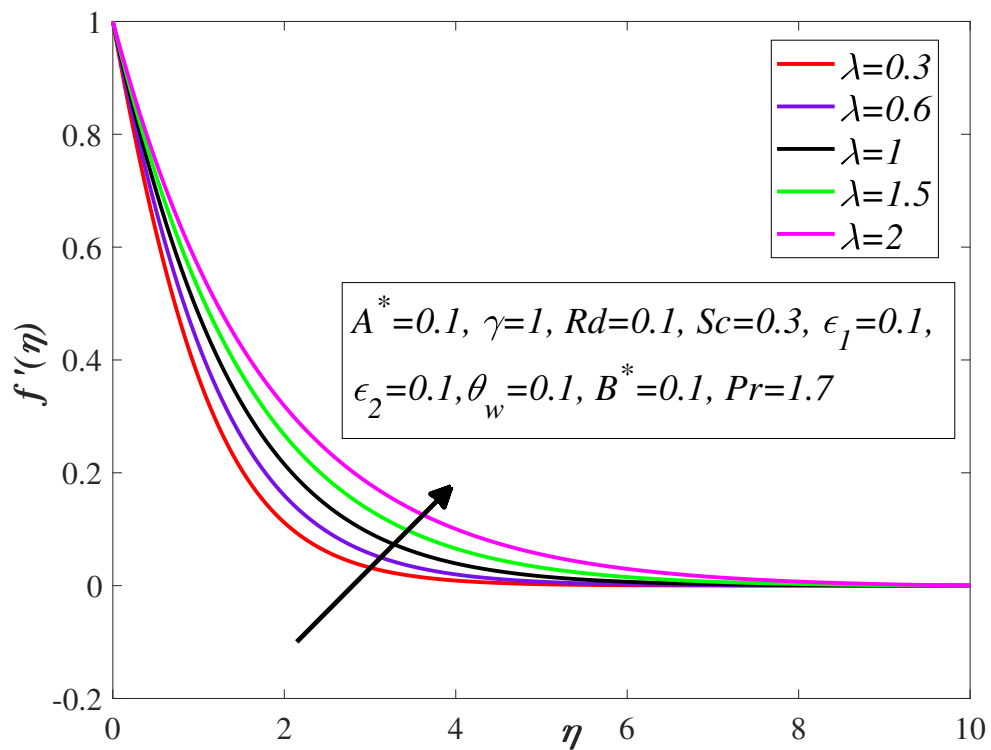


FIGURE 3.3: Influence of λ on f' .

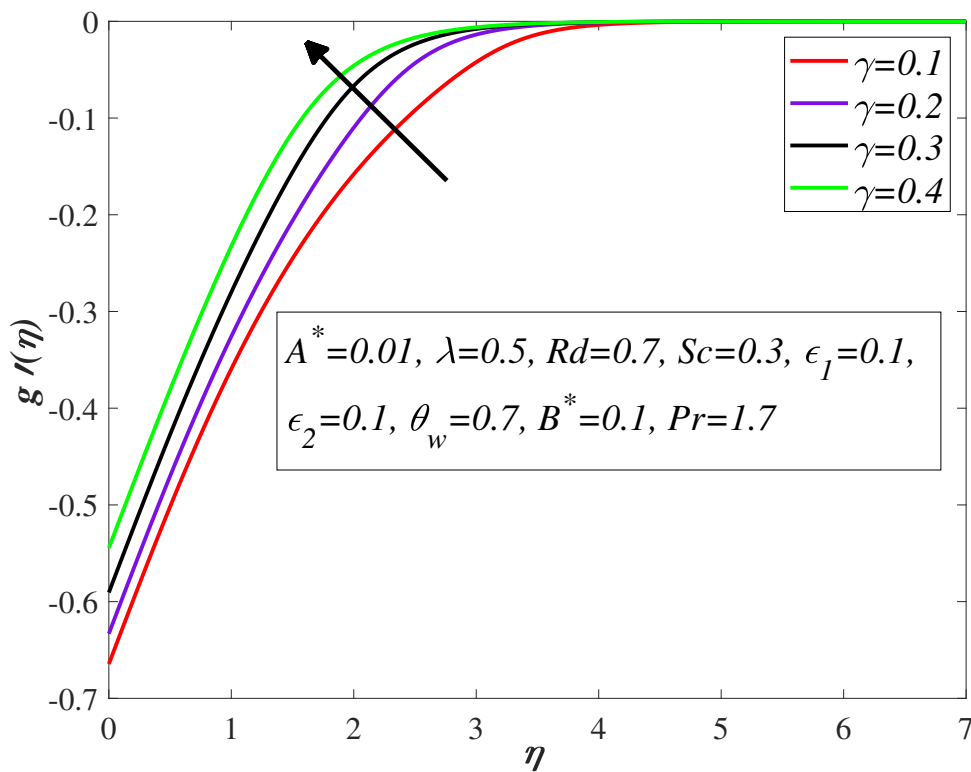


FIGURE 3.4: Impact of γ on g' .

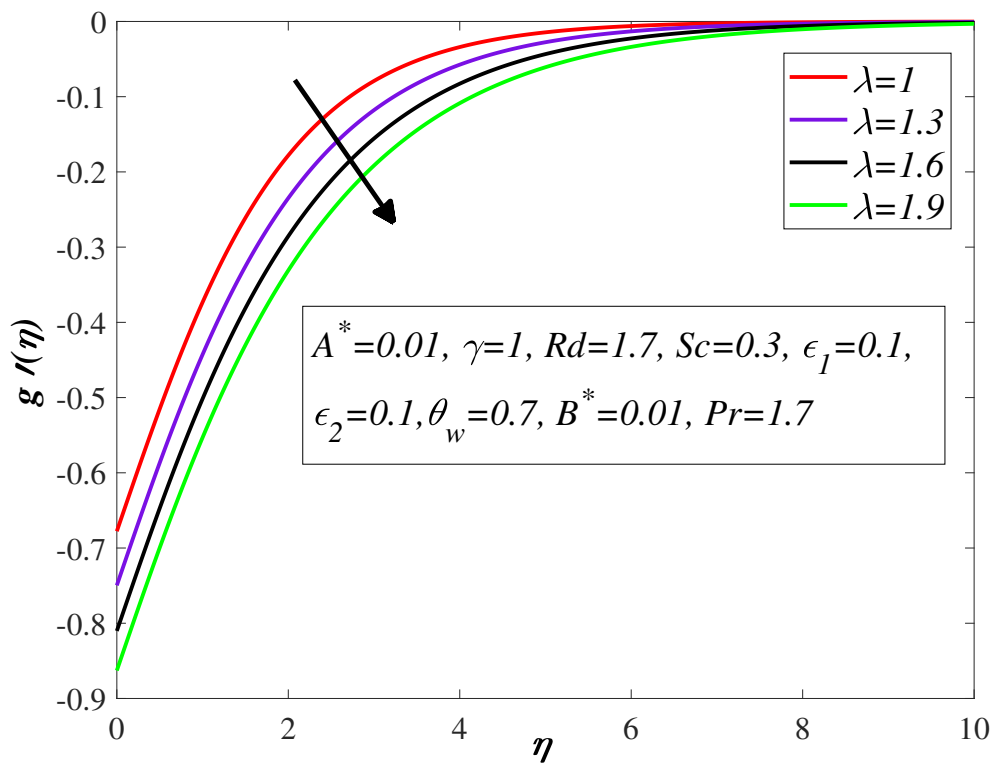


FIGURE 3.5: Effect of λ on g' .

3.3.2 Impact of A^* , B^* , Pr , ϵ_1 , Rd and θ_w on $\theta(\eta)$

Figures 3.6 and 3.7 demonstrate the impact of A^* and B^* on the temperature field. Evidently, a magnification in A^* and B^* produces more heat inside the fluid which magnifies the temperature field. Figure 3.8 reflects the conduct of Prandtl number Pr on $\theta(\eta)$. It is notable that a magnification in Pr weakens the thermal diffusivity and depreciates the temperature field. Figure 3.9 reflects the impact of ϵ_1 on θ_η . Physically, a more frequent collision of molecules delivers more heat energy inside the fluid and brings about a magnification in $\theta(\eta)$. Figure 3.10 is sketched for the investigation of the temperature profile in response to the thermal radiation parameter Rd . Physically, a magnification in Rd provides additional heat to the operating fluid which amplifies the temperature field. Figure 3.11 displays the impact of ambient to wall temperature ratio θ_w on $\theta(\eta)$ and observed that a magnification in θ_w produces more heat and further augments the temperature profile.

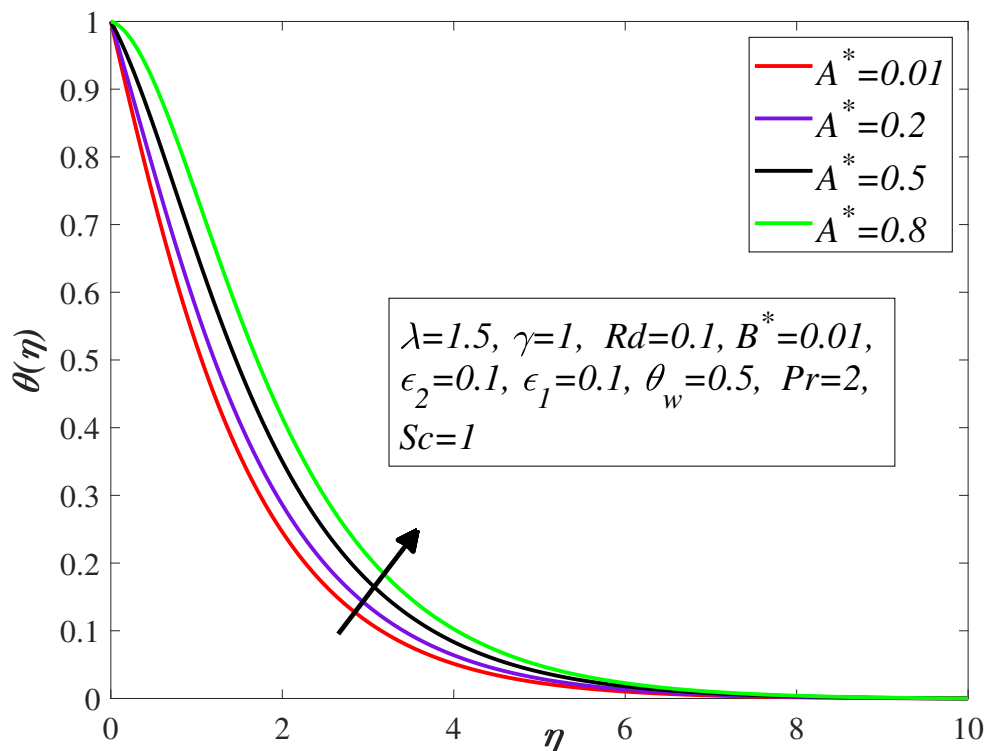
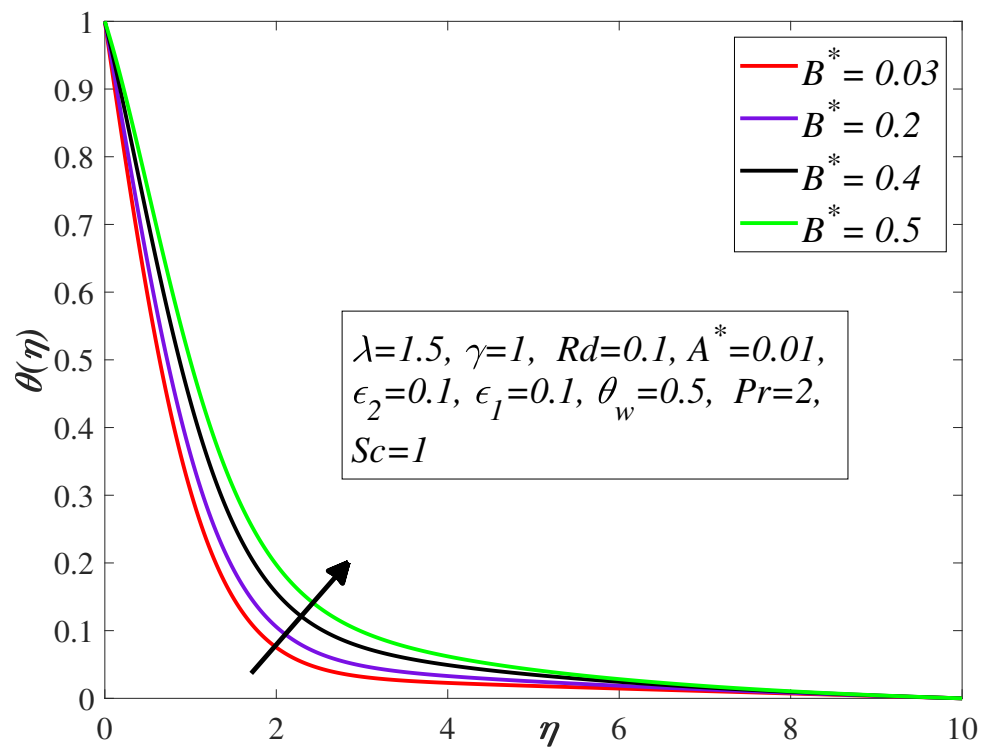
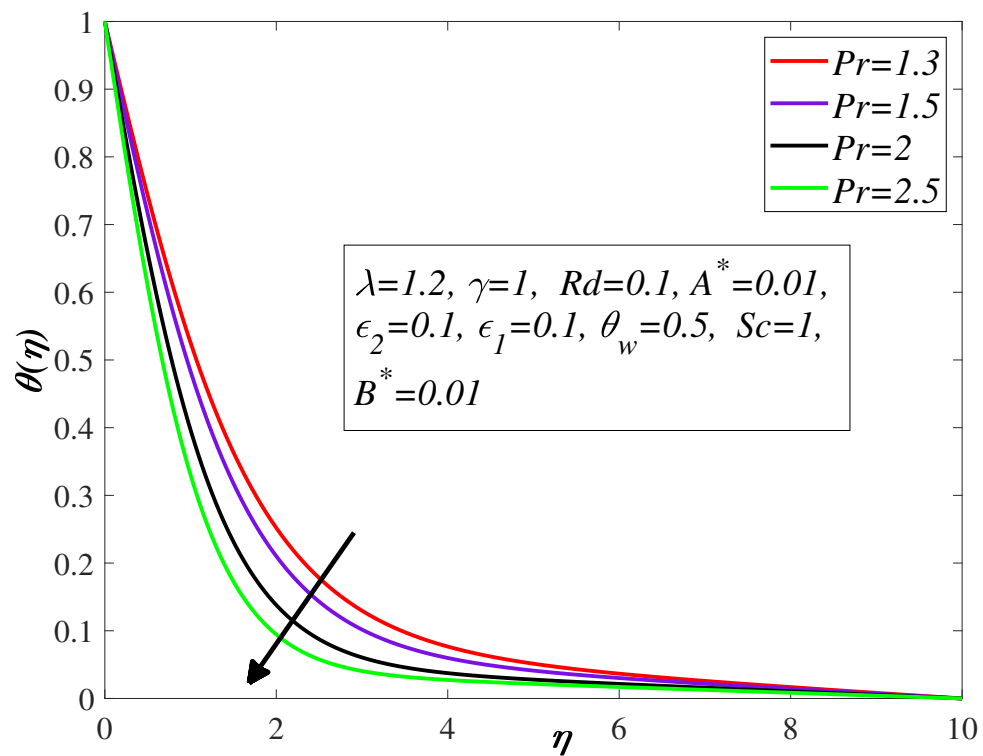


FIGURE 3.6: Effect of A^* on θ .

FIGURE 3.7: Impact of B^* on θ .FIGURE 3.8: Impact of Pr on θ .

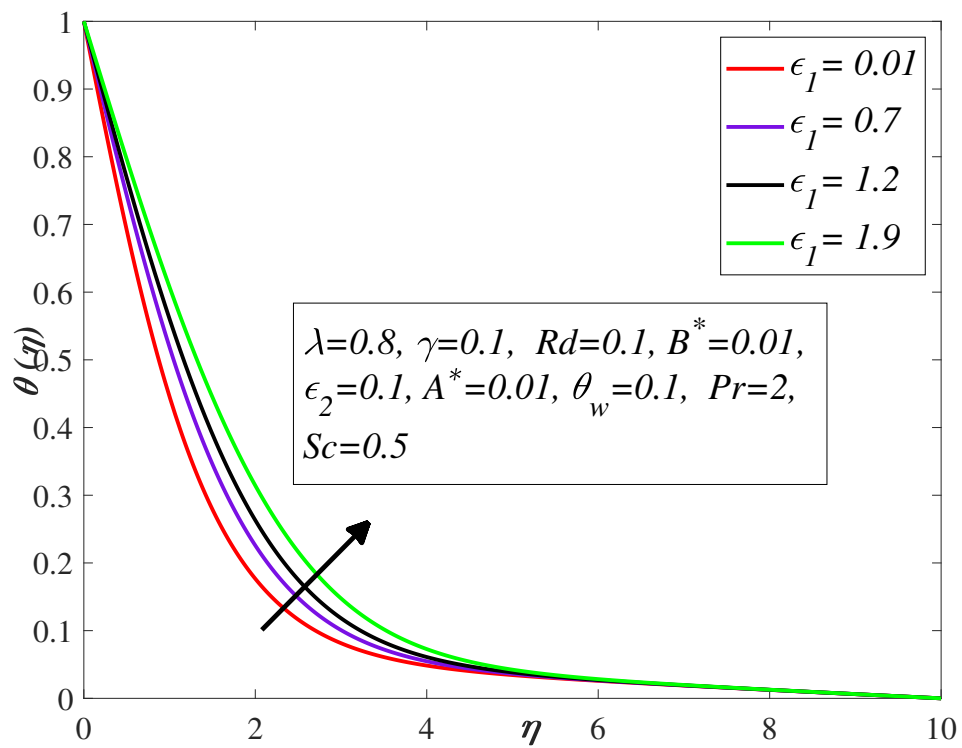


FIGURE 3.9: Effect of ϵ_1 on θ .

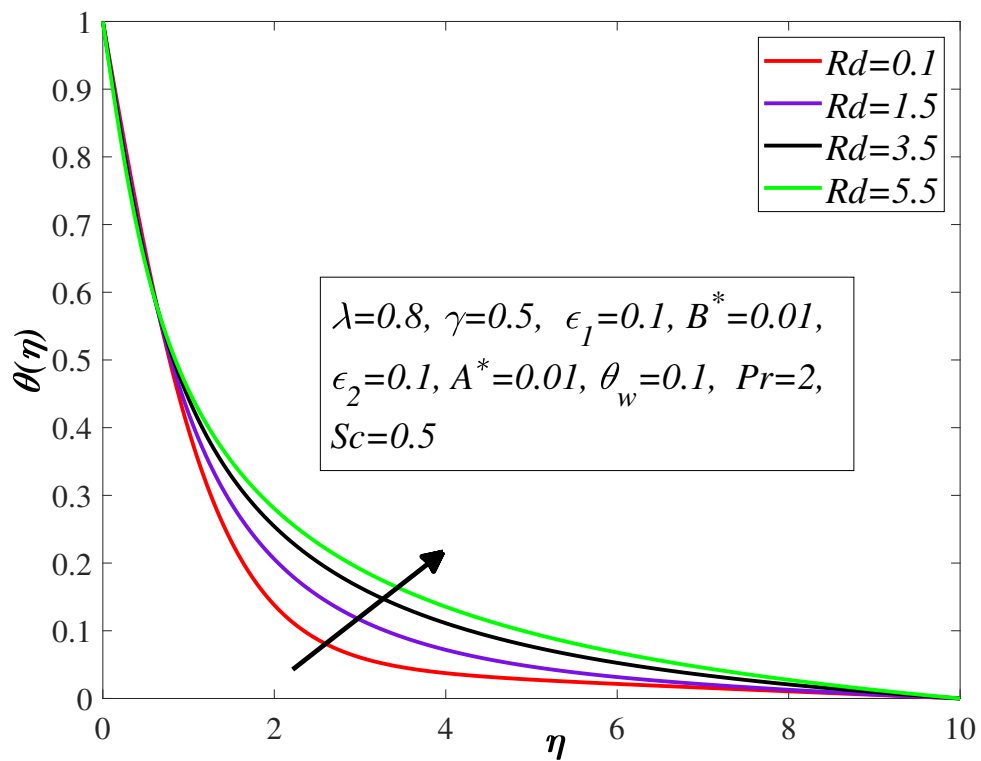
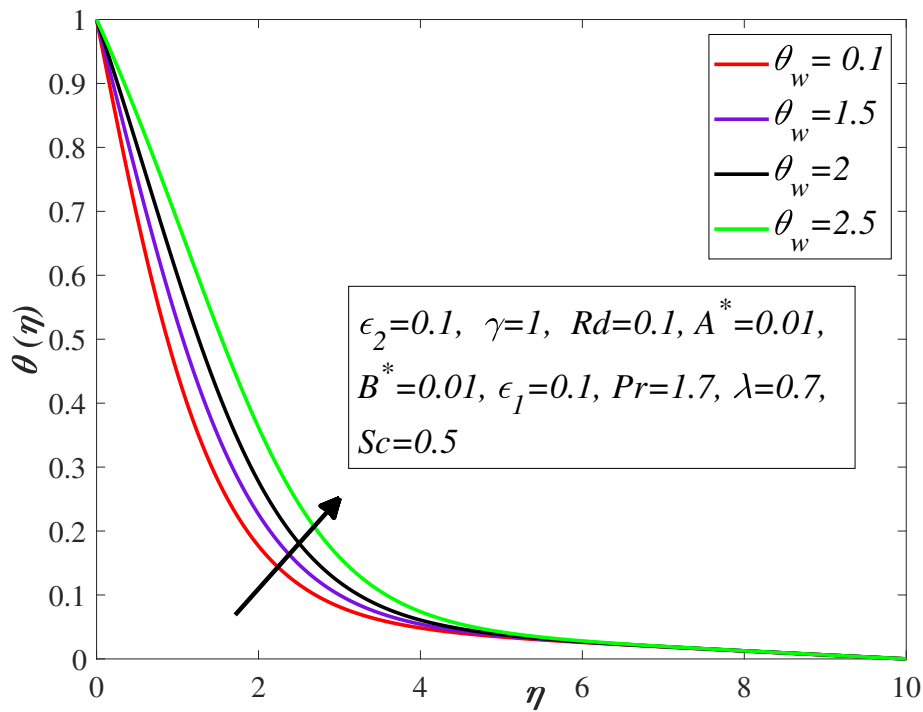
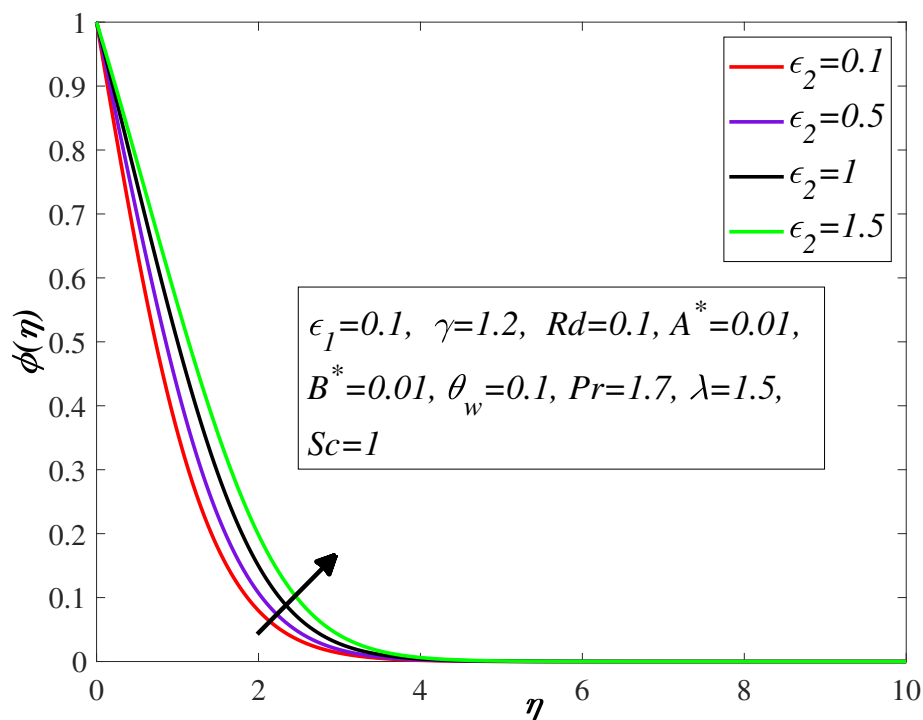


FIGURE 3.10: Influence of Rd on θ .

FIGURE 3.11: Effect of θ_w on θ .

3.3.3 Impact of ϵ_2 and Sc on Concentration Field $\phi(\eta)$

A magnification in ϵ_2 and Sc elevates $\phi(\eta)$ as shown in Figure 3.12 and 3.13.

FIGURE 3.12: Impact of ϵ_2 on ϕ .

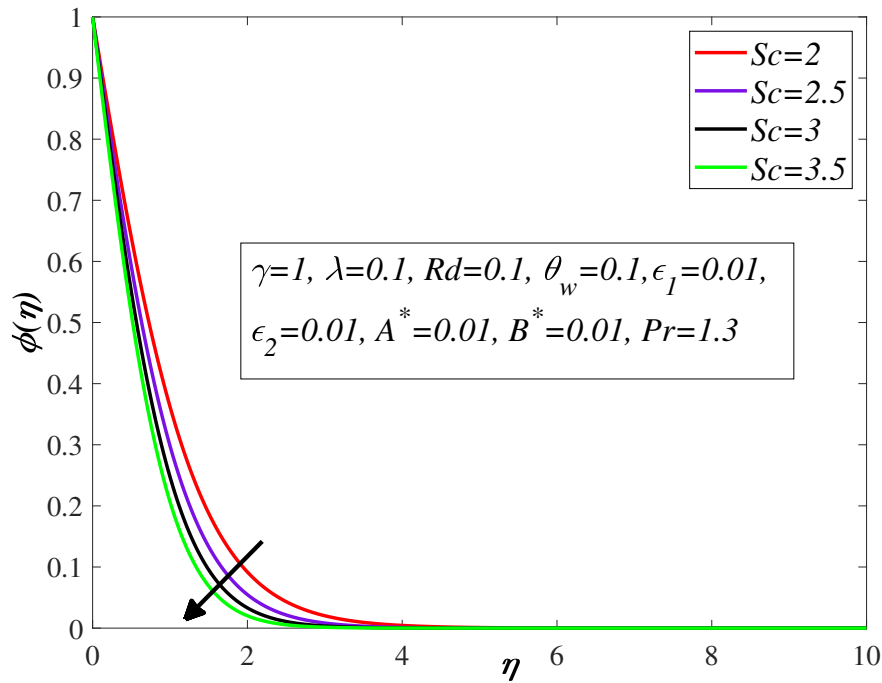


FIGURE 3.13: Influence of Sc on ϕ .

3.3.4 Impact of γ and λ on surface drag coefficient $Cf_x Re_x^{\frac{1}{2}}$

Fluid becomes shear thinning due to an increase in γ which lessens λ and amplifies $Cf_x Re_x^{\frac{1}{2}}$ as shown in Figure 3.14. In the case of $\lambda < 1$, the fluid becomes less viscous amplifies $Cf_x Re_x^{\frac{1}{2}}$ but decreases in the case of $\lambda > 1$ as shown in Figure 3.15.

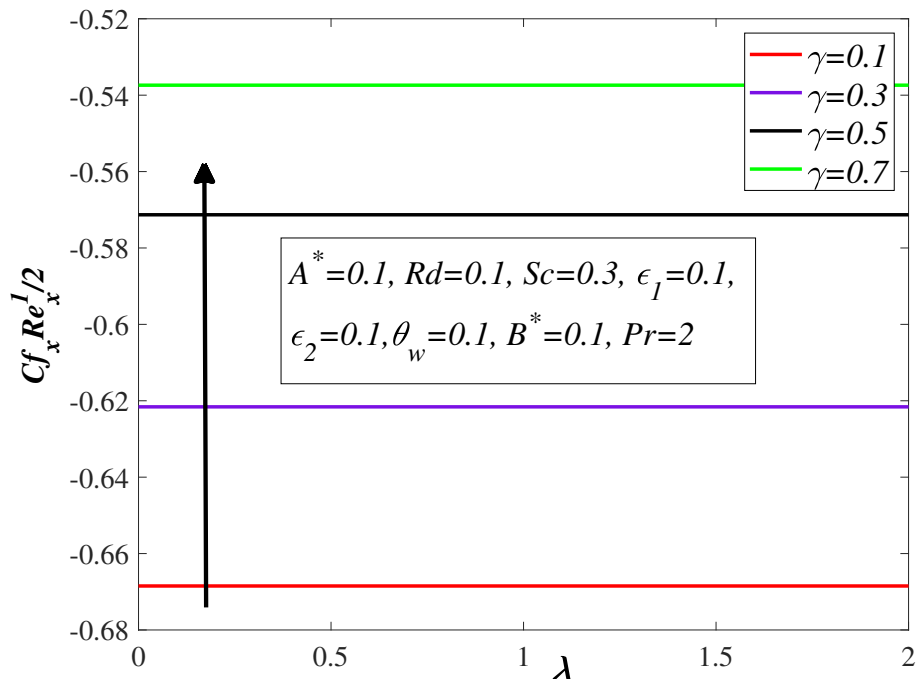
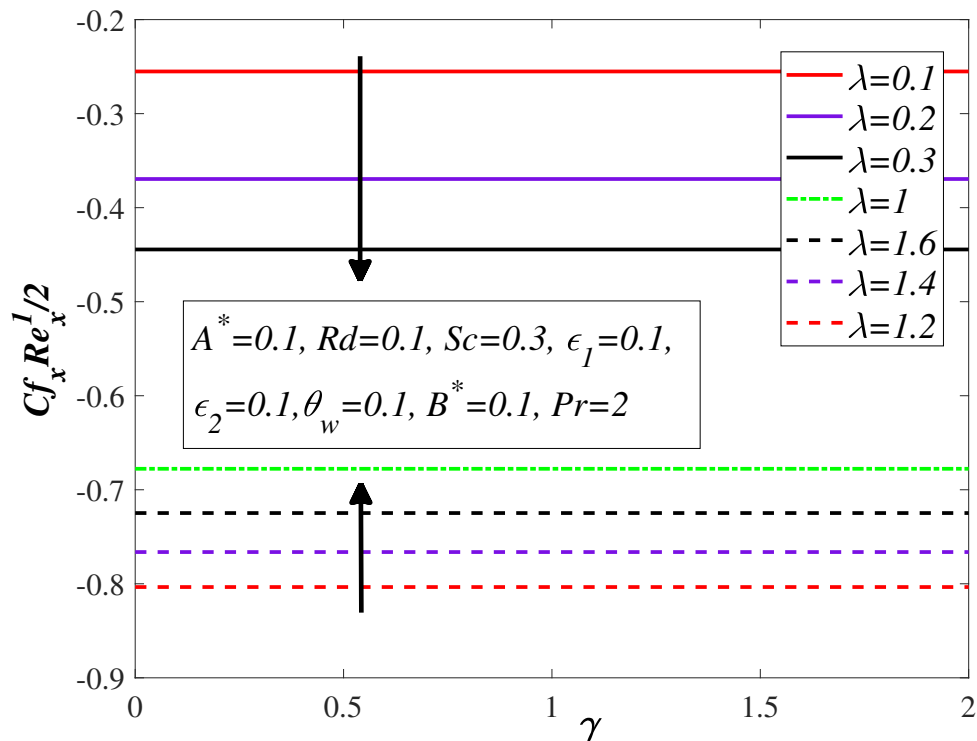


FIGURE 3.14: Impact of γ versus λ on $Cf_x Re_x^{\frac{1}{2}}$.


 FIGURE 3.15: λ versus γ on $Cf_x Re_x^{-\frac{1}{2}}$.

3.3.5 Impact of Rd and θ_w versus Pr , A^* and B^* versus θ_w , λ versus γ on heat transfer rate $Nu_x Re_x^{-\frac{1}{2}}$

Figure 3.16 depicts the impact of Pr on the Nusselt number with respect to the change in Rd . In the presence of both Pr and Rd , more heat is released which amplifies the heat transport rate. Figure 3.17 demeanour Pr versus θ_w impact on heat transport phenomenon and noticed that a positive variation in Pr and θ_w causes an increment in nonlinear thermal radiation phenomenon and moreover deliver substantial heat which magnifies $Nu_x Re_x^{-\frac{1}{2}}$. Figure 3.18 and 3.19 elaborate the impact of A^* , B^* on θ_w against the heat transport effect and canvassed that more heat is generated inside the fluid in the case of $A^* > 0$ and $B^* > 0$, which prompts an enhancement in θ_w and $Nu_x Re_x^{-\frac{1}{2}}$. Figure 3.20 sketches the influence of λ on the Nusselt number in terms of a change in gamma. The viscosity of the fluid decreases as a result of an abatement in fluid parameter $\lambda < 1$ which lessens the Nusselt number but a magnification in $\lambda > 1$ improves heat transfer.

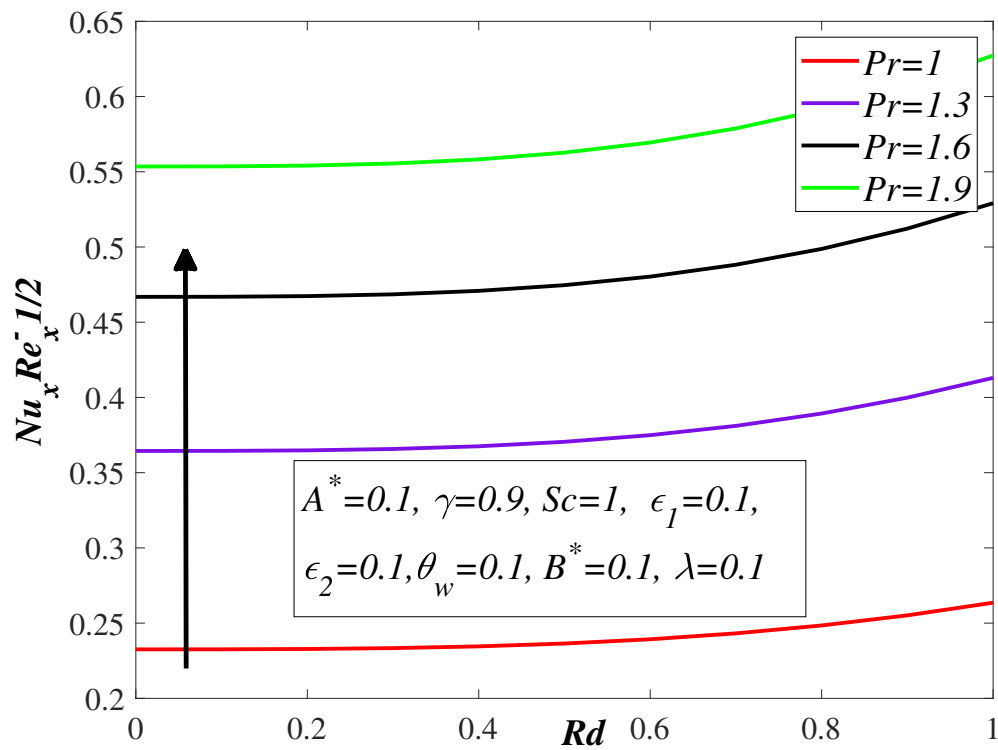


FIGURE 3.16: Pr versus Rd on $Nu_x Re_x^{-1/2}$.

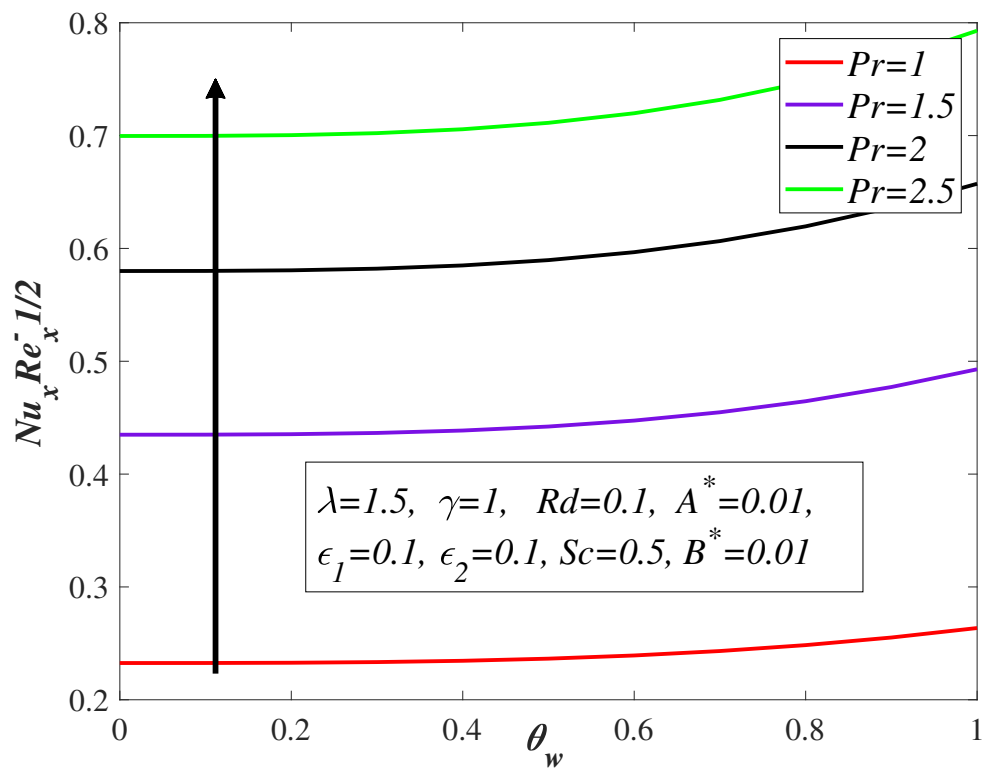


FIGURE 3.17: Pr versus θ_w on $Nu_x Re_x^{-1/2}$.

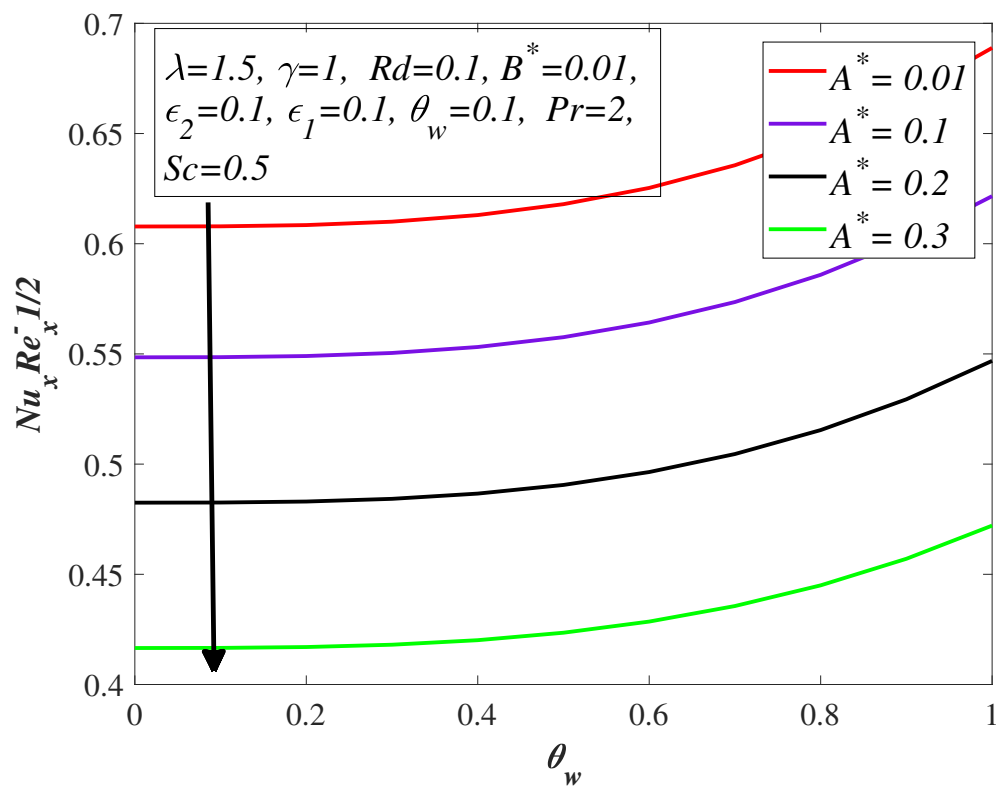


FIGURE 3.18: A^* versus θ_w on $Nu_x Re_x^{-1/2}$.

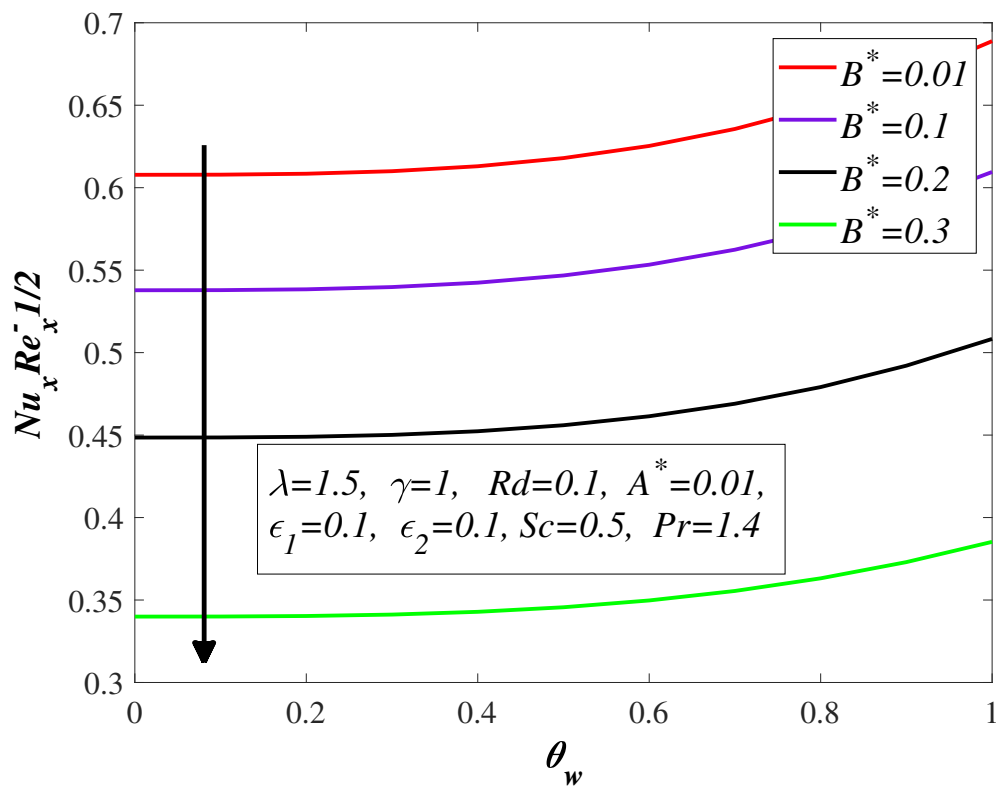


FIGURE 3.19: B^* versus θ_w on $Nu_x Re_x^{-1/2}$.

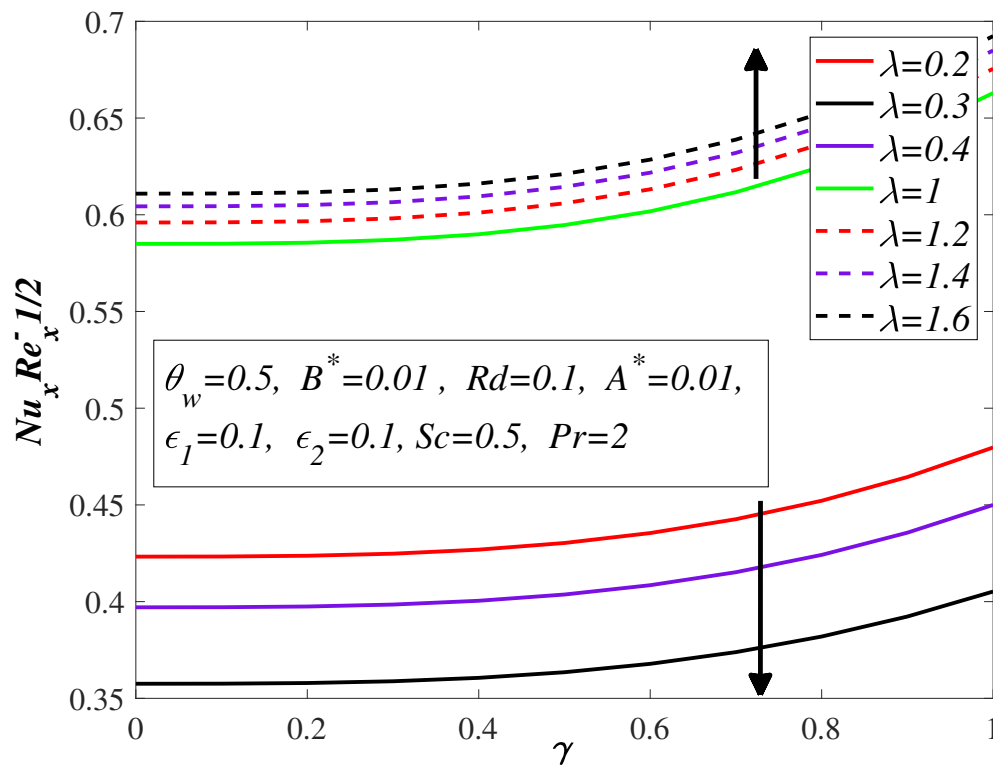


FIGURE 3.20: λ versus γ on $Nu_x Re_x^{-\frac{1}{2}}$.

3.3.6 Impact of Sc versus variable species diffusivity ϵ_2 on mass transfer rate $Sh_x Re_x^{-\frac{1}{2}}$

Figure 3.21 exhibits the effect of Sc on the mass fraction field with change in ϵ_2 . Schmidt number can be defined as momentum to the mass diffusivity responsible for mass transport. Schmidt number is applicable in the case of the fluid in which both momentum as well as mass diffusion convection are involved. Mass diffusivity is actually the molecules transport from region having higher concentration towards the lower region. That's why diffusivity phenomenon is related to the concentration. The role of variable species diffusivity in mass transfer is same as thermal conductivity in the heat transfer. It is quite clear from the above discussion that Sc and ϵ_2 relies on the diffusion process and species diffusivity varies due to a variation in the concentration of the molecules. A gradual change in the species diffusivity causes an embellishment in concentration which escalates the mass transfer rate.

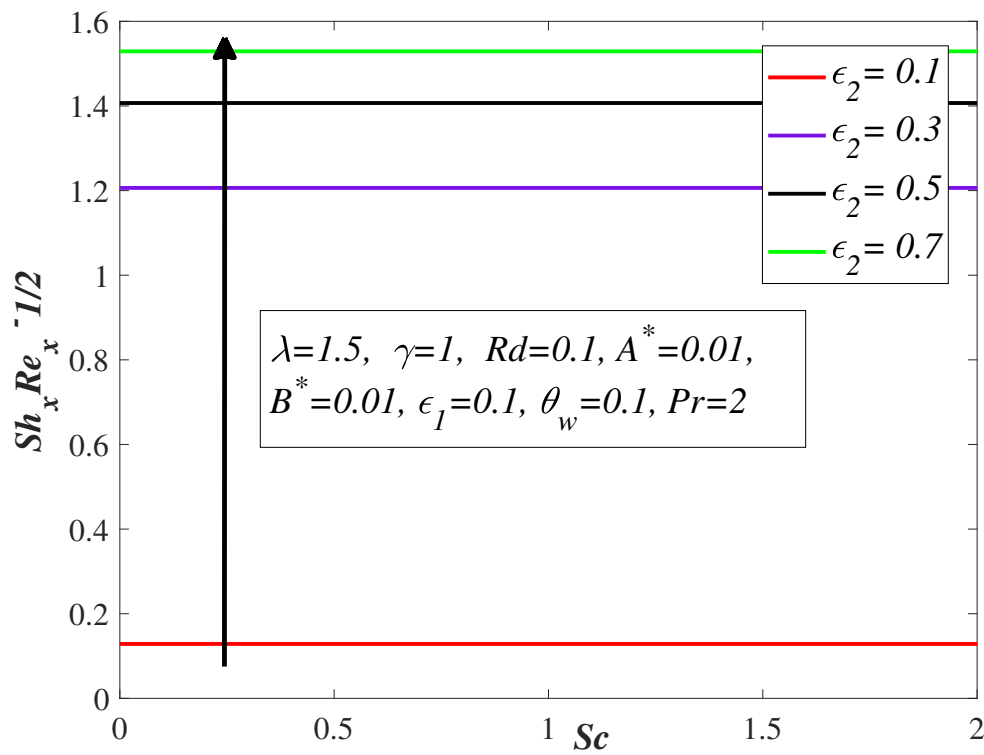


FIGURE 3.21: Impact of ϵ_2 and Sc on $Sh_x Re_x^{-1/2}$.

Table 3.2 depicts the influence of sundry physical parameters on the physical quantities like surface drag coefficient, heat as well as mass transport numbers. These physical quantities are quite necessary in order to study the momentum, heat and concentration aspects of the fluid. Amplification in Bingham number γ brings about a magnification in surface drag coefficient but the surface drag coefficient diminishes owing to an improvement in the Reiner-Philippoff fluid parameter λ . Moreover, a magnification in λ , thermal radiation Rd , temperature ratio parameter θ_w and Prandtl number Pr generates an enhancement in the Nusselt number however an opposite behaviour is observed for Bingham number γ , thermal conductivity ϵ_1 , species diffusivity ϵ_2 , heat generation/absorption coefficients A^* and B^* and Schmidt number Sc . The mass transfer rate escalates as a result of an enhancement in λ and Sc but depreciates in the case of an augmentation in γ and ϵ_2 . Table 3.3 reflects the effectiveness of distinguished parameters against Nusselt number by keeping $Sc=0.1$ and $\epsilon_2=0.1$. Heat transfer amplified more for nonlinear thermal radiation rather than thermal radiation.

TABLE 3.2: Numerical values of skin friction, Nusselt and Sherwood numbers for various physical parameters.

γ	λ	Rd	θ_w	ϵ_1	ϵ_2	A^*	B^*	Pr	Sc	$\frac{1}{2}Cf_xRe_x^{\frac{1}{2}}$	$Nu_xRe_x^{-\frac{1}{2}}$	$Sh_xRe_x^{-\frac{1}{2}}$
0.1	0.1	0.1	0.1	0.01	0.01	0.01	0.01	1.7	0.1	-0.660273	0.674889	0.133592
	0.5									-0.380604	0.514999	0.118724
	1									-0.246415	0.403716	0.113661
	2									-1.143974	0.382161	0.112794
		0.3								-0.664497	0.673753	0.134262
		0.5								-0.668484	0.674594	0.134825
		0.7								-0.672282	0.675268	0.135308
			0.3							-0.660271	0.678065	0.133592
			0.5							-0.660271	0.683150	0.133592
			0.7							-0.660271	0.687991	0.133592
				0.3						-0.660271	0.674792	0.133592
				0.6						-0.660271	0.681787	0.133592
				0.9						-0.660271	0.694968	0.133592
					0.03					-0.660271	0.662843	0.133592
					0.05					-0.660271	0.653468	0.133592
					0.07					-0.660271	0.644409	0.133592
						0.03				-0.660271	0.672563	0.131896
						0.05				-0.660271	0.672561	0.130263
						0.07				-0.660271	0.672567	0.128701
							0.03			-0.660271	0.658104	0.133592
							0.05			-0.660271	0.643647	0.133592
							0.07			-0.660271	0.629192	0.133592
								0.03		-0.660271	0.656931	0.133592
								0.05		-0.660271	0.640894	0.133592
								0.07		-0.660271	0.624428	0.133592
									1.9	-0.660271	0.723241	0.133592
									2.1	-0.660271	0.771130	0.133592
									2.3	-0.660271	0.816659	0.133592
									0.3	-0.660271	0.672562	0.212701
									0.5	-0.660271	0.672562	0.296095
									0.7	-0.660271	0.672562	0.375564

TABLE 3.3: Effect of physical parameters on Nusselt number.

								$Nu_x Re_x^{-\frac{1}{2}}$					
Dimensionless Parameters								Absence of Rd			Presence of Rd		
γ	Pr	Rd	θ_w	A^*	B^*	ϵ_1		$\lambda=0.5$	$\lambda=1$	$\lambda=1.5$	$\lambda=0.5$	$\lambda=1$	$\lambda=1.5$
0.1	0.5	0.7	0.7	0.01	0.01	0.1		0.23001	0.23340	0.23559	0.30364	0.30812	0.31102
							0.2	0.22513	0.23340	0.23847	0.29720	0.30812	0.31482
							0.3	0.22008	0.23340	0.24109	0.29054	0.30812	0.31827
							1	0.37713	0.38129	0.38390	0.49787	0.50335	0.50680
							1.5	0.50633	0.50981	0.51197	0.66842	0.67302	0.67587
							2	0.61823	0.62084	0.62246	0.81614	0.81959	0.82173
							1	0.22412	0.22721	0.22922	0.32661	0.33112	0.33405
							1.5	0.21711	0.21978	0.22154	0.36604	0.37056	0.37352
							2	0.21222	0.21458	0.21613	0.40633	0.41085	0.41381
							1	0.17481	0.17759	0.17941	0.33798	0.34335	0.34685
							1.5	0.10134	0.10295	0.10403	0.42059	0.42726	0.43173
							2	0.06562	0.06639	0.06693	0.55561	0.56218	0.56669
							0.1	0.17418	0.17777	0.18010	0.22994	0.23468	0.23776
							0.2	0.11217	0.11599	0.11846	0.14808	0.15312	0.15639
							0.3	0.05019	0.05423	0.05685	0.06626	0.07160	0.07506
							0.02	0.21193	0.21570	0.21814	0.27977	0.28475	0.28798
							0.03	0.19258	0.19681	0.19955	0.25423	0.25981	0.26343
							0.04	0.17173	0.17652	0.17961	0.22671	0.23303	0.23711
							0.5	0.18914	0.19209	0.19401	0.24969	0.25358	0.25612
							1	0.15709	0.15965	0.16132	0.20738	0.21076	0.21296
							1.5	0.13612	0.13836	0.13983	0.17970	0.18266	0.18460

3.4 Concluding Remarks

The radiative Reiner-Philippoff fluid impinging on an extendable surface accompanied with heat generation/absorption, thermal conductivity and variable molecular diffusivity is debated in detail. The computations indicate the following major findings

- A positive variation in γ diminishes the shear stress field $g'(\eta)$ but situation is entirely different in the case of λ which magnifies $g'(\eta)$.
- A magnification in ϵ_1 escalates the temperature field.
- An improvement in heat transport phenomenon is observed owing to a magnification in the values of θ_w and Rd .
- Heat transport Nusselt number is depressed in the case of shear thickening fluid.
- The upshots revealed that a positive variation in heat source/sink parameters A^* and B^* generate more heat which produces an enlargement in the temperature field.
- The mass fraction field amplifies owing to a magnification in ϵ_2 .
- Sherwood number abates for the larger values of Sc and ϵ_2 .

Chapter 4

Impact of Double-Diffusive Convection and Motile Gyrotactic Microorganisms on Bioconvection Tangent Hyperbolic Nanofluid

The motive behind this chapter is to investigate the non-Newtonian double diffusive tangent hyperbolic nanofluid containing motile gyrotactic microorganisms. The modeled PDEs are renovated into ODEs with the utilization of necessary transformations and moreover tackled numerically by adopting the well known numerical procedure called Keller-box scheme. The behaviour of working fluid against various parameters of physical nature has been analyzed through graphs and tables. The impact of various dimensionless quantities appearing during the numerical simulation on the drag force, Nusselt amount, microorganisms density field and the mass transport field is analyzed in terms of tables and figures. The noteworthy outcome of this analysis is that a magnification in Dufour and Brownian motion parameters produces an amplification in the temperature profile. The velocity field decays when both Weissenberg number and magnetic parameters are increased. It is noted that a magnification in Dufour and moreover nanofluid Lewis number magnifies the solutal field.

4.1 Mathematical Formulation

Figure 4.1 reflects the movement of a tangent hyperbolic nanofluid flow subjected to an expandable sheet having expanding rate $u_w = ax$. The induced magnetic field under the assumption of small Reynolds number is neglected as compared to the applied magnetic field B_0 which is applied transversely to the surface. The expressions T_w, γ_w, C_w and N_w represent the temperature, solute concentration, nanoparticles concentration and microorganisms concentration at the wall whereas ambient temperature, solute concentration, nanoparticles as well as microorganisms concentration are denoted as $T_\infty, \gamma_\infty, C_\infty$ and N_∞ . The diffusion-thermo (Dufour) and thermo-diffusion (Soret) are also considered in terms of heat and mass transport analysis.

The constitutive equation of tangent hyperbolic fluid is [24]:

$$\mathbf{S} = -p\mathbf{I} + \tau, \tag{4.1}$$

in which symbol \mathbf{I} denotes the identity matrix, μ_∞ as well as μ_0 is zero and infinite shear rates, Γ symbolizes the relaxation time, n expresses the flow behaviour index and deformation rate $\dot{\gamma}$ can be expressed as

$$\dot{\gamma} = \sqrt{\frac{1}{2}\Sigma\Sigma\dot{\gamma}_{ij}\dot{\gamma}_{ji}} = \sqrt{\frac{1}{2}\mathbf{\Pi}}, \tag{4.2}$$

where

$$\mathbf{\Pi} = \frac{1}{2}\text{trac}(\text{grad}\mathbf{V} + (\text{grad}\mathbf{V})^T)^2. \tag{4.3}$$

The equation mentioned is valid for the case $\mu = 0$ because the fluid behaviour is impossible to study at $\mu = \infty$ and moreover utilizing tangent hyperbolic based fluid characterizing shear thinning phenomenon $\Gamma\dot{\gamma} < 1$.

The above equation written as

$$\begin{aligned} \tau &= \mu_0[(\Gamma\dot{\gamma})^n]\dot{\gamma}, \\ &= \mu_0[(1 + n(\Gamma\dot{\gamma} - 1)]\dot{\gamma}. \end{aligned} \tag{4.4}$$

Under the above assumptions and boundary approximation, the governing expressions regarding continuity, temperature, solutal as well as mass concentration regarding tangent hyperbolic model accompanied with nanoparticles written as

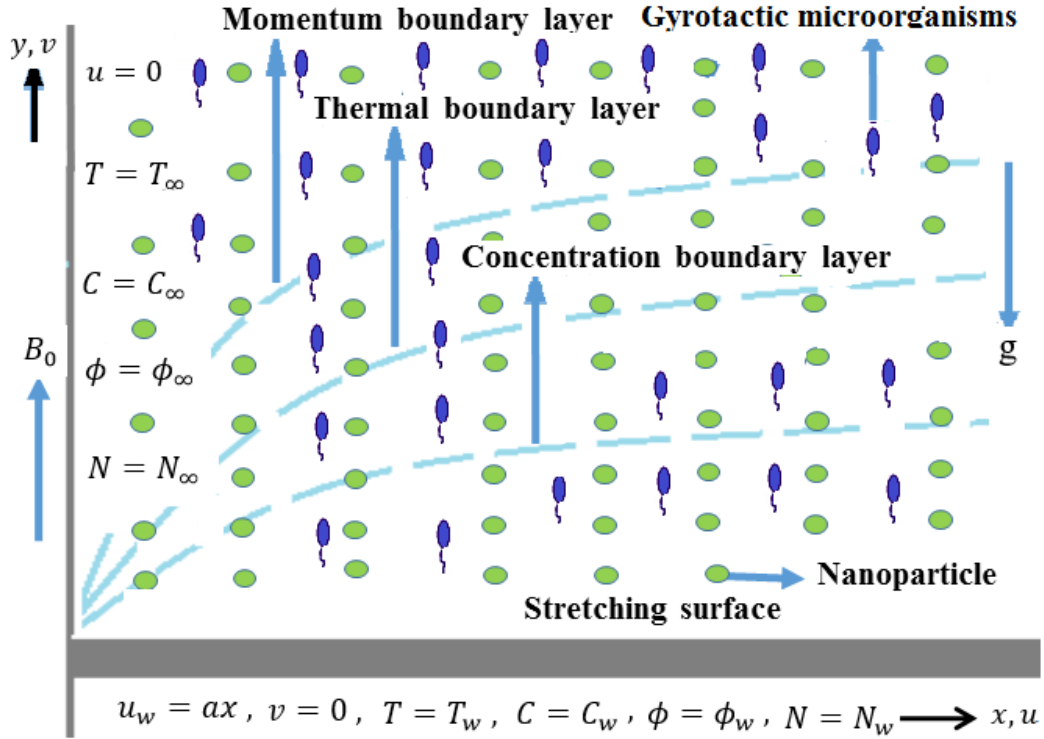


FIGURE 4.1: Geometry of the problem.

$$u \frac{\partial u}{\partial x} + v \frac{\partial v}{\partial y} = 0, \quad (4.5)$$

$$u \frac{\partial u}{\partial x} + v \frac{\partial u}{\partial y} = \nu(1-n) \frac{\partial^2 u}{\partial y^2} + \sqrt{2} \Gamma \nu n \frac{\partial u}{\partial x} \frac{\partial^2 u}{\partial y^2} + \left((1-\phi_\infty) \rho_f g \beta (T - T_\infty) - g(\rho_p - \rho_f)(\phi - \phi_\infty) - g(\rho_p - \rho_f) \gamma (N - N_\infty) \right) - \frac{\sigma_1}{\rho_f} B_0^2 u, \quad (4.6)$$

$$u \frac{\partial T}{\partial x} + v \frac{\partial T}{\partial y} = \alpha \frac{\partial^2 T}{\partial y^2} + \tau \left(D_B \left(\frac{\partial C}{\partial y} \right) \left(\frac{\partial T}{\partial y} \right) + \frac{D_T}{T_\infty} \left(\frac{\partial T}{\partial y} \right)^2 \right) + D_{TC} \left(\frac{\partial^2 C}{\partial y^2} \right), \quad (4.7)$$

$$u \frac{\partial C}{\partial x} + v \frac{\partial C}{\partial y} = D_s \frac{\partial^2 C}{\partial y^2} + D_{CT} \left(\frac{\partial^2 T}{\partial y^2} \right), \quad (4.8)$$

$$u \frac{\partial \phi}{\partial x} + v \frac{\partial \phi}{\partial y} = D_B \frac{\partial^2 \phi}{\partial y^2} + \frac{D_T}{T_\infty} \left(\frac{\partial^2 T}{\partial y^2} \right), \quad (4.9)$$

$$u \frac{\partial N}{\partial x} + v \frac{\partial N}{\partial y} = D_m \frac{\partial^2 N}{\partial y^2} - \frac{bW_\phi}{(\phi_w - \phi_\infty)} \frac{\partial}{\partial y} \left(N \frac{\partial \phi}{\partial y} \right). \quad (4.10)$$

The conditions at the boundary are:

$$\left. \begin{aligned} u = u_w = ax, \quad v = 0, \quad T = T_w, \quad C = C_w, \quad \phi = \phi_w, \quad N = N_w \quad \text{at } y = 0, \\ u \longrightarrow 0, \quad T \longrightarrow T_\infty, \quad C \longrightarrow C_\infty, \quad \phi \longrightarrow \phi_\infty, \quad N \longrightarrow N_\infty \quad \text{as } y \longrightarrow \infty. \end{aligned} \right\} \quad (4.11)$$

Here ρ_f and ρ_p depict the density fluid and nanoparticles respectively. By adopting the following similarity transformations [37], the PDEs are converted into ODEs.

$$\left. \begin{aligned} \eta = \sqrt{\frac{a}{\nu}}y, \quad u = axf'(\eta), \quad v = -\sqrt{a\nu}f(\eta), \quad \theta = \frac{T - T_\infty}{T_w - T_\infty}, \\ \gamma = \frac{C - C_\infty}{C_w - C_\infty}, \quad \xi = \frac{\phi - \phi_\infty}{\phi_w - \phi_\infty}, \quad \chi = \frac{N - N_\infty}{N_w - N_\infty}. \end{aligned} \right\} \quad (4.12)$$

The detailed procedure for conversion of Eqs. (4.1)-(4.6) into dimensionless ODEs are given below

- $\frac{\partial u}{\partial x} = \frac{\partial}{\partial x}(axf'(\eta)) = af'(\eta) \tag{4.13}$

- $\begin{aligned} \frac{\partial v}{\partial y} &= \frac{\partial}{\partial y}(-\sqrt{a\nu}f(\eta)) \\ &= -\sqrt{a\nu} \frac{\partial f'(\eta)}{\partial \eta} \frac{\partial \eta}{\partial y} \\ &= -\sqrt{a\nu} \sqrt{\frac{a}{\nu}} f'(\eta) \\ &= -af'(\eta). \end{aligned} \tag{4.14}$

- $\begin{aligned} \frac{\partial u}{\partial y} &= \frac{\partial u}{\partial \eta} \cdot \frac{\partial \eta}{\partial y} \\ &= \frac{\partial}{\partial \eta}(axf'(\eta)) \cdot \frac{\partial}{\partial y} \left(\sqrt{\frac{a}{\nu}}y \right) \\ &= ax \sqrt{\frac{a}{\nu}} f''(\eta). \end{aligned} \tag{4.15}$

- $\begin{aligned} \frac{\partial^2 u}{\partial y^2} &= \frac{\partial}{\partial y} \left(\frac{\partial u}{\partial y} \right) \\ &= ax \sqrt{\frac{a}{\nu}} \frac{\partial f''(\eta)}{\partial \eta} \cdot \frac{\partial \eta}{\partial y} \\ &= ax \left(\sqrt{\frac{a}{\nu}} \right)^2 f'''(\eta). \end{aligned} \tag{4.16}$

$$\bullet \left(\frac{\partial u}{\partial y} \right) \left(\frac{\partial^2 u}{\partial y^2} \right) = a^2 x^2 \left(\sqrt{\frac{a}{\nu}} \right)^3 f'' f''' \quad (4.17)$$

$$\bullet u \frac{\partial u}{\partial x} = ax f'(\eta) \cdot a f'(\eta),$$

$$= a^2 x f'^2. \quad (4.18)$$

$$\bullet v \frac{\partial u}{\partial y} = -\sqrt{a\nu} f(\eta) \cdot \frac{\partial u}{\partial \eta} \cdot \frac{\partial \eta}{\partial y}$$

$$= a^2 x f' f''. \quad (4.19)$$

$$\bullet \sqrt{2}\Gamma\nu n \left(\frac{\partial u}{\partial y} \right) \left(\frac{\partial^2 u}{\partial y^2} \right) = \sqrt{2}\Gamma\nu n a^2 x^2 \left(\sqrt{\frac{a}{\nu}} \right)^3 f'' f'''.$$

$$= \sqrt{2}\Gamma n a^3 x^2 \sqrt{\frac{a}{\nu}} f'' f'''. \quad (4.20)$$

$$\bullet \nu(1-n) \frac{\partial^2 u}{\partial y^2} = \nu(1-n) \left(\frac{a}{\nu} \right) ax f'''$$

$$= a^2 x(1-n) f'''. \quad (4.21)$$

$$\bullet \frac{\sigma_1}{\rho_f} B_0^2 u = \frac{\sigma_1}{\rho_f} B_0^2 ax f'. \quad (4.22)$$

$$\bullet (1 - \phi_\infty) \rho_f g \beta (T - T_\infty) - g(\rho_p - \rho_f)(\phi - \phi_\infty)$$

$$- g(\rho_p - \rho_f) \gamma (N - N_\infty)$$

$$= (1 - \phi_\infty) \rho_f g \beta (T_w - T_\infty) \left[\frac{T - T_\infty}{T_w - T_\infty} - \frac{g(\rho_p - \rho_f)(\phi - \phi_\infty)}{(1 - \phi_\infty) g \rho_f \beta (T_w - T_\infty)} \right.$$

$$\left. - \frac{g \gamma (\rho_p - \rho_f)(N - N_\infty)}{(1 - \phi_\infty) g \rho_f \beta (T_w - T_\infty)} \right]$$

$$= (1 - \phi_\infty) \rho_f g \beta (T_w - T_\infty) \left[\theta - \frac{(\rho_p - \rho_f)(\phi_w - \phi_\infty)}{(1 - \phi_\infty) \rho_f \beta (T_w - T_\infty)} \frac{\phi - \phi_\infty}{\phi_w - \phi_\infty} \right.$$

$$\left. - \frac{\gamma (\rho_p - \rho_f)(N_w - N_\infty)}{(1 - \phi_\infty) \rho_f \beta (T_w - T_\infty)} \frac{N - N_\infty}{N_w - N_\infty} \right]$$

$$= (1 - \phi_\infty) \rho_f g \beta (T_w - T_\infty) [\theta - Nr\xi - Nc\chi]. \quad (4.23)$$

$$\bullet T = (T_w - T_\infty)\theta(\eta) + T_\infty \quad (4.24)$$

$$\bullet \frac{\partial T}{\partial x} = \frac{\partial}{\partial x} ((T_w - T_\infty)\theta(\eta) + T_\infty) = 0. \quad (4.25)$$

$$\bullet u \frac{\partial T}{\partial x} = ax f'(\eta) \cdot 0 = 0. \quad (4.26)$$

$$\begin{aligned}
\bullet \frac{\partial T}{\partial y} &= (T_w - T_\infty) \frac{\partial \theta}{\partial \eta} \frac{\partial \eta}{\partial y} \\
&= (T_w - T_\infty) \theta' \frac{\partial \eta}{\partial y} \\
&= \sqrt{\frac{a}{\nu}} (T_w - T_\infty) \theta'.
\end{aligned} \tag{4.27}$$

$$\begin{aligned}
\bullet v \frac{\partial T}{\partial y} &= -\sqrt{a\nu} f(\eta) \cdot \sqrt{\frac{a}{\nu}} (T_w - T_\infty) \theta' \\
&= -a(T_w - T_\infty) f \theta'.
\end{aligned} \tag{4.28}$$

$$\begin{aligned}
\bullet \alpha \frac{\partial^2 T}{\partial y^2} &= \alpha \frac{\partial}{\partial y} \left(\frac{\partial T}{\partial y} \right) \\
&= \alpha \frac{\partial}{\partial y} \left(\sqrt{\frac{a}{\nu}} (T_w - T_\infty) \theta' \right) \\
&= \alpha \sqrt{\frac{a}{\nu}} (T_w - T_\infty) \frac{\partial \theta'}{\partial \eta} \frac{\partial \eta}{\partial y} \\
&= \alpha \sqrt{\frac{a}{\nu}} (T_w - T_\infty) \theta'' \frac{\partial \eta}{\partial y} \\
&= \alpha (T_w - T_\infty) \left(\sqrt{\frac{a}{\nu}} \right)^2 \theta''.
\end{aligned} \tag{4.29}$$

$$\bullet \frac{\partial C}{\partial y} = \sqrt{\frac{a}{\nu}} (C_w - C_\infty) \gamma'. \tag{4.30}$$

$$\begin{aligned}
\bullet D_B \frac{\partial T}{\partial y} \frac{\partial C}{\partial y} &= D_B \sqrt{\frac{a}{\nu}} (T_w - T_\infty) \theta' \sqrt{\frac{a}{\nu}} (C_w - C_\infty) \gamma' \\
&= D_B (T_w - T_\infty) \left(\frac{a}{\nu} \right) (C_w - C_\infty) \theta' \gamma'.
\end{aligned} \tag{4.31}$$

$$\begin{aligned}
\bullet \left(\frac{\partial T}{\partial y} \right)^2 &= \left((T_w - T_\infty) \sqrt{\frac{a}{\nu}} \theta' \right)^2 \\
&= (T_w - T_\infty)^2 \left(\frac{a}{\nu} \right) \theta'^2.
\end{aligned} \tag{4.32}$$

$$\bullet \frac{D_T}{T_\infty} \left(\frac{\partial T}{\partial y} \right)^2 = \frac{D_T}{T_\infty} (T_w - T_\infty)^2 \left(\frac{a}{\nu} \right) \theta'^2. \tag{4.33}$$

$$\begin{aligned}
\bullet D_{TC} \frac{\partial^2 C}{\partial y^2} &= D_{TC} \frac{\partial}{\partial y} \left(\frac{\partial C}{\partial y} \right) \\
&= D_{TC} \frac{\partial}{\partial y} \left(\sqrt{\frac{a}{\nu}} (C_w - C_\infty) \gamma' \right) \\
&= D_{TC} \left(\frac{a}{\nu} \right) (C_w - C_\infty) \gamma''.
\end{aligned} \tag{4.34}$$

$$\bullet C = (C_w - C_\infty) \gamma + C_\infty \tag{4.35}$$

$$\bullet \frac{\partial C}{\partial x} = \frac{\partial}{\partial x}((C_w - C_\infty)\gamma + C_\infty) = 0. \quad (4.36)$$

$$\bullet u \frac{\partial C}{\partial x} = ax f'(\eta).0 = 0. \quad (4.37)$$

$$\bullet \frac{\partial C}{\partial y} = \sqrt{\frac{a}{\nu}}(C_w - C_\infty)\gamma'. \quad (4.38)$$

$$\begin{aligned} \bullet D_B \frac{\partial^2 C}{\partial y^2} &= D_B \frac{\partial}{\partial y} \left(\sqrt{\frac{a}{\nu}}(C_w - C_\infty)\gamma' \right) \\ &= D_B \sqrt{\frac{a}{\nu}}(C_w - C_\infty) \frac{\partial \gamma'}{\partial \eta} \frac{\partial \eta}{\partial y} \\ &= D_B \left(\frac{a}{\nu} \right) (C_w - C_\infty)\gamma''. \end{aligned} \quad (4.39)$$

$$\begin{aligned} \bullet \frac{D_T}{T_\infty} \frac{\partial^2 T}{\partial y^2} &= \frac{D_T}{T_\infty} \frac{\partial}{\partial y} \left(\sqrt{\frac{a}{\nu}}(T_w - T_\infty)\theta' \right) \\ &= \frac{D_T}{T_\infty} \left(\frac{a}{\nu} \right) (T_w - T_\infty)\theta''. \end{aligned} \quad (4.40)$$

$$\begin{aligned} \bullet v \frac{\partial C}{\partial y} &= -\sqrt{a\nu}f \cdot \sqrt{\frac{a}{\nu}}(C_w - C_\infty)\gamma' \\ &= -a(C_w - C_\infty)f\gamma'. \end{aligned} \quad (4.41)$$

$$\bullet \phi = (\phi_w - \phi_\infty)\xi + \phi_\infty \quad (4.42)$$

$$\bullet \frac{\partial \phi}{\partial x} = \frac{\partial}{\partial x}((\phi_w - \phi_\infty)\xi + \phi_\infty) = 0. \quad (4.43)$$

$$\bullet u \frac{\partial \phi}{\partial x} = 0 \quad (4.44)$$

$$\bullet \frac{\partial \phi}{\partial y} = \sqrt{\frac{a}{\nu}}(\phi_w - \phi_\infty)\xi'. \quad (4.45)$$

$$\begin{aligned} \bullet v \frac{\partial \phi}{\partial y} &= -\sqrt{a\nu}f \cdot \sqrt{\frac{a}{\nu}}(\phi_w - \phi_\infty)\xi' \\ &= -a(\phi_w - \phi_\infty)f\xi'. \end{aligned} \quad (4.46)$$

$$\begin{aligned} \bullet \frac{\partial^2 \phi}{\partial y^2} &= \frac{\partial}{\partial y} \left(\sqrt{\frac{a}{\nu}}(\phi_w - \phi_\infty)\xi' \right) \\ &= \sqrt{\frac{a}{\nu}}(\phi_w - \phi_\infty) \frac{\partial \xi'}{\partial \eta} \frac{\partial \eta}{\partial y} \\ &= \left(\frac{a}{\nu} \right) (\phi_w - \phi_\infty)\xi''. \end{aligned} \quad (4.47)$$

$$\bullet D_s \frac{\partial^2 C}{\partial y^2} = D_s \left(\frac{a}{\nu} \right) (\gamma_w - \gamma_\infty)\gamma''. \quad (4.48)$$

$$\bullet D_{CT} \frac{\partial^2 T}{\partial y^2} = D_{CT} \left(\frac{a}{\nu} \right) (T_w - T_\infty) \theta''.$$
 (4.49)

$$\bullet N = (N_w - N_\infty) \chi + N_\infty.$$
 (4.50)

$$\bullet \frac{\partial N}{\partial x} = \frac{\partial N}{\partial \eta} \frac{\partial \eta}{\partial x} = 0.$$
 (4.51)

$$\bullet u \frac{\partial N}{\partial x} = 0.$$
 (4.52)

$$\begin{aligned} \bullet \frac{\partial N}{\partial y} &= \frac{\partial N}{\partial \eta} \frac{\partial \eta}{\partial y} \\ &= \sqrt{\frac{a}{\nu}} (N_w - N_\infty) \chi'. \end{aligned}$$
 (4.53)

$$\begin{aligned} \bullet v \frac{\partial N}{\partial y} &= -\sqrt{a\nu} f \cdot \sqrt{\frac{a}{\nu}} (N_w - N_\infty) \chi' \\ &= -a(N_w - N_\infty) f \chi'. \end{aligned}$$
 (4.54)

$$\begin{aligned} \bullet \frac{\partial^2 N}{\partial y^2} &= \frac{\partial}{\partial y} \left(\sqrt{\frac{a}{\nu}} (N_w - N_\infty) \chi' \right) \\ &= \sqrt{\frac{a}{\nu}} (N_w - N_\infty) \frac{\partial \chi'}{\partial \eta} \frac{\partial \eta}{\partial y} \\ &= \left(\frac{a}{\nu} \right) (N_w - N_\infty) \chi''. \end{aligned}$$
 (4.55)

$$\bullet D_m \frac{\partial^2 N}{\partial y^2} = D_m \left(\frac{a}{\nu} \right) (N_w - N_\infty) \chi''.$$
 (4.56)

$$\begin{aligned} \bullet \frac{\partial}{\partial y} \left(N \frac{\partial \phi}{\partial y} \right) &= N \frac{\partial^2 \phi}{\partial y^2} + \frac{\partial N}{\partial y} \frac{\partial \phi}{\partial y} \\ &= \left(\frac{a(\phi_w - \phi_\infty)}{\nu} \right) \left(((N_w - N_\infty) \chi \right. \\ &\quad \left. + N_\infty) \xi'' (N_w - N_\infty) \chi' \xi' \right) \end{aligned}$$
 (4.57)

$$\begin{aligned} \bullet \frac{bW_\phi}{(\phi_w - \phi_\infty)} \frac{\partial}{\partial y} \left(N \frac{\partial \phi}{\partial y} \right) &= \frac{bW_\phi \left(\frac{a}{\nu} \right)}{(\phi_w - \phi_\infty)} (\phi_w - \phi_\infty) \left((N_w - N_\infty) \chi' \xi' \right. \\ &\quad \left. + ((N_w - N_\infty) \chi + N_\infty) \xi'' \right). \end{aligned}$$
 (4.58)

The continuity equation (4.5) is straightforwardly satisfied by utilizing (4.13) and (4.14) as below.

$$\frac{\partial u}{\partial x} + \frac{\partial v}{\partial y} = a f'(\eta) - a f'(\eta) = 0.$$
 (4.59)

Using (4.15)-(4.23) in (4.6), the dimensionless momentum equation is given by

$$\begin{aligned}
a^2 x f'^2 - a^2 x f f'' &= a^2 x (1-n) f''' + \sqrt{2} \Gamma n a^3 x^2 \sqrt{\frac{a}{\nu}} f'' f''' - \frac{\sigma_1 B_0^2 a x f'}{\rho_f} \\
&\quad + (1 - \phi_\infty) \rho_f g \beta (T_w - T_\infty) [\theta - Nr\xi - Nc\chi] \\
\Rightarrow f'^2 - f f'' &= (1-n) f''' + \frac{(1 - \phi_\infty) \rho_f g \beta (T_w - T_\infty)}{a^2 x} [\theta - Nr\xi - Nc\chi] \\
&\quad + \sqrt{2} \Gamma n a x \sqrt{\frac{a}{\nu}} f'' f''' - \frac{\sigma_1 B_0^2}{\rho_f a} f' \\
\Rightarrow f'^2 - f f'' &= (1-n) f''' + \frac{(1 - \phi_\infty) \rho_f g \beta (T_w - T_\infty)}{a^2 x} [\theta - Nr\xi - Nc\chi] \\
&\quad + \sqrt{2} \Gamma n a x \sqrt{\frac{a}{\nu}} f'' f''' - \frac{\sigma_1 B_0^2}{\rho_f a} f' \\
\Rightarrow f'^2 - f f'' &= (1-n) f''' + \frac{(1 - \phi_\infty) \rho_f g \beta (T_w - T_\infty) x^3 \nu^2}{a^2 x^4 \nu^2} [\theta - Nr\xi - Nc\chi] \\
&\quad + \sqrt{2} \Gamma n a x \sqrt{\frac{a}{\nu}} f'' f''' - \frac{\sigma_1 B_0^2}{\rho_f a} f' \\
\Rightarrow f'^2 - f f'' &= (1-n) f''' + \frac{\left(\frac{(1 - \phi_\infty) \rho_f g \beta (T_w - T_\infty) x^3}{\nu^2} \right)}{\left(\frac{a^2 x^4}{\nu^2} \right)} [\theta - Nr\xi - Nc\chi] \\
&\quad + \sqrt{2} \Gamma n a x \sqrt{\frac{a}{\nu}} f'' f''' - \frac{\sigma_1 B_0^2}{\rho_f a} f' \\
\Rightarrow 0 &= (1-n) f''' + \frac{Gr}{Re_x^2} (\theta - Nr\xi - Nc\chi) - f'^2 + f f'' + \sqrt{2} \Gamma n a x \sqrt{\frac{a}{\nu}} f'' f''' \\
&\quad - \frac{\sigma_1 B_0^2}{\rho_f a} f' \\
\Rightarrow ((1-n) + nWe f'') f''' &+ \Lambda (\theta - Nr\xi - Nc\chi) - f'^2 + f f'' \\
&- M f' = 0. \tag{4.60}
\end{aligned}$$

Temperature equation (4.7) after using (4.24)-(4.34) is given by

$$\begin{aligned}
-a(T_w - T_\infty) f \theta' &= \left(\frac{a}{\nu} \right) \left(\alpha (T_w - T_\infty) \theta'' + \left(\tau D_B (T_w - T_\infty) (C_w - C_\infty) \theta' \gamma' \right. \right. \\
&\quad \left. \left. + \frac{\tau D_T}{T_\infty} (T_w - T_\infty)^2 \theta'^2 \right) + D_{TC} (C_w - C_\infty) \gamma'' \right) \\
\Rightarrow -f \theta' &= \left(\frac{\tau \left(\frac{a}{\nu} \right) D_B (C_w - C_\infty) \theta' \gamma'}{a} + \frac{\tau \frac{D_T}{T_\infty} \left(\frac{a}{\nu} \right) (T_w - T_\infty)^2 \theta'^2}{a (T_w - T_\infty)} \right) \\
&\quad + \frac{\alpha}{\nu} \theta'' + \frac{D_{TC} \left(\frac{a}{\nu} \right) (C_w - C_\infty) \gamma''}{a (T_w - T_\infty)}
\end{aligned}$$

$$\begin{aligned}
\Rightarrow 0 &= \frac{\theta''}{Pr} + \left(\frac{\tau D_B (C_w - C_\infty) \theta' \gamma'}{\nu} + \frac{\tau \frac{D_T}{T_\infty} (T_w - T_\infty) \theta'^2}{\nu} \right) \\
&\quad + \frac{D_{TC} (C_w - C_\infty) \gamma''}{\nu (T_w - T_\infty)} + f \theta'. \\
\Rightarrow \theta'' + Pr (Nb \theta' \gamma' + Nt \theta'^2) + Pr Nd \gamma'' + Pr f \theta' &= 0. \tag{4.61}
\end{aligned}$$

After using derivatives (4.35)-(4.41) in the concentration equation (4.8) give

$$\begin{aligned}
-a(C_w - C_\infty) f \gamma' &= D_B \left(\frac{a}{\nu} \right) (C_w - C_\infty) \gamma'' + \frac{D_T}{T_\infty} \left(\frac{a}{\nu} \right) (T_w - T_\infty) \theta'' \\
\Rightarrow -f \gamma' &= \frac{D_B \left(\frac{a}{\nu} \right) (C_w - C_\infty)}{a(C_w - C_\infty)} \gamma'' + \frac{\frac{D_T}{T_\infty} \left(\frac{a}{\nu} \right) (T_w - T_\infty)}{a(C_w - C_\infty)} \theta'' \\
\Rightarrow -f \gamma' &= \frac{D_B}{\nu} \gamma'' + \frac{\frac{D_T (T_w - T_\infty)}{T_\infty}}{(C_w - C_\infty)} \theta'' \\
\Rightarrow 0 &= \gamma'' + \frac{\frac{D_T}{T_\infty} \left(\frac{a}{\nu} \right) (T_w - T_\infty)}{\frac{D_B}{\nu} (C_w - C_\infty)} \theta'' + \left(\frac{\nu}{D_B} \right) f \gamma' \\
\Rightarrow 0 &= \left(\frac{\tau}{\tau} \right) \gamma'' + \left(\frac{\tau}{\tau} \right) \frac{\frac{D_T}{T_\infty} \left(\frac{a}{\nu} \right) (T_w - T_\infty)}{\frac{D_B}{\nu} (C_w - C_\infty)} \theta'' + \left(\frac{\tau}{\tau} \right) \left(\frac{\nu}{D_B} \right) f \gamma' \\
\Rightarrow 0 &= \gamma'' + \frac{\tau \frac{D_T}{T_\infty} \left(\frac{a}{\nu} \right) (T_w - T_\infty)}{\tau \left(\frac{D_B}{\nu} \right) (C_w - C_\infty)} + \left(\frac{\nu}{D_B} \right) f \gamma' \\
\Rightarrow 0 &= \gamma'' + \frac{Nt}{Nb} \theta'' + \frac{\nu}{\alpha} \frac{\alpha}{D_B} f \gamma' \\
\Rightarrow \gamma'' + \frac{Nt}{Nb} \theta'' + Pr Ln f \gamma' &= 0. \tag{4.62}
\end{aligned}$$

Using (4.42)-(4.49), the dimensionless form of (4.9) takes the form

$$\begin{aligned}
-a(\phi_w - \phi_\infty) f \xi' &= D_s \left(\frac{a}{\nu} \right) (\phi_w - \phi_\infty) \xi'' + D_{CT} \left(\frac{a}{\nu} \right) (T_w - T_\infty) \theta'' \\
\Rightarrow -f \xi' &= \frac{D_s \left(\frac{a}{\nu} \right) (\phi_w - \phi_\infty)}{a(\phi_w - \phi_\infty)} \xi'' + \frac{D_{CT} \left(\frac{a}{\nu} \right) (T_w - T_\infty)}{a(\phi_w - \phi_\infty)} \theta'' \\
\Rightarrow -f \xi' &= \frac{D_s}{\nu} \xi'' + \left(\frac{D_{CT}}{\nu} \right) \left(\frac{T_w - T_\infty}{(\phi_w - \phi_\infty)} \right) \theta'' \\
\Rightarrow - \left(\frac{\nu}{D_s} \right) f \xi' &= \xi'' + \left(\frac{D_{CT}}{\nu} \right) \frac{\nu}{D_s} \left(\frac{T_w - T_\infty}{(\phi_w - \phi_\infty)} \right) \theta'' \\
\Rightarrow -Pr Le f \xi' &= \xi'' + Pr Ld \theta'' \\
\Rightarrow \xi'' + Pr Ld \theta'' + Pr Le f \xi' &= 0. \tag{4.63}
\end{aligned}$$

The motile gyrotactic microorganisms equation (4.10), using (4.50)-(4.58) gets the following form

$$\begin{aligned}
D_m \left(\frac{a}{\nu} \right) (N_w - N_\infty) \chi'' &= -a(N_w - N_\infty) f \chi' + \frac{bW_c \left(\frac{a}{\nu} \right)}{(\phi_w - \phi_\infty)} (\phi_w - \phi_\infty) \\
&\quad \left(((N_w - N_\infty)\chi + N_\infty) \xi'' + (N_w - N_\infty) \chi' \xi' \right) \\
\Rightarrow D_m \left(\frac{a}{\nu} \right) (N_w - N_\infty) \chi'' - bW_c \left(\frac{a}{\nu} \right) \left(((N_w - N_\infty)\chi + N_\infty) \xi'' + \right. \\
&\quad \left. (N_w - N_\infty) \chi' \xi' \right) + a(N_w - N_\infty) f \chi' = 0 \\
\Rightarrow \chi'' - \frac{bW_c \left(\frac{a}{\nu} \right) (N_w - N_\infty)}{D_m \left(\frac{a}{\nu} \right) (N_w - N_\infty)} \left(\left(\chi + \left(\frac{N_\infty}{N_w - N_\infty} \right) \right) \xi'' + \chi' \xi' \right) + \\
&\quad \frac{a(N_w - N_\infty)}{D_m \left(\frac{a}{\nu} \right) (N_w - N_\infty)} f \chi' = 0 \\
\Rightarrow \chi'' - \frac{bW_c}{D_m} ((\chi + \sigma) \xi'' + \chi' \xi') + \frac{1}{\frac{D_m}{\nu}} f \chi' = 0 \\
\Rightarrow \chi'' - Pe ((\chi + \sigma) \xi'' + \chi' \xi') + Lbf \chi' = 0. \tag{4.64}
\end{aligned}$$

The dimensionless form of the boundary conditions (4.11), is achieved through the following procedure

$$\begin{aligned}
\bullet u = ax &\quad \text{at } y = 0 \\
\Rightarrow ax f'(\eta) = ax &\quad \text{at } \eta = 0 \\
\Rightarrow f'(\eta) = 1 &\quad \text{at } \eta = 0. \tag{4.65}
\end{aligned}$$

$$\begin{aligned}
\bullet v = 0 &\quad \text{at } y = 0 \\
\Rightarrow -\sqrt{a\nu} f(\eta) = 0 &\quad \text{at } \eta = 0 \\
\Rightarrow -f(\eta) = 0. &\quad \text{at } \eta = 0 \tag{4.66}
\end{aligned}$$

$$\begin{aligned}
\bullet T(x, y) = T_w &\quad \text{at } y = 0 \\
\Rightarrow (T_w - T_\infty) \theta(\eta) + T_\infty = T_w &\quad \text{at } \eta = 0 \\
\Rightarrow (T_w - T_\infty) \theta(\eta) = T_w - T_\infty &\quad \text{at } \eta = 0 \\
\Rightarrow \theta = 1. &\quad \text{at } \eta = 0 \tag{4.67}
\end{aligned}$$

$$\begin{aligned}
\bullet C(x, y) = C_w &\quad \text{at } y = 0 \\
\Rightarrow (C_w - C_\infty) \gamma(\eta) + C_\infty = C_w &\quad \text{at } \eta = 0 \\
\Rightarrow (C_w - C_\infty) \gamma(\eta) = C_w - C_\infty &\quad \text{at } \eta = 0 \\
\Rightarrow \gamma = 1. &\quad \text{at } \eta = 0 \tag{4.68}
\end{aligned}$$

$$\begin{aligned}
\bullet \phi(x, y) &= \phi_w && \text{at } y = 0 \\
&\Rightarrow (\phi_w - \phi_\infty)\xi(\eta) + \phi_\infty = \phi_w && \text{at } \eta = 0 \\
&\Rightarrow (\phi_w - \phi_\infty)\xi(\eta) = \phi_w - \phi_\infty && \text{at } \eta = 0 \\
&\Rightarrow \xi = 1. && \text{at } \eta = 0
\end{aligned} \tag{4.69}$$

$$\begin{aligned}
\bullet N(x, y) &= N_w && \text{at } y = 0 \\
&\Rightarrow (N_w - N_\infty)\chi(\eta) + N_\infty = N_w && \text{at } \eta = 0 \\
&\Rightarrow (N_w - N_\infty)\chi(\eta) = N_w - N_\infty && \text{at } \eta = 0 \\
&\Rightarrow \chi = 1. && \text{at } \eta = 0
\end{aligned} \tag{4.70}$$

$$\begin{aligned}
\bullet u(x) &\rightarrow 0 && \text{at } y \rightarrow \infty \\
&\Rightarrow axf'(\eta) \rightarrow 0 && \text{at } \eta \rightarrow \infty \\
&\Rightarrow f' \rightarrow 0. && \text{at } \eta \rightarrow \infty
\end{aligned} \tag{4.71}$$

$$\begin{aligned}
\bullet T(x, y) &\rightarrow T_\infty && \text{at } y \rightarrow \infty \\
&\Rightarrow (T_w - T_\infty)\theta(\eta) + T_\infty \rightarrow T_\infty && \text{at } \eta \rightarrow \infty \\
&\Rightarrow (T_w - T_\infty)\theta(\eta) \rightarrow T_\infty - T_\infty && \text{at } \eta \rightarrow \infty \\
&\Rightarrow (T_w - T_\infty)\theta(\eta) \rightarrow 0 && \text{at } \eta \rightarrow \infty \\
&\Rightarrow \theta \rightarrow 0. && \text{at } \eta \rightarrow \infty
\end{aligned} \tag{4.72}$$

$$\begin{aligned}
\bullet C(x, y) &\rightarrow C_\infty && \text{at } y \rightarrow \infty \\
&\Rightarrow (C_w - C_\infty)\gamma(\eta) + C_\infty \rightarrow C_\infty && \text{at } \eta \rightarrow \infty \\
&\Rightarrow (C_w - C_\infty)\gamma(\eta) \rightarrow C_\infty - C_\infty && \text{at } \eta \rightarrow \infty \\
&\Rightarrow (C_w - C_\infty)\gamma(\eta) \rightarrow 0 && \text{at } \eta \rightarrow \infty \\
&\Rightarrow \gamma \rightarrow 0. && \text{at } \eta \rightarrow \infty
\end{aligned} \tag{4.73}$$

$$\begin{aligned}
\bullet \phi(x, y) &\rightarrow \phi_\infty && \text{at } y \rightarrow \infty \\
&\Rightarrow (\phi_w - \phi_\infty)\gamma(\eta) + \phi_\infty \rightarrow \phi_\infty && \text{at } \eta \rightarrow \infty \\
&\Rightarrow (\phi_w - \phi_\infty)\xi(\eta) \rightarrow \phi_\infty - \phi_\infty && \text{at } \eta \rightarrow \infty \\
&\Rightarrow (\phi_w - \phi_\infty)\xi(\eta) \rightarrow 0 && \text{at } \eta \rightarrow \infty \\
&\Rightarrow \xi \rightarrow 0. && \text{at } \eta \rightarrow \infty
\end{aligned} \tag{4.74}$$

$$\begin{aligned}
\bullet \quad & N(x, y) \rightarrow N_\infty && \text{at } y \rightarrow \infty \\
& \Rightarrow (N_w - C_\infty)\chi(\eta) + N_\infty \rightarrow N_\infty && \text{at } \eta \rightarrow \infty \\
& \Rightarrow (N_w - N_\infty)\chi(\eta) \rightarrow N_\infty - N_\infty && \text{at } \eta \rightarrow \infty \\
& \Rightarrow \chi \rightarrow 0. && \text{at } \eta \rightarrow \infty
\end{aligned} \tag{4.75}$$

The dimensionless expression of drag force C_{fx} is given by

$$C_{fx} = \frac{\tau_w}{\frac{1}{2}\rho U_w^2},$$

where

$$\begin{aligned}
\tau_w &= \mu(1-n) \left(\frac{\partial u}{\partial y} \right) + \mu \frac{n\Gamma}{\sqrt{2}} \left(\frac{\partial u}{\partial y} \right)^2, \\
&= \mu(1-n)ax \sqrt{\frac{a}{\nu}} f'' + \mu \frac{n\Gamma}{\sqrt{2}} \left(ax \sqrt{\frac{a}{\nu}} \right)^2 f''^2.
\end{aligned}$$

Therefore,

$$\begin{aligned}
C_{fx} &= \frac{\mu(1-n)ax \sqrt{\frac{a}{\nu}} f'' + \mu \frac{n\Gamma}{\sqrt{2}} \left(ax \sqrt{\frac{a}{\nu}} \right)^2 f''^2}{\frac{1}{2}\rho a^2 x^2}, \\
&= \frac{\sqrt{\frac{a}{\nu}} x \left(\mu(1-n)af'' + \mu \frac{n\Gamma}{\sqrt{2}} \sqrt{\frac{a}{\nu}} a^2 x f''^2 \right)}{\frac{1}{2}\rho a^2 x^2}, \\
&= \frac{2\sqrt{\frac{a}{\nu}} ax \mu \left((1-n)f'' + \frac{n\Gamma}{\sqrt{2}} \sqrt{\frac{a^3 x^2}{\nu}} f''^2 \right)}{\rho a^2 x^2}, \\
\Rightarrow \frac{C_{fx}}{2} &= \frac{\sqrt{\frac{a}{\nu}} ax \mu \left((1-n)f'' + \frac{n\Gamma}{\sqrt{2}} \sqrt{\frac{a^3 x^2}{\nu}} f''^2 \right)}{\rho a^2 x^2}. \\
\Rightarrow \frac{C_{fx}}{2} \sqrt{Re_x} &= \frac{\sqrt{\frac{a}{\nu}} x \sqrt{\frac{a}{\nu}} ax \mu \left((1-n)f'' + \frac{n\Gamma}{\sqrt{2}} \sqrt{\frac{a^3 x^2}{\nu}} f''^2 \right)}{\rho a^2 x^2}, \\
&= \frac{\sqrt{\frac{a}{\nu}} x \sqrt{\frac{a}{\nu}} ax \mu \left((1-n)f'' + \frac{n\Gamma}{2} \sqrt{\frac{2a^3 x^2}{\nu}} f''^2 \right)}{\rho a^2 x^2}, \\
&= \frac{a^2 x^2 \nu \mu \left((1-n)f'' + \frac{n}{2} We f''^2 \right)}{\rho a^2 x^2}, \\
&= \frac{\mu}{\rho \nu} \left((1-n)f'' + \frac{n}{2} We f''^2 \right), \\
&= \left((1-n)f'' + \frac{n}{2} We f''^2 \right).
\end{aligned} \tag{4.76}$$

The dimensionless form of Nusselt amount is given by

$$Nu_x = \frac{xq_w}{\kappa(T_w - T_\infty)}, \text{ where}$$

$$q_w = -\kappa \frac{\partial T}{\partial y}$$

$$= -\kappa \sqrt{\frac{a}{\nu}} (T_w - T_\infty) \theta'.$$

Therefore,

$$Nu_x = \frac{-x\kappa \sqrt{\frac{a}{\nu}} (T_w - T_\infty) \theta'}{\kappa(T_w - T_\infty)}$$

$$= \sqrt{\frac{a}{\nu}} x \frac{-\kappa(T_w - T_\infty) \theta'}{\kappa(T_w - T_\infty)}$$

$$= -\sqrt{Re_x} \theta', \quad (4.77)$$

solutal Sherwood number can be mathematically expressed as

$$Sh_x = \frac{xq_m}{D_B(C_w - C_\infty)}, \text{ where}$$

$$q_m = -D_B \frac{\partial C}{\partial y},$$

$$= -D_B \sqrt{\frac{a}{\nu}} (C_w - C_\infty) \phi'.$$

Therefore,

$$Sh_x = \frac{-xD_B \sqrt{\frac{a}{\nu}} (C_w - C_\infty) \phi'}{D_B(C_w - C_\infty)}$$

$$= -\sqrt{Re_x} \phi'. \quad (4.78)$$

The dimensionless form of the motile gyrotactic microorganisms is given by

$$Nn_x = \frac{xq_n}{D_n(N_w - N_\infty)}, \text{ where}$$

$$q_n = -D_n \frac{\partial N}{\partial y},$$

$$= -D_n \sqrt{\frac{a}{\nu}} (N_w - N_\infty) \chi'.$$

Therefore,

$$Nn_x = \frac{-xD_n \sqrt{\frac{a}{\nu}} (N_w - N_\infty) \chi'}{D_n(N_w - N_\infty)}$$

$$= \sqrt{\frac{a}{\nu}} x \frac{-D_n(N_w - N_\infty) \chi'}{D_n(N_w - N_\infty)}$$

$$= -\sqrt{Re_x} \chi'. \quad (4.79)$$

Distinct physical parameters arising during the conversion of PDEs into ODEs are:

$$\left. \begin{aligned}
 We &= \Gamma x \sqrt{\frac{2a^3}{\nu}}, \quad Nb = \frac{\tau D_B}{\nu} (C_w - C_\infty), \quad Nt = \frac{D_T \tau}{T_\infty \nu} (T_w - T_\infty), \\
 Pr &= \frac{\nu}{\alpha}, \quad Le = \frac{\alpha}{D_s}, \quad Lb = \frac{\alpha}{D_m}, \quad Ln = \frac{\alpha}{D_B}, \quad Pe = \frac{bW_c}{D_m}, \quad Ld = \frac{\alpha}{D_m}, \\
 Nd &= \frac{\alpha D_{TC} (C_w - C_\infty)}{\nu (T_w - T_\infty)}, \quad M = \frac{\sigma B_0^2}{a \rho_f}, \quad Nr = \frac{(\rho_p - \rho_f)(\phi_w - \phi_\infty)}{(1 - \phi_\infty) \rho_f \beta (T_w - T_\infty)}, \\
 G_T &= \frac{x^3 (1 - C_\infty) \rho_f g \beta_T (T_w - T_\infty)}{\nu^2}, \quad Nc = \frac{(\rho_p - \rho_f) \gamma (N_w - N_\infty)}{(1 - \phi_\infty) \rho_f \beta (T_w - T_\infty)}, \\
 \Lambda &= \frac{G_T}{Re_x^2}, \quad \tau = \frac{\rho C_p}{\rho C_f}, \quad \sigma = \frac{N_\infty}{N_w - N_\infty}
 \end{aligned} \right\} \quad (4.80)$$

4.2 Solution Methodology

The dimensionless system of ODEs along with boundary conditions can be tackled numerically with the utilization of well established scheme called Keller-box method. There are four steps involved in Keller box method to obtained the solution of an equation. These factors are mentioned below

1. Transform the system of equations into first order system.
2. Convert first order system od equations into difference equations utilizing central differences.
3. Linearize system of equations and furthermore arrange them in matrix vector form.
4. At the end solve those linear system of equations with block-tridiagonal elimination method.

In the light of above mentioned points the dimensionless ODEs (4.56)-(4.60) in association with the boundary conditions (4.61)-(4.71) have been handled with the help of Keller box technique [121] for distinguished parameters emerged during the

numerical simulation of the problem. This numerical technique is quite effective and flexible to solve parabolic type boundary value problems of any order, unconditionally stable and attains remarkable accuracy. Keller box scheme [121] is numerically more stable and converges using less iterations as compared to other numerical techniques. Figure 4.2 describes the flow chart procedure of Keller box method. By adopting the new variables

$$f' = z_1, z_1' = z_2, \theta' = z_3, \gamma' = z_4, \xi' = z_5, \chi' = z_6, \tag{4.81}$$

The dimensionless Eqs. (4.56)-(4.60) mentioned above are converted into first order ODEs given below:

$$\begin{aligned} &((1 - n) + nWez_1)z_2 - z_1^2 + fz_2 - M^2z_1 + \\ &\Lambda(\theta - Nr\xi - Nc\chi) = 0, \end{aligned} \tag{4.82}$$

$$z_3' + Pr(fz_3 + Nbz_3z_5) + Ntz_3^2 + Ndz_4' = 0, \tag{4.83}$$

$$z_4' + PrLefz_4 + LdPrz_3' = 0, \tag{4.84}$$

$$z_5' + PrLnz_5 + \frac{Nt}{Nb}z_3' = 0, \tag{4.85}$$

$$z_6' + Lbfz_6 - Pe(z_6z_5 + z_5'(\sigma + \chi)) = 0. \tag{4.86}$$

The surface boundary conditions are given below:

$$\left. \begin{aligned} &f(\eta) = 0, \quad z_1(\eta) = 1, \quad \theta(\eta) = 1, \quad \gamma(\eta) = 1, \\ &\xi(\eta) = 1, \quad \chi(\eta) = 1 \quad \text{at} \quad \eta = 0, \\ &z_1(\eta) \rightarrow 0, \quad \theta(\eta) \rightarrow 0, \quad \gamma(\eta) \rightarrow 0, \quad \xi(\eta) \rightarrow 0, \\ &\chi(\eta) \rightarrow 0 \quad \text{at} \quad \eta \rightarrow \infty. \end{aligned} \right\} \tag{4.87}$$

Figure 4.3 portrays the mesh structure for central difference approximations. The stepping procedure for the selection of nodes in the case of domain discretization is mentioned given below:

$$\eta_0 = 0, \quad \eta_j = \eta_{j-1} + h_j, \quad j = 1, 2, 3, \dots, J, \quad \eta_J = \eta_{max}. \tag{4.88}$$

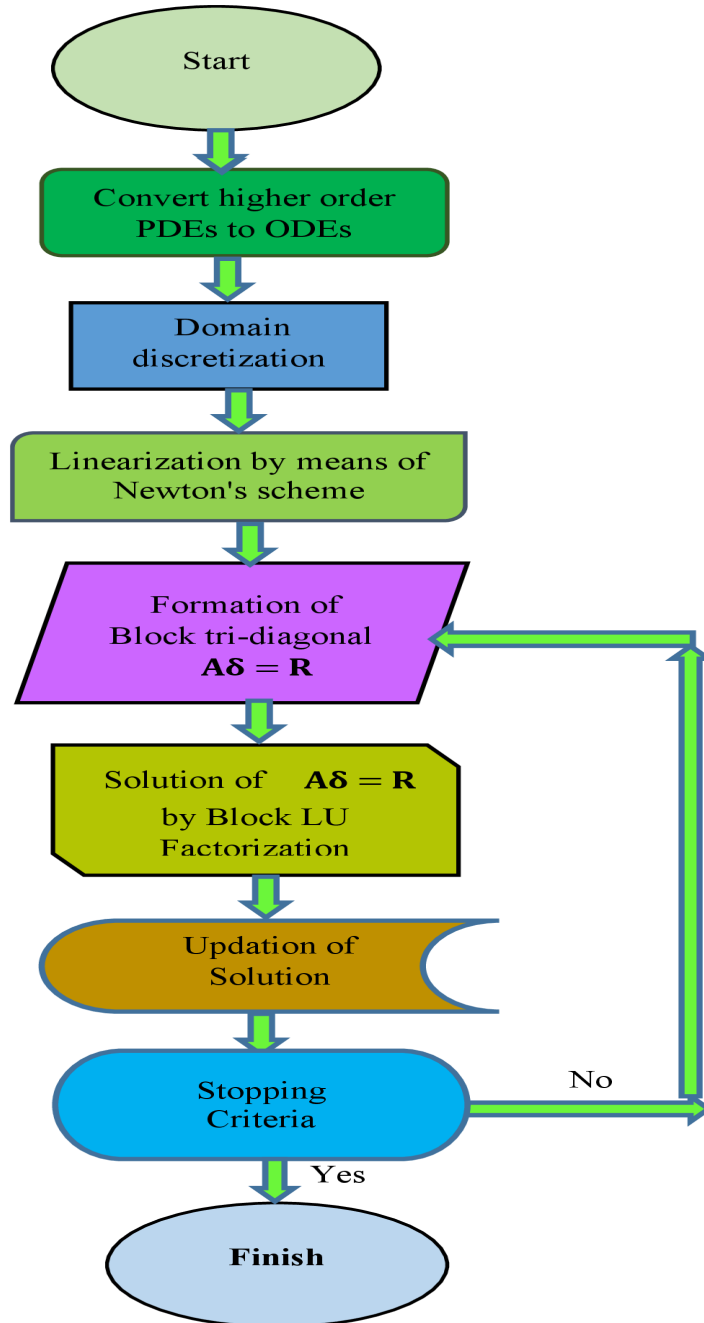


FIGURE 4.2: Mechanism of the present technique

The derivatives of Eqs. (4.78)-(4.82) are approximated by employing the central difference at the midpoint $\eta_{j-\frac{1}{2}}$ mentioned underneath

$$\frac{f_j - f_{j-1}}{h_j} = \frac{(z_1)_j + (z_1)_{j-1}}{2}, \quad (4.89)$$

$$\frac{(z_1)_j - (z_1)_{j-1}}{h_j} = \frac{(z_2)_j + (z_2)_{j-1}}{2}, \quad (4.90)$$

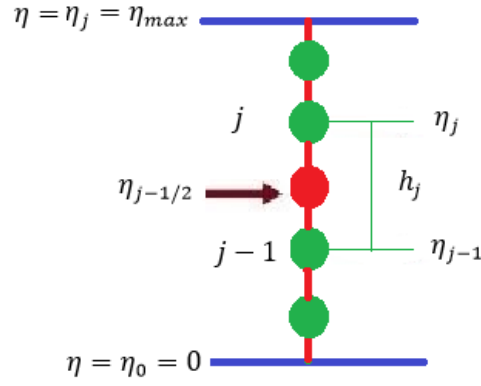


FIGURE 4.3: One-dimensional mesh for difference approximations.

$$\frac{\theta_j - \theta_{j-1}}{h_j} = \frac{(z_3)_j + (z_3)_{j-1}}{2}, \quad (4.91)$$

$$\frac{\gamma_j - \gamma_{j-1}}{h_j} = \frac{(z_4)_j + (z_4)_{j-1}}{2}, \quad (4.92)$$

$$\frac{\xi_j - \xi_{j-1}}{h_j} = \frac{(z_5)_j + (z_5)_{j-1}}{2}, \quad (4.93)$$

$$\frac{\chi_j - \chi_{j-1}}{h_j} = \frac{(z_6)_j + (z_6)_{j-1}}{2}, \quad (4.95)$$

$$\begin{aligned} & \left[(1-n) + nWe \left(\frac{(z_2)_j + (z_2)_{j-1}}{2} \right) \right] z_2 - \left(\frac{(z_1)_j + (z_1)_{j-1}}{2} \right)^2 \\ & - M^2 \left(\frac{(z_1)_j + (z_1)_{j-1}}{2} \right) + \left(\frac{f_j + f_{j-1}}{2} \right) \left(\frac{(z_2)_j + (z_2)_{j-1}}{2} \right) \\ & + \Lambda \left(\frac{\theta_j + \theta_{j-1}}{2} \right) - \Lambda Nr \left(\frac{\xi_j + \xi_{j-1}}{2} \right) - \Lambda Nc \left(\frac{\chi_j + \chi_{j-1}}{2} \right) = 0. \end{aligned} \quad (4.96)$$

$$\begin{aligned} & \left(\frac{(z_3)_j + (z_3)_{j-1}}{h_j} \right) + Pr \left(\frac{(z_3)_j + (z_3)_{j-1}}{2} \right) \left(\frac{f_j + f_{j-1}}{2} \right) \\ & + PrNb \left(\frac{(z_3)_j + (z_3)_{j-1}}{2} \right) \left(\frac{(z_5)_j + (z_5)_{j-1}}{2} \right) \\ & + Nt \left(\frac{(z_3)_j + (z_3)_{j-1}}{2} \right)^2 + Nd \left(\frac{(z_4)_j + (z_4)_{j-1}}{2} \right) = 0. \end{aligned} \quad (4.97)$$

$$\begin{aligned} & \left(\frac{(z_4)_j + (z_4)_{j-1}}{h_j} \right) + PrLd \left(\frac{(z_3)_j + (z_3)_{j-1}}{h_j} \right) \\ & + PrLe \left(\frac{f_j + f_{j-1}}{2} \right) \left(\frac{(z_4)_j + (z_4)_{j-1}}{2} \right) = 0. \end{aligned} \quad (4.98)$$

$$\begin{aligned} & \left(\frac{(z_5)_j + (z_5)_{j-1}}{h_j} \right) + \left(\frac{N_t}{N_b} \right) \left(\frac{(z_3)_j + (z_3)_{j-1}}{h_j} \right) \\ & + PrLn \left(\frac{f_j + f_{j-1}}{2} \right) \left(\frac{(z_5)_j + (z_5)_{j-1}}{2} \right) = 0. \end{aligned} \quad (4.99)$$

$$\begin{aligned} & \left(\frac{(z_6)_j + (z_6)_{j-1}}{h_j} \right) + Lb \left(\frac{(z_6)_j + (z_6)_{j-1}}{2} \right) \\ & \left(\frac{f_j + f_{j-1}}{2} \right) - Pe \left(\frac{(z_6)_j + (z_6)_{j-1}}{2} \right) \\ & \left(\frac{(z_5)_j + (z_5)_{j-1}}{2} \right) - Pe \left(\frac{(z_5)_j + (z_5)_{j-1}}{h_j} \right) \\ & \left(\sigma + \left(\frac{\chi_j + \chi_{j-1}}{2} \right) \right) = 0. \end{aligned} \quad (4.100)$$

Equations (4.91)-(4.95) are nonlinear in nature and will be linearized with the utilization of any well established iterative scheme termed as Newton's method which is used to find the roots of a given equation.

To achieve this objective of linerization, Newton iterative scheme is implemented with the philosophy illustrated in the equations mentioned below.

The detailed procedure for the linerization of discretized equations are given by procedure mentioned underneath

$$\left. \begin{aligned} f_j^{n+1} &= f_j^n + \delta f_j^n, & (z_1)_j^{n+1} &= (z_1)_j^n + \delta(z_1)_j^n, \\ (z_2)_j^{n+1} &= (z_2)_j^n + \delta(z_2)_j^n, & (z_3)_j^{n+1} &= (z_3)_j^n + \delta(z_3)_j^n, \\ (z_4)_j^{n+1} &= (z_4)_j^n + \delta(z_4)_j^n, & (z_5)_j^{n+1} &= (z_5)_j^n + \delta(z_5)_j^n, \\ (z_6)_j^{n+1} &= (z_6)_j^n + \delta(z_6)_j^n, & \theta_j^{n+1} &= \theta_j^n + \delta\theta_j^n, \\ \gamma_j^{n+1} &= \gamma_j^n + \delta\gamma_j^n, & \xi_j^{n+1} &= \xi_j^n + \delta\xi_j^n \\ \chi_j^{n+1} &= \chi_j^n + \delta\chi_j^n. \end{aligned} \right\} \quad (4.96)$$

By putting (4.96) into (4.85)-(4.95) and moreover ignoring the quadratic as well as higher order terms in δf_j^n , etc.

The power n mentioned in the above equations represent the iteration.

The linear tri-diagonal matrix can be written as

$$[A][\delta] = [R] \quad (4.101)$$

TABLE 4.1: Numerical comparison of the obtained results with Khan et al. [37] for various values of Pr .

Pr	Khan et al. [37]	Present study
0.00	1.0000	1.00000
0.25	1.1180	1.11802
1.00	1.4142	1.41411

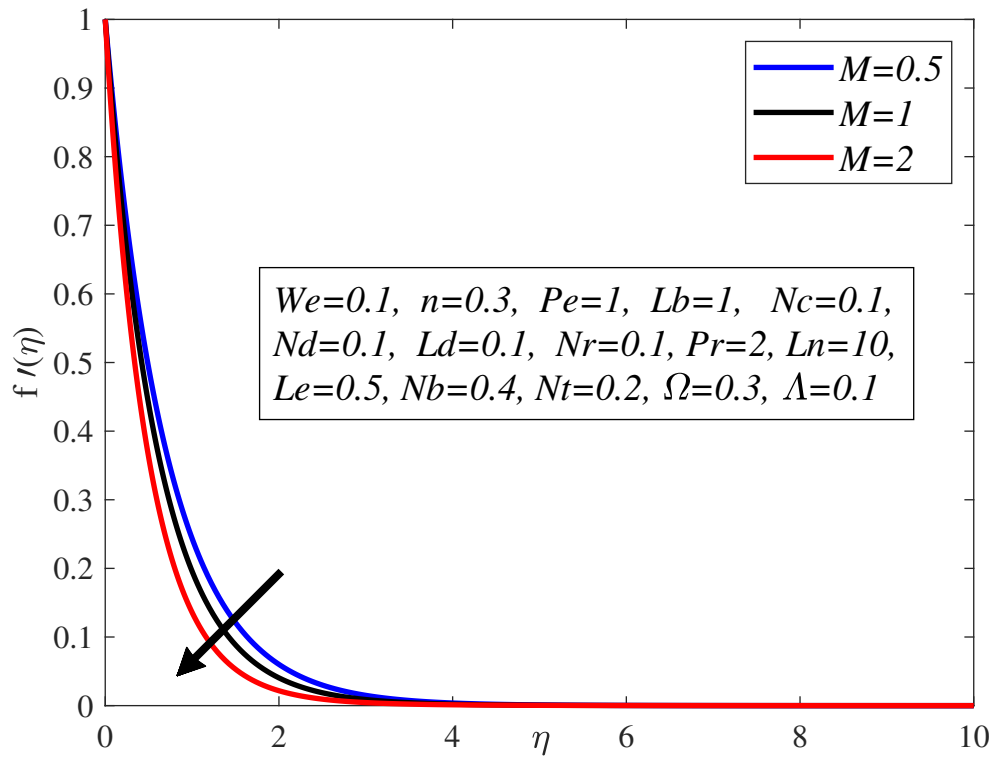
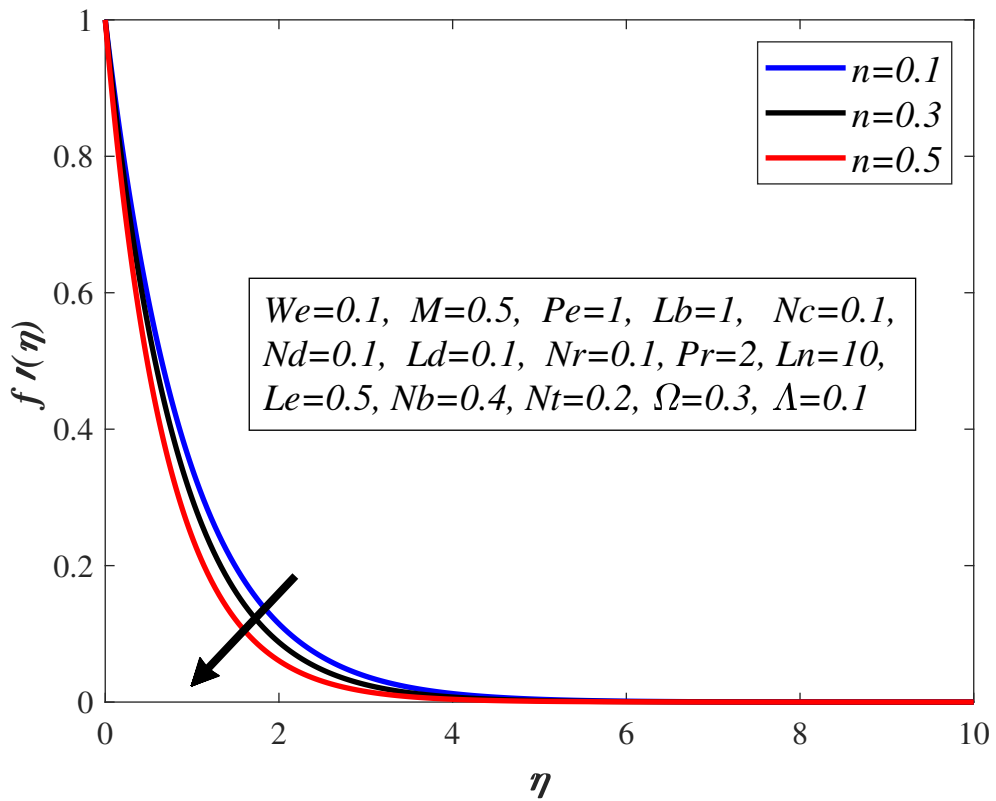
The initial profile taken for the case of Keller-box procedure $f = xe^x$, $u = e^{-x} - xe^{-x}$, $v = -2e^{-x} + xe^{-x}$, $\theta = e^{-x}$, $\xi = e^{-x}$, $\gamma = e^{-x}$, $\chi = e^{-x}$, $t = e^{-x}$, $c = e^{-x}$, $g = e^{-x}$. The simulation of Keller-box procedure has been done in Matlab 2016 software.

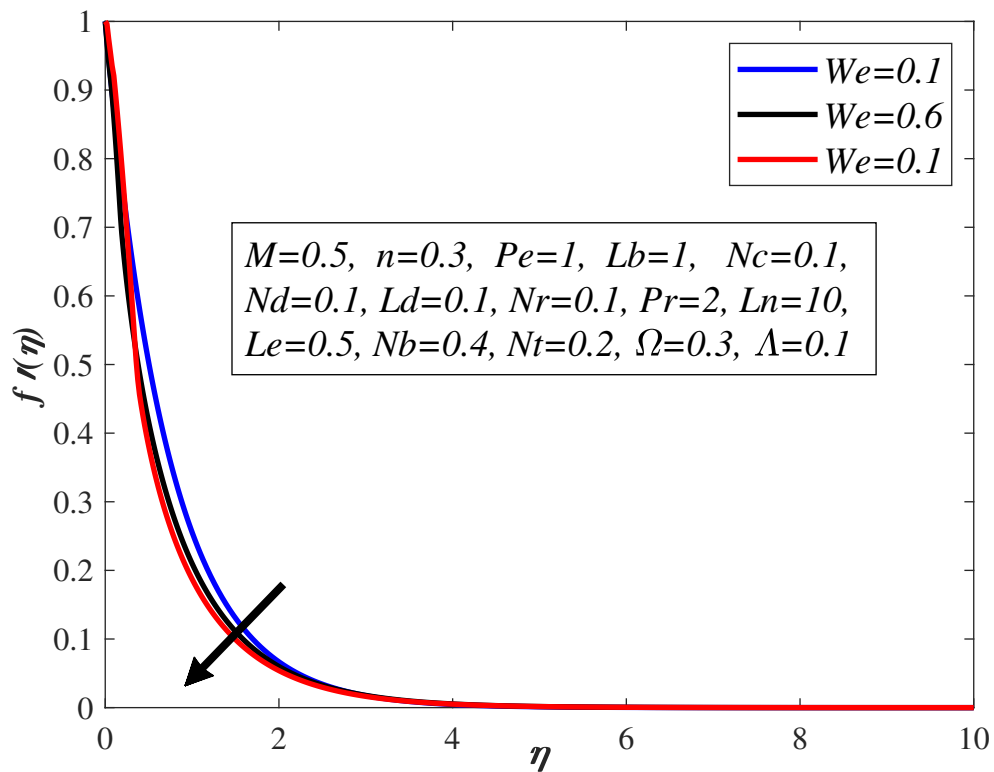
4.3 Results and Discussion

The influence of various parameters against velocity, temperature, mass fraction and microorganisms density fields have been discussed in detail and portrayed in the form of figures and tables.

4.3.1 Impact of M , n and We on the Velocity Field $f'(\eta)$

Figure 4.4 highlights the impact of M on the velocity field $f'(\eta)$. Actually, the resistive force called Lorentz force is produced due to an amplification in M which slows down the fluid motion. Figure 4.5 elaborates the impact of n on $f'(\eta)$. The value of n decides the viscosity of fluid. The fluid is less viscous for $n < 1$, more viscous in the case of $n > 1$ and not viscous in the case of $n = 1$. In the case of $n > 1$ depreciation in fluid velocity occurs. Figure 4.6 depicts the effect of We on $f'(\eta)$. According to the definition, We is viscous forces by inertial forces depicts the elastic nature of the fluid. For greater values of Weissenberg number, the fluids behave like solids, while lower values of Weissenberg number indicate the liquid nature of the fluid. The fluid viscosity amplifies during this time. It is quite clear that an augmentation in We reduces $f'(\eta)$ which brings about a decrement in the velocity field.

FIGURE 4.4: Impact of M on $f'(\eta)$.FIGURE 4.5: Effect of n on $f'(\eta)$.

FIGURE 4.6: Influence of We on $f'(\eta)$.

4.3.2 Impact of M , Pr , Nb and Nt , Nd on $\theta(\eta)$

Figure 4.7 reflects the impact of M on $\theta(\eta)$. It is observed that a positive variation in magnetic number reduces the fluid velocity, therefore additional heat is produced which enhances the fluid temperature. Figure 4.8 highlights the influence of Pr on the temperature field $\theta(\eta)$. The thermal conductivity debacles owing to an improvement in Pr which decelerates the fluid temperature. Figure 4.9 portrays the impact of Nb on $\theta(\eta)$. A magnification in Nb enhances the molecular collision which augments the fluid temperature and $\theta(\eta)$.

Figure 4.10 portrays the performance of Nt on $\theta(\eta)$. In the case of thermophoresis process, smaller particles migrated from high temperature region towards colder one which ultimately improves $\theta(\eta)$ Figure 4.11 is designed to investigate the influence of Dufour effect Nd on $\theta(\eta)$. The parameter Nd plays the role of concentration to the thermal energy flux inside the fluid which produces a monotonic enhancement in $\theta(\eta)$.

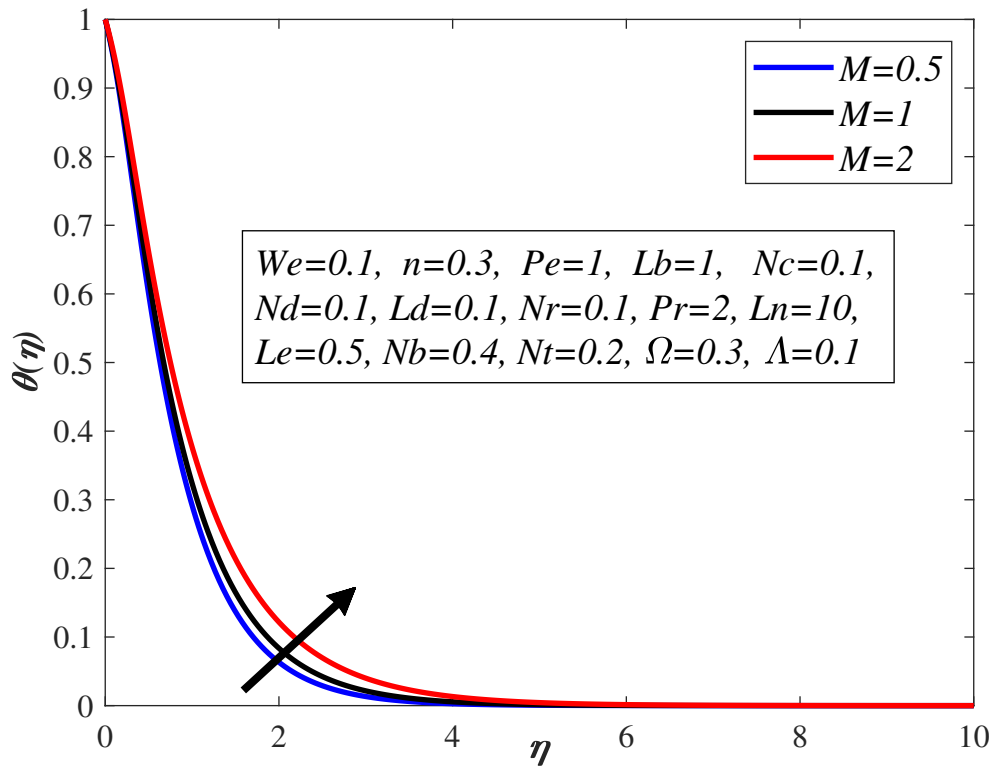


FIGURE 4.7: Impact M on $\theta(\eta)$.

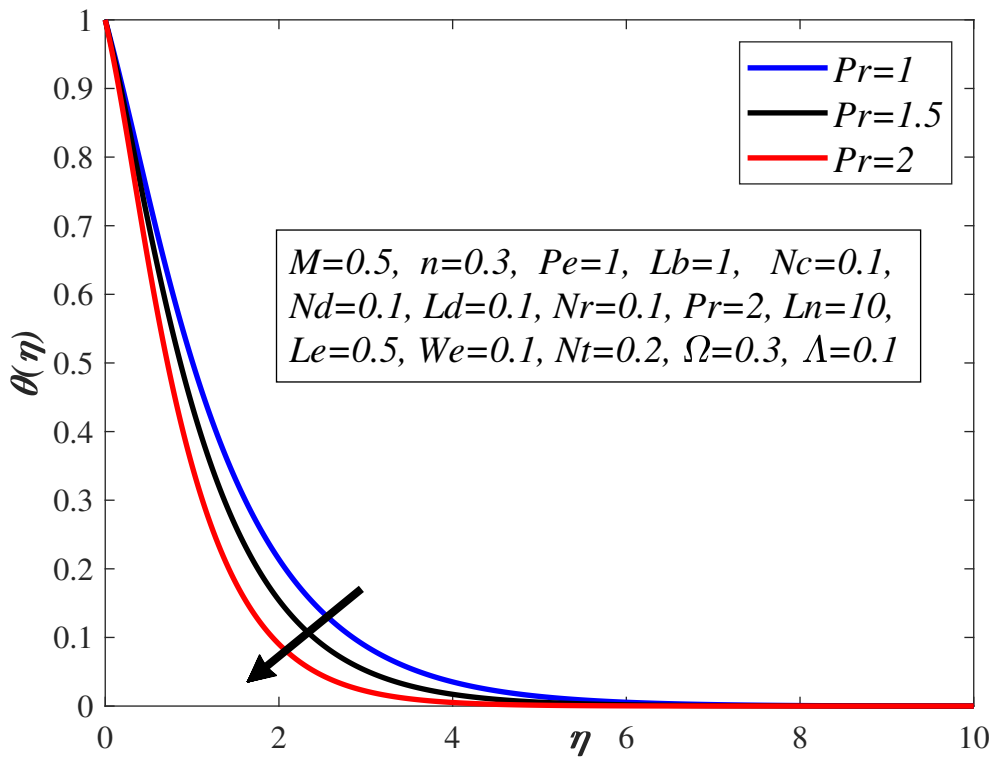
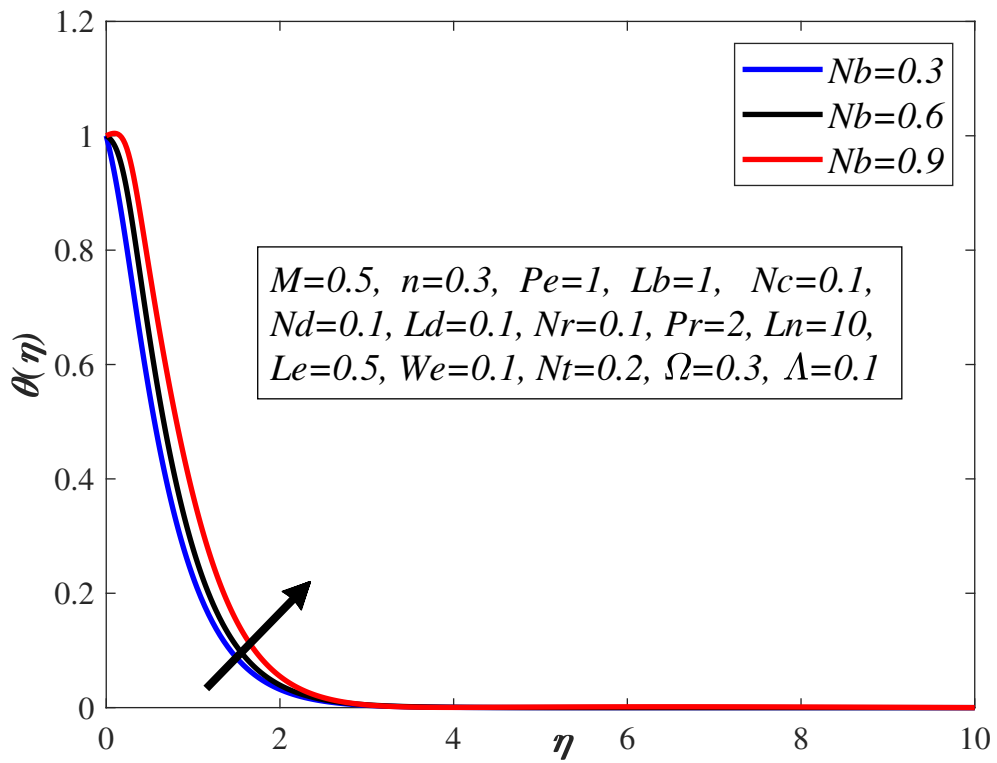
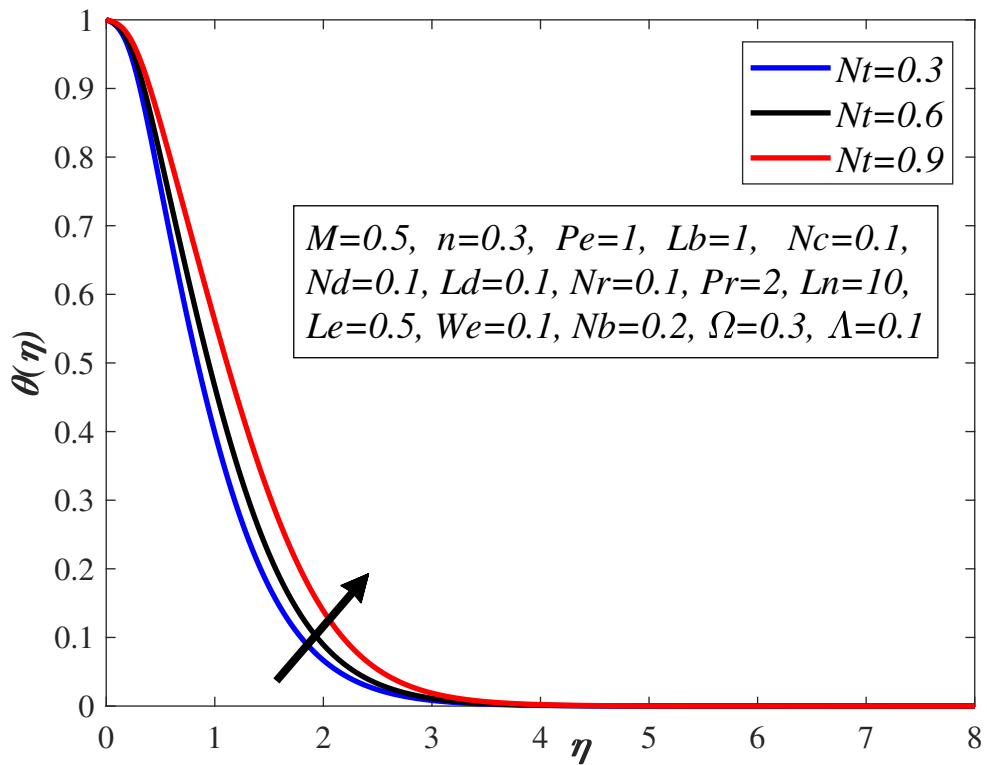
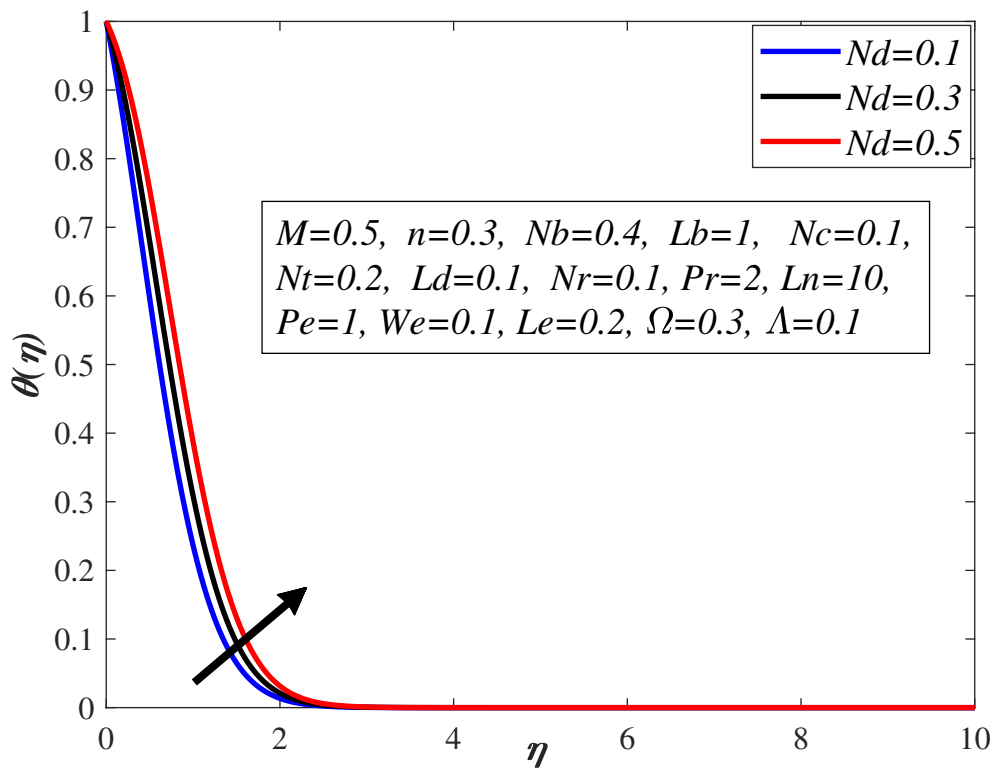


FIGURE 4.8: Effect of Pr on $\theta(\eta)$.

FIGURE 4.9: Implication of Nb on $\theta(\eta)$.FIGURE 4.10: Impact of Nt on $\theta(\eta)$.

FIGURE 4.11: Implication of Nd on $\theta(\eta)$.

4.3.3 Impact of Nb , Nt , Ln on the Mass Fraction Field $\xi(\eta)$

Figure 4.12 highlights the impact of Nb on the mass fraction field. Brownian diffusion and thermophoresis parameter emerges as a result of an amalgamation of nanoparticles as well as the fluid. It is verified that an escalation in Nb boost the phenomenon of random collision amongst the nanoparticles present inside the base fluid which promotes a reduction in mass fraction field. Figure 4.13 shows that an improvement in Nt push nanoparticles away from the warm surface. The density of concentration boundary layer upsurges due to an augmentation in the value of Nt , which brings about an embellishment in $\xi(\eta)$.

Figure 4.14 sways the performance of nanofluid Lewis parameter Ln on the mass $\xi(\eta)$. Lewis number is thermal diffusivity divided by the mass diffusivity. Concentration profile abates by virtue of Lewis number Ln dependence on Brownian diffusion D_B and plays a major role in the mass transfer scrutinizing. As a result, an augmentation in D_B depreciates $\xi(\eta)$ and Ln .

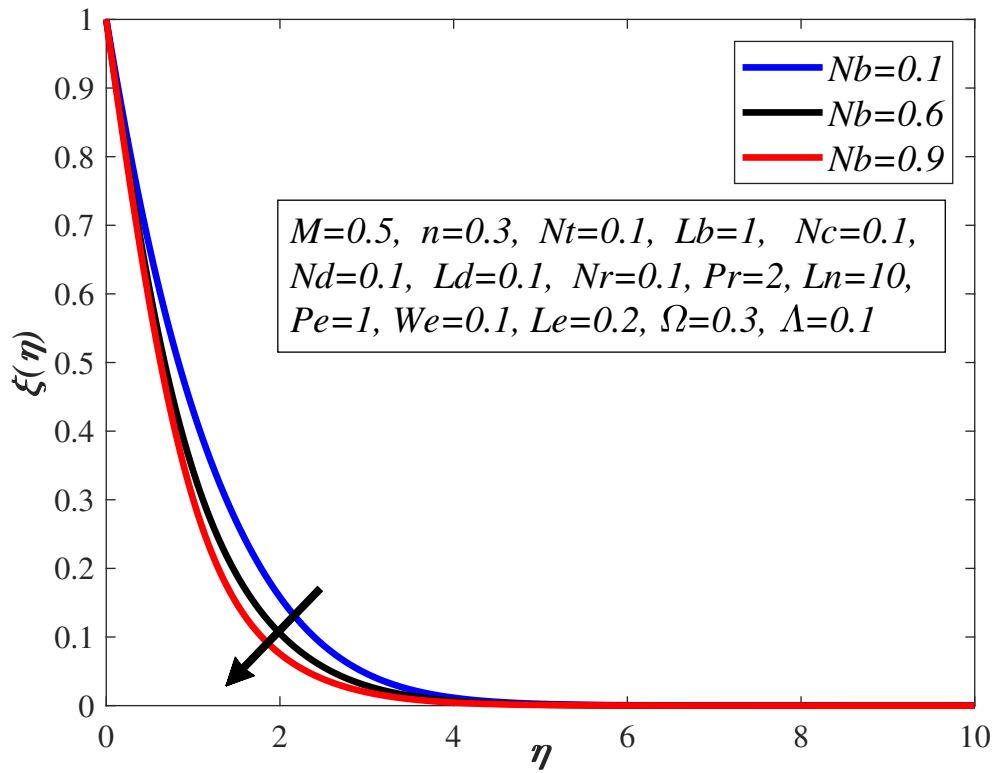


FIGURE 4.12: Implication of Nb on $\xi(\eta)$

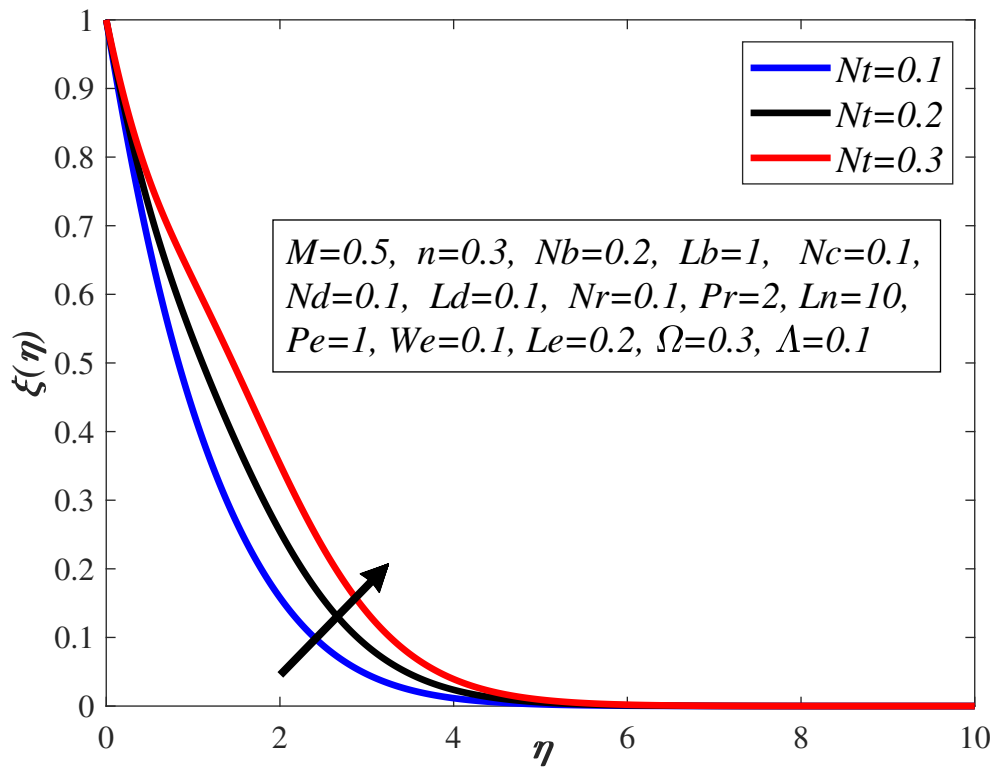
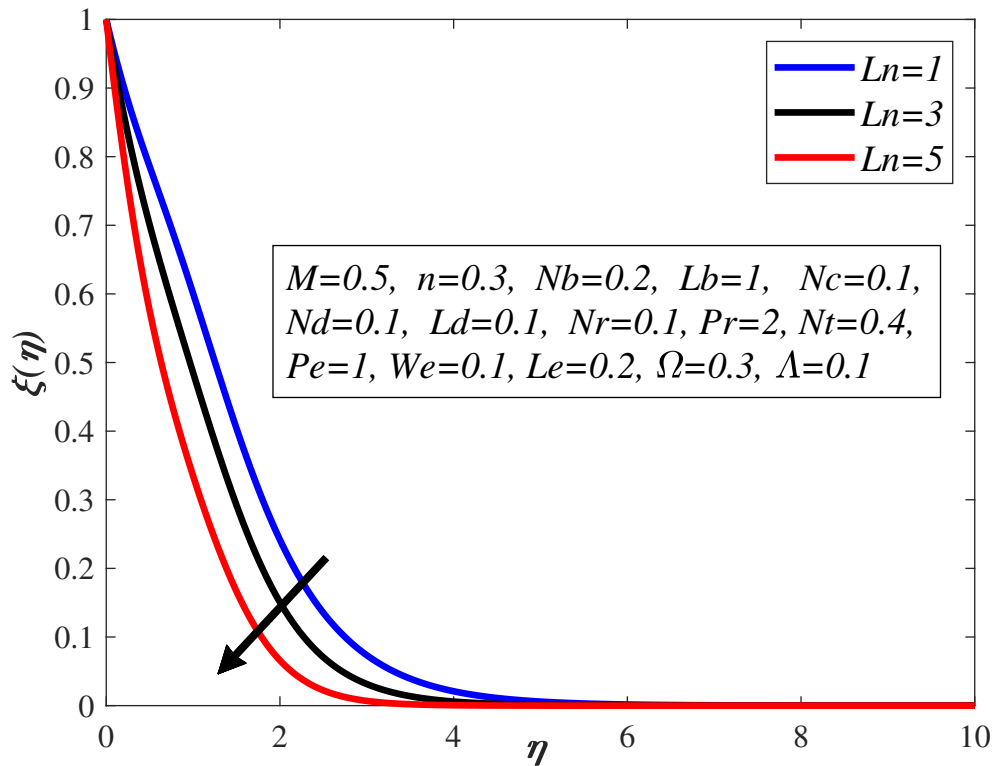


FIGURE 4.13: Impact of Nt on $\xi(\eta)$.

FIGURE 4.14: Effect of Ln on $\xi(\eta)$.

4.3.4 Impact of Pe , Lb , Ω on $\chi(\eta)$

Figure 4.15 describes the effect of Peclet number Pe on the microrotation distribution $\chi(\eta)$. During the diffusion process species migrate from area of high concentration to lower one. It is found that the diffusivity of microorganisms decreases in the case of an augmentation in Pe . As a result density of motile microorganism declines.

Figure 4.16 displays impact of bioconvection Lewis parameter Lb on the density of motile microorganism. Similarly like Figure 4.14 an augmentation in Lb results an abatement in the diffusivity of microorganisms, which results in the density of motile microorganism.

Figure 4.17 portrays the influence of microorganisms concentration difference parameter Ω and $\chi(\eta)$ on the density of motile microorganism. An amplification in σ , the concentration of microorganisms at ambient fluid diminishes which brings about a reduction in $\chi(\eta)$.

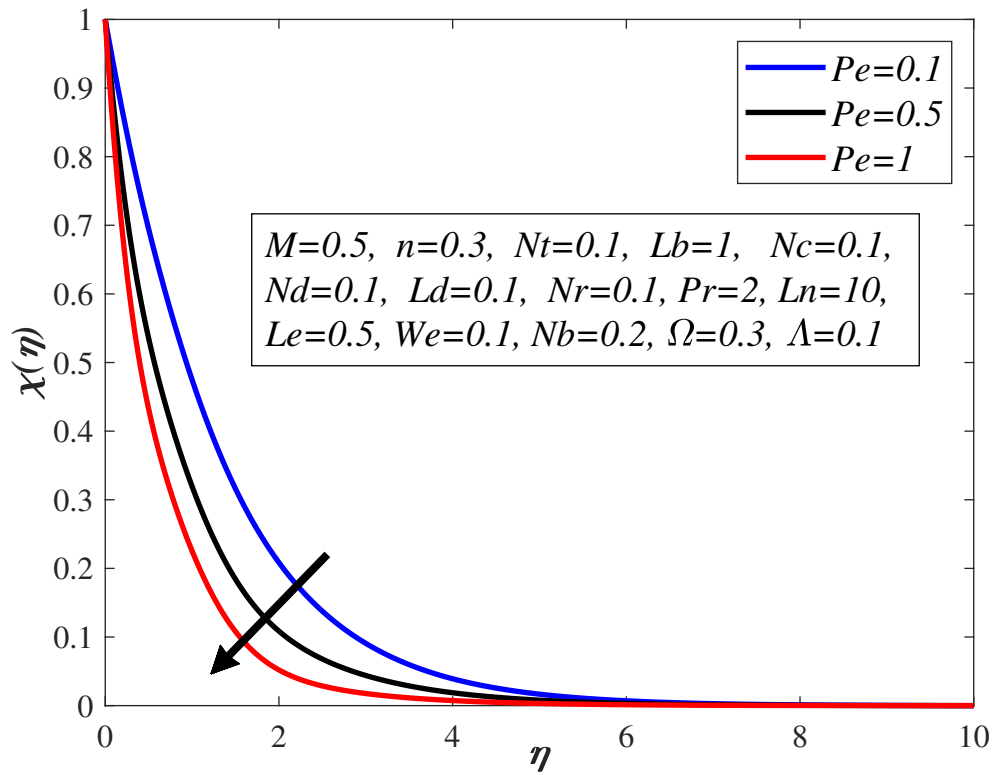


FIGURE 4.15: Effect of Pe on $\chi(\eta)$.

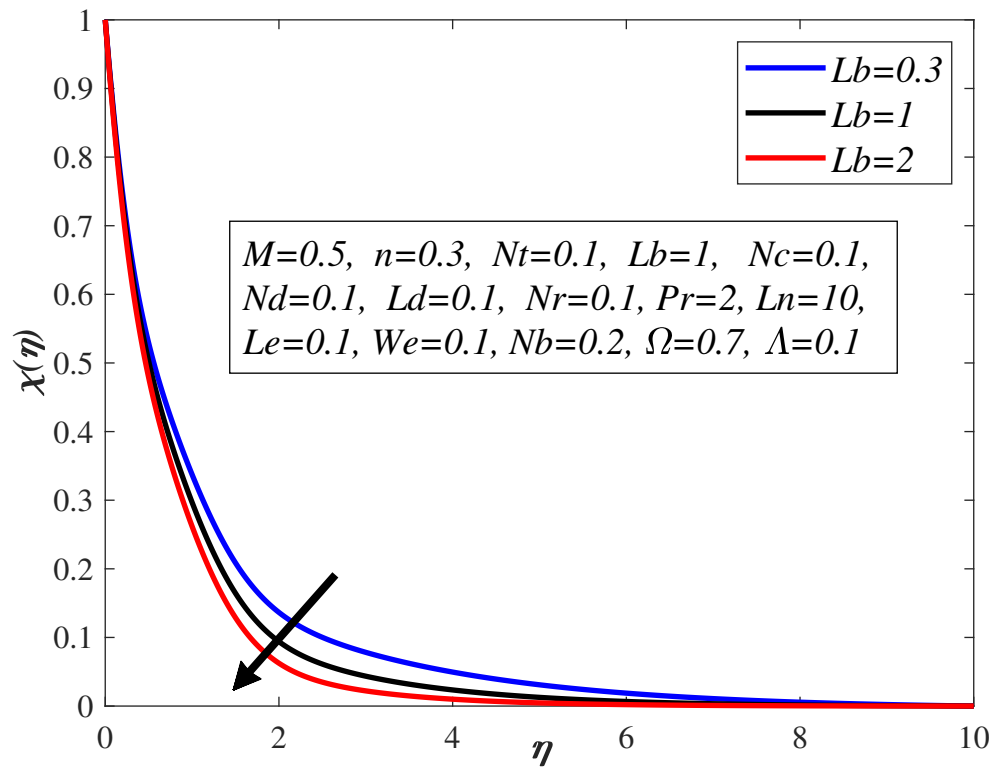
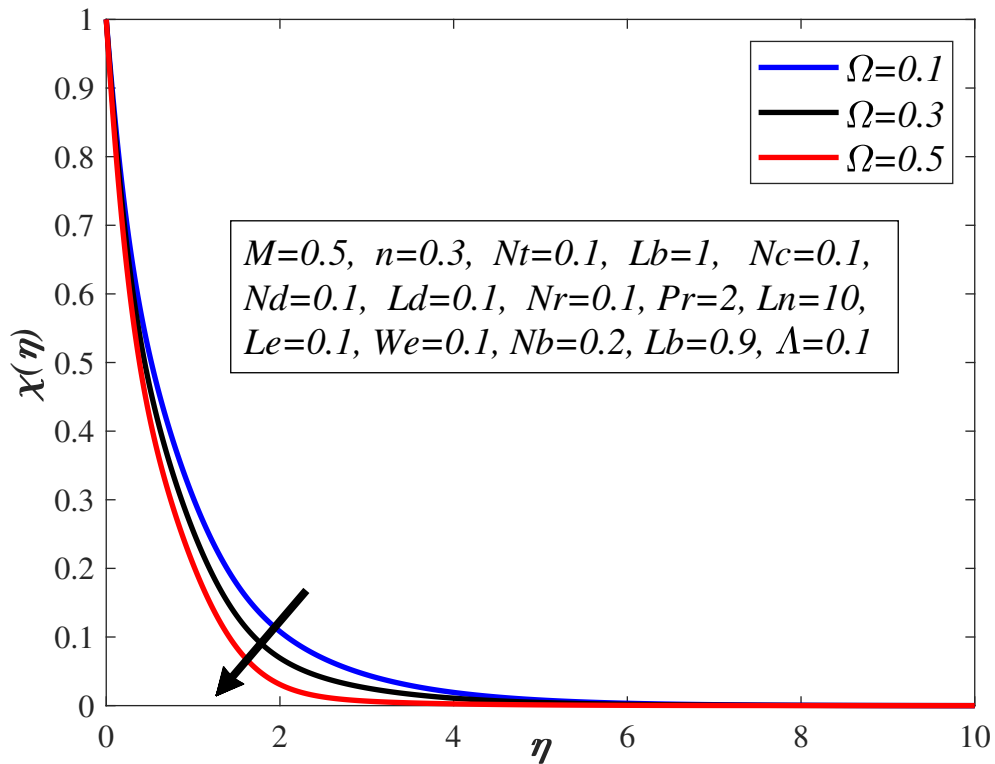


FIGURE 4.16: Impact of Lb on $\chi(\eta)$.

FIGURE 4.17: Influence of Ω on $\chi(\eta)$.

4.3.5 Impact of Ld and Le on the solute profile $\gamma(\eta)$

Figure 4.18 portrays the impact of Ld and $\gamma(\eta)$ on the solute profile. Dufour Lewis number illustrates the effect of temperature gradient on the mass fraction field. The diffusion process increases owing to an amplification in concentration phenomenon. It is observed that a positive change in concentration excites the fluid flow by virtue of an enhancement in the thermal energy which amplifies the solute profile. Figure 4.19 reflects Lewis number Le influence on the solute profile $\gamma(\eta)$. According to the definition, Le is thermal diffusivity α_1 divide by Brownian diffusivity D_B . Actually Le is inversely related to D_B .

The concentration of nanoparticles increases by the virtue of an augmentation in D_B . The collision of the nanoparticles increases as a result of a magnification in D_B . It is observed that a positive variation in D_B guides to an abatement in the concentration of particles and depreciates. Thats why a positive variation in Le produces an abatement in $\gamma(\eta)$.

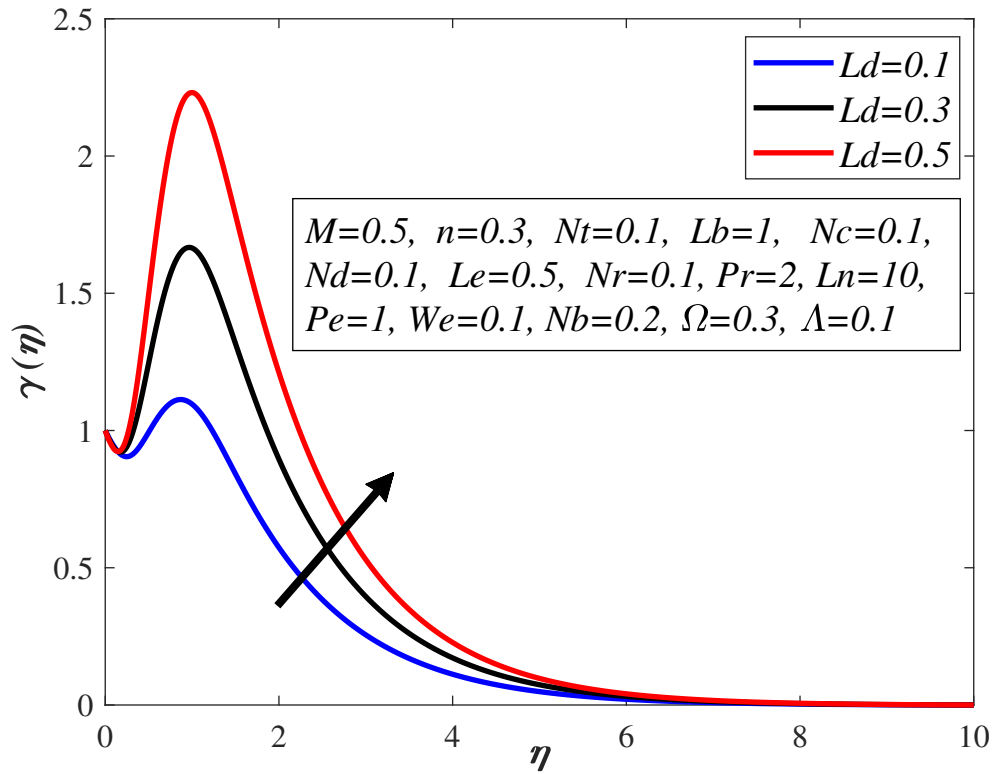


FIGURE 4.18: Impact of Ld on $\gamma(\eta)$.

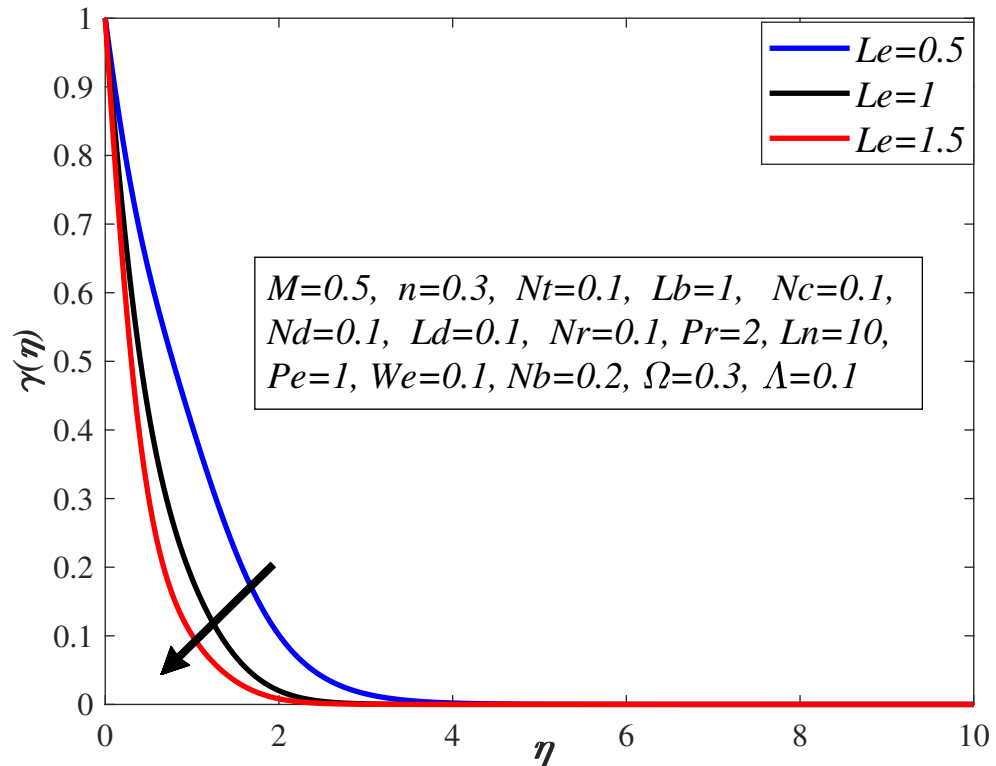


FIGURE 4.19: Effect of Le on $\gamma(\eta)$.

4.3.6 Impact of Ld , Nt versus Ln on $-\xi'$

Figure 4.20 describes the influence of nanofluid Lewis number Ln on mass fraction field for distinguished values of Dufour Lewis number Ln . Lewis number is defined as thermal diffusion by the mass diffusion. The phenomenon of diffusivity relies on the concentration. Both nanofluid and Dufour Lewis number are inversely related to the diffusion. A positive variation in the Lewis number depreciates the concentration of the fluid and mass transfer rate as well.

Figure 4.21 elucidates the influence of Nt on the mass fraction field as a result of a variation in Ln . In the occurrence of thermophoretic force the nanoparticles situated close to the surface having high temperature towards the surface having lower temperature which abates the thermal boundary layer and heightens the nanofluid Lewis number and amplifies Nt .

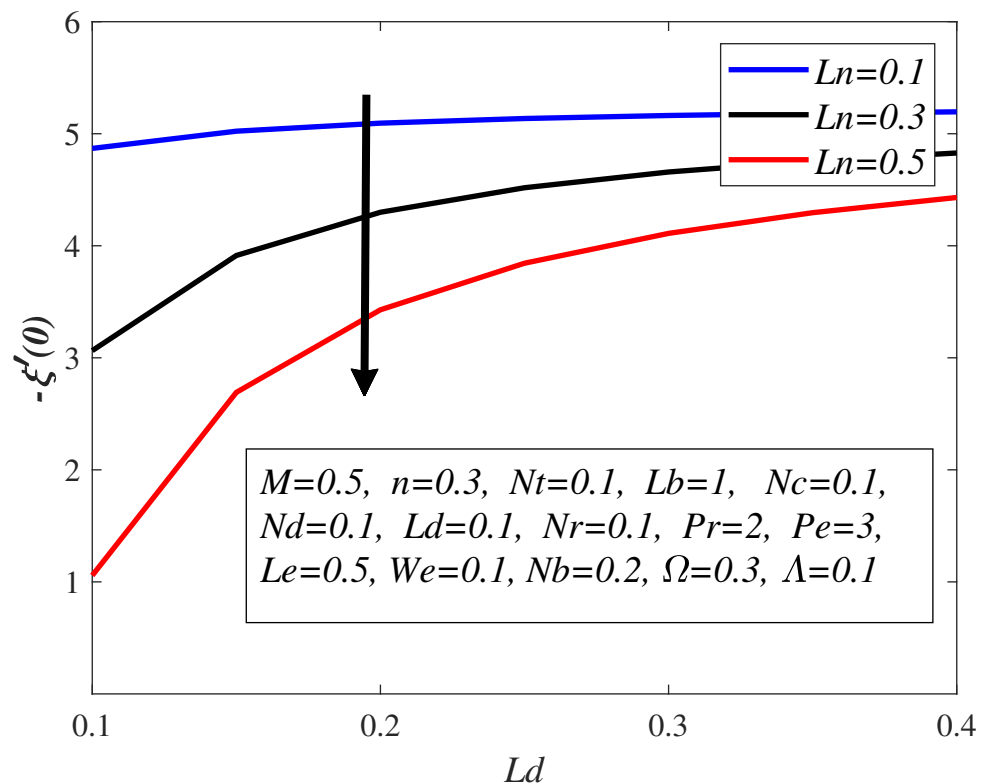
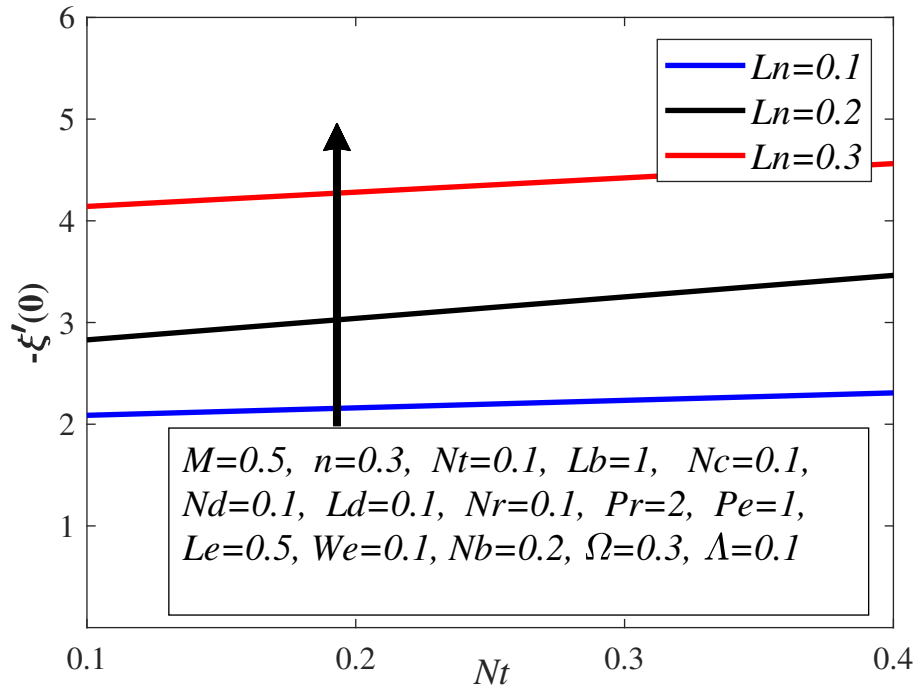


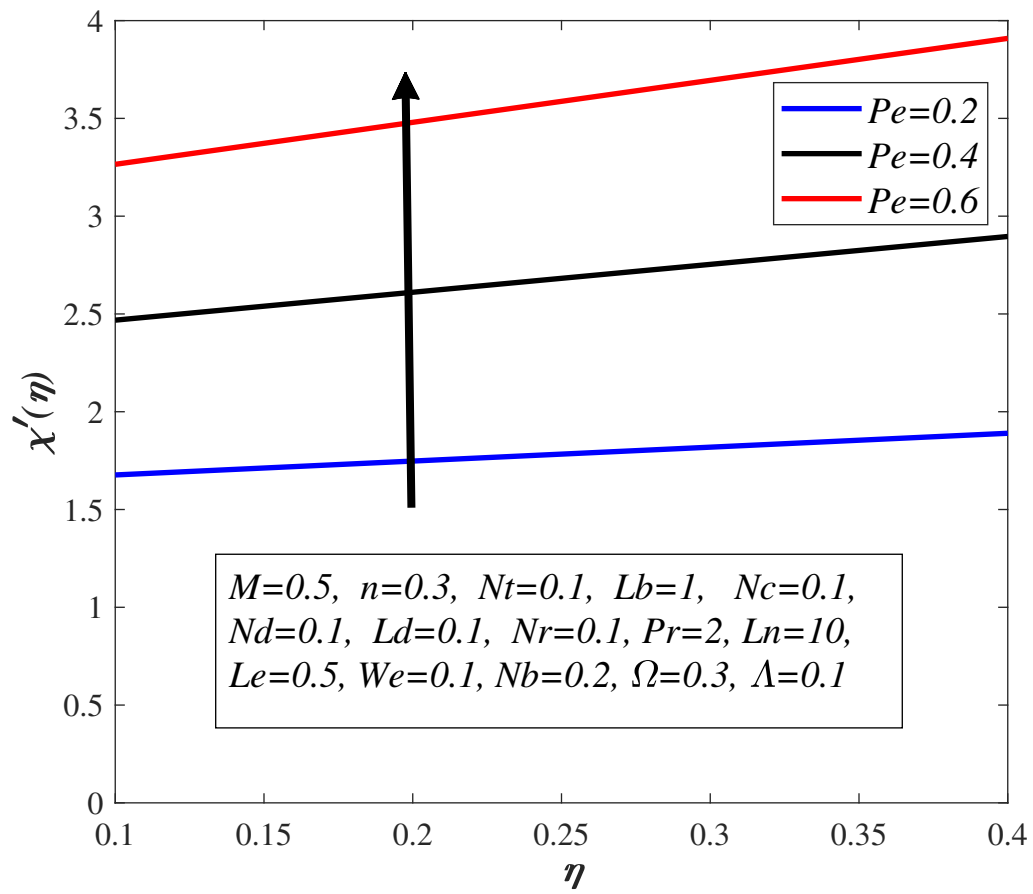
FIGURE 4.20: Effect of Nb on $\xi'(0)$.

FIGURE 4.21: Impact of Nt on $\xi'(0)$.

4.3.7 Impact of Pe on the density of motile microorganisms profile $-\chi'(0)$

Figure 4.22 presents the effect of microorganism concentration difference parameter Ω on density of motile microorganism $-\chi'(0)$ with a positive change in Peclet number Pe . Peclet number is the ratio of cell swimming speed of the microorganisms to the microorganisms concentration difference. The swimming speed of the microorganisms increases by the virtue of an incremental change in the Peclet number which drives to a increment in the fluid density. The concentration difference of microorganisms depreciates as a result of an augmentation in Pe . It is quite clear that both σ and Pe are responsible for an incremental change in the microorganisms concentration. As a result both microorganism boundary layer thickness and microorganisms density profile $-\chi'(0)$ increases.

Table 4.2 depicts the effect of various parameters on temperature field, mass fraction field and motile microorganisms density profile when $Nt=0.1$, $Pr=6.2$, $Le=0.5$, $Ld=0.1$ and $\Lambda=0.1$. Nusselt number abates owing to an amplification in

FIGURE 4.22: Effect of σ on $\chi'(0)$.

magnetic parameter M , Weissenberg number We , modified Dufour parameter Nd , power-law index n , nanofluid Lewis number Ln , buoyancy ratio parameter Nr but an amplification in Nusselt number has been observed for the case of Brownian motion parameter Nb and bioconvective Rayleigh number Nc . It is noteworthy that the heat transfer rate indicates no variation in terms of an augmentation in the microorganism concentration difference parameter σ , Peclet number Pe , bioconvective Lewis number Lb . The mass fraction field decays by the virtue of an improvement in M , Nc , nanofluid Lewis number Ln and buoyancy ratio parameter Nr , but behaviour of mass fraction field is increasing owing to a magnification in Nb , We , Nd and n whereas no change has been seen for σ , Pe and Lb . It is noted that a positive variation in motile microorganisms density profile has been monitored as a result of an elevation in M , σ , Pe , Lb and Ln , but motile microorganisms density profile diminishes in the case of Nr , Nc , n , We , Nd , Nb .

TABLE 4.2: Variation of $Nu_x Re_x^{-1/2}$, $Shu_x Re_x^{-1/2}$ and $Nn_x Re_x^{-1/2}$ for diverse parameters when $Nt=0.1$, $Pr=6.2$, $Le=0.5$, $Ld=0.1$ and $\Lambda=0.1$ are fixed.

M	Nc	Nr	Nb	We	n	σ	Pe	Lb	Nd	Ln	$-\theta'(0)$	$-\xi'(0)$	$-\chi'(0)$
0.1	0.5	0.5	0.1	0.3	0.2	0.5	1	1	0.1	2	0.93786	1.48950	1.30837
											0.93815	1.50424	1.32242
											0.93841	1.51812	1.33562
										0.1	2.03841	2.71812	3.45016
										0.3	2.03853	2.72591	2.63562
										0.5	2.03865	2.73339	2.64400
										0.1	2.05487	3.12893	2.93505
										0.2	2.05483	3.12731	2.93360
										0.3	2.05480	3.12569	2.93214
										0.4	0.33911	7.72999	11.6733
										0.5	0.55922	7.70119	11.6306
										0.6	0.68789	7.69032	11.6146
										0.1	0.82446	4.07381	6.23334
										0.2	0.82438	4.06941	6.22659
										0.3	0.82431	4.06476	6.21943
										0.3	0.82367	4.03450	6.17277
										0.4	0.82271	3.98592	6.09800
										0.5	0.82134	3.90893	5.97975
										0.1	0.82438	4.06941	4.69593
										0.2	0.82438	4.06941	5.07859
										0.3	0.82438	4.06941	5.46126
										0.1	0.82438	4.06941	1.03179
										0.5	0.82438	4.06941	3.31479
										1	0.82438	4.06941	6.22659
										0.5	0.82438	4.06941	3.31479
										1	0.82438	4.06941	6.22659
										1.5	0.82438	4.06941	9.18276
										0.1	0.89710	2.21688	3.50681
										0.2	0.81434	2.20547	3.48796
										0.3	0.78569	2.18375	3.45366
										1	0.89710	2.21688	3.50681
										2	0.85497	3.26596	5.04071
										3	0.82438	4.06941	6.22659

4.4 Concluding Remarks

The consequences of various effects like nanoparticles, double diffusive convection along with motile gyrotatic microorganisms on incompressible fluid moving along a stretching sheet has been discussed in this chapter. The numerical solution of the developed model has been achieved with the help of well established scheme termed as Keller box method. The prominent outcomes from the present study are enumerated underneath:

- An improvement in We augments $f'(\eta)$.
- The mass fraction field portrays an opposite behaviour as a result of an amplification in Ln .
- A positive variation in Pe drives to an abatement in the solute profile.
- The microrotation distribution profile declines in the case of an improvement in Lb and σ .
- The solute profile diminishes for the case of an embellishment in the regular Lewis number Le .

Chapter 5

Darcy-Forchheimer Flow of Maxwell Nanofluid Moving over a Stretching Sheet

The current chapter elucidates the performance of magneto Maxwell nanofluid moving over a Darcy porous stretching medium. The heat and mass transfer phenomena with regard to fluid flow under the effect of thermal conductivity, nonlinear based thermal radiation and activation energy have been debated. The temperature of the expandable sheet is controlled by the mechanism of convective heat transfer. The concentration of the nanoparticles is zero at the surface of the sheet. Buongiorno nanofluid model is considered for the analysis of nanoparticles on the non-Newtonian fluid. The modelled nonlinear modeled PDEs have been further transformed into ODEs by adopting a suitable transformation which are further handled by shooting scheme. The influence of sundry parameters like Biot number, Brownian as well as thermophoresis nanofluid parameters, radiation parameter, wall to ambient temperature parameter and reaction rate constant have been observed on the velocity, temperature and concentration profiles in terms of tables and figures. It is quite interesting that the mass concentration decreases by the virtue of an improvement in the activation energy parameter but temperature field heightens owing to an enhancement in the temperature ratio parameter.

5.1 Mathematical Formulation

The model depicted in Figure 5.1 describes the Maxwell magneto nanofluid moving over a stretching surface having pores in it. The sheet is stretching horizontally with velocity $u_w(x) = ax$ and furthermore the applied magnetic field B_0 direction is perpendicular to the fluid flow. The fluid flow is laminar under the effect of small Reynolds number which furthermore dismisses the influence of induced magnetic effect. The convective heat transfer phenomenon denoted by h_f is responsible for the temperature adjustment of the expandable sheet. Zero mass flux condition has been considered along with Brownian and thermophoresis effects.

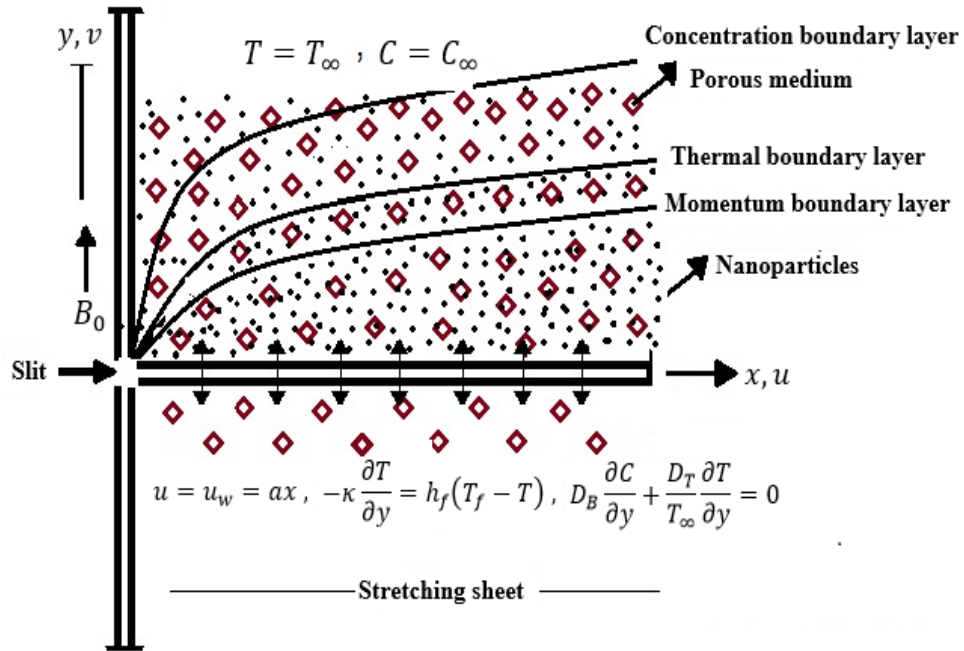


FIGURE 5.1: Flow geometry.

The extra stress tensor for Maxwell fluid [61] are defined as

$$\bar{\mathbf{S}} + \lambda_1 \frac{D\bar{\mathbf{S}}}{Dt} = \mu \bar{\mathbf{A}}_1, \quad (5.1)$$

where μ as well as λ_1 indicates the fluid viscosity and relaxation time of the material respectively. $\bar{\mathbf{A}}_1$ is the Rivlin-Ericksen tensor defined by

$$\bar{\mathbf{A}}_1 = \bar{\mathbf{L}} + \bar{\mathbf{L}}^T. \quad (5.2)$$

where $\bar{\mathbf{L}}$ denote the change in velocity and $\bar{\mathbf{L}}^T$ represents the transpose of velocity components matrix defined as

$$\bar{\mathbf{L}} = \begin{pmatrix} \frac{\partial u}{\partial x} & \frac{\partial u}{\partial y} & 0 \\ \frac{\partial v}{\partial x} & \frac{\partial v}{\partial y} & 0 \\ 0 & 0 & 0 \end{pmatrix}, \quad \bar{\mathbf{L}}^T = \begin{pmatrix} \frac{\partial u}{\partial x} & \frac{\partial v}{\partial x} & 0 \\ \frac{\partial u}{\partial y} & \frac{\partial v}{\partial y} & 0 \\ 0 & 0 & 0 \end{pmatrix}. \quad (5.3)$$

The operator $\frac{D}{Dt}$ is defined for contravariant vector and for a contravariant tensor of rank(2) respectively in Eq. (5.4) and Eq. (5.5) given below

$$\frac{D\bar{\mathbf{S}}}{Dt} = \frac{d\bar{\mathbf{S}}}{dt} - \bar{\mathbf{L}}\bar{\mathbf{S}}, \quad (5.4)$$

$$\frac{D\bar{\mathbf{S}}}{Dt} = \frac{d\bar{\mathbf{S}}}{dt} - \bar{\mathbf{L}}\bar{\mathbf{S}} - \bar{\mathbf{S}}\bar{\mathbf{L}}^T, \quad (5.5)$$

Applying divergence on both sides of Eq. (5.1), we get

$$\left(1 - \lambda_1 \frac{D}{Dt}\right) \nabla \cdot \bar{\mathbf{S}} = \mu \nabla \cdot \bar{\mathbf{A}}_1, \quad (5.6)$$

operating $(1 + \lambda_1(\frac{D}{Dt}))$ on both sides of $\rho \frac{d\bar{\mathbf{V}}}{dt} = -\nabla p + Div \bar{\mathbf{S}}$ and then eliminating $(1 + \lambda_1(\frac{D}{Dt})) \nabla \cdot \bar{\mathbf{S}}$ from Eq. (5.6), we obtain the mathematical expression of the form enumerated below

$$\left(1 - \lambda_1 \frac{D}{Dt}\right) \left(\rho \frac{d\bar{\mathbf{V}}}{dt} + \nabla p\right) = \mu \nabla \cdot \bar{\mathbf{A}}_1. \quad (5.7)$$

Eq. (5.7) in components form are mentioned below

$$\begin{aligned} u \frac{\partial u}{\partial x} + v \frac{\partial u}{\partial y} &= -\frac{1}{p} \frac{\partial p}{\partial x} - \frac{\lambda_1}{p} \left(u \frac{\partial^2 p}{\partial x^2} + v \frac{\partial^2 p}{\partial x \partial y} - \frac{\partial u}{\partial x} \frac{\partial p}{\partial x} - \frac{\partial u}{\partial y} \frac{\partial p}{\partial y} \right) + \\ &\mathbf{v} \left(\frac{\partial^2 u}{\partial x^2} + \frac{\partial^2 u}{\partial y^2} \right) - \lambda_1 \left(v^2 \frac{\partial^2 u}{\partial y^2} + 2uv \frac{\partial^2 u}{\partial x \partial y} + u^2 \frac{\partial^2 u}{\partial x^2} \right), \end{aligned} \quad (5.8)$$

and

$$\begin{aligned} u \frac{\partial v}{\partial x} + v \frac{\partial v}{\partial y} &= -\frac{1}{p} \frac{\partial p}{\partial y} - \frac{\lambda_1}{p} \left(v \frac{\partial^2 p}{\partial y^2} + u \frac{\partial^2 p}{\partial x \partial y} - \frac{\partial v}{\partial x} \frac{\partial p}{\partial x} - \frac{\partial v}{\partial y} \frac{\partial p}{\partial y} \right) + \\ &\mathbf{v} \left(\frac{\partial^2 v}{\partial x^2} + \frac{\partial^2 v}{\partial y^2} \right) - \lambda_1 \left(v^2 \frac{\partial^2 v}{\partial y^2} + 2uv \frac{\partial^2 v}{\partial x \partial y} + u^2 \frac{\partial^2 v}{\partial x^2} \right), \end{aligned} \quad (5.9)$$

after ignoring the pressure gradient we get

$$u \frac{\partial u}{\partial x} + v \frac{\partial u}{\partial y} + \lambda_1 \left(v^2 \frac{\partial^2 v}{\partial y^2} + 2uv \frac{\partial^2 v}{\partial x \partial y} + u^2 \frac{\partial^2 v}{\partial x^2} \right) = \mathbf{v} \left(\frac{\partial^2 v}{\partial x^2} + \frac{\partial^2 u}{\partial y^2} \right), \quad (5.10)$$

and

$$u \frac{\partial u}{\partial x} + v \frac{\partial u}{\partial y} + \lambda_1 \left(v^2 \frac{\partial^2 v}{\partial y^2} + 2uv \frac{\partial^2 v}{\partial x \partial y} + u^2 \frac{\partial^2 v}{\partial x^2} \right) = \mathbf{v} \left(\frac{\partial^2 v}{\partial x^2} + \frac{\partial^2 u}{\partial y^2} \right). \quad (5.11)$$

The governing modeled PDEs under the effect of boundary layer assumption are enumerated underneath

$$\frac{\partial u}{\partial x} + \frac{\partial v}{\partial y} = 0, \quad (5.12)$$

$$u \frac{\partial u}{\partial x} + v \frac{\partial u}{\partial y} = \nu \frac{\partial^2 u}{\partial y^2} - \frac{\sigma_1 B_0^2}{\rho_f} \left(u + \lambda_1 v \frac{\partial u}{\partial y} \right) - \frac{\nu}{K_2} u - F u^2 - \lambda_1 \left(u^2 \frac{\partial^2 u}{\partial x^2} + v^2 \frac{\partial^2 u}{\partial y^2} + 2uv \frac{\partial^2 u}{\partial x \partial y} \right), \quad (5.13)$$

$$u \frac{\partial T}{\partial x} + v \frac{\partial T}{\partial y} = \frac{1}{\rho c_p} \frac{\partial}{\partial y} \left(\kappa \frac{\partial T}{\partial y} \right) + \tau \left[D_B \frac{\partial C}{\partial y} \frac{\partial T}{\partial y} + \frac{D_T}{T_\infty} \left(\frac{\partial T}{\partial y} \right)^2 \right] - \frac{1}{\rho c_p} \frac{\partial q_r}{\partial y}, \quad (5.14)$$

$$u \frac{\partial C}{\partial x} + v \frac{\partial C}{\partial y} = D_B \frac{\partial^2 C}{\partial y^2} + \frac{D_T}{T_\infty} \frac{\partial^2 T}{\partial y^2} - K_r^2 (C - C_\infty) \left(\frac{T}{T_\infty} \right)^n \exp \left(\frac{-E_a}{\kappa T} \right), \quad (5.15)$$

with the boundary conditions

$$\left. \begin{aligned} y = 0 : u = ax, v = 0, -k \frac{\partial T}{\partial y} = h_f (T_w - T), D_B \frac{\partial C}{\partial y} + \frac{D_T}{T_\infty} \frac{\partial T}{\partial y} = 0, \\ y \rightarrow \infty : u \rightarrow 0, T \rightarrow T_\infty, C \rightarrow C_\infty. \end{aligned} \right\} \quad (5.16)$$

The parameter $F = \frac{C_b}{x K^{\frac{1}{2}}}$ depicts the inertia coefficient and the thermal conductivity is denoted by

$$\kappa(T) = \kappa_\infty \left(1 + \epsilon_1 \frac{T - T_\infty}{T_w - T_\infty} \right). \quad (5.17)$$

The last expression in the right side of governing modeled energy equation (5.14) is termed as thermal radiation heat flux based on the Rosseland approximation. Rosseland approximation relies on the hypotheses that the participating medium (fluid) is an optically thick and radiation propagates over a small distance before encounter a scattering phenomenon. The penetration length of radiation is small

compare to the characteristic length and moreover photon mean free length is very small. The equation regarding Rosseland heat approximation [94] is exhibited by

$$q_r = -\frac{4\sigma^*}{3\kappa^*} \frac{\partial T^4}{\partial y}. \quad (5.18)$$

The terms σ^* and κ^* indicates Boltzmann as well as absorption coefficients accordingly. The generalized form of the radiation heat flux is given by

$$\frac{\partial q_r}{\partial y} = -\frac{16\sigma^*T_\infty^3}{3\kappa^*} \frac{\partial^2 T}{\partial y^2}, \quad (5.19)$$

where $K_r^2 (C - C_\infty) \left(\frac{T}{T_\infty}\right)^n \exp\left(\frac{-E_a}{\kappa T}\right)$ represents the Arrhenius expression.

To convert PDEs to ODEs, we adopt the following similarity transformation [98]:

$$\left. \begin{aligned} u &= axf'(\eta), \quad v = -\sqrt{a\nu}f(\eta), \quad \eta = \sqrt{\frac{a}{\nu}}y, \\ \phi(\eta) &= \frac{C - C_\infty}{C_w - C_\infty}, \quad \theta(\eta) = \frac{T - T_\infty}{T_w - T_\infty}. \end{aligned} \right\} \quad (5.20)$$

The detailed mechanism for conversion of (5.12)-(5.15) into dimensionless ODEs is given below:

$$\begin{aligned} \bullet \quad \frac{\partial u}{\partial x} &= \frac{\partial}{\partial x} (axf'(\eta)) \\ &= af'(\eta). \end{aligned} \quad (5.21)$$

$$\begin{aligned} \bullet \quad \frac{\partial v}{\partial y} &= \frac{\partial}{\partial y} (-\sqrt{a\nu}f(\eta)) \\ &= -\sqrt{a\nu} \sqrt{\frac{a}{\nu}} f'(\eta) \\ &= -af'(\eta). \end{aligned} \quad (5.22)$$

$$\begin{aligned} \bullet \quad \frac{\partial u}{\partial y} &= \frac{\partial}{\partial y} (axf'(\eta)) \\ &= ax \sqrt{\frac{a}{\nu}} f''(\eta). \end{aligned} \quad (5.23)$$

$$\begin{aligned} \bullet \quad u \frac{\partial u}{\partial x} &= axf' \cdot \frac{\partial}{\partial x} (axf') \\ &= a^2 x f'^2. \end{aligned} \quad (5.23)$$

$$\begin{aligned}
\bullet \quad v \frac{\partial u}{\partial y} &= -\sqrt{a\nu} f(\eta) \cdot ax \sqrt{\frac{a}{\nu}} f''(\eta) \\
&= -ax \sqrt{a\nu} \sqrt{\frac{a}{\nu}} f(\eta) f''(\eta) \\
&= -a^2 x f f''(\eta).
\end{aligned} \tag{5.24}$$

$$\begin{aligned}
\bullet \quad \nu \frac{\partial^2 u}{\partial y^2} &= \nu \frac{\partial}{\partial y} \left(\frac{\partial u}{\partial y} \right) \\
&= ax \left(\sqrt{\frac{a}{\nu}} \right)^2 f'''(\eta) \\
&= ax \left(\frac{a}{\nu} \right) f'''(\eta) \\
&= \frac{a^2 x}{\nu} f'''(\eta).
\end{aligned} \tag{5.25}$$

$$\begin{aligned}
\bullet \quad v^2 \frac{\partial^2 u}{\partial y^2} &= (-\sqrt{a\nu} f(\eta))^2 \cdot \frac{a^2 x}{\nu} f''' \\
&= a^3 x f^2 f'''.
\end{aligned} \tag{5.26}$$

$$\begin{aligned}
\bullet \quad u^2 \frac{\partial^2 u}{\partial x^2} &= (ax f')^2 \cdot \frac{\partial}{\partial x} \left(\frac{\partial u}{\partial x} \right) \\
&= (ax f')^2 \cdot \frac{\partial}{\partial x} (a f'(\eta)) \\
&= (ax f')^2 \cdot 0 \\
&= 0.
\end{aligned} \tag{5.27}$$

$$\begin{aligned}
\bullet \quad \frac{\partial^2 u}{\partial x \partial y} &= \frac{\partial}{\partial x} \left(\frac{\partial u}{\partial y} \right) \\
&= \frac{\partial}{\partial x} \left(ax \sqrt{\frac{a}{\nu}} f''(\eta) \right) \\
&= a \sqrt{\frac{a}{\nu}} f''(\eta).
\end{aligned} \tag{5.28}$$

$$\begin{aligned}
\bullet \quad 2uv \frac{\partial^2 u}{\partial x \partial y} &= -2ax f' \cdot \sqrt{a\nu} f \cdot a \sqrt{\frac{a}{\nu}} f'' \\
&= -2ax f' \cdot a^2 f f'' \\
&= -2a^3 x f f' f''.
\end{aligned} \tag{5.29}$$

$$\bullet \quad \lambda_1 \left(u^2 \frac{\partial^2 u}{\partial x^2} + v^2 \frac{\partial^2 u}{\partial y^2} + 2uv \frac{\partial^2 u}{\partial x \partial y} \right) = \lambda_1 a^3 x (f^2 f''' - 2f f' f''). \tag{5.30}$$

$$\begin{aligned}
\bullet \quad u + \lambda_1 v \frac{\partial u}{\partial y} &= ax f' - \lambda_1 \sqrt{a\nu} f \cdot ax \sqrt{\frac{a}{\nu}} f'' \\
&= ax f' - \lambda_1 a^2 x f f'' \\
&= ax(f' - \lambda_1 a f f'').
\end{aligned} \tag{5.31}$$

$$\bullet \quad \frac{\sigma_1 B_0^2}{\rho_f} \left(u + \lambda_1 v \frac{\partial u}{\partial y} \right) = \frac{\sigma_1 B_0^2}{\rho_f} (ax f' - \lambda_1 a^2 x f f''). \tag{5.32}$$

$$\begin{aligned}
\bullet \quad F u^2 &= F(ax f')^2 \\
&= F a^2 x^2 f'^2 \\
&= a^2 x^2 F f'^2.
\end{aligned} \tag{5.33}$$

$$\bullet \quad \frac{\partial T}{\partial x} = (T_w - T_\infty) \frac{\partial \theta(\eta)}{\partial \eta} \cdot \frac{\partial \eta}{\partial x} = 0. \tag{5.34}$$

$$\bullet \quad u \frac{\partial T}{\partial x} = ax f'(\eta) \cdot (T_w - T_\infty) \frac{\partial \theta(\eta)}{\partial \eta} \cdot \frac{\partial \eta}{\partial x} = 0. \tag{5.35}$$

$$\begin{aligned}
\bullet \quad \frac{\partial T}{\partial y} &= (T_w - T_\infty) \frac{\partial \theta(\eta)}{\partial \eta} \cdot \frac{\partial \eta}{\partial y} \\
&= (T_w - T_\infty) \sqrt{\frac{a}{\nu}} \theta'
\end{aligned} \tag{5.36}$$

$$\begin{aligned}
\bullet \quad \frac{\partial^2 T}{\partial y^2} &= (T_w - T_\infty) \frac{\partial}{\partial y} \left(\frac{\partial \theta(\eta)}{\partial \eta} \cdot \frac{\partial \eta}{\partial y} \right) \\
&= (T_w - T_\infty) \frac{\partial}{\partial y} \left(\sqrt{\frac{a}{\nu}} \theta' \right) \\
&= (T_w - T_\infty)^2 \sqrt{\frac{a}{\nu}} \sqrt{\frac{a}{\nu}} \theta'' \\
&= (T_w - T_\infty)^2 \left(\frac{a}{\nu} \right) \theta''
\end{aligned} \tag{5.37}$$

$$\begin{aligned}
\bullet \quad v \frac{\partial T}{\partial y} &= -\sqrt{a\nu} f(\eta) \cdot (T_w - T_\infty) \frac{\partial \theta(\eta)}{\partial \eta} \cdot \frac{\partial \eta}{\partial y}, \\
&= -a(T_w - T_\infty) f \theta'.
\end{aligned} \tag{5.38}$$

$$\begin{aligned}
\bullet \quad \frac{\partial C}{\partial y} &= (C_w - C_\infty) \frac{\partial \phi(\eta)}{\partial \eta} \cdot \frac{\partial \eta}{\partial y} \\
&= (C_w - C_\infty) \sqrt{\frac{a}{\nu}} \phi'.
\end{aligned} \tag{5.39}$$

$$\bullet \quad D_B \frac{\partial C}{\partial y} = D_B (C_w - C_\infty) \sqrt{\frac{a}{\nu}} \phi'. \tag{5.40}$$

$$\begin{aligned}
\bullet \quad D_B \frac{\partial C}{\partial y} \frac{\partial T}{\partial y} &= D_B (C_w - C_\infty) \sqrt{\frac{a}{\nu}} \phi' \cdot (T_w - T_\infty) \sqrt{\frac{a}{\nu}} \theta' \\
&= D_B (C_w - C_\infty) (T_w - T_\infty) \left(\frac{a}{\nu}\right) \phi' \theta'.
\end{aligned} \tag{5.41}$$

$$\begin{aligned}
\bullet \quad \frac{\partial T}{\partial y} &= (T_w - T_\infty) \frac{\partial \theta(\eta)}{\partial \eta} \cdot \frac{\partial \eta}{\partial y} \\
&= \sqrt{\frac{a}{\nu}} (T_w - T_\infty) \theta'(\eta).
\end{aligned} \tag{5.42}$$

$$\begin{aligned}
\bullet \quad \frac{D_T}{T_\infty} \left(\frac{\partial T}{\partial y}\right)^2 &= \frac{D_T}{T_\infty} \left(\sqrt{\frac{a}{\nu}} (T_w - T_\infty) \theta'(\eta)\right)^2 \\
&= \frac{D_T}{T_\infty} \left(\frac{a}{\nu}\right) (T_w - T_\infty)^2 \theta'^2.
\end{aligned} \tag{5.43}$$

$$\begin{aligned}
\bullet \quad D_B \frac{\partial C}{\partial y} \frac{\partial T}{\partial y} + \frac{D_T}{T_\infty} \left(\frac{\partial T}{\partial y}\right)^2 &= \frac{a(T_w - T_\infty)}{\nu} \left(D_B (C_w - C_\infty) \theta' \phi' + \right. \\
&\quad \left. \frac{D_T}{T_\infty} (T_w - T_\infty) \theta'^2\right).
\end{aligned} \tag{5.44}$$

$$\begin{aligned}
\bullet \quad \kappa \frac{\partial^2 T}{\partial y^2} &= \kappa \frac{\partial}{\partial y} \left(\frac{\partial T}{\partial y}\right) \\
&= \kappa_\infty \left(1 + \epsilon_1 \frac{T - T_\infty}{T_w - T_\infty}\right) \cdot (T_w - T_\infty) \left(\frac{a}{\nu}\right) \theta'' \\
&= \kappa_\infty (1 + \epsilon_1 \theta) \cdot (T_w - T_\infty) \left(\frac{a}{\nu}\right) \theta'' \\
&= \kappa_\infty (T_w - T_\infty) \left(\frac{a}{\nu}\right) (1 + \epsilon_1 \theta) \theta''.
\end{aligned} \tag{5.45}$$

$$\begin{aligned}
\bullet \quad \frac{\partial \kappa}{\partial y} \frac{\partial T}{\partial y} &= \frac{\partial}{\partial y} \left(\kappa_\infty \left(1 + \epsilon_1 \frac{T - T_\infty}{T_w - T_\infty}\right)\right) \cdot (T_w - T_\infty) \sqrt{\frac{a}{\nu}} \theta' \\
&= \kappa_\infty \left(\frac{\epsilon_1}{T_w - T_\infty}\right) \frac{\partial T}{\partial y} \cdot (T_w - T_\infty) \sqrt{\frac{a}{\nu}} \theta' \\
&= \kappa_\infty \left(\frac{\epsilon_1}{T_w - T_\infty}\right) (T_w - T_\infty)^2 \left(\sqrt{\frac{a}{\nu}}\right)^2 \theta'^2 \\
&= \kappa_\infty \epsilon_1 (T_w - T_\infty) \left(\frac{a}{\nu}\right) \theta'^2.
\end{aligned} \tag{5.46}$$

$$\begin{aligned}
\bullet \quad \frac{\partial}{\partial y} \left(\kappa \frac{\partial T}{\partial y}\right) &= \kappa \frac{\partial^2 T}{\partial y^2} + \frac{\partial \kappa}{\partial y} \frac{\partial T}{\partial y} \\
&= \kappa_\infty (T_w - T_\infty) \left(\frac{a}{\nu}\right) (1 + \epsilon_1 \theta) \theta'' + \kappa_\infty \epsilon_1 (T_w - T_\infty) \left(\frac{a}{\nu}\right) \theta'^2 \\
&= \left(\frac{a \kappa_\infty (T_w - T_\infty)^2}{\nu}\right) (1 + \epsilon_1 \theta) \theta'' + \epsilon_1 \theta'^2.
\end{aligned} \tag{5.47}$$

$$\bullet \quad T^3 \frac{\partial^2 T}{\partial y^2} = \left(\frac{a}{\nu}\right) ((T_w - T_\infty) \theta + T_\infty)^3 (T_w - T_\infty) \theta''. \tag{5.48}$$

$$\begin{aligned}
\bullet \quad T^2 &= ((T_w - T_\infty)\theta(\eta) + T_\infty)^2 \\
3T^2 &= 3((T_w - T_\infty)\theta(\eta) + T_\infty)^2 \\
3T^2 \left(\frac{\partial T}{\partial y} \right)^2 &= 3((T_w - T_\infty)\theta(\eta) + T_\infty)^2 \left(\frac{a}{v} \right) (T_w - T_\infty)^2 \theta'^2. \quad (5.49)
\end{aligned}$$

$$\begin{aligned}
\bullet \quad T^3 \frac{\partial^2 T}{\partial y^2} + 3T^2 \left(\frac{\partial T}{\partial y} \right)^2 &= \left(((T_w - T_\infty)\theta(\eta) + T_\infty)^3 \left(\frac{a}{v} \right) \right. \\
&\quad \left. (T_w - T_\infty)\theta'' \right) + \left(3 \left(\frac{a}{v} \right) (T_w - T_\infty)^2 \right. \\
&\quad \left. ((T_w - T_\infty)\theta(\eta) + T_\infty)^2 \theta'^2 \right). \quad (5.50)
\end{aligned}$$

$$\begin{aligned}
\bullet \quad \frac{\partial q_r}{\partial y} &= -\frac{16\sigma^*}{3\kappa^*} \frac{\partial}{\partial y} \left(T^3 \frac{\partial T}{\partial y} \right) \\
&= -\frac{16\sigma^*}{3\kappa^*} \left(\left(T^3 \frac{\partial^2 T}{\partial y^2} \right) + 3T^2 \left(\frac{\partial T}{\partial y} \right)^2 \right) \\
&= -\frac{16\sigma^*}{3\kappa^*} \left(\left(((T_w - T_\infty)\theta(\eta) + T_\infty)^3 \left(\frac{a}{v} \right) \right. \right. \\
&\quad \left. \left. (T_w - T_\infty)\theta'' \right) + \left(3 \left(\frac{a}{v} \right) (T_w - T_\infty)^2 \right. \right. \\
&\quad \left. \left. ((T_w - T_\infty)\theta(\eta) + T_\infty)^2 \theta'^2 \right) \right) \quad (5.51)
\end{aligned}$$

$$\begin{aligned}
\bullet \quad \frac{1}{\rho C_p} \frac{\partial q_r}{\partial y} &= -\frac{16\sigma^*}{3\kappa^* \rho C_p} \left(\left(((T_w - T_\infty)\theta(\eta) T_\infty)^3 \left(\frac{a}{v} \right) (T_w - T_\infty)\theta'' \right) \right. \\
&\quad \left. + \left(3 \left(\frac{a}{v} \right) (T_w - T_\infty)^2 ((T_w - T_\infty)\theta(\eta) + T_\infty)^2 \theta'^2 \right) \right). \quad (5.52)
\end{aligned}$$

$$\begin{aligned}
\bullet \quad \frac{1}{\rho C_p} \frac{\partial}{\partial y} \left(\kappa \frac{\partial T}{\partial y} \right) - \frac{1}{\rho C_p} \frac{\partial q_r}{\partial y} &= \frac{a(T_w - T_\infty)\kappa_\infty}{\rho \nu C_p} \left((1 + \epsilon_1 \theta) \theta'' + \epsilon_1 \theta'^2 \right) + \frac{16\sigma^* a}{3\kappa^* \rho \nu C_p} \left(((T_w - T_\infty)\theta \right. \\
&\quad \left. + T_\infty)^3 (T_w - T_\infty)\theta'' + 3((T_w - T_\infty)\theta + T_\infty)^2 (T_w - T_\infty)^2 \theta'^2 \right) \\
&= \frac{a\kappa_\infty (T_w - T_\infty)}{\rho \nu C_p} \left(\left(\frac{16\sigma^* T_\infty^3}{3\kappa^* \kappa_\infty} \left(\left(\left(\frac{T_w}{T_\infty} - 1 \right) \theta(\eta) + 1 \right)^3 \theta'' \right. \right. \right. \\
&\quad \left. \left. + 3 \left(\frac{T_w}{T_\infty} - 1 \right) \left(\left(\frac{T_w}{T_\infty} - 1 \right) \theta(\eta) + 1 \right)^2 \theta'^2 \right) \right) + ((1 + \epsilon_1 \theta)\theta'' + \epsilon_1 \theta'^2) \right) \\
&= \frac{a\kappa_\infty (T_w - T_\infty)}{\rho \nu C_p} \left((1 + \epsilon_1 \theta) \theta'' + \epsilon_1 \theta'^2 + \left(\frac{4}{3} \right) Rd \left(((\theta_w - 1) \theta + 1)^3 \theta'' \right. \right. \\
&\quad \left. \left. + 3(\theta_w - 1) ((\theta_w - 1) \theta + 1)^2 \theta'^2 \right) \right)
\end{aligned}$$

$$\begin{aligned}
&= \frac{a(T_w - T_\infty)}{\left(\frac{\mu C_p}{\kappa_\infty}\right)} \left(\left((1 + \epsilon_1 \theta) \theta'' + \epsilon_1 \theta'^2 \right) + \left(\frac{4}{3} \right) Rd \left(((\theta_w - 1) \theta + 1)^3 \theta'' \right. \right. \\
&\quad \left. \left. + 3(\theta_w - 1) ((\theta_w - 1) \theta + 1)^2 \theta'^2 \right) \right) \\
&= \frac{a(T_w - T_\infty)}{Pr} \left(\left((1 + \epsilon_1 \theta) \theta'' + \epsilon_1 \theta'^2 \right) + \left(\frac{4}{3} \right) Rd \left(((\theta_w - 1) \theta + 1)^3 \theta'' \right. \right. \\
&\quad \left. \left. + 3(\theta_w - 1) ((\theta_w - 1) \theta + 1)^2 \theta'^2 \right) \right) \\
&= \frac{a(T_w - T_\infty)}{Pr} \left(\left((1 + \epsilon_1 \theta) + \frac{4}{3} Rd \left(((\theta_w - 1) \theta + 1)^3 \right) \right) \theta'' \right. \\
&\quad \left. + (\epsilon_1 + 4Rd(\theta_w - 1) ((\theta_w - 1) \theta + 1)^2) \theta'^2 \right). \tag{5.53}
\end{aligned}$$

$$\bullet \frac{\partial C}{\partial x} = (C_w - C_\infty) \frac{\partial \phi(\eta)}{\partial \eta} \cdot \frac{\partial \eta}{\partial x} = 0. \tag{5.54}$$

$$\bullet u \frac{\partial C}{\partial x} = ax f'(\eta) \cdot (C_w - C_\infty) \frac{\partial \phi(\eta)}{\partial \eta} \cdot \frac{\partial \eta}{\partial x} = 0. \tag{5.55}$$

$$\begin{aligned}
\bullet \frac{\partial C}{\partial y} &= (C_w - C_\infty) \frac{\partial \phi(\eta)}{\partial \eta} \cdot \frac{\partial \eta}{\partial y} \\
&= (C_w - C_\infty) \sqrt{\frac{a}{\nu}} \phi'. \tag{5.56}
\end{aligned}$$

$$\begin{aligned}
\bullet \frac{\partial^2 C}{\partial y^2} &= \frac{\partial}{\partial y} \left(\frac{\partial C}{\partial y} \right) \\
\frac{\partial^2 C}{\partial y^2} &= \frac{\partial \left((C_w - C_\infty) \sqrt{\frac{a}{\nu}} \phi' \right)}{\partial y} \\
&= (C_w - C_\infty) \left(\frac{a}{\nu} \right) \phi''. \tag{5.57}
\end{aligned}$$

$$\begin{aligned}
\bullet D_B \frac{\partial^2 C}{\partial y^2} &= D_B \frac{\partial}{\partial y} \left((C_w - C_\infty) \sqrt{\frac{a}{\nu}} \phi' \right) \\
&= D_B (C_w - C_\infty) \left(\frac{a}{\nu} \right) \phi''
\end{aligned}$$

$$\begin{aligned}
\bullet \left(\frac{T}{T_\infty} \right)^n &= \left(\frac{(T_w - T_\infty) \theta + T_\infty}{T_\infty} \right)^n \\
&= \left(\frac{T_\infty \left(\left(\frac{T_w - T_\infty}{T_\infty} \right) \theta + 1 \right)}{T_\infty} \right)^n \\
&= \left(\frac{T_\infty (\delta_2 \theta + 1)}{T_\infty} \right)^n \\
&= (1 + \delta_2 \theta)^n. \tag{5.58}
\end{aligned}$$

$$\begin{aligned}
\bullet \exp\left(\frac{-E_a}{\kappa T}\right) &= \exp\left(\frac{-E_a}{\kappa((T_w - T_\infty)\theta + T_\infty)}\right) \\
&= \exp\left(\frac{-E_a}{\kappa T_\infty\left(\left(\frac{T_w - T_\infty}{T_\infty}\right)\theta + 1\right)}\right) \\
&= \exp\left(\frac{-E}{(1 + \delta_2\theta)}\right).
\end{aligned} \tag{5.59}$$

The continuity equation after utilizing (5.21) and (5.22) in (5.12) is given below

$$\frac{\partial u}{\partial x} + \frac{\partial v}{\partial y} = af'(\eta) - af'(\eta) = 0. \tag{5.60}$$

Inserting (5.23)-(5.33) in (5.13) to get dimensionless momentum equation

$$\begin{aligned}
a^2xf'^2 - a^2xf f'' + \lambda_1(a^3xf^2f''' - 2a^3xf f' f'') &= a^2xf''' \\
- \frac{\sigma_1 B_0^2 a^2 x}{\rho_f}(f' - \lambda_1 f f'') - \frac{\nu}{k_2} a x f' - F a^2 x^2 f'^2 \\
\Rightarrow \nu \frac{a^2 x}{\nu} f''' - \frac{\sigma_1 B_0^2}{\rho_f}(a x f' - \lambda_1 a^2 x f f'') - \frac{\nu}{k_2} a x f' - F a^2 x^2 f'^2 \\
- a^2 x f'^2 + a^2 x f f'' - \lambda_1(a^3 x f^2 f''' - 2a^3 x f f' f'') &= 0 \\
\Rightarrow f''' - \frac{\sigma_1 B_0^2 a x}{\rho_f a^2 x}(f' - \lambda_1 a f f'') - \frac{\nu}{k_2 a} f' - F x f'^2 - f'^2 + f f'' \\
- \lambda_1 a(f^2 f''' - 2f f' f'') &= 0 \\
\Rightarrow f''' - \frac{\sigma_1 B_0^2}{\rho_f a}(f' - \lambda_1 a f f'') - \frac{\nu}{k_2 a} f' - F x f'^2 - f'^2 + f f'' \\
- \lambda_1 a(f^2 f''' - 2f f' f'') &= 0 \\
\Rightarrow f''' - M^2(f' - \beta_2 f f'') - \lambda_2 f' - F r f'^2 - f'^2 + f f'' \\
- \beta_2(f^2 f''' - 2f f' f'') &= 0 \\
\Rightarrow f''' - M^2(f' - \beta_2 f f'') - \lambda_2 f' - F r f'^2 - f'^2 + f f'' \\
- \beta_2(f^2 f''' - 2f f' f'') &= 0 \\
\Rightarrow f''' - M^2 f' + M^2 \beta_2 f f'' - \lambda_2 f' - F r f'^2 - f'^2 + f f'' \\
- \beta_2 f^2 f''' + 2\beta_2 f f' f'' &= 0 \\
\Rightarrow (1 - \beta_2 f^2) f''' - (M^2 + \lambda_2) f' - (M^2 \beta_2 + 1) f f'' \\
- (1 + F r) f'^2 - 2\beta_2 f f' f'' &= 0.
\end{aligned} \tag{5.61}$$

Utilizing (5.34)-(5.53) in (5.14), we get dimensionless energy equation

$$\begin{aligned}
 -a(T_w - T_\infty)f\theta' &= a(T_w - T_\infty) \left(\frac{1}{Pr} \left(\left((1 + \epsilon_1\theta) + \frac{4}{3}Rd((\theta_w - 1)\theta + 1)^3 \right) \right. \right. \\
 &\quad \left. \left. + (\epsilon_1 + 4Rd(\theta_w - 1)((\theta_w - 1)\theta + 1)^2)\theta'^2 \right) \right. \\
 &\quad \left. + \frac{\tau}{\nu} \left(D_B(C_w - C_\infty)\theta'\phi' + \frac{D_T}{T_\infty}(T_w - T_\infty)\theta'^2 \right) \right) \\
 \Rightarrow -f\theta' &= \frac{1}{Pr} \left(\left((1 + \epsilon_1\theta) + \frac{4}{3}Rd((\theta_w - 1)\theta + 1)^3 \right) + \right. \\
 &\quad \left. (\epsilon_1 + 4Rd(\theta_w - 1)((\theta_w - 1)\theta + 1)^2)\theta'^2 \right) + \\
 &\quad \left(\frac{\tau D_B}{\nu}(C_w - C_\infty)\theta'\phi' + \frac{\tau D_T}{\nu T_\infty}(T_w - T_\infty)\theta'^2 \right). \\
 \Rightarrow \left((1 + \epsilon_1\theta) + \frac{4}{3}Rd((\theta_w - 1)\theta + 1)^3 \right)\theta'' &+ (\epsilon_1 + 4Rd(\theta_w - 1)) \\
 &\quad ((\theta_w - 1)\theta + 1)^2\theta'^2 + Pr(Nb\theta'\phi' + Nt\theta'^2) + Prf\theta' = 0. \quad (5.62)
 \end{aligned}$$

Using (5.54)-(5.59) in (5.15), the dimensionless concentration equation is given by

$$\begin{aligned}
 -a(C_w - C_\infty)f\phi' &= D_B(C_w - C_\infty) \left(\frac{a}{\nu} \right) \phi'' + \left(\frac{D_T}{T_\infty} \right) (T_w - T_\infty) \left(\frac{a}{\nu} \right) \theta'' - \\
 &\quad Kr^2(C - C_\infty)(1 + \delta_2\theta)^n \exp\left(\frac{-E}{(1 + \delta_2\theta)}\right) \\
 \Rightarrow \phi'' - \left(\frac{\nu}{D_B} \right) \frac{Kr^2}{a} \frac{(C - C_\infty)}{(C_w - C_\infty)} (1 + \delta_2\theta)^n \exp\left(\frac{-E}{(1 + \delta_2\theta)}\right) &+ \\
 &\quad \left(\frac{\left(\frac{D_T}{\nu T_\infty} \right)}{\left(\frac{D_B}{\nu} \right)} \right) \frac{(T_w - T_\infty)}{(C_w - C_\infty)} \theta'' + f\phi' = 0 \\
 \Rightarrow \phi'' - \left(\frac{\nu}{D_B} \right) \frac{Kr^2}{a} \frac{(C - C_\infty)}{(C_w - C_\infty)} (1 + \delta_2\theta)^n \exp\left(\frac{-E}{(1 + \delta_2\theta)}\right) &+ \\
 &\quad \left(\frac{\left(\frac{\tau D_T}{\nu T_\infty} (T_w - T_\infty) \right)}{\left(\frac{\tau D_B}{\nu} \right) (C_w - C_\infty)} \right) \theta'' + \left(\frac{\nu}{D_B} \right) f\phi' = 0 \\
 \Rightarrow \phi'' - PrLe \left(Sc\sigma_2 (1 + \delta\theta)^n \exp\left(\frac{-E}{(1 + \delta\theta)}\right) \phi \right. & \\
 \left. + f\phi' \right) + \left(\frac{Nt}{Nb} \right) \theta'' = 0. \quad (5.63)
 \end{aligned}$$

Dimensionless momentum boundary condition is given by

$$\begin{aligned}
 \bullet \quad u &= ax && \text{at } y = 0 \\
 \Rightarrow axf'(\eta) &= ax && \text{at } \eta = 0 \\
 \Rightarrow f'(\eta) &= 1 && \text{at } \eta = 0. \quad (5.64)
 \end{aligned}$$

$$\begin{aligned}
\bullet \quad v &= 0 && \text{at } y = 0 \\
&\Rightarrow -\sqrt{a\nu}f(\eta) = 0 && \text{at } \eta = 0 \\
&\Rightarrow f(\eta) = 0 && \text{at } \eta = 0 \\
&\Rightarrow f = 0 && \text{at } \eta = 0. \quad (5.65)
\end{aligned}$$

$$\begin{aligned}
\bullet \quad -k \frac{\partial T}{\partial y} &= h_f(T_w - T) && \text{at } y = 0 \\
&\Rightarrow -k\sqrt{\frac{a}{\nu}}\theta' = h_f(T_w - T_\infty + T_\infty - T) && \text{at } \eta = 0 \\
&\Rightarrow = h_f \frac{(T_w - T_\infty + T_\infty - T)}{(T_w - T_\infty)} && \text{at } \eta = 0 \\
&\Rightarrow = h_f \left(1 - \frac{(T - T_\infty)}{(T_w - T_\infty)}\right) && \text{at } \eta = 0 \\
&\Rightarrow = h_f(1 - \theta) && \text{at } \eta = 0 \\
&\Rightarrow = -h_f(1 - \theta) && \text{at } \eta = 0 \\
&\Rightarrow \theta' = -\left(\frac{h_f}{k(\sqrt{\frac{a}{\nu}})}\right)(1 - \theta) && \text{at } \eta = 0 \\
&= -\gamma_2(1 - \theta) && \text{at } \eta = 0. \quad (5.66)
\end{aligned}$$

$$\begin{aligned}
\bullet \quad D_B \frac{\partial C}{\partial y} + \frac{D_T}{T_\infty} \frac{\partial T}{\partial y} &= 0 && \text{at } y = 0 \\
&\Rightarrow \sqrt{\frac{a}{\nu}} \left(D_B(C_w - C_\infty)\phi' + \frac{D_T}{T_\infty}(T_w - T_\infty)\theta' \right) = 0 && \text{at } \eta = 0 \\
&\Rightarrow D_B(C_w - C_\infty)\phi' + \frac{D_T}{T_\infty}(T_w - T_\infty)\theta' = 0 && \text{at } \eta = 0 \\
&\Rightarrow \frac{\frac{\tau}{\nu} D_B(C_w - C_\infty)\phi' + \frac{\tau}{\nu} \frac{D_T}{T_\infty}(T_w - T_\infty)\theta'}{\left(\frac{\tau}{\nu}\right)} = 0 && \text{at } \eta = 0 \\
&\Rightarrow \frac{\tau}{\nu} D_B(C_w - C_\infty)\phi' + \frac{\tau}{\nu} \frac{D_T}{T_\infty}(T_w - T_\infty)\theta' = 0 && \text{at } \eta = 0 \\
&\Rightarrow Nb\phi' + Nt\theta' = 0 && \text{at } \eta = 0. \quad (5.67)
\end{aligned}$$

$$\begin{aligned}
\bullet \quad u &\rightarrow 0 && \text{as } y \rightarrow \infty \\
&\Rightarrow axf'(\eta) = 0 && \text{as } \eta \rightarrow \infty \\
&\Rightarrow f'(\eta) = 0 && \text{as } \eta \rightarrow \infty. \quad (5.68)
\end{aligned}$$

$$\begin{aligned}
\bullet \quad T &\rightarrow T_\infty && \text{as } y \rightarrow \infty \\
&\Rightarrow (T_w - T_\infty)\theta + T_\infty \rightarrow T_\infty && \text{as } \eta \rightarrow \infty \\
&\Rightarrow (T_w - T_\infty)\theta \rightarrow 0 && \text{as } \eta \rightarrow \infty \\
&\Rightarrow \theta \rightarrow 0 && \text{as } \eta \rightarrow \infty. \quad (5.69)
\end{aligned}$$

$$\begin{aligned}
 \bullet \quad C &\rightarrow C_\infty && \text{as } y \rightarrow \infty \\
 &\Rightarrow (C_w - C_\infty)\phi + C_\infty \rightarrow C_\infty && \text{as } \eta \rightarrow \infty \\
 &\Rightarrow (C_w - C_\infty)\phi \rightarrow 0 && \text{as } \eta \rightarrow \infty \\
 &\Rightarrow \phi \rightarrow 0. && \text{as } \eta \rightarrow \infty \quad (5.70)
 \end{aligned}$$

Different dimensionless parameters appearing during the numerical simulation are enumerated underneath

$$\left. \begin{aligned}
 Re_x &= \frac{u_e(x)x}{\nu}, \quad b = a/c, \quad E = \left(\frac{E_a}{\kappa T_\infty} \right), \quad \delta_2 = \frac{T_w - T_\infty}{T_\infty} \\
 \beta_2 &= \lambda_1 a, \quad \lambda_2 = \frac{\nu}{Ka}, \quad Pr = \frac{\nu}{\alpha}, \quad Le = \frac{\alpha}{D_B}, \quad \gamma_2 = \frac{h}{k} \sqrt{\frac{\nu}{c}}, \\
 Nb &= \frac{\tau D_B}{\nu} (C_w - C_\infty), \quad Nt = \frac{D_T \tau}{T_\infty \nu} (T_w - T_\infty), \quad Fr = \frac{C_b}{K^{\frac{1}{2}}}, \\
 Rd &= \frac{4\sigma T_\infty^3}{k^* k_\infty}, \quad \sigma_2 = \frac{k_r^2}{c}, \quad \tau = \frac{\rho C_p}{\rho C_f}.
 \end{aligned} \right\} \quad (5.71)$$

Derivation regarding heat transfer rate is given by

$$\begin{aligned}
 Nu_x &= -\frac{x}{(T_w - T_\infty)} \left. \frac{\partial T}{\partial y} \right|_{y=0} + \frac{x q_r}{k(T_w - T_\infty)} \Big|_{y=0}, \text{ where} \\
 q_r &= -\frac{4\sigma^* \partial T^4}{3\kappa^* \partial y} \\
 &\Rightarrow = -\frac{16\sigma^*}{3\kappa^*} T^3 \frac{\partial T}{\partial y} \\
 &\Rightarrow = -\frac{16\sigma^*}{3\kappa^*} ((T_w - T_\infty)\theta(\eta) + T_\infty)^3 \sqrt{\frac{a}{v}} \theta'(\eta) \\
 &\Rightarrow = -\frac{16\sigma^* T_\infty^3}{3\kappa^*} (1 + (\theta_w - 1)\theta(\eta))^3 (T_w - T_\infty) \sqrt{\frac{a}{v}} \theta'(\eta) \\
 &\Rightarrow = -\left(\frac{4}{3}\right) Rd (1 + (\theta_w - 1)\theta(\eta))^3 (T_w - T_\infty) \sqrt{\frac{a}{v}} \theta'(\eta).
 \end{aligned}$$

Therefore,

$$\begin{aligned}
 Nu_x &= \frac{-x \sqrt{\frac{a}{v}} (T_w - T_\infty) \theta'}{(T_w - T_\infty)} - \frac{x \left(\frac{4}{3}\right) Rd (1 + (\theta_w - 1)\theta)^3 (T_w - T_\infty) \sqrt{\frac{a}{v}} \theta'}{(T_w - T_\infty)} \\
 &\Rightarrow = -x \sqrt{\frac{a}{v}} \theta'(\eta) - x \sqrt{\frac{a}{v}} \left(\frac{4}{3}\right) Rd (1 + (\theta_w - 1)\theta(\eta))^3 \theta'(\eta) \\
 &\Rightarrow = -x \sqrt{\frac{a}{v}} \left(\theta' + \left(\frac{4}{3}\right) Rd (1 + (\theta_w - 1)\theta(\eta))^3 \theta' \right) \\
 &\Rightarrow = -\left(1 + \frac{4}{3} Rd (1 + (\theta_w - 1)\theta(\eta))^3 \right) \theta' \sqrt{Re_x}. \quad (5.72)
 \end{aligned}$$

5.2 Solution Methodology

The solutions of dimensionless system of equations (5.61)-(5.63) are numerically achieved with the employment of well established shooting scheme [120]. The interval of integration has been taken $[0, 7]$ instead of $[0, \infty]$. To transform the boundary value problem (BVP) into initial value problem (IVP) comprising of ODEs having order one, f has been denoted by y_1 , θ by y_4 and ϕ by y_6 . The resulting first order ODEs are given by

$$\left. \begin{aligned} y_1' &= y_2, \\ y_2' &= y_3, \\ y_3' &= \frac{[(M^2 + \lambda_2) y_2 + (1 + F_r) y_2^2 - (M^2 \beta_2 + 1) y_1 y_3 - 2\beta_2 y_1 y_2 y_3]}{1 - \beta_2 y_1^2}, \\ y_4' &= y_5, \\ y_5' &= -\frac{\left[(\epsilon_1 + 4Rd(\theta_w - 1)(1 + (\theta_w - 1)y_4)^2 y_5^2) + Pr f y_1 y_5 + Pr (Nb y_5 y_7 + Nt y_5^2) \right]}{\left((1 + \epsilon_1 y_4) + \frac{4}{3} Rd (1 + (\theta_w - 1) y_4)^3 \right)}, \\ y_6' &= y_7, \\ y_7' &= PrLe \sigma_2 (1 + \delta_2 y_4)^n \exp\left(\frac{-E}{1 + \delta_2 y_4}\right) y_6 - PrLe y_1 y_7 - \left(\frac{Nt}{Nb}\right) y_5', \end{aligned} \right\} \quad (5.73)$$

together with the boundary conditions:

$$\left. \begin{aligned} \eta = 0 : \quad & y_1(0) = 0, \quad y_2(0) = 1, \quad y_3(0) = s, \quad y_4(0) = t, \\ & y_5(0) = -\gamma(1 - t), \quad y_6(0) = u, \quad y_7(0) = \frac{Nb}{Nt} \gamma(1 - t). \\ \eta \rightarrow \infty : \quad & y_2(\infty) \rightarrow 0, \quad y_4(\infty) \rightarrow 0, \quad y_6(\infty) \rightarrow 0. \end{aligned} \right\} \quad (5.74)$$

For some appropriate choice of the missing initial conditions s , t and u , the IVP is solved numerically with the utilization of RK4 scheme. The iterative scheme called Newton's method is employed to refine the initial guesses s , t and u until mentioned below is fulfilled.

$$\max\{|y_2(\eta_\infty)|, |y_4(\eta_\infty)|, |y_6(\eta_\infty)|\} < \varepsilon, \quad (5.75)$$

where η_∞ is a finite number and $\epsilon > 0$ represents any positive number with tolerance level $\epsilon = 10^{-6}$. Tolerance is actually the level of error acceptable for any numerical scheme. Solution is convergent with an error less than tolerance level.

5.3 Results and Discussion

The impact of various dimensionless parameters appear during numerical simulation of the problem on velocity, temperature as well as concentration fields are discussed and displayed the results in terms of figures and tables mentioned below.

5.3.1 Impact of β_2 , Fr , λ_2 and M on the velocity field $f'(\eta)$

The impact of Deborah number on $f'(\eta)$ is sketched in Figure 5.2. It can be seen that the field $f'(\eta)$ depreciates by increasing the value of Deborah number. A smaller change in the Deborah number change the material state from solid to the fluid however a converse finding means that the material acts like a solid. That's why a magnification in β_2 diminishes the fluid velocity and moreover the velocity field likewise. A positive variation in the case of inertia coefficient brings about a decrement in the velocity field as displayed in figure 5.3. It is found that by increasing the inertia coefficient, the thermal boundary layer becomes more thick and the fluid cannot move easily. Figure 5.4 is potted for the varying values of porosity parameter on $f'(\eta)$. It can be seen that an incremental variation in the porosity parameter debacles $f'(\eta)$. It is noted that the fluid speed diminishes when moving across a porous expandable medium. Figure 5.5 displays the change in $f'(\eta)$ in response to the deviation in M . When we increase the value of M , the profile $f'(\eta)$ decreases because of the magnetic field. An electrically conducting fluid along with the magnetic field produces a Lorentz force which provide hurdle to the fluid flow. Collision of molecules increases as a result of this resistive force. Due to this, the temperature of fluid rises and a reduction in fluid flow velocity is observed within the boundary layer. As a result decrement in the velocity field is observed by the virtue of an amplification in magnetic field.

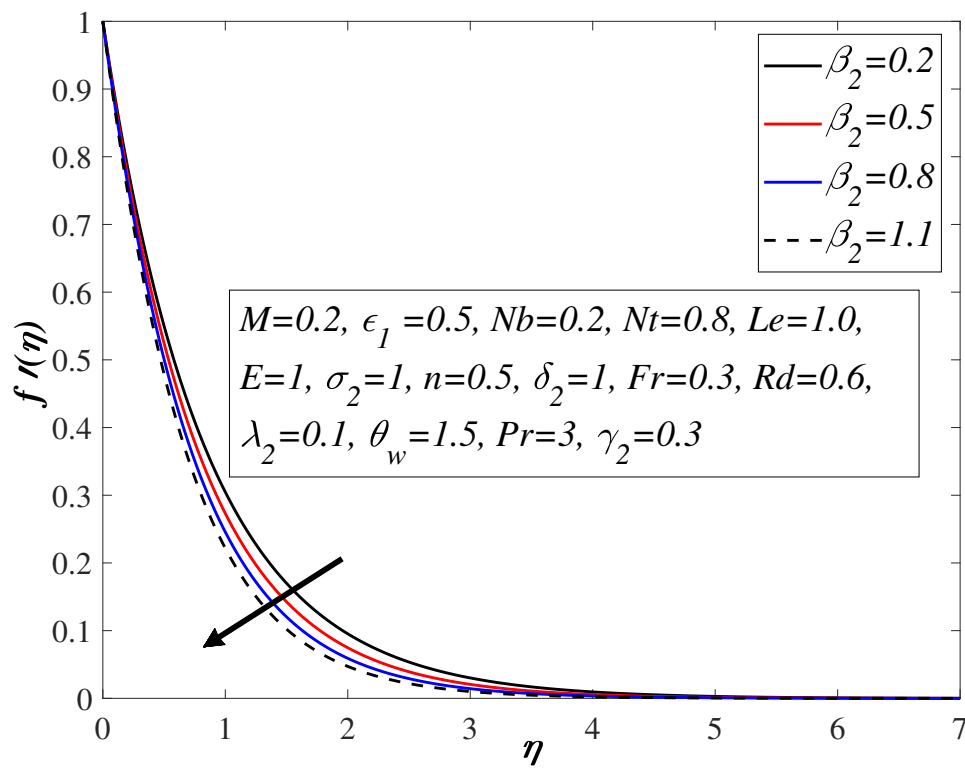


FIGURE 5.2: Impact of β_2 on f' .

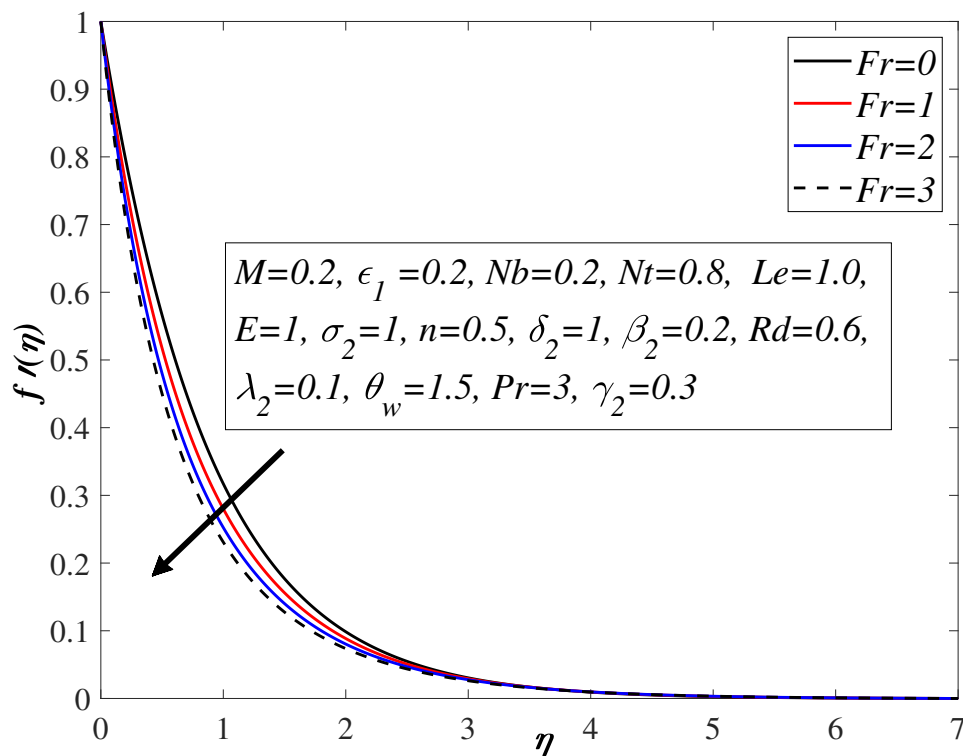


FIGURE 5.3: Effect of Fr on f' .

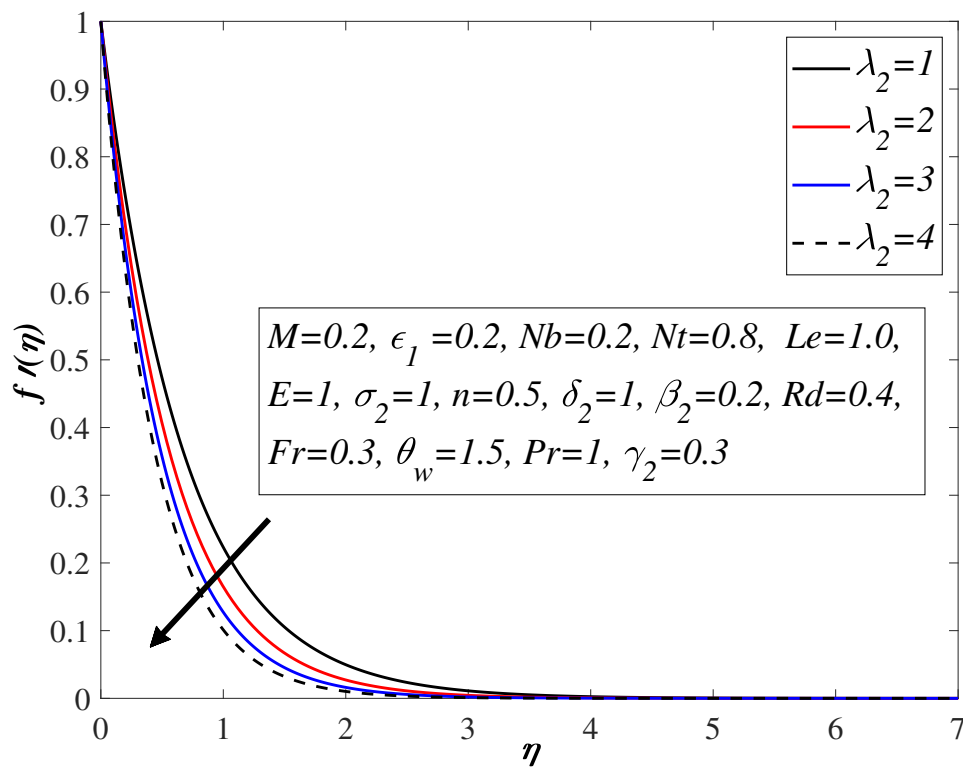


FIGURE 5.4: Influence of λ_2 on f' .

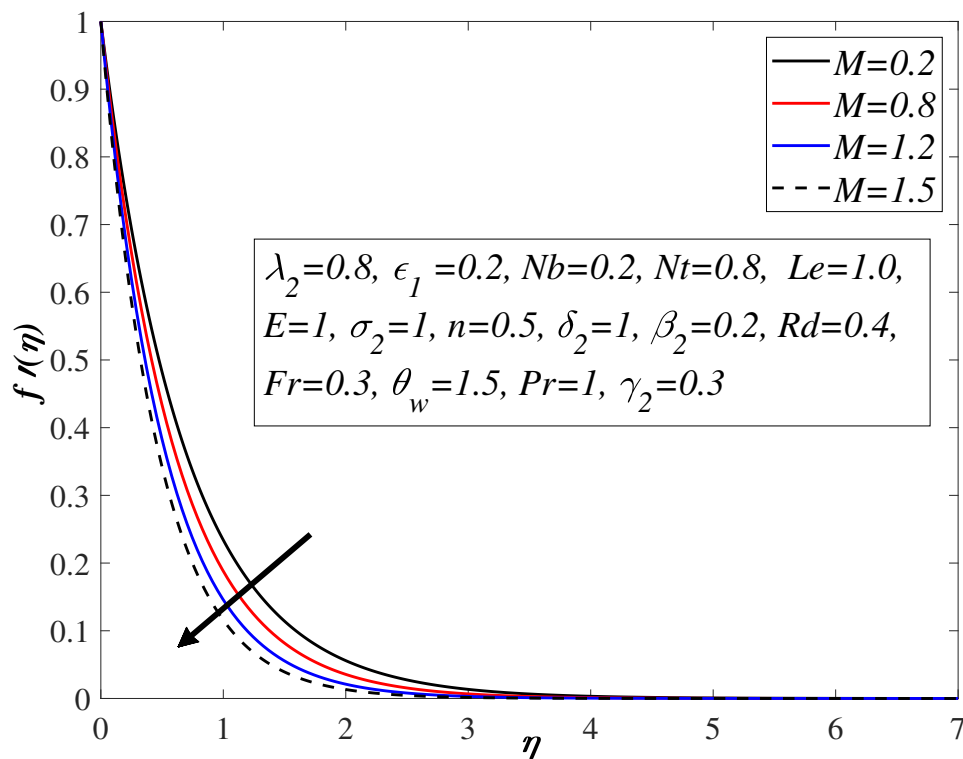


FIGURE 5.5: Impact of M on f' .

5.3.2 Impact of β_2 , Fr , ϵ_1 , λ_2 , M , Nt , Pr , Rd , θ_w , γ_2 on $\theta(\eta)$

Figure 5.6 represents the fact that when the Deborah number increase, the temperature field $\theta(\eta)$ increases. It is note worthy that a magnification in β_2 turn liquids into solids which reduces the fluid speed and velocity field as well. The influence of the variable thermal conductivity on $\theta(\eta)$ has been discussed in Figure 5.7. The impact of variable thermal conductivity ϵ amplifies $\theta(\eta)$ meaningfully but reverse in the case of the volume fraction nanoparticles, thats why the cooling rate is more faster in the case of coolant possesses minimum thermal based conductivity parameter. Figure 5.8 displays the relationship between the inertia coefficient Fr and the temperature profile $\theta(\eta)$. An increase in Fr brings about a magnification in the temperature field. Figure 5.9 is portrayed to analyze the relationship between the porosity parameter λ_2 and the temperature profile $\theta(\eta)$. It is noticed that the presence of porous media creates an increment in the resistance against the fluid flow which magnifies the temperature profile. Figure 5.10 indicates that the temperature profile is enhanced owing to a magnification in M in the presence of resistive force which increases the fluid viscosity and amplifies the temperature field. The behavior of the thermophoresis parameter on the temperature field has been discussed in Figure 5.11. The nanoparticles scattered around the boundary region possesses high temperature migrate towards the region possesses low temperature subject to the availability of thermophoretic force which amplifies the temperature field. Figure 5.12 displays the Prandtl number influence on $\theta(\eta)$. When the Prandtl number increases, a decrease in the thermal conductivity takes place which ultimately guides to a reduction in the temperature field $\theta(\eta)$. Figure 5.13 shows that an increment in the thermal radiation Rd gives more heat to the fluid which results an increment in the temperature. Thermal radiation is one of the pertinent parameter in order to determine the heat transfer analysis. Figure 5.14 sketches the impact of θ_w on the temperature profile. It is quite clear that the temperature increases with a decrease in θ_w . Figure 5.15 depicts that a magnification in Biot number γ results an increase in the temperature profile $\theta(\eta)$. When the Biot number increases, higher convective heat transfer increases.

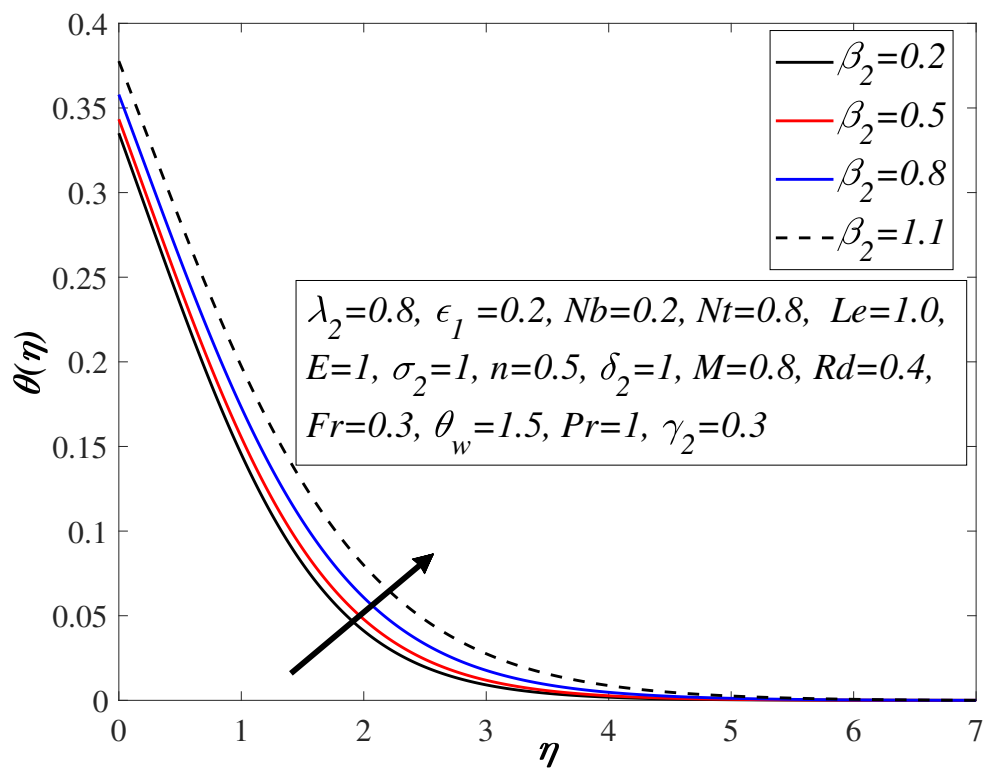


FIGURE 5.6: Effect of β_2 on θ .

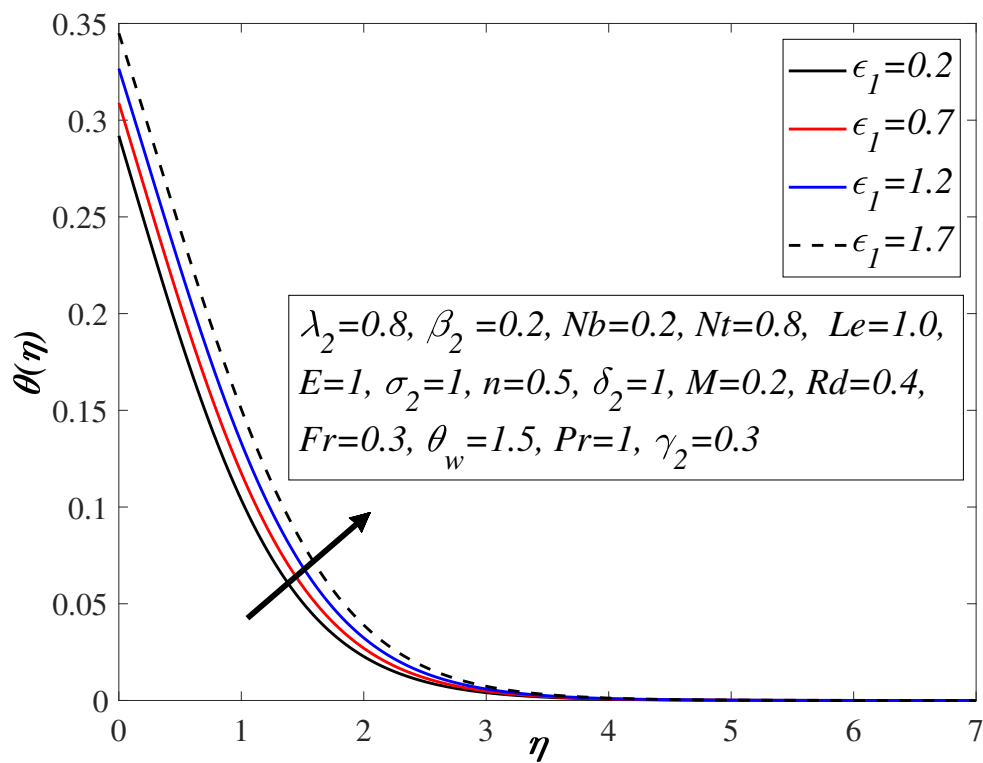


FIGURE 5.7: Influence of ϵ_1 on θ .

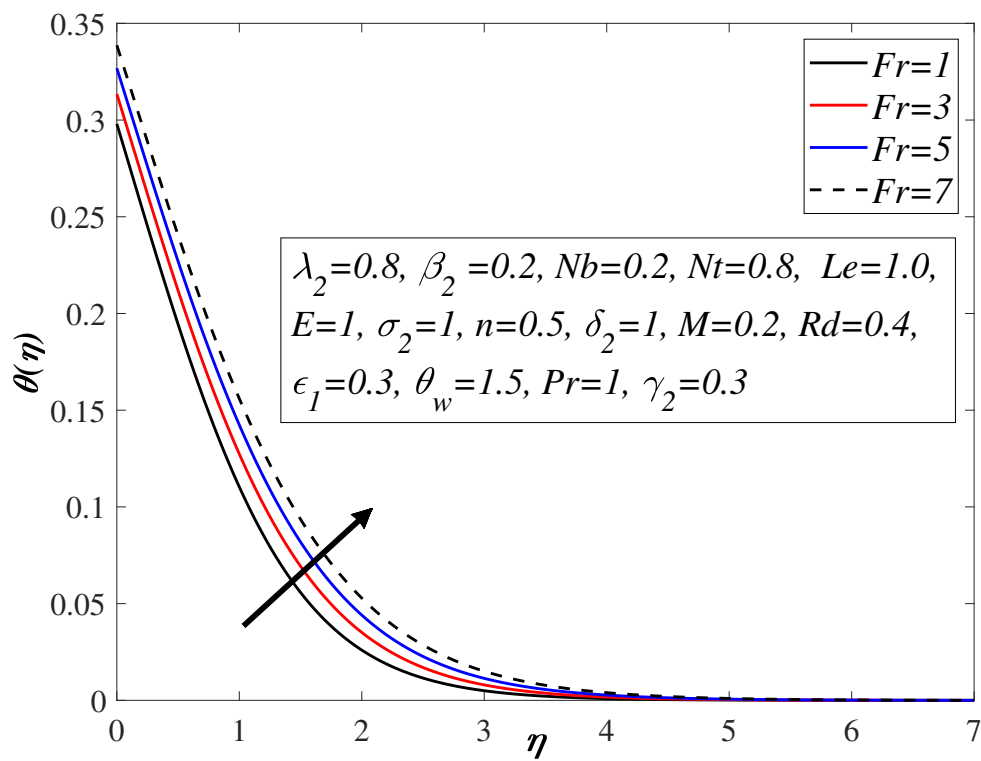


FIGURE 5.8: Impact of Fr on θ .

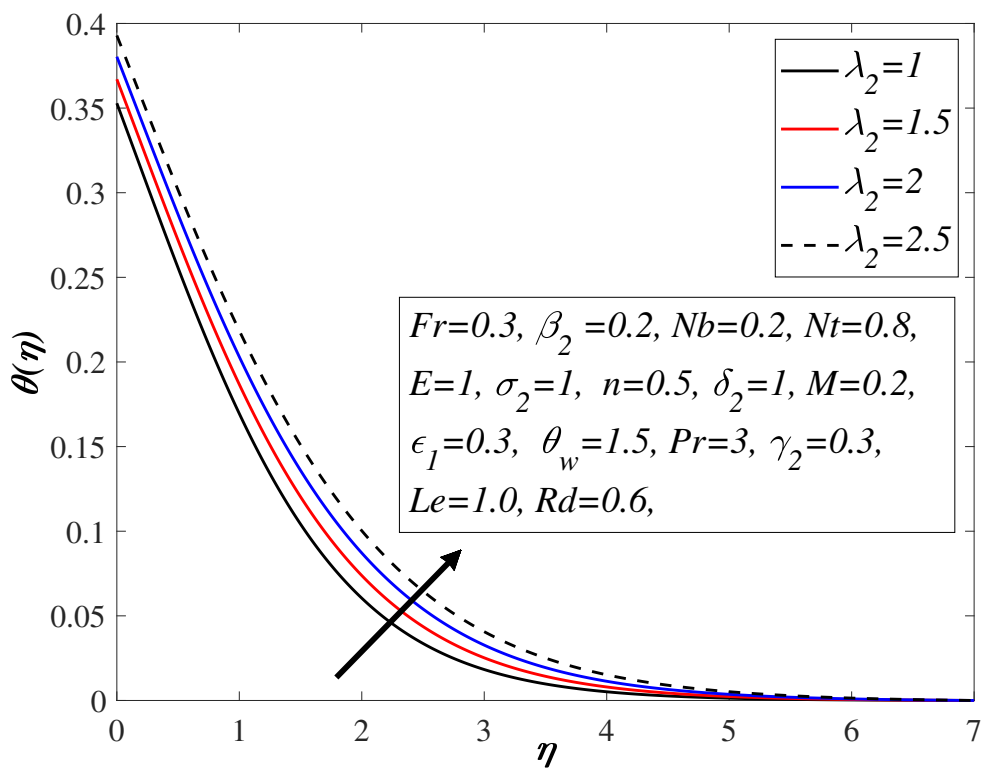


FIGURE 5.9: Effect of λ_2 on θ .

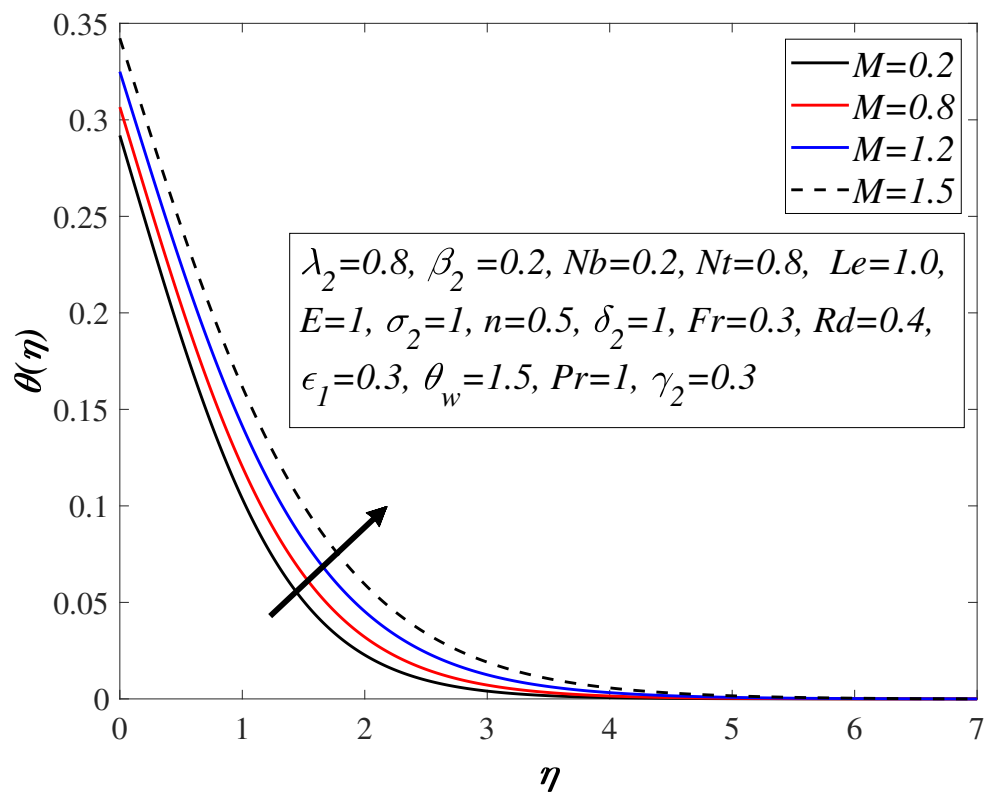


FIGURE 5.10: Influence of M on θ .

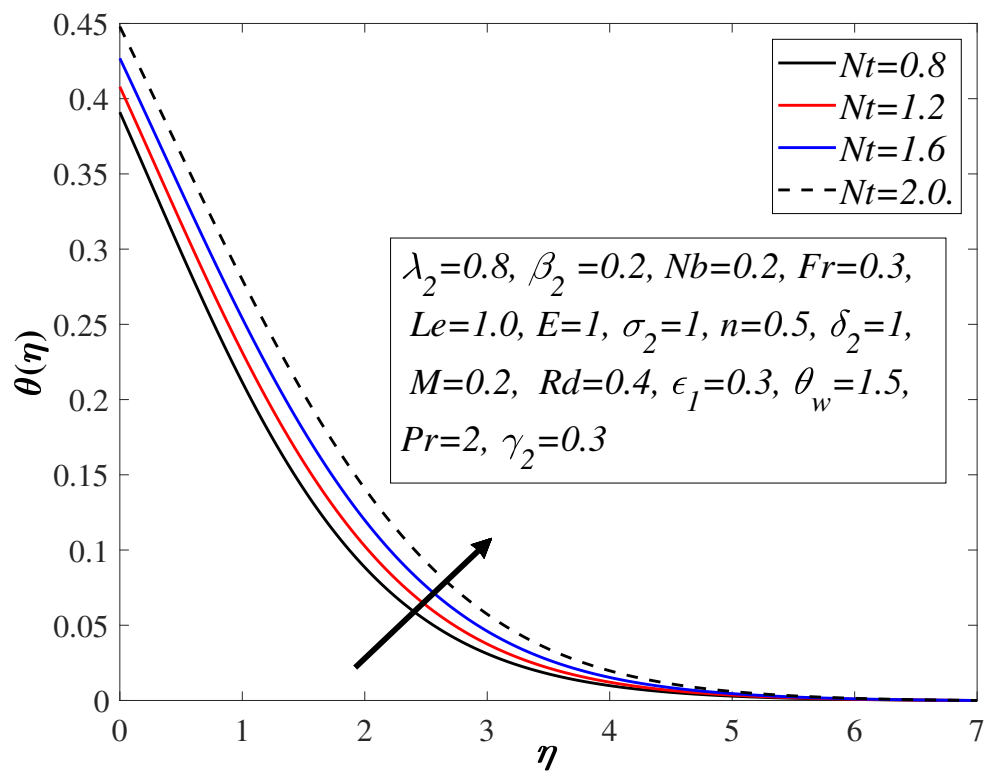


FIGURE 5.11: Influence of N_t on θ .

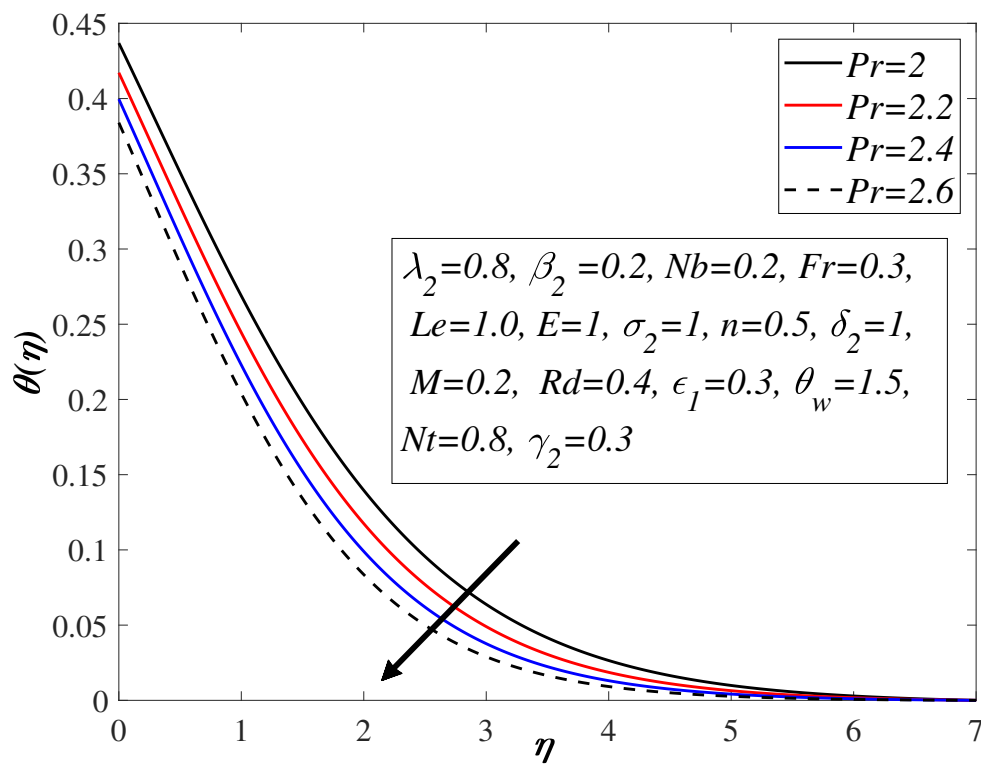


FIGURE 5.12: Impact of Pr on θ .

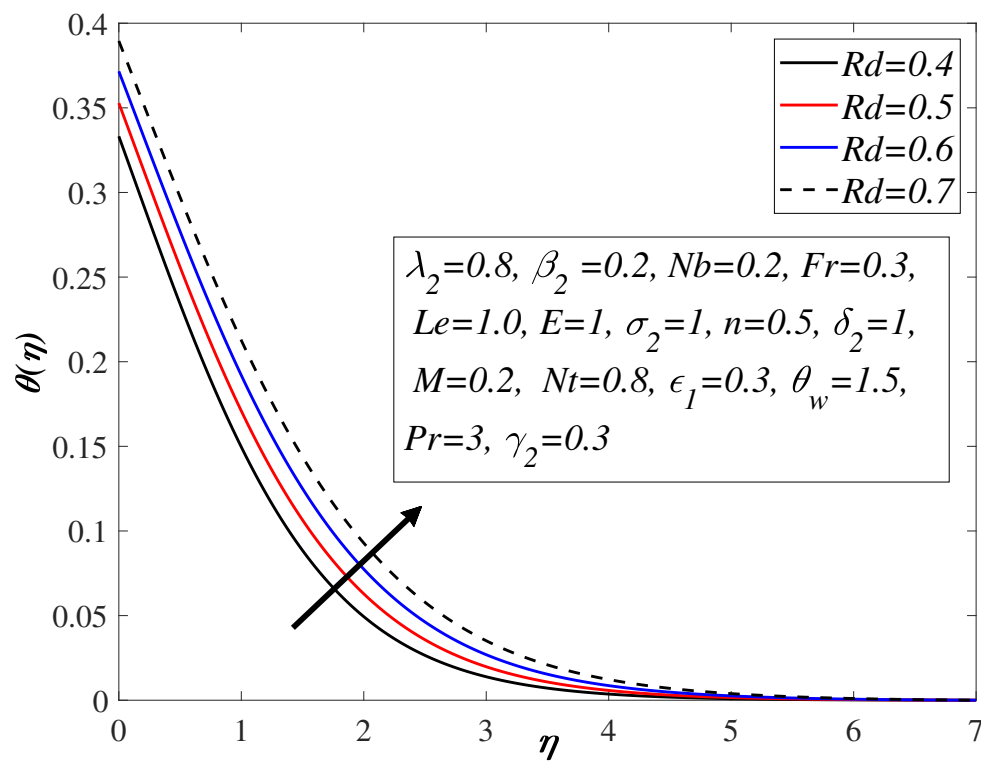


FIGURE 5.13: Effect of Rd on θ .

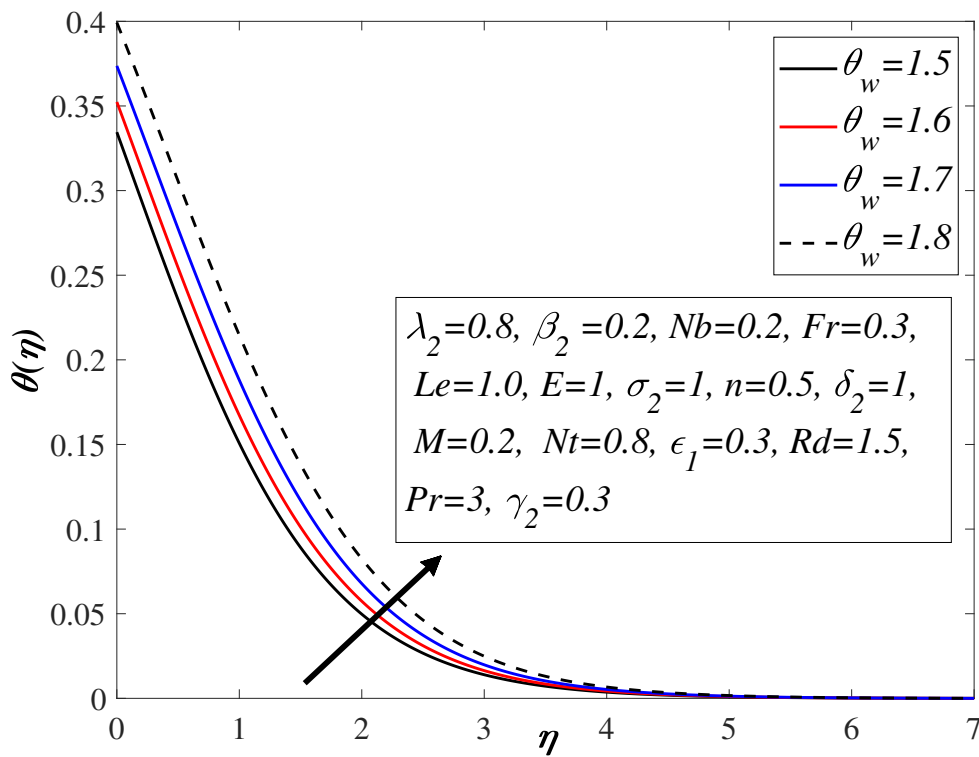


FIGURE 5.14: Influence of θ_w on θ .

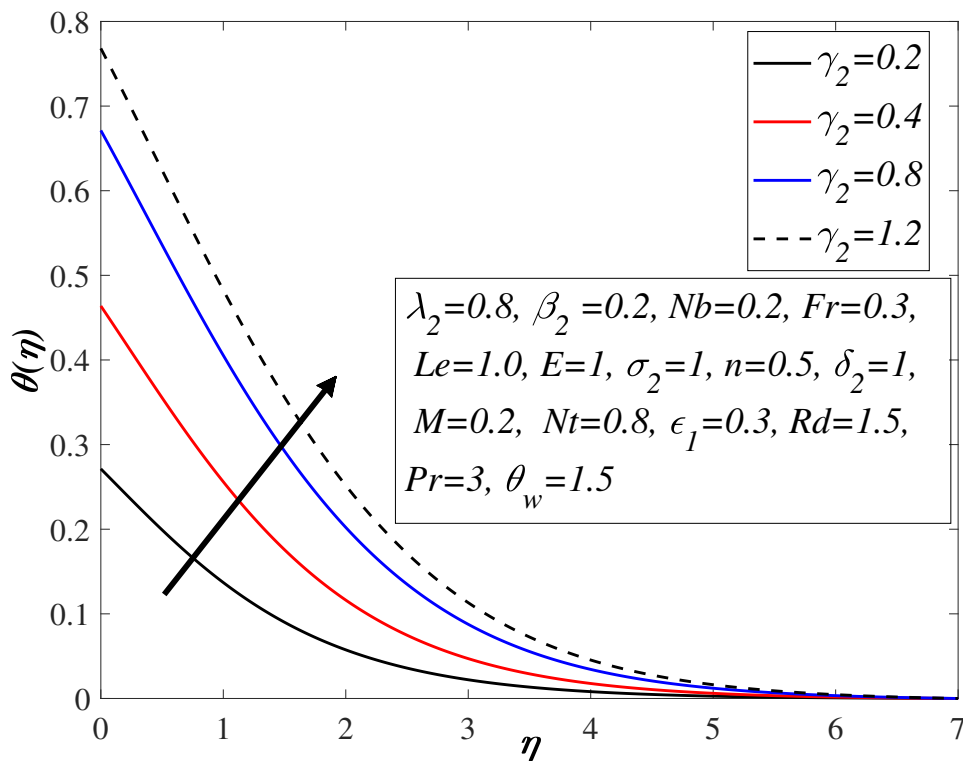


FIGURE 5.15: Impact of γ_2 on θ .

5.3.3 Impact of γ_2 , λ_2 , Le , Nt , σ_2 , β_2 and E on the concentration field $\phi(\eta)$

Figures 5.19-5.22 are designed to study the impact of various dimensionless parameters γ_2 , λ_2 , Le , Nt , σ_2 , β_2 , E arise during numerical simulation of the problem on mass fraction field $\phi(\eta)$. The impact of γ_2 against $\phi(\eta)$ is sketched in Figure 5.16. It is quite evident that a magnification in γ_2 escalates $\phi(\eta)$ and furthermore elevates the concentration thickness in the case of boundary layer. In Figure 5.17, a variation in porosity parameter λ , magnifies the mass fraction field and thickness of the concentration boundary layer. Figure 5.18 is utilized to represent the influence of Le on $\phi(\eta)$. Diffusion process relies on the concentration of the species. The net flux of the molecules move from the region of higher concentration towards the lower one. The parameter Le is related to the diffusivity phenomenon. It is analyzed that an increment in the Lewis number amplifies the Brownian diffusion which elevates $\phi(\eta)$. Diffusion in the fluid elevates the concentration of the species. 5.19 illustrate the influence of Nt on $\phi(\eta)$. In the occurrence of Nt , little particles migrated away from surface having high temperature towards the surface having low temperature. It is researched that by enlarging the estimation of Nt brings about a magnification in the nanoparticle mass fraction profile. Figure 5.20 displays the behaviour of σ_2 on $\phi(\eta)$ and found that a magnification in σ_2 results in a decrement of nanoparticle concentration. Thus a destructive chemical reaction takes place. As a result $\phi(\eta)$ escalates. Impact of Deborah effect on the concentration profile is portrayed in Figure 5.21. It is observed that an amplification in relaxation to retardation time in the fluid give ascent to $\phi(\eta)$, yet reverse in the case of smaller value of relaxation time to retardation time brings about an abatement in the concentration profile. Figure 5.22 is designed to investigate the influence of E on $\phi(\eta)$. It is quite interesting that the value of Arrhenius function declines as a result of a magnification in the parameter E , which contributes a lot in the process to generate a chemical reaction results in an augmentation in $\phi(\eta)$. In the presence of low temperature and high energy brings about an increment in σ_2 which elevates chemical reaction and moreover $\phi(\eta)$ diminishes.

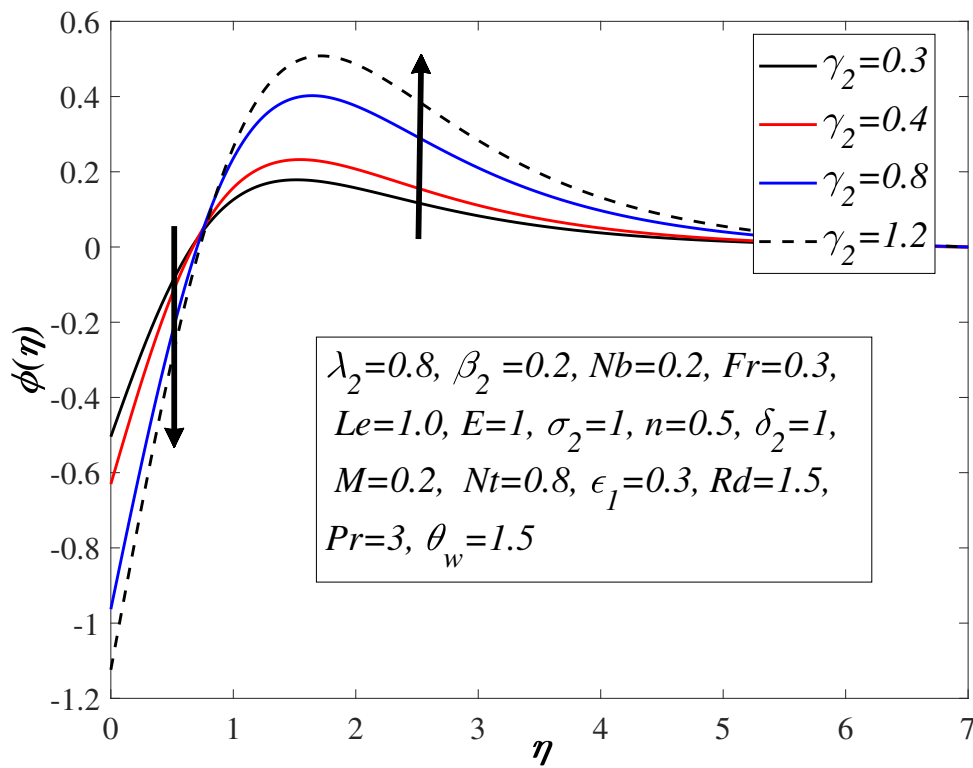


FIGURE 5.16: Effect of γ_2 on ϕ .

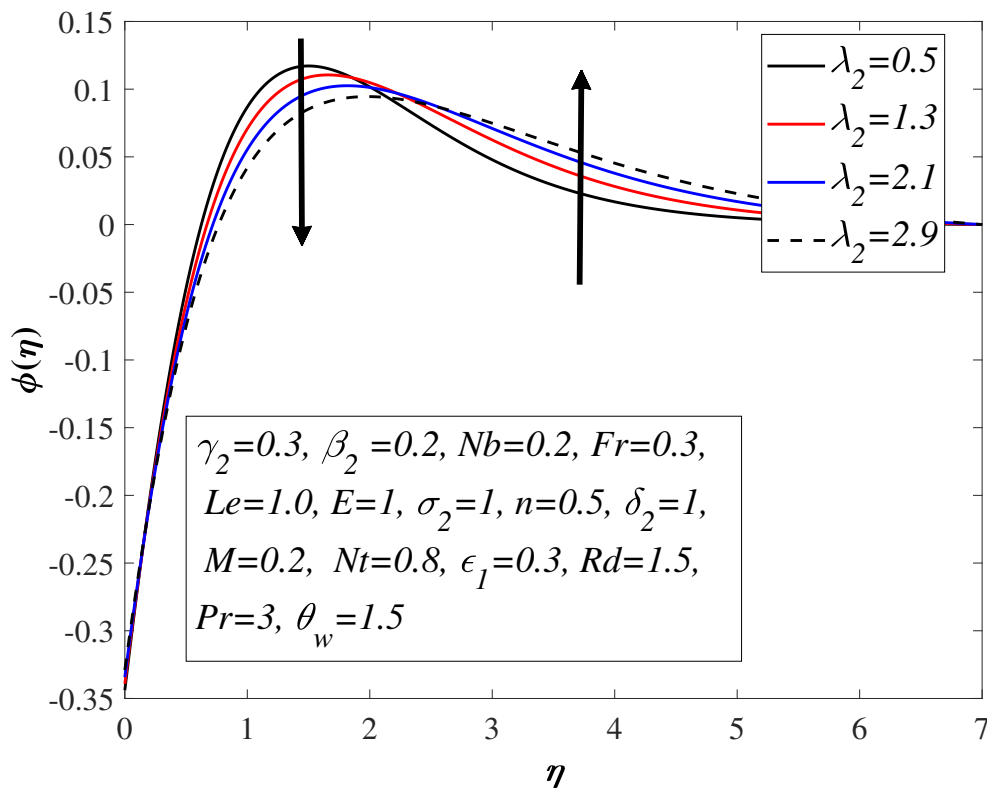


FIGURE 5.17: Influence of λ_2 on ϕ .

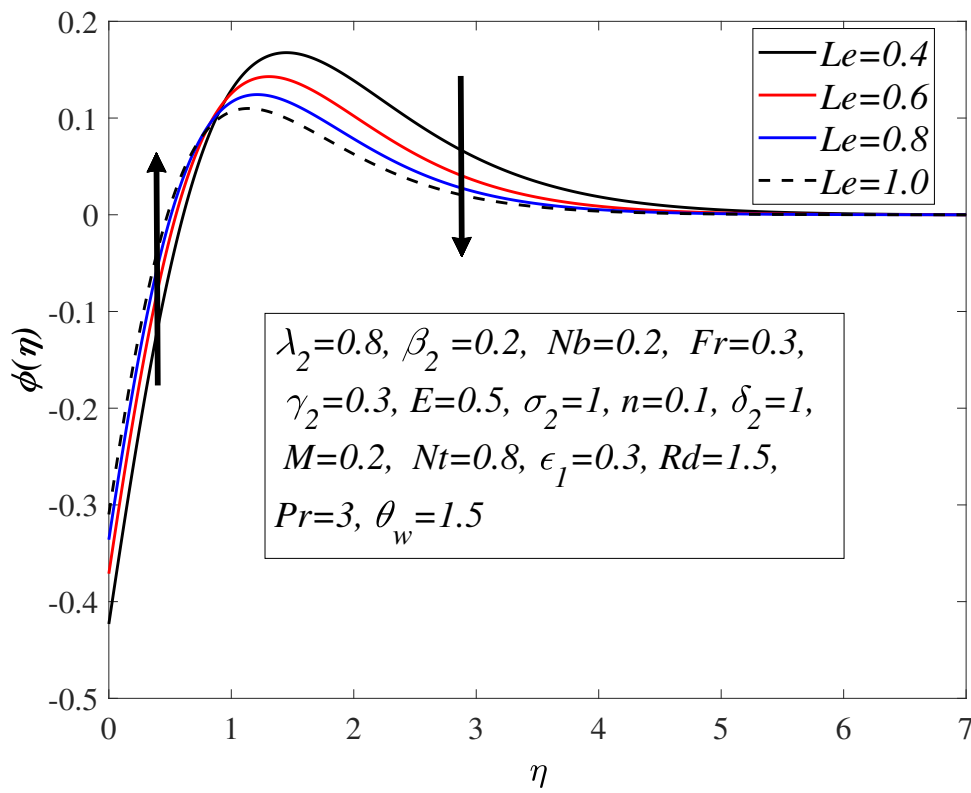


FIGURE 5.18: Impact of Le on ϕ .

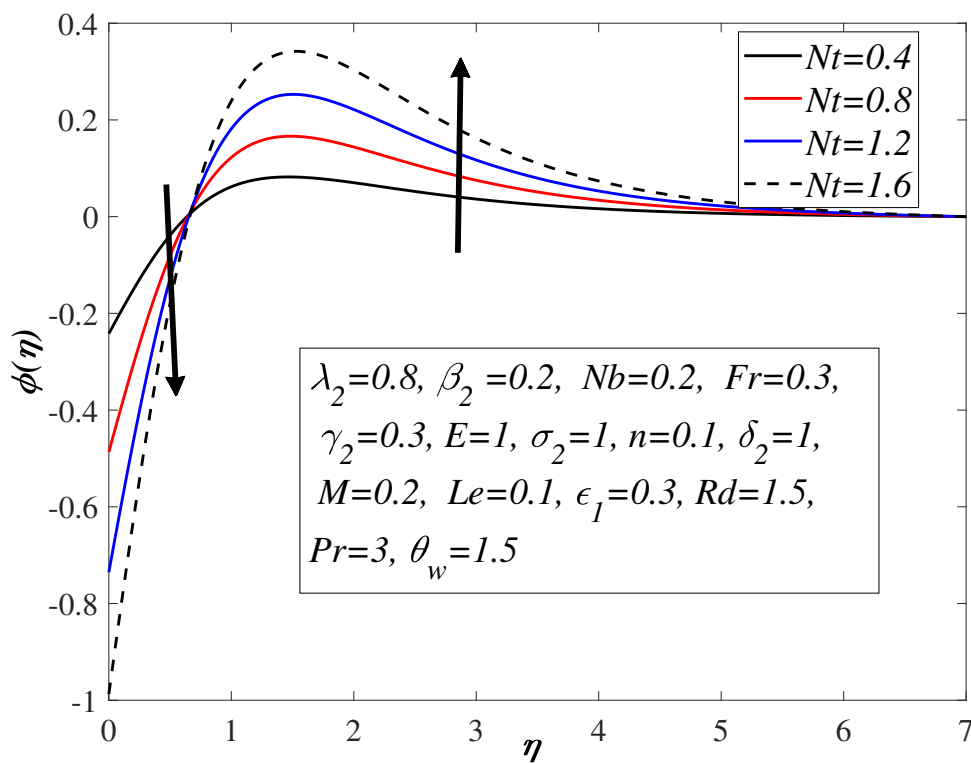


FIGURE 5.19: Effect of N_t on ϕ .

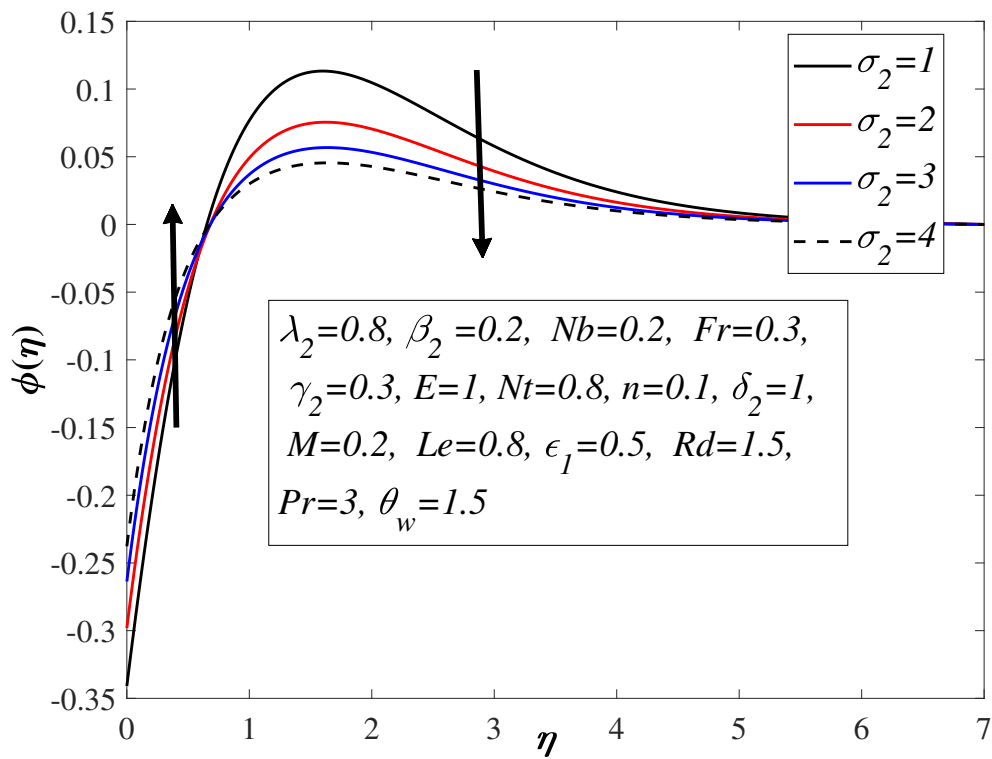


FIGURE 5.20: Influence of σ_2 on ϕ .

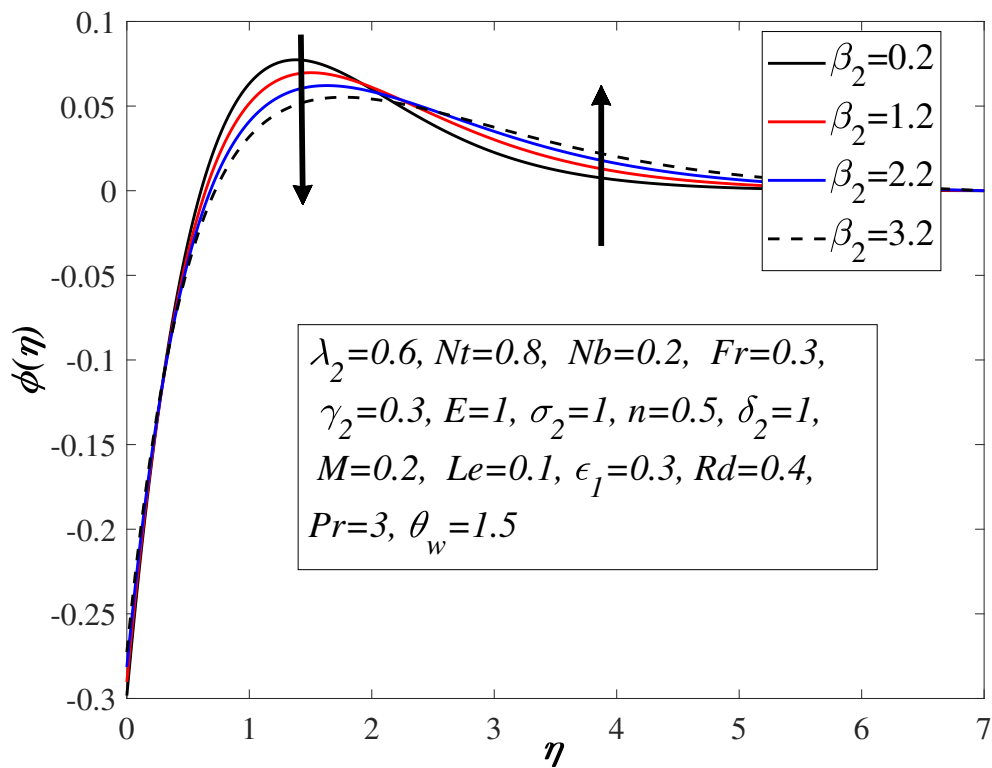
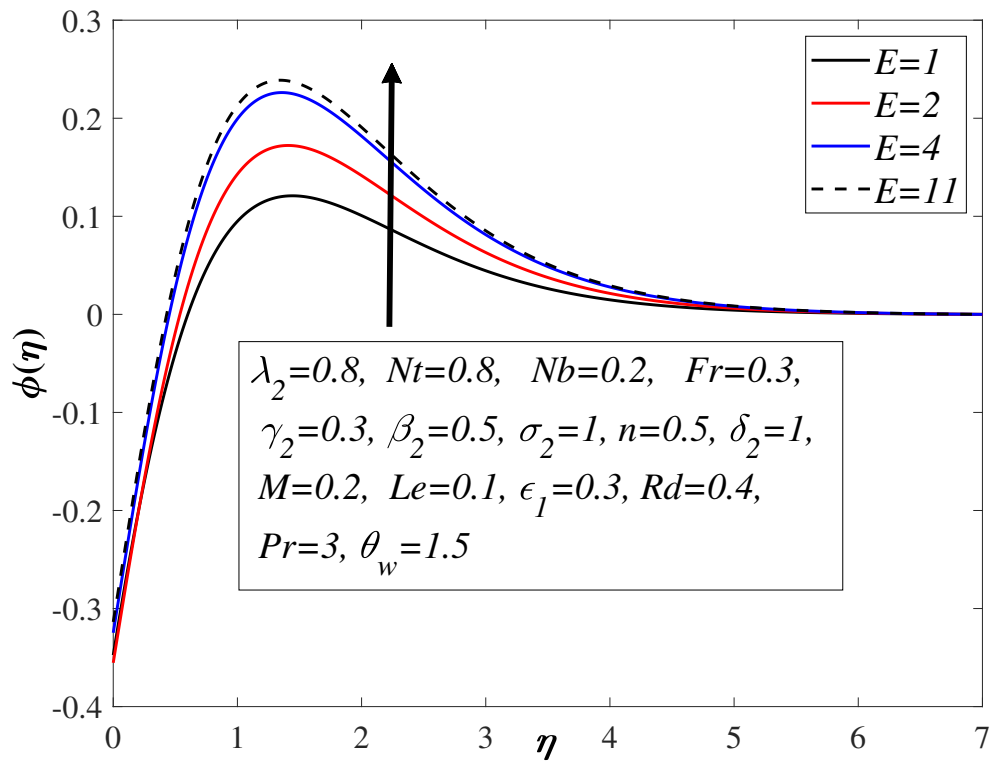


FIGURE 5.21: Impact of β_2 on ϕ .

FIGURE 5.22: Impact of E on ϕ .

In Table 5.1, the present results for Nusselt number are compared with those obtained by Muhammad et al. [55] for different parameters, which shows a very good agreement. Through Table 5.2, it can be observed that an increase in the Biot number β_2 , Rd , Pr brings about an amplification in Nusselt number, whereas incremental change in M , ϵ_2 , Nt , Le depreciates the Nusselt number. From Table 5.3, an enhancement in β_2 , reaction rate constant σ , fitted rate constant n , porosity parameter λ , temperature difference parameter δ leads to a magnification in the heat transfer phenomenon. In the case of an augmentation in β_2 more heat is entered into the system which improves heat transfer rate. Thermal radiation occurs due thermal motion of the molecules and non-linear thermal radiation is used where temperature difference is large. An augmentation in non-linear thermal radiation increases the heat transfer rate. An amplification in the Prandtl number delivers more heat to the fluid which brings about an amplification in the heat transport phenomenon. More heat diffuses into the fluid brings about an escalation in M and the Nusselt number.

TABLE 5.1: Computation of $-\theta'(0)$ showing resemblance with Ref. [55]

β_2	M	λ_2	Fr	Le	Pr	γ_2	N_t	Ref. [55]	Shooting
0.0								0.20321	0.20325
0.5								0.19945	0.19955
1.0								0.19587	0.19606
	0.0							0.20178	0.20185
	0.5							0.19954	0.19939
	0.8							0.19633	0.19592
		0.0						0.20358	0.20361
		0.4						0.19990	0.19999
		0.8						0.19656	0.19676
			0.0					0.20203	0.20207
			0.5					0.20042	0.20050
			1.0					0.19895	0.19905
				0.5				0.20203	0.20188
				1.0				0.20169	0.20175
				1.5				0.20160	0.20166
					0.5			0.15592	0.15955
					1.0			0.19306	0.19326
					1.5			0.21147	0.21146
						0.2		0.15100	0.15103
						0.7		0.32691	0.32708
						1.2		0.40532	0.40559
							0.0	0.20204	0.20120
							0.5	0.20022	0.20028
							1.0	0.19828	0.19883

TABLE 5.2: Computation of Nusselt number against various values of embedded parameters.

M	Rd	β_2	ϵ_1	N_t	Pr	Le	$Nu_x Re_x^{-\frac{1}{2}}$ Shooting
0.2							0.288567
0.4							0.286350
0.6							0.282915
0.7							0.280399
	0.5						0.315386
	0.6						0.341821
	0.7						0.367946
		1.6					0.301540
		1.7					0.315907
		1.8					0.331768
			0.3				0.285396
			0.4				0.282241
			0.5				0.279105
				0.9			0.287217
				1.0			0.285850
				1.2			0.283961
					1.2		0.303084
					1.4		0.315554
					1.6		0.326182
						1.2	0.288249
						1.4	0.287996
						1.6	0.287789

TABLE 5.3: Computation of Nusselt number for different embedded parameters.

E	σ_2	n	δ_2	β_2	λ_2	F_r	γ_2	$Nu_x Re_x^{-\frac{1}{2}}$
								Shooting
0.3								0.288891
0.5								0.289222
0.7								0.289553
	1.2							0.288281
	1.4							0.288048
	1.5							0.287947
		0.7						0.288402
		0.9						0.288239
		1.1						0.288079
			1.8					0.288389
			2.0					0.288156
			2.2					0.288048
				0.4				0.285732
				0.6				0.283048
				0.8				0.280507
					1.0			0.285352
					1.2			0.282384
					1.4			0.279635
						0.3		0.287491
						0.5		0.286455
						0.7		0.285455
							0.5	0.360750
							0.7	0.399335
							0.9	0.422897

5.4 Concluding Remarks

The present investigation is carried out to analyze the magnetohydrodynamics (MHD) stretchedflow of Maxwell nanofluid with the convective boundary condition and consideration of some relevantphysical parameters like activation energy, radiative heat flux and variable thermal conductivity. Someof the conclusive remarks for the present work are presented below.

- The velocity profile $f'(\eta)$ show an opposite impact against the magnetic parameter M and inertia coefficient Fr .
- The temperature profile $\theta(\eta)$ has increasing behavior for the thermal conductivity ϵ_1 , porosity parameter λ_2 and Deborah number β_2 .
- Incremental change in thermophoresis quantity N_t , radiation effect Rd boosts $\theta(\eta)$.
- Magnification in β and λ_2 show an enhancing effect on $\phi(\eta)$ but opposite behaviour is observed in case of Le and σ .
- Rising value of γ_2 amplifies both the velocity and the concentration profiles.
- Nusselt number decreases for boosting the value of thermophoresis parameter N_t .

Chapter 6

Role of Maxwell Velocity and Smoluchowski Temperature Jump Slip Boundary Conditions on Carreau Fluid

The motive behind this chapter is to study three dimensional magneto Carreau fluid past a bidirectional stretchable surface accompanied with Joule heating, non-linear Rosseland thermal radiation and homogenous/heterogenous reaction process. Both velocity and temperature slips boundary conditions have also been taken at the sheet surface. Heat and mass transport phenomena have been studied for the effects like nonlinear Rosseland thermal radiation and cubic autocatalysis chemical reaction. By adopting a suitable transformation, the PDEs regarding continuity, momentum, temperature and homogenous/heterogenous reaction have been converted into ODEs and the shooting scheme is adopted to handle the differential equations numerically. The effect of relevant dimensionless physical quantities on velocity field, temperature as well as mass fraction fields are debated and displayed. The velocity field depreciates owing to an increment in the velocity slip parameter and the temperature field escalates by the virtue of an enhancement in the radiative parameter.

6.1 Mathematical Formulation

Three dimensional electrically conducting magneto radiative Carreau fluid flow subjected to an expandable medium with expanding sheet velocities $U_w(x) = ax$ and $V_w(x) = by$ has been portrayed in Figure 6.1. A magnetic effect of strength B_0 is utilized normal to the expandable sheet. Furthermore the induced magnetic field is not considered because of low Reynold’s number. The Maxwell velocity slip [122] and Smoluchowski temperature jump [123] boundary conditions are also considered. The stress tensor behaviour of Carreau rheological model [89] is premeditated by the expression mentioned below

$$\tau = -p\mathbf{I} + \eta\mathbf{A}_1, \tag{6.1}$$

with

$$\eta = \eta_\infty + (\eta_0 - \eta_\infty)[1 + (I\dot{\gamma})^2]^{\frac{n-1}{2}}, \tag{6.2}$$

where p is the symbol of pressure, identity tensor is denoted by the symbol \mathbf{I} , η_0 and η_∞ symbolizes the fluid thickness at zero as well as infinite-shear rate, n

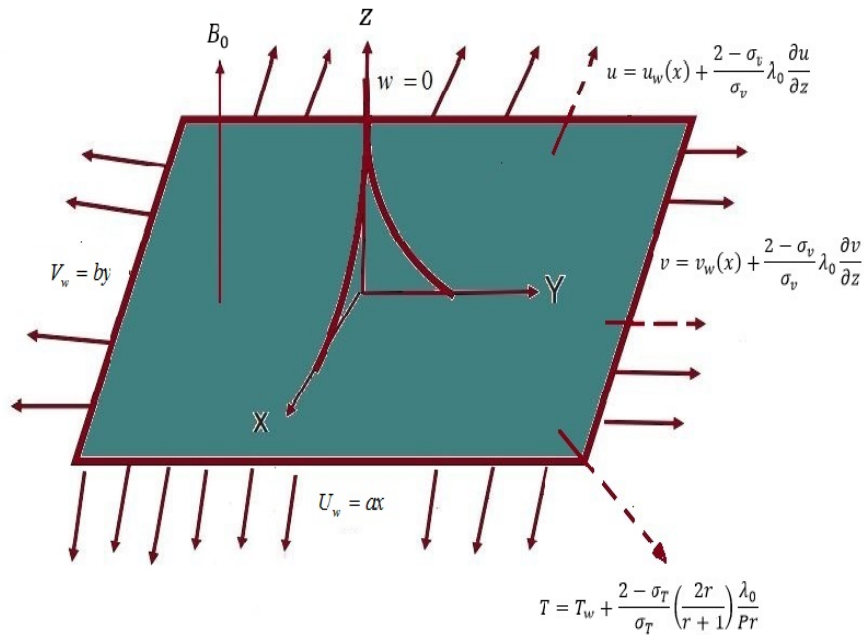


FIGURE 6.1: Physical model of the problem.

expresses the power law index, and Γ a material time expression. The shear rate $\dot{\gamma}$ is expressed as

$$\begin{aligned}\dot{\gamma} &= \sqrt{\frac{1}{2} \Sigma \Sigma \dot{\gamma}_{ij} \dot{\gamma}_{ji}}, \\ &= \sqrt{\frac{1}{2} \mathbb{II}}, \\ &= \sqrt{\frac{1}{2} \text{tr}(\mathbf{A}_1^2)}.\end{aligned}\quad (6.3)$$

Here \mathbb{II} is the second invariant strain rate tensor and \mathbf{A}_1 is the Rivlin-Ericksen tensor given by

$$\mathbf{A}_1 = (\text{grad}\mathbf{V}) + (\text{grad}\mathbf{V})^T. \quad (6.4)$$

We consider the most practical cases where in $\eta_0 \gg \eta_\infty$. Hence η_∞ represent the shear rate at the infinity and moreover taken to be zero and consequently Eq. (6.1) reduces as

$$\tau = -p\mathbf{I} + \eta_0 [1 + (\Gamma\dot{\gamma})^2]^{\frac{n-1}{2}} \mathbf{A}_1, \quad (6.5)$$

where A_1 is the Rivlin-Ericksen tensor. Carreau fluid model is a four parameter model derived from power law model. The expression n in Carreau-model usually lie between $0 < n < 1$ determine how much viscous the fluid is. In the case of $n > 1$ the fluid behaviour is dilatant but shear thickening as a result of $n < 1$. The velocity components of the Carreau fluid flow subjected to an expandable surface and temperature are premeditated by the mathematical expressions mentioned below

$$\mathbf{V} = [u(x, y), v(x, y), 0], \quad T = T(x, y), \quad (6.6)$$

symbols u and v indicates the direction of fluid flow along the x -axis and y -axis. Implementing Eq. (6.4) and Eq. (6.6) in Eq. (6.3), the strain rate $\dot{\gamma}$ is expressed as:

$$\dot{\gamma} = \left[4 \left(\frac{\partial u}{\partial x} \right)^2 + \left(\frac{\partial u}{\partial y} + \frac{\partial v}{\partial x} \right)^2 \right]^{\frac{1}{2}}. \quad (6.7)$$

The fundamental equation regarding Carreau fluid flow rheological model is mentioned below

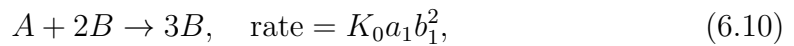
$$\tau = \mu_\infty + (\mu_0 + \mu_\infty) [1 + \Gamma^2 \dot{\gamma}^2]^{\frac{n-1}{2}} \dot{\gamma}, \quad (6.8)$$

whereas the terms μ_0 and μ_∞ symbolize the shear rate at zero and infinity and moreover the parameter n denotes the power-law index. The symbol n represents the nature of the fluid and viscosity of the fluid. The fluid behaviour is dilatant for $n > 1$, pseudoplastic in the case of $n < 1$ and the behaviour is Newtonian as $n = 1$.

In the current formulation of the problem the viscosity effect at infinity termed as μ_∞ is considered as zero. Then stress tensor regarding Carreau fluid model reduces to

$$\tau = \mu_0 \left[1 + \Gamma^2 \dot{\gamma}^2 \right]^{\frac{n-1}{2}} \dot{\gamma}, \quad (6.9)$$

where Γ is the material constant and generally represent the relaxation time. The parameter $\dot{\gamma}$ symbolizes the movement of the layer of the liquid over another layer. The symbol $\dot{\gamma}$ is used to represent the deformation rate. The homogeneous as well as the heterogeneous reaction between species A and B is premeditated by Mansur et al. [124]. Both of the reaction processes exhibit the isothermal phenomenon, bestowed by



The concentration of chemical species A and B is established by the symbols a_1 and b_1 whereas the terms K_0 and K_s represent the homogeneous as well as heterogeneous reaction rate constants. It is reported that homogeneous and heterogeneous chemical reactions have immense utilizations in engineering and industrial applications like manufacturing of polymer products, design of chemical processing equipment, and food processing, etc.

In the light of boundary layer assumptions and the inclusion of effects like nonlinear thermal radiation and chemical reactions the modeled partial differential equations (PDEs) regarding continuity, momentum, energy and homogeneous/heterogeneous reactions along with temperature and velocity slip boundary conditions are enumerated below:

$$\frac{\partial u}{\partial x} + \frac{\partial v}{\partial y} + \frac{\partial w}{\partial z} = 0, \quad (6.12)$$

$$u \frac{\partial u}{\partial x} + v \frac{\partial u}{\partial y} + w \frac{\partial u}{\partial z} = \nu(n-1) \Gamma^2 \left(\frac{\partial u}{\partial z} \right)^2 \frac{\partial^2 u}{\partial z^2} \left(1 + \Gamma^2 \left(\frac{\partial u}{\partial z} \right)^2 \right)^{\frac{n-3}{2}} \tag{6.13}$$

$$+ \nu \frac{\partial^2 u}{\partial z^2} \left(1 + \Gamma^2 \left(\frac{\partial u}{\partial z} \right)^2 \right)^{\frac{n-1}{2}} - \frac{\sigma_1 B_0^2}{\rho_f} u,$$

$$u \frac{\partial v}{\partial x} + v \frac{\partial v}{\partial y} + w \frac{\partial v}{\partial z} = \nu(n-1) \Gamma^2 \left(\frac{\partial v}{\partial z} \right)^2 \frac{\partial^2 v}{\partial z^2} \left(1 + \Gamma^2 \left(\frac{\partial v}{\partial z} \right)^2 \right)^{\frac{n-3}{2}} \tag{6.14}$$

$$+ \nu \frac{\partial^2 v}{\partial z^2} \left(1 + \Gamma^2 \left(\frac{\partial v}{\partial z} \right)^2 \right)^{\frac{n-1}{2}} - \frac{\sigma_1 B_0^2}{\rho_f} v,$$

$$u \frac{\partial T}{\partial x} + v \frac{\partial T}{\partial y} + w \frac{\partial T}{\partial z} = \frac{\mu}{\rho C_p} \left(\left(\frac{\partial u}{\partial z} \right)^2 + \left(\frac{\partial v}{\partial z} \right)^2 \right) + \frac{\sigma_1 B_0^2}{\rho C_p} (u^2 + v^2) \tag{6.15}$$

$$+ \alpha \frac{\partial^2 T}{\partial z^2} - \frac{1}{\rho C_p} \frac{\partial q_r}{\partial z},$$

$$u \frac{\partial a_1}{\partial x} + v \frac{\partial a_1}{\partial y} + w \frac{\partial a_1}{\partial z} = D_A \frac{\partial^2 a_1}{\partial z^2} - K_0 a_1 b_1^2, \tag{6.16}$$

$$u \frac{\partial b_1}{\partial x} + v \frac{\partial b_1}{\partial y} + w \frac{\partial b_1}{\partial z} = D_B \frac{\partial^2 b_1}{\partial z^2} + K_0 a_1 b_1^2. \tag{6.17}$$

The relevant boundary conditions have been included below

$$\left. \begin{aligned} z = 0 : \quad & u = ax + \frac{2 - \sigma_v}{\sigma_v} \lambda_0 \frac{\partial u}{\partial z}, \quad v = by + \frac{2 - \sigma_v}{\sigma_v} \lambda_0 \frac{\partial v}{\partial z}, \quad w = 0, \\ & T = T_w + \frac{2 - \sigma_T}{\sigma_T} \left(\frac{2r}{r+1} \right) \frac{\lambda_0}{Pr} \frac{\partial T}{\partial z}, \quad D_A \frac{\partial a_1}{\partial z} \Big|_{y=0} = K_s a_1(0), \\ & D_B \frac{\partial b_1}{\partial z} \Big|_{y=0} = -K_s a_1(0). \\ z \rightarrow \infty : \quad & u \rightarrow 0, v \rightarrow 0, T \rightarrow T_\infty, a_1 \rightarrow a_0, b_1 \rightarrow 0, \end{aligned} \right\} \tag{6.18}$$

where σ_v and σ_T are the velocity and temperature accomodation coefficients, λ_0 is the mean free path, r is the gas constant respectively, The mathematical expression of Rosseland approximation is premeditated by:

$$q_r = -\frac{4\sigma^*}{3\kappa^*} \frac{\partial T^4}{\partial z} = -\frac{4\sigma^*}{3\kappa^*} T^3 \frac{\partial T}{\partial z}. \tag{6.19}$$

The symbol σ^* and κ^* in the above mentioned expression represents the Stefan-Boltzmann constant and absorption coefficient of the medium. The Rosseland approximation regarding radiative heat flux is applicable where the medium is

optically thick.

By introducing the following non-dimensional variables

$$\left. \begin{aligned} u &= axf'(\eta), \quad v = ayg'(\eta), \quad w = -\sqrt{av}(f(\eta) + g(\eta)), \quad \eta = z\sqrt{\frac{a}{\nu}}, \\ \theta(\eta) &= \frac{T - T_\infty}{T_w - T_\infty}, \quad h(\eta) = \frac{a_1}{a_0}, \quad q(\eta) = \frac{b_1}{a_0}, \end{aligned} \right\} \quad (6.20)$$

the modelled PDEs are converted into the ODEs. The detailed procedure for transformation of Eqs. (6.12)-(6.17) are given below.

$$\begin{aligned} \bullet \quad \frac{\partial u}{\partial x} &= \frac{\partial}{\partial x} (axf'(\eta)) \\ &= af'(\eta). \end{aligned} \quad (6.21)$$

$$\begin{aligned} \bullet \quad \frac{\partial v}{\partial y} &= \frac{\partial}{\partial y} (ayg'(\eta)) \\ &= ag'(\eta). \end{aligned} \quad (6.22)$$

$$\begin{aligned} \bullet \quad \frac{\partial w}{\partial z} &= -\sqrt{(av)} \left(\frac{\partial f}{\partial \eta} \frac{\partial \eta}{\partial z} + \frac{\partial g}{\partial \eta} \frac{\partial \eta}{\partial z} \right) \\ &= -\sqrt{(av)} \sqrt{\frac{a}{v}} (f'(\eta) + g'(\eta)) \\ &= -a(f'(\eta) + g'(\eta)). \end{aligned} \quad (6.23)$$

$$\bullet \quad u \frac{\partial u}{\partial x} = axf'(\eta) \cdot af'(\eta) = a^2 x f'^2(\eta) \quad (6.24)$$

$$\begin{aligned} \bullet \quad \frac{\partial u}{\partial y} &= \frac{\partial}{\partial y} (axf'(\eta)) \\ &= ax \frac{\partial f'}{\partial \eta} \frac{\partial \eta}{\partial y} \\ &= ax \left(\sqrt{\frac{a}{v}} \right) f''. \end{aligned} \quad (6.25)$$

$$\begin{aligned} \bullet \quad v \frac{\partial u}{\partial y} &= ayg'(\eta) \cdot ax \left(\sqrt{\frac{a}{v}} \right) f'' \\ &= 0. \end{aligned} \quad (6.26)$$

$$\begin{aligned} \bullet \quad \frac{\partial u}{\partial z} &= ax \frac{\partial}{\partial \eta} (f'(\eta)) \cdot \frac{\partial \eta}{\partial z} \\ &= ax \sqrt{\frac{a}{v}} f''(\eta). \end{aligned} \quad (6.27)$$

$$\begin{aligned}
 \bullet \quad w \frac{\partial u}{\partial z} &= -\sqrt{av}(f+g)ax\sqrt{\frac{a}{v}}f''(\eta) \\
 &= -(a^2xf+a^2xg)f''(\eta) \\
 &= -a^2x(f+g)f''(\eta).
 \end{aligned} \tag{6.28}$$

$$\bullet \quad v(n-1)I^2 \left(\frac{\partial u}{\partial z} \right)^2 = v(n-1)I^2 \left(ax\sqrt{\frac{a}{v}}f'' \right)^2 \tag{6.29}$$

$$\bullet \quad \left(\frac{\partial u}{\partial z} \right)^2 = \left(\frac{a^3x^2}{v} \right) f''^2(\eta) \tag{6.30}$$

$$\begin{aligned}
 \bullet \quad \frac{\partial^2 u}{\partial z^2} &= \frac{\partial}{\partial z} \left(\frac{\partial u}{\partial z} \right) \\
 &= \frac{\partial}{\partial z} \left(ax\sqrt{\frac{a}{v}}f'(\eta) \right) \\
 &= ax \left(\sqrt{\frac{a}{v}} \right) \frac{\partial f''(\eta)}{\partial \eta} \cdot \frac{\partial \eta}{\partial z} \\
 &= ax \left(\sqrt{\frac{a}{v}} \right)^2 f'''(\eta) \\
 &= \left(\frac{a^2x}{v} \right) f'''.
 \end{aligned} \tag{6.31}$$

$$\begin{aligned}
 \bullet \quad v \frac{\partial^2 u}{\partial z^2} \left(1 + I^2 \left(\frac{\partial u}{\partial z} \right)^2 \right)^{\frac{n-1}{2}} &= v \left(\frac{a^2x}{v} \right) f'''(\eta) \left(1 + I^2 \left(ax\sqrt{\frac{a}{v}}f''(\eta) \right)^2 \right)^{\frac{n-1}{2}} \\
 &= a^2x f''' \left(1 + I^2 \left(\frac{a^3x^2}{v} \right) f''^2 \right)^{\frac{n-1}{2}} \\
 &= a^2x f''' (1 + We_1^2 f''^2)^{\frac{n-1}{2}}.
 \end{aligned} \tag{6.32}$$

$$\begin{aligned}
 \bullet \quad v(n-1)I^2 \left(\frac{\partial u}{\partial z} \right)^2 \frac{\partial^2 u}{\partial z^2} \left(1 + I^2 \left(\frac{\partial u}{\partial z} \right)^2 \right)^{\frac{n-3}{2}} \\
 &= v(n-1)I^2 \left(\frac{a^3x^2}{v} \right) f''^2 \left(ax \left(\sqrt{\frac{a}{v}} \right)^2 f''' \right) \left(1 + I^2 \left(\frac{a^3x^2}{v} \right) f''^2 \right)^{\frac{n-3}{2}} \\
 &= v(n-1)I^2 \left(\frac{a^3x^2}{v} \right) f''^2 \left(\left(\frac{a^2x}{v} \right) f''' \right) \left(1 + I^2 \left(\frac{a^3x^2}{v} \right) f''^2 \right)^{\frac{n-3}{2}} \\
 &= v(n-1) \left(\left(\frac{a^2x}{v} \right) f''' \right) \left(1 + \left(I^2 \frac{a^3x^2}{v} \right) f''^2 \right)^{\frac{n-3}{2}} \left(I^2 \frac{a^3x^2}{v} \right) f''^2 \\
 &= v(n-1) \left(\left(\frac{a^2x}{v} \right) f''' \right) (1 + We_1^2 f''^2)^{\frac{n-3}{2}} We_1^2 f''^2
 \end{aligned} \tag{6.33}$$

$$\bullet \quad \frac{\sigma_1 B_0^2}{\rho_f} u = \frac{\sigma B_0^2}{\rho_f} (axf'(\eta)). \tag{6.34}$$

$$\bullet \frac{\partial v}{\partial x} = \frac{\partial}{\partial x}(ayg'(\eta)) = 0 \quad (6.35)$$

$$\bullet u \frac{\partial v}{\partial x} = ayg'(\eta) \cdot \frac{\partial}{\partial x}(ayg'(\eta)) = 0. \quad (6.36)$$

$$\begin{aligned} \bullet \frac{\partial v}{\partial y} &= \frac{\partial}{\partial y}(ayg'(\eta)) \\ &= ag'(\eta). \end{aligned} \quad (6.37)$$

$$\bullet v \frac{\partial v}{\partial y} = ayg'(\eta) \cdot ag'(\eta) = a^2 yg'(\eta)^2. \quad (6.38)$$

$$\begin{aligned} \bullet \frac{\partial v}{\partial z} &= \frac{\partial v}{\partial \eta} \cdot \frac{\partial \eta}{\partial z} \\ &= \frac{\partial}{\partial \eta}(ayg'(\eta)) \cdot \frac{\partial \eta}{\partial z} \\ &= ayg''(\eta) \cdot \sqrt{\frac{a}{v}} \\ &= ay \sqrt{\frac{a}{v}} g''(\eta). \end{aligned} \quad (6.39)$$

$$\begin{aligned} \bullet w \frac{\partial v}{\partial z} &= -\sqrt{(av)}(f+g) \cdot ay \sqrt{\frac{a}{v}} g''(\eta) \\ &= -(a^2 y f + a^2 y g) g''(\eta) \\ &= -a^2 y (f+g) g''(\eta). \end{aligned} \quad (6.40)$$

$$\begin{aligned} \bullet v(n-1)I^2 \left(\frac{\partial v}{\partial z} \right)^2 &= v(n-1)I^2 \left(ay \sqrt{\frac{a}{v}} g'' \right)^2 \\ &= v(n-1)I^2 \left(\frac{a^3 y^2}{v} \right) g''^2 \\ &= v(n-1)W e_2^2 g''^2. \end{aligned} \quad (6.41)$$

$$\begin{aligned} \bullet \left(\frac{\partial v}{\partial z} \right)^2 &= \left(ay \sqrt{\frac{a}{v}} g'' \right)^2 \\ &= \left(\frac{a^3 y^2}{v} \right) g''^2(\eta). \end{aligned} \quad (6.42)$$

$$\begin{aligned} \bullet \frac{\partial^2 v}{\partial z^2} &= \frac{\partial}{\partial z} \left(ay \sqrt{\frac{a}{v}} g'' \right) \\ &= ay \left(\sqrt{\frac{a}{v}} \right) \frac{\partial g''(\eta)}{\partial \eta} \cdot \frac{\partial \eta}{\partial z} \\ &= ay \left(\sqrt{\frac{a}{v}} \right) g'''(\eta) \cdot \left(\sqrt{\frac{a}{v}} \right) \\ &= \left(\frac{a^2 y}{v} \right) g'''. \end{aligned} \quad (6.43)$$

$$\begin{aligned}
 \bullet \quad v \frac{\partial^2 v}{\partial z^2} \left(1 + \Gamma^2 \left(\frac{\partial v}{\partial z} \right)^2 \right)^{\frac{n-1}{2}} &= v \left(\frac{a^2 y}{v} \right) g''' \left(1 + \Gamma^2 \left(\frac{a^3 y^2}{v} \right) g''^2 \right)^{\frac{n-1}{2}} \\
 &= a^2 y g''' \left(1 + \Gamma^2 \left(\frac{a^3 y^2}{v} \right) g''^2 \right)^{\frac{n-1}{2}} \\
 &= a^2 y g''' (1 + We_2^2 g''^2)^{\frac{n-1}{2}}. \tag{6.44}
 \end{aligned}$$

$$\begin{aligned}
 \bullet \quad v(n-1) \Gamma^2 \left(\frac{\partial v}{\partial z} \right)^2 \frac{\partial^2 v}{\partial z^2} \left(1 + \Gamma^2 \left(\frac{\partial v}{\partial z} \right)^2 \right)^{\frac{n-3}{2}} \\
 &= v(n-1) \Gamma^2 \left(\frac{a^3 y^2}{v} g''' \right) \left(\frac{a^y x^2}{v} \right) g''^2 \left(1 + \Gamma^2 \left(\frac{a^3 y^2}{v} \right) g''^2 \right)^{\frac{n-3}{2}} \\
 &= v(n-1) \Gamma^2 \left(\left(\frac{a^2 y}{v} \right) g''' \right) \left(1 + \Gamma^2 \left(\frac{a^3 y^2}{v} \right) g''^2 \right)^{\frac{n-3}{2}} \left(\frac{a^3 y^2}{v} \right) g''^2 \\
 &= v(n-1) \left(\left(\frac{a^2 y}{v} \right) g''' \right) \left(1 + \left(\Gamma^2 \frac{a^3 y^2}{v} \right) g''^2 \right)^{\frac{n-3}{2}} \left(\Gamma^2 \frac{a^3 y^2}{v} \right) g''^2 \\
 &= a^2 y (n-1) g''' We_2^2 g''^2 (1 + We_2^2 g''^2)^{\frac{n-3}{2}}. \tag{6.45}
 \end{aligned}$$

$$\bullet \quad \frac{\sigma_1 B_0^2}{\rho_f} v = \frac{\sigma_1 B_0^2}{\rho_f} (ayg'(\eta)). \tag{6.46}$$

$$\begin{aligned}
 \bullet \quad \frac{\partial T}{\partial x} &= (T_w - T_\infty) \frac{\partial \theta(\eta)}{\partial \eta} \cdot \frac{\partial \eta}{\partial x} \\
 &= (T_w - T_\infty) \frac{\partial \theta(\eta)}{\partial \eta} \cdot 0 = 0. \tag{6.47}
 \end{aligned}$$

$$\bullet \quad u \frac{\partial T}{\partial x} = axf'(\eta) \cdot (T_w - T_\infty) \frac{\partial \theta(\eta)}{\partial \eta} \cdot \frac{\partial \eta}{\partial x} = 0. \tag{6.48}$$

$$\bullet \quad \frac{\partial T}{\partial y} = (T_w - T_\infty) \frac{\partial \theta(\eta)}{\partial \eta} \cdot \frac{\partial \eta}{\partial y} = 0. \tag{6.49}$$

$$\bullet \quad v \frac{\partial T}{\partial y} = ayg'(\eta) \cdot (T_w - T_\infty) \frac{\partial \theta(\eta)}{\partial \eta} \cdot \frac{\partial \eta}{\partial y} = 0. \tag{6.50}$$

$$\begin{aligned}
 \bullet \quad \frac{\partial T}{\partial z} &= (T_w - T_\infty) \frac{\partial \theta(\eta)}{\partial \eta} \cdot \frac{\partial \eta}{\partial z} \\
 &= \sqrt{\frac{a}{v}} (T_w - T_\infty) \theta'(\eta). \tag{6.51}
 \end{aligned}$$

$$\bullet \quad \alpha \frac{\partial^2 T}{\partial z^2} = \alpha \left(\sqrt{\frac{a}{v}} \right)^2 (T_w - T_\infty) \theta'' \tag{6.52}$$

$$\begin{aligned}
 \bullet \quad w \frac{\partial T}{\partial z} &= -\sqrt{av}(f+g) \sqrt{\frac{a}{v}} (T_w - T_\infty) \theta'(\eta) \\
 &= -a(T_w - T_\infty)(f+g) \theta'(\eta). \tag{6.53}
 \end{aligned}$$

$$\bullet \frac{\mu}{\rho C_p} \left(\left(\frac{\partial u}{\partial z} \right)^2 + \left(\frac{\partial v}{\partial z} \right)^2 \right) = \frac{\mu}{\rho C_p} \left(\frac{a^3}{v} \right) (x^2 f''^2(\eta) + y^2 g''^2(\eta)). \quad (6.54)$$

$$\begin{aligned} \bullet \frac{\sigma_1 B_0^2}{\rho C_p} (u^2 + v^2) &= \frac{\sigma_1 B_0^2}{\rho C_p} (a^2 x^2 f'^2 + a^2 y^2 g'^2) \\ &= \frac{\sigma_1 B_0^2 a^2}{\rho C_p} (x^2 f'^2 + y^2 g'^2). \end{aligned} \quad (6.55)$$

$$\begin{aligned} \bullet \quad q_r &= -\frac{16\sigma^*}{3\kappa^*} T^3 \frac{\partial T}{\partial z}. \\ \frac{\partial q_r}{\partial z} &= -\frac{16\sigma^*}{3\kappa^*} \frac{\partial}{\partial z} \left(T^3 \frac{\partial T}{\partial z} \right) \\ &= -\frac{16\sigma^*}{3\kappa^*} \left(\left(T^3 \frac{\partial^2 T}{\partial z^2} \right) + 3T^2 \left(\frac{\partial T}{\partial z} \right)^2 \right). \end{aligned} \quad (6.56)$$

$$\bullet T^3 \frac{\partial^2 T}{\partial z^2} = ((T_w - T_\infty)\theta + T_\infty)^3 \left(\frac{a}{v} \right) (T_w - T_\infty) \theta''. \quad (6.57)$$

$$\bullet 3T^2 \left(\frac{\partial T}{\partial z} \right)^2 = 3((T_w - T_\infty)\theta + T_\infty)^2 \left(\frac{a}{v} \right) (T_w - T_\infty)^2 \theta'^2. \quad (6.58)$$

$$\begin{aligned} \bullet T^3 \frac{\partial^2 T}{\partial z^2} + 3T^2 \left(\frac{\partial T}{\partial z} \right)^2 &= \left(\frac{a}{v} \right) \left(((T_w - T_\infty)\theta + T_\infty)^3 (T_w - T_\infty) \theta'' + \right. \\ &\quad \left. 3((T_w - T_\infty)\theta + T_\infty)^2 (T_w - T_\infty)^2 \theta'^2 \right). \end{aligned} \quad (6.59)$$

$$\begin{aligned} \bullet \frac{1}{\rho C_p} \frac{\partial q_r}{\partial z} &= -\frac{16\sigma^*}{3\kappa^* \rho C_p} \left(((T_w - T_\infty)\theta(\eta) + T_\infty)^3 \left(\frac{a}{v} \right) \right. \\ &\quad \left. (T_w - T_\infty) \theta'' + 3 \left(\frac{a}{v} \right) (T_w - T_\infty)^2 \right. \\ &\quad \left. ((T_w - T_\infty)\theta(\eta) + T_\infty)^2 \theta'^2 \right). \end{aligned} \quad (6.60)$$

$$\begin{aligned} \bullet \alpha \frac{\partial^2 T}{\partial z^2} - \frac{1}{\rho C_p} \frac{\partial q_r}{\partial z} &= \frac{16\sigma^*}{3\kappa^* \rho C_p} \left(((T_w - T_\infty)\theta(\eta) + T_\infty)^3 \left(\frac{a}{v} \right) (T_w - T_\infty) \theta'' + \right. \\ &\quad \left. 3((T_w - T_\infty)\theta(\eta) + T_\infty)^2 \left(\frac{a}{v} \right) (T_w - T_\infty)^2 \theta'^2 \right) + \\ &\quad \alpha \left(\frac{a}{v} \right) (T_w - T_\infty) \theta'' \\ &= \alpha \left(\frac{a}{v} \right) (T_w - T_\infty) \left(1 + \frac{16\sigma^* T_\infty^3}{3\kappa^* \rho C_p \alpha} (1 + (\theta_w - 1)\theta)^3 \theta'' + \right. \\ &\quad \left. 3(1 + (\theta_w - 1)\theta(\eta))^2 (\theta_w - 1) \theta'^2 \right) \theta''. \end{aligned} \quad (6.61)$$

$$\begin{aligned} \bullet \quad a_1 &= a_0 h(\eta) \\ \frac{\partial a_1}{\partial x} &= a_0 \frac{\partial h}{\partial \eta} \cdot \frac{\partial \eta}{\partial x} = 0. \end{aligned} \quad (6.62)$$

$$\begin{aligned} \bullet \frac{\partial a_1}{\partial y} &= a_0 \frac{\partial h}{\partial \eta} \cdot \frac{\partial \eta}{\partial y} \\ &= a_0 \frac{\partial h}{\partial \eta} \cdot 0 = 0. \end{aligned} \quad (6.63)$$

$$\begin{aligned} \bullet \frac{\partial a_1}{\partial z} &= a_0 \frac{\partial h}{\partial \eta} \cdot \frac{\partial \eta}{\partial z} \\ &= a_0 h'(\eta) \sqrt{\frac{a}{v}}. \end{aligned} \quad (6.64)$$

$$\bullet u \frac{\partial a_1}{\partial x} = ax f'(\eta) \cdot 0 = 0. \quad (6.65)$$

$$\bullet v \frac{\partial a_1}{\partial y} = ay g'(\eta) \cdot a_0 \frac{\partial h}{\partial \eta} \cdot \frac{\partial \eta}{\partial y} = 0. \quad (6.66)$$

$$\begin{aligned} \bullet v \frac{\partial a_1}{\partial y} &= ay g'(\eta) \cdot a_0 \frac{\partial h}{\partial \eta} \cdot \frac{\partial \eta}{\partial y} \\ &= ay g'(\eta) \cdot 0 = 0. \end{aligned} \quad (6.67)$$

$$\bullet w \frac{\partial a_1}{\partial z} = -\sqrt{av}(f(\eta) + g(\eta))a_0 \sqrt{\frac{a}{v}} h'(\eta) \quad (6.68)$$

$$\begin{aligned} \bullet \frac{\partial^2 a_1}{\partial z^2} &= a_0 \sqrt{\frac{a}{v}} \frac{\partial h'(\eta)}{\partial \eta} \cdot \frac{\partial \eta}{\partial z} \\ &= a_0 \left(\sqrt{\frac{a}{v}} \right)^2 h''(\eta) \\ &= a_0 \frac{a}{v} h''(\eta). \end{aligned} \quad (6.69)$$

$$\bullet D_A \frac{\partial^2 a_1}{\partial z^2} = D_A a_0 \left(\frac{a}{v} \right) h''(\eta). \quad (6.70)$$

$$\begin{aligned} \bullet K_0 a_1 b_1^2 &= K_0 h(\eta) a_0 a_0^2 q^2(\eta) \\ &= K_0 h(\eta) a_0^3 q^2(\eta). \end{aligned} \quad (6.71)$$

$$\bullet \frac{\partial b_1}{\partial x} = a_0 \frac{\partial q}{\partial \eta} \cdot \frac{\partial \eta}{\partial x} = 0. \quad (6.72)$$

$$\begin{aligned} \bullet \frac{\partial b_1}{\partial y} &= a_0 \frac{\partial q}{\partial \eta} \cdot \frac{\partial \eta}{\partial y} \\ &= a_0 q'(\eta) \cdot 0 \\ &= 0. \end{aligned} \quad (6.73)$$

$$\begin{aligned} \bullet \frac{\partial b_1}{\partial z} &= a_0 \frac{\partial q}{\partial \eta} \cdot \frac{\partial \eta}{\partial z} \\ &= a_0 q'(\eta) \sqrt{\frac{a}{v}}. \end{aligned} \quad (6.74)$$

$$\bullet u \frac{\partial b_1}{\partial x} = axf'(\eta).0 = 0. \quad (6.75)$$

$$\bullet v \frac{\partial b_1}{\partial y} = axf'(\eta).0 = 0. \quad (6.76)$$

$$\begin{aligned} \bullet w \frac{\partial b_1}{\partial z} &= -\sqrt{av}(f(\eta) + g(\eta))a_0\sqrt{\frac{a}{v}}q'(\eta) \\ &= aa_0(f(\eta) + g(\eta))q'(\eta) \end{aligned} \quad (6.77)$$

$$\begin{aligned} \bullet \frac{\partial^2 b_1}{\partial z^2} &= a_0\sqrt{\frac{a}{v}}\frac{\partial q'(\eta)}{\partial \eta} \cdot \frac{\partial \eta}{\partial z} \\ &= a_0\sqrt{\frac{a}{v}}q'' \cdot \sqrt{\frac{a}{v}} \\ &= a_0\left(\sqrt{\frac{a}{v}}\right)^2 q''(\eta) \\ &= a_0\left(\frac{a}{v}\right) q''(\eta). \end{aligned} \quad (6.78)$$

$$\bullet D_B \frac{\partial^2 b_1}{\partial z^2} = D_B a_0 \left(\frac{a}{v}\right) q''(\eta). \quad (6.79)$$

$$\begin{aligned} \bullet K_0 a_1 b_1^2 &= K_0 h(\eta) a_0 a_0^2 q^2(\eta) \\ &= K_0 h(\eta) a_0^3 q^2(\eta). \end{aligned} \quad (6.80).$$

Using (6.24)-(6.34) in the momentum equation (6.13), we get

$$\begin{aligned} a^2 x f'^2 - a^2 x (f + g) f'' &= a^2 x f''' (1 + We_1^2 f''^2)^{\frac{n-1}{2}} + v(n-1) \left(\frac{a^2 x}{v}\right) f''' \\ &\quad We_1^2 f''^2 (1 + We_1^2 f''^2)^{\frac{n-3}{2}} - \frac{\sigma_1 B_0^2}{\rho_f} (axf') \\ a^2 (x f'^2 - (f + g) f'') &= a^2 x \left(f''' (1 + We_1^2 f''^2)^{\frac{n-1}{2}} + v(n-1) \left(\frac{1}{v}\right) f''' \right. \\ &\quad \left. We_1^2 f''^2 (1 + We_1^2 f''^2)^{\frac{n-3}{2}} - \frac{a^2 \sigma_1 B_0^2}{\rho_f} (axf') \right) \\ \Rightarrow f'^2(\eta) - (f + g) f''(\eta) &= (n-1) f''' f''^2 (1 + We_1^2 f''^2)^{\frac{n-3}{2}} We_1^2 - \\ &\quad \frac{\sigma_1 B_0^2}{\rho_f a} (f'(\eta)) + f''' (1 + We_1^2 f''^2)^{\frac{n-1}{2}} \\ \Rightarrow f'^2(\eta) - (f + g) f''(\eta) &= f''' (1 + We_1^2 f''^2)^{\frac{n-3}{2}} \left((n-1) We_1^2 f''^2 + \right. \\ &\quad \left. (1 + We_1^2 f''^2) \right) - M f' \\ \Rightarrow f''' (1 + We_1^2 f''^2)^{\frac{n-3}{2}} (1 + n We_1^2 f''^2) &- f'^2 + (f + g) f'' - M f' = 0. \end{aligned} \quad (6.81)$$

After utilizing (6.35)-(6.46) in (6.14), we get

$$\begin{aligned}
 a^2 y g'^2 - a^2 y (f + g) g'' &= a^2 y g''' (1 + We_2^2 g''^2)^{\frac{n-1}{2}} + v(n-1) \left(\frac{a^2 y}{v} \right) g''' \\
 &\quad We_2^2 g''^2 (1 + We_2^2 g''^2)^{\frac{n-3}{2}} - \frac{\sigma_1 B_0^2}{\rho_f} (a y g') \\
 \Rightarrow g'^2(\eta) - (f + g) g''(\eta) &= (n-1) g''' g''^2 (1 + We_1^2 f''^2)^{\frac{n-3}{2}} We_1^2 - \\
 &\quad \frac{\sigma_1 B_0^2}{\rho_f a} (g'(\eta)) + g''' (1 + We_2^2 g''^2)^{\frac{n-1}{2}} \\
 \Rightarrow g''' (1 + We_2^2 g''^2)^{\frac{n-3}{2}} &\left((n-1) We_2^2 g''^2 + (1 + We_2^2 g''^2) \right) - M g' \\
 &- g'^2 + (f + g) g'' = 0. \\
 \Rightarrow g''' (1 + We_2^2 g''^2)^{\frac{n-3}{2}} &(1 + n We_2^2 g''^2) - g'^2 + (f + g) g'' - M g' = 0. \quad (6.82)
 \end{aligned}$$

After utilizing (6.47)-(6.61) in (6.15), the following is achieved

$$\begin{aligned}
 -a(T_w - T_\infty)(f + g)\theta' &= \frac{\alpha a(T_w - T_\infty)}{v} \left(1 + \frac{16\sigma^* T_\infty^3}{3\kappa^* \kappa} ((1 + (\theta_w - 1)\theta)^3 \theta'' \right. \\
 &\quad \left. + 3(1 + (\theta_w - 1)\theta)^2 (\theta_w - 1)\theta'^2 \right) + \frac{\sigma_1 B_0^2}{\rho C_p} \left(a^2 x^2 f'^2 \right. \\
 &\quad \left. + a^2 y^2 g'^2 \right) + \frac{\mu}{\rho C_p} \left(\frac{a^3 x^2}{v} f''^2 + \frac{a^3 y^2}{v} g''^2 \right) \\
 \Rightarrow -(f + g)\theta' &= \frac{(1 + Rd((1 + (\theta_w - 1)\theta))^3 \theta'' + 3(1 + (\theta_w - 1)\theta)^2 (\theta_w - 1)\theta'^2)}{\left(\frac{v}{\alpha} \right)} \\
 &\quad + \frac{\sigma_1 B_0^2}{\rho a} \left(\frac{a^2 x^2 f'^2}{C_p(T_w - T_\infty)} + \frac{a^2 y^2 g'^2}{C_p(T_w - T_\infty)} \right) \\
 &\quad + \frac{\mu}{\rho C_p a} \left(\frac{a^3 x^2 f''^2}{v(T_w - T_\infty)} + \frac{a^3 y^2 g''^2}{v(T_w - T_\infty)} \right) \\
 \Rightarrow -Pr(f + g)\theta' &= (1 + Rd((1 + (\theta_w - 1)\theta))^3 \theta'' + 3(1 + (\theta_w - 1)\theta)^2 (\theta_w - 1)\theta'^2)) \\
 &\quad + Pr \left(\left(\frac{Ma^2 x^2 f'^2}{C_p(T_w - T_\infty)} + \frac{Ma^2 y^2 g'^2}{C_p(T_w - T_\infty)} \right) + \frac{\mu}{\rho v} \left(\frac{a^2 x^2 f''^2}{C_p(T_w - T_\infty)} \right. \right. \\
 &\quad \left. \left. + \frac{a^2 y^2 g''^2}{C_p(T_w - T_\infty)} \right) \right). \\
 \Rightarrow (1 + Rd((1 + (\theta_w - 1)\theta))^3 \theta'' &+ 3(1 + (\theta_w - 1)\theta(\eta))^2 (\theta_w - 1)\theta'^2)) + \\
 Pr((f + g)\theta' + M(Ec_x f'^2 + Ec_y g'^2) &+ (Ec_x f''^2 + Ec_y g''^2)) = 0. \quad (6.83)
 \end{aligned}$$

Using (6.62)-(6.71) in (6.16), the dimensionless concentration equation is

$$\begin{aligned}
 -aa_0h'(\eta)(f(\eta) + g(\eta)) &= D_Aa_0 \left(\frac{a}{v}\right) h''(\eta) - K_0h(\eta)a_0^3q^2(\eta). \\
 -aa_0h'(\eta)(f(\eta) + g(\eta)) &= D_Aa_0 \left(\frac{a}{v}\right) h''(\eta) - K_0h(\eta)a_0^3q^2(\eta) \\
 \Rightarrow -h'(\eta)(f(\eta) + g(\eta)) &= \frac{D_A \left(\frac{a}{v}\right) h''}{a} - \frac{K_0h(\eta)a_0^2q^2(\eta)}{a}. \\
 \Rightarrow -h'(\eta)(f(\eta) + g(\eta)) &= \left(\frac{D_A}{v}\right) h'' - \frac{K_0a_0^2}{a}h(\eta)q^2(\eta) \\
 \Rightarrow \frac{1}{\left(\frac{v}{D_A}\right)}h'' + h'(\eta)(f(\eta) + g(\eta)) - Kh(\eta)q^2(\eta) &= 0 \\
 \Rightarrow \frac{1}{Sc}h'' + h'(\eta)(f(\eta) + g(\eta)) - Kh(\eta)q^2(\eta) &= 0 \\
 \Rightarrow h'' + Sc h'(\eta)(f(\eta) + g(\eta)) - K Sc h(\eta)q^2(\eta) &= 0. \tag{6.84}
 \end{aligned}$$

After using (6.72)-(6.80) in (6.17) gets the following form

$$\begin{aligned}
 -aa_0q'(\eta)(f(\eta) + g(\eta)) &= D_Ba_0 \left(\frac{a}{v}\right) q''(\eta) + K_0h(\eta)a_0^3q^2(\eta) \\
 \Rightarrow -\left(\frac{D_A}{D_A}\right)q'(\eta)(f(\eta) + g(\eta)) &= \frac{D_B}{D_A} \left(\frac{a}{v}\right) q''a + \frac{K_0h(\eta)a_0^2q^2(\eta)}{a} \\
 \Rightarrow -q'(\eta)(f(\eta) + g(\eta)) &= \frac{D_B}{D_A} \frac{1}{\left(\frac{v}{D_A}\right)}h'' - \frac{K_0a_0^2}{a}h(\eta)q^2(\eta) \\
 \Rightarrow \frac{D_B}{D_A} \frac{1}{\left(\frac{v}{D_A}\right)}h'' + h'(\eta)(f(\eta) + g(\eta)) + Kh(\eta)q^2(\eta) &= 0. \\
 \Rightarrow \frac{\xi}{Sc}q'' + q'(\eta)(f(\eta) + g(\eta)) + Kh(\eta)q^2(\eta) &= 0. \tag{6.85}
 \end{aligned}$$

The species diffusions are of comparable size by taking $D_A=D_B=1$. [104]

In this case,

$$\begin{aligned}
 h(\eta) + q(\eta) &= 1, \\
 q(\eta) &= 1 - h(\eta), \tag{6.86}
 \end{aligned}$$

and hence (6.84) and (6.85) reduce to

$$\frac{1}{Sc}h'' + h'(\eta)(f(\eta) + g(\eta)) - Kh(\eta)(1 - h)^2(\eta) = 0, \tag{6.87}$$

having boundary conditions given in (6.92) at $\eta = 0$ and (6.97) at $\eta \rightarrow \infty$. The dimensionless boundary conditions are achieved through the procedure mentioned below

$$\begin{aligned}
 \bullet \quad u &= ax + \frac{2 - \sigma_v}{\sigma_v} \lambda_0 a \frac{\partial u}{\partial z} && \text{at } z = 0 \\
 \Rightarrow ax f'(\eta) &= ax + \frac{2 - \sigma_v}{\sigma_v} \lambda_0 a \sqrt{\frac{a}{v}} x f'' && \text{at } \eta = 0 \\
 &= \frac{ax + \frac{2 - \sigma_v}{\sigma_v} \lambda_0 a x \sqrt{\frac{a}{v}} f''}{ax} && \text{at } \eta = 0 \\
 &= 1 + \frac{2 - \sigma_v}{\sigma_v} \lambda_0 \sqrt{\frac{a}{v}} f''(\eta) && \text{at } \eta = 0 \\
 &= 1 + \gamma_3 f''(\eta). && \text{at } \eta = 0 \quad (6.88)
 \end{aligned}$$

$$\begin{aligned}
 \bullet \quad v &= by + \frac{2 - \sigma_v}{\sigma_v} \lambda_0 a \frac{\partial v}{\partial z} && \text{at } z = 0 \\
 \Rightarrow ay g'(\eta) &= by + \frac{2 - \sigma_v}{\sigma_v} \lambda_0 a y g'' \sqrt{\frac{a}{v}} && \text{at } \eta = 0 \\
 &= \frac{b}{a} + \frac{2 - \sigma_v}{\sigma_v} \lambda_0 g'' \sqrt{\frac{a}{v}} && \text{at } \eta = 0 \\
 &= \beta_3 + \gamma_3 g''(\eta). && \text{at } \eta = 0 \quad (6.89)
 \end{aligned}$$

$$\begin{aligned}
 \bullet \quad w &= 0 && \text{at } z = 0 \\
 \Rightarrow f(\eta) + g(\eta) &= 0 && \text{at } \eta = 0 \\
 \Rightarrow f(\eta) &= 0 && \text{at } \eta = 0 \\
 \Rightarrow g(\eta) &= 0 && \text{at } \eta = 0. \quad (6.90)
 \end{aligned}$$

$$\begin{aligned}
 \bullet \quad T &= T_w + \frac{2 - \sigma_T}{\sigma_T} \frac{2r}{r+1} \frac{\lambda_0}{Pr} \frac{\partial T}{\partial z} && \text{at } z = 0 \\
 \Rightarrow (T_w - T_\infty)\theta + T_\infty &= && \\
 T_w + \frac{2 - \sigma_T}{\sigma_T} \frac{2r}{r+1} \frac{\lambda_0}{Pr} \sqrt{\frac{a}{v}} (T_w - T_\infty)\theta' &&& \text{at } \eta = 0 \\
 \Rightarrow (T_w - T_\infty)\theta &= && \\
 T_w - T_\infty + \frac{2 - \sigma_T}{\sigma_T} \frac{2r}{r+1} \frac{\lambda_0}{Pr} \sqrt{\frac{a}{v}} (T_w - T_\infty)\theta' &&& \text{at } \eta = 0 \\
 \Rightarrow \theta(\eta) &= 1 + \frac{2 - \sigma_T}{\sigma_T} \frac{2r}{r+1} \frac{\lambda_0}{Pr} \sqrt{\frac{a}{v}} \theta'(\eta) && \text{at } \eta = 0 \\
 \Rightarrow &= 1 + \delta_3 \theta'(\eta). && \text{at } \eta = 0 \quad (6.91)
 \end{aligned}$$

$$\begin{aligned}
 \bullet \quad D_A \left. \frac{\partial a_1}{\partial z} \right|_{y=0} &= +K_s a_1(0) && \text{at } z = 0 \\
 D_A a_0 h'(\eta) \sqrt{\frac{a}{v}} &= +K_s a_0 h(\eta) && \text{at } \eta = 0
 \end{aligned}$$

$$\begin{aligned} \Rightarrow h'(\eta) &= \frac{+K_s}{\sqrt{\frac{a}{v}}D_A}h(\eta) && \text{at } \eta = 0 \\ \Rightarrow h'(\eta) &= K_1h(\eta) && \text{at } \eta = 0. \end{aligned} \quad (6.92)$$

$$\begin{aligned} \bullet D_B \frac{\partial b_1}{\partial z} \Big|_{y=0} &= -K_s a_1(0) && \text{at } z = 0 \\ \Rightarrow D_B a_0 q'(\eta) \sqrt{\frac{a}{v}} &= -K_s a_0 h(\eta) && \text{at } \eta = 0 \\ \Rightarrow \left(\frac{D_A}{D_B}\right) D_B a_0 q'(\eta) \sqrt{\frac{a}{v}} &= -\left(\frac{D_A}{D_A}\right) K_s a_0 h(\eta) && \text{at } \eta = 0 \\ \Rightarrow \left(\frac{D_B}{D_A}\right) D_A a_0 q'(\eta) \sqrt{\frac{a}{v}} &= -\left(\frac{D_A}{D_A}\right) K_s a_0 h(\eta) && \text{at } \eta = 0 \\ \Rightarrow \left(\frac{D_B}{D_A}\right) q'(\eta) &= -\frac{+K_s}{\sqrt{\frac{a}{v}}D_A}h(\eta) && \text{at } \eta = 0 \\ \Rightarrow \varphi q'(\eta) &= -K_1 h(\eta). && \text{at } \eta = 0. \end{aligned} \quad (6.93)$$

$$\begin{aligned} \bullet u &\rightarrow 0 && \text{as } z \rightarrow \infty \\ \Rightarrow axf'(\eta) &\rightarrow 0 && \text{as } \eta \rightarrow \infty \\ \Rightarrow f' &\rightarrow 0. && \text{as } \eta \rightarrow \infty \end{aligned} \quad (6.94)$$

$$\begin{aligned} \bullet v &\rightarrow 0 && \text{as } z \rightarrow \infty \\ \Rightarrow ayg'(\eta) &\rightarrow 0 && \text{as } \eta \rightarrow \infty \\ \Rightarrow g' &\rightarrow 0. && \text{as } \eta \rightarrow \infty \end{aligned} \quad (6.95)$$

$$\begin{aligned} \bullet T &\rightarrow T_\infty && \text{as } z \rightarrow \infty \\ \Rightarrow (T_w - T_\infty)\theta + T_\infty &\rightarrow T_\infty && \text{as } \eta \rightarrow \infty \\ \Rightarrow (T_w - T_\infty)\theta &\rightarrow 0 && \text{as } \eta \rightarrow \infty \\ \Rightarrow \theta &\rightarrow 0. && \text{as } \eta \rightarrow \infty \end{aligned} \quad (6.96)$$

$$\begin{aligned} \bullet a_1 &\rightarrow a_0 && \text{as } z \rightarrow \infty \\ \Rightarrow a_0 h &\rightarrow a_0 && \text{as } \eta \rightarrow \infty \\ \Rightarrow h &\rightarrow 1. && \text{as } \eta \rightarrow \infty \end{aligned} \quad (6.97)$$

$$\begin{aligned} \bullet b_1 &\rightarrow 0 && \text{as } z \rightarrow \infty \\ \Rightarrow a_0 q &\rightarrow 0 && \text{as } \eta \rightarrow \infty \\ \Rightarrow q &\rightarrow 0 && \text{as } \eta \rightarrow \infty. \end{aligned} \quad (6.98)$$

The dimensionless Nusselt number is given by

$$\bullet Nu_x = -\frac{x}{(T_w - T_\infty)} \frac{\partial T}{\partial z} \Big|_{z=0} + \frac{xq_r}{k(T_w - T_\infty)} \Big|_{z=0}, \text{ where}$$

$$\begin{aligned}
 q_r &= -\frac{16\sigma^*}{3\kappa^*}T^3\frac{\partial T}{\partial z} \\
 &= -\frac{16\sigma^*}{3\kappa^*}((T_w - T_\infty)\theta(\eta) + T_\infty)^3\sqrt{\frac{a}{v}}\theta'(\eta) \\
 &= -\frac{16\sigma^*T_\infty^3}{3\kappa^*}(1 + (\theta_w - 1)\theta(\eta))^3(T_w - T_\infty)\sqrt{\frac{a}{v}}\theta'(\eta) \\
 &= -Rd(1 + (\theta_w - 1)\theta(\eta))^3(T_w - T_\infty)\sqrt{\frac{a}{v}}\theta'(\eta).
 \end{aligned}$$

Therefore,

$$\begin{aligned}
 Nu_x &= \frac{-x\sqrt{\frac{a}{v}}(T_w - T_\infty)\theta'}{(T_w - T_\infty)} - \frac{xRd(1 + (\theta_w - 1)\theta(\eta))^3(T_w - T_\infty)\sqrt{\frac{a}{v}}\theta'}{(T_w - T_\infty)} \\
 &= -x\sqrt{\frac{a}{v}}\theta'(\eta) - xRd(1 + (\theta_w - 1)\theta(\eta))^3\theta'(\eta) \\
 &= -x\sqrt{\frac{a}{v}}(\theta'(\eta) + Rd(1 + (\theta_w - 1)\theta(\eta))^3\theta'(\eta)) \\
 &= -(1 + Rd(1 + (\theta_w - 1)\theta(\eta))^3)\theta'(\eta)\sqrt{Re_x}. \tag{6.99}
 \end{aligned}$$

The dimensionless form of skin friction coefficients along x - axis and y - axis are given by

- $C_{fx} = \frac{\tau_{xz}}{\frac{1}{2}\rho_f U_w^2}$, where

$$\begin{aligned}
 \tau_{xz} &= \mu \frac{\partial u}{\partial z} \left(1 + I^2 \left(\frac{\partial u}{\partial z} \right)^2 \right)^{\frac{n-1}{2}} \\
 &= \mu a \sqrt{\frac{a}{v}} x f'' (1 + We_1^2 f''(\eta)^2)^{\frac{n-1}{2}}.
 \end{aligned}$$

Therefore,

$$\begin{aligned}
 C_{fx} &= \frac{\tau_{xz}}{\frac{1}{2}\rho_f U_w^2} \\
 &= \frac{2\mu a \sqrt{\frac{a}{v}} x f'' (1 + We_1^2 f''(\eta)^2)^{\frac{n-1}{2}}}{\rho_f a^2 x^2} \\
 &= \frac{2\mu a \sqrt{\frac{a}{v}} x f'' (1 + We_1^2 f''(\eta)^2)^{\frac{n-1}{2}}}{\rho_f a^2 x^2}. \\
 \frac{1}{2}C_{fx} Re_x^{\frac{1}{2}} &= \frac{\mu a \sqrt{\frac{a}{v}} x \sqrt{\frac{a}{v}} x f'' (1 + We_1^2 f''(\eta)^2)^{\frac{n-1}{2}}}{\rho_f a^2 x^2} \\
 &= \frac{\mu a^2 x^2 f'' (1 + We_1^2 f''(\eta)^2)^{\frac{n-1}{2}}}{\rho_f \nu a^2 x^2} \\
 &= \frac{\mu a^2 x^2 f'' (1 + We_1^2 f''(\eta)^2)^{\frac{n-1}{2}}}{\mu a^2 x^2} \\
 &= f'' (1 + We_1^2 f''^2)^{\frac{n-1}{2}}. \tag{6.100}
 \end{aligned}$$

$$\bullet \frac{1}{2}C_{fy} = \frac{\tau_{yz}}{\rho_f U_w^2}, \text{ where}$$

$$\begin{aligned} \tau_{yz} &= \mu \frac{\partial v}{\partial z} \left(1 + I^2 \left(\frac{\partial v}{\partial z} \right)^2 \right)^{\frac{n-1}{2}} \\ &= \mu \sqrt{\frac{a}{v}} y g'' \left(1 + I^2 \left(ay \sqrt{\frac{a}{v}} g'' \right)^2 \right)^{\frac{n-1}{2}} \\ &= \sqrt{\frac{a}{v}} y g'' (1 + We_2^2 g''(\eta)^2)^{\frac{n-1}{2}}. \end{aligned}$$

Therefore,

$$\frac{1}{2}C_{fy} = \frac{\tau_{yz}}{\rho_f U_w^2}$$

$$= \frac{\mu a \sqrt{\frac{a}{v}} y g'' (1 + We_2^2 g''(\eta)^2)^{\frac{n-1}{2}}}{\rho_f a^2 x^2}$$

$$= \frac{\mu a \sqrt{\frac{a}{v}} y g'' (1 + We_2^2 g''(\eta)^2)^{\frac{n-1}{2}}}{\rho_f a^2 x^2}$$

$$\frac{1}{2}C_{fy} \left(\frac{U_w}{V_w} \right) = \frac{\mu a \sqrt{\frac{a}{v}} a x y g'' (1 + We_2^2 g''(\eta)^2)^{\frac{n-1}{2}}}{\rho_f a^2 x^2 a y}$$

$$\frac{1}{2}C_{fy} \left(\frac{U_w}{V_w} \right) Re_x^{\frac{1}{2}} = \frac{\mu a^2 x^2 \sqrt{\frac{a}{v}} y \sqrt{\frac{a}{v}} g'' (1 + We_2^2 g''(\eta)^2)^{\frac{n-1}{2}}}{\rho_f a^2 x^2 a y}$$

$$= \frac{\mu a^3 x^2 y g'' (1 + We_2^2 g''(\eta)^2)^{\frac{n-1}{2}}}{\rho_f a^3 x^2 y v}$$

$$= \frac{\mu a^3 x^2 y g'' (1 + We_2^2 g''(\eta)^2)^{\frac{n-1}{2}}}{\mu a^3 x^2 y}$$

$$= g'' (1 + We_2^2 g''^2)^{\frac{n-1}{2}}.$$

(6.101)

Various dimensionless parameters appearing during numerical simulation are given by

$$\left. \begin{aligned} We_1 &= I^2 \frac{a^3 x^2}{\nu}, \quad Pr = \frac{\nu}{\alpha}, \quad M = \frac{\sigma_1 B_0^2}{\rho a}, \quad Ec_x = \frac{a^2 x^2}{C_P (T_w - T_\infty)}, \\ We_2 &= I^2 a \frac{b^2 y^3}{\nu}, \quad \mu = \rho \nu, \quad \varphi = \frac{D_B}{D_A}, \quad Ec_y = \frac{b^2 y^2}{C_P (T_w - T_\infty)}, \\ Rd &= \frac{16 \sigma^* T_\infty^3}{3 k^* \kappa}, \quad \theta_w = \frac{T_w}{T_\infty}, \quad K = \frac{K_s}{D_A a_0} \sqrt{\frac{v}{a}}, \quad Sc = \frac{\nu}{D_A}, \quad \beta_3 = \frac{b}{a}, \\ K_1 &= \frac{K_c a_0^2}{a}, \quad \gamma_3 = \frac{2 - \sigma_v}{\sigma_v} \lambda_0 \sqrt{\frac{a}{v}}, \quad \delta_3 = \frac{2 - \sigma_T}{\sigma_T} \left(\frac{2r}{r+1} \right) \frac{\lambda_0}{Pr} \sqrt{\frac{a}{v}}. \end{aligned} \right\} \quad (6.102)$$

6.2 Solution Methodology

The nonlinear, non-dimensional system of equations (6.81)-(6.87) along with boundary conditions (6.88)-(6.98) can be comprehended with the assistance of the shooting strategy [99] utilizing the RK4 integrated scheme. For numerical solution, the unbounded domain $[0, \infty)$ has been replaced by $[0, \eta_\infty]$ where η_∞ is a real number chosen in such a way that the solution doesn't show significant variations for $\eta > \eta_\infty$. After giving different values to η_∞ , it is observed that $\eta_\infty = 7$ guarantees an asymptotic convergence for all the results presented in this article. For convenience in the choice of missing conditions and computational efficiency, first the momentum Eqs. (6.81) and (6.82) are solved numerically by the shooting method. Later on, using f and g as known functions, the energy Eq. (6.83) will be treated numerically. Finally the concentration Eq. (6.87) can be handled numerically with the assistance of shooting technique. The momentum equations (6.81) and (6.82) have been converted into first order ODEs signifying f by y_1 , f' by y_2 , f'' by y_3 , g by y_4 , g' by y_5 , g'' by y_6 , $y_3(0)$ by l_1 and $y_6(0)$ by l_2 . The symbols l_1 as well as l_2 denote the missing initial conditions of the modeled problem. The resulting system of equations along with the initial conditions is:

$$\left. \begin{aligned} y_1' &= y_2, & y_1(0) &= 0, \\ y_2' &= y_3, & y_2(0) &= 1 + \gamma_3 l_1, \\ y_3' &= \frac{[y_2^2 - y_3(y_1 + y_4) + M y_2]}{(1 + W e_1^2 y_3^2)^{\frac{n-3}{2}} (1 + n W e_1^2 y_3^2)}, & y_3(0) &= l_1, \\ y_4' &= y_5, & y_4(0) &= 0, \\ y_5' &= y_6, & y_5(0) &= \beta_3 + \gamma_3 l_2, \\ y_6' &= \frac{[y_5^2 - y_6(y_1 + y_4) + M y_5]}{(1 + W e_2^2 y_6^2)^{\frac{n-3}{2}} (1 + n W e_2^2 y_6^2)}, & y_6(0) &= l_2, \end{aligned} \right\} \quad (6.103)$$

To reach close enough to the missing initial conditions, Newton's method is iteratively applied until the following criteria is met.

$$\max\{|y_2(\eta_\infty)|, |y_5(\eta_\infty)|\} < \epsilon, \quad (6.104)$$

where ϵ denotes a small positive number.

The energy equation (6.83) has been converted in to first order ODEs by taking θ by w_1 , θ' by w_2 and $w_2(0)$ by l_3 , we get

$$\left. \begin{aligned} w_1' &= w_2, & w_1(0) &= 1 + \delta_3 l_3, \\ w_2' &= \frac{\left[\begin{aligned} &Pr(f + g)w_1 + Pr(Ec_x f''^2 + \\ &Ec_y g''^2) + MPr(Ec_x f'^2 + Ec_y g'^2) \\ &+ 3Rd(1 + (\theta_w - 1)y_1)^2(\theta_w - 1)w_2^2 \end{aligned} \right]}{- (1 + Rd(1 + (\theta_w - 1)w_1)^3)}, & w_2(0) &= l_3, \end{aligned} \right\} \quad (6.105)$$

For the refinement of the initial guess l_3 , Newton’s method is applied unless the condition underneath is fulfilled.

$$|w_1(\eta_\infty) - 0| < \epsilon, \quad (6.106)$$

where $\epsilon = 10^{-6}$ is the tolerance level. Tolerance is actually the level of error acceptable for any numerical scheme. If solution at the boundary is achieved with in the tolerance level value then solution is said to be convergent otherwise divergent. In divergent case refine the initial guess with the help of Newton’s method until the solution within the tolerance level is achieved.

The concentration eq. (6.87) is converted into the first order ODEs by denoting h by z_1 , h' by z_2 . The first order ODEs are then given by:

$$\left. \begin{aligned} z_1' &= z_2, & z_1(0) &= l_4, \\ z_2' &= Sc(-z_2(f + g) + Kz_1(1 - z_1)^2), & z_2(0) &= K_1 l_4. \end{aligned} \right\} \quad (6.107)$$

For the improvement of the initial guess l_4 , the iterative scheme called Newton’s iterative method has been considered unless the condition mentioned below is achieved.

$$|z_1(\eta_\infty) - 1| < \epsilon. \quad (6.108)$$

Tables (6.1)-(6.3) give a comparison analysis of the presently computed values of

different physical quantities with those already published in literature.

TABLE 6.1: Comparison of $f''(0)$.

	$f''(0)$	
β_3	Ariel [125]	Present
0.1	1.01702	1.02038
0.2	1.03458	1.03958
0.3	1.05747	1.05802
0.4	1.07052	1.07583
0.5	1.08866	1.09313

TABLE 6.2: Comparison of $g''(0)$.

	$g''(0)$	
β_3	Ariel [125]	Present
0	0	0
0.1	0.0668	0.0668
0.2	0.1487	0.1487
0.3	0.2433	0.2433
0.4	0.3492	0.3492
0.5	0.4652	0.4652

TABLE 6.3: Comparison of Nu_x .

	Nu_x	
β_3	Liu [126]	Present
0.25	0.6659	0.6661
0.50	0.7353	0.7354
0.75	0.7964	0.7965

6.3 Results and Discussion

This portion discusses the impact of various physical parameters on velocity, temperature and concentration distributions. The numerical solution of the dimensionless mathematical model has been presented and analyzed.

6.3.1 Impact of M , n , We_1 , γ_3 , We_2 , β_3 on the velocity fields f' and g'

Figure 6.2 exhibits the dynamics of the velocity fields f' as well as g' under the effect of M . Within an amplification in the dimensionless magnetic parameter M , velocity profiles depreciate. It is observed that the current carrying fluid passing through a magnetic field produces a resistive force termed as Lorentz force which depreciates fluid speed inside the boundary layer and moreover lessens the velocity field. Figure 6.3 delineates the impact of n on f' and g' . The power law index n is the important parameter of the non-Newtonian fluid and determines how much viscus the fluid is. The values of n have been taken for $n < 1$, $n > 1$ and $n = 1$. Actually parameter n tells us how much viscous the fluid is. From this figure, it can be clearly seen that a boost in f' and g' happens due to an embellishment in n . The impact of Weissenberg number We_1 on f' is manifested in Figure 6.4. Weissenberg number describes the shear rate time divided by relaxation time. Relaxation time is the time in which the fluid is allowed to relax after the application of shear stress. Viscosity of the fluid decreases by the virtue of an amplification in We_1 . Liquids turn out to be more thicker because of an augmentation in the Weissenberg number. Therefore velocity profile is reduced with an enrichment in the Weissenberg number. The execution of γ_3 on f' is displayed in Figure 6.5. Rising γ_3 lessens the fluid velocity. The impact of the Wessenberg number We_2 on g' is considered in Figure 6.6. The fluid thickness improves on the behalf of an improvement in We_2 which depreciates the value of g' . Figure 6.7 elucidates the dynamics of γ_3 on g' . The fluid velocity depreciates as a result of an incremental change in γ_3 . The physical reason behind the velocity decrement is actually an increment in the frictional resistance existing between the surface and the fluid particles. Figure 6.8 displays the impact of the stretching parameter β_3 on g' . Actually β_3 depicts the ratio of fluid flow velocity. More precisely the parameter β_3 is directly related to y -axis instead of x -axis. Change in y -axis tkes place as a result of an amplification in β_3 . As a result of this diminishment in g' take place.

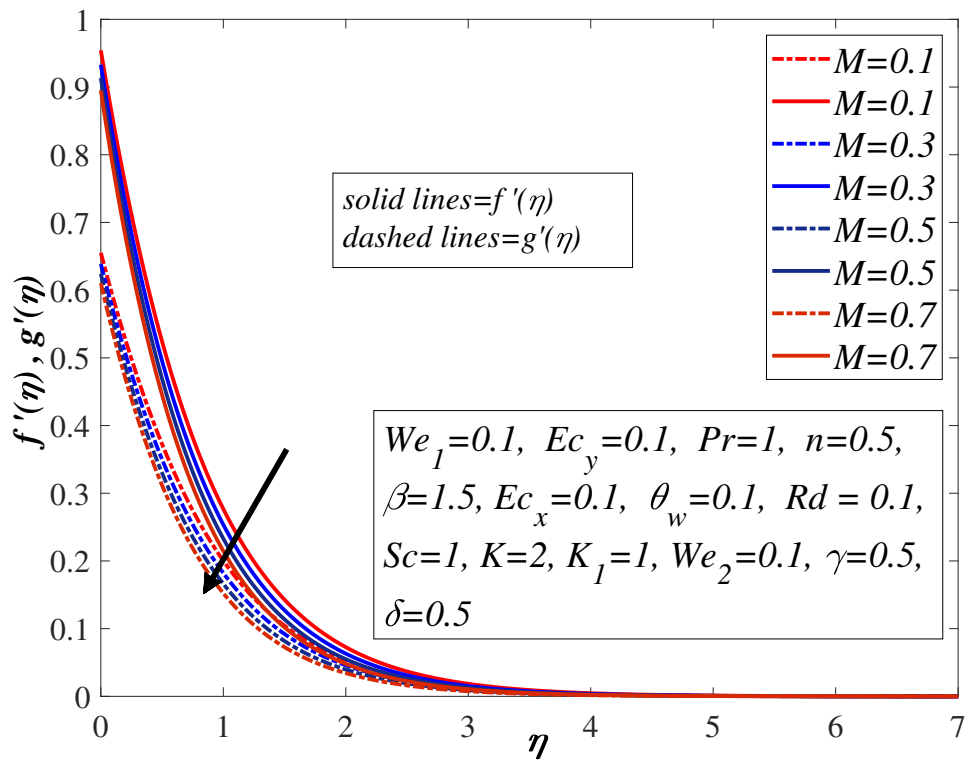


FIGURE 6.2: Impact of M on f' and g' .

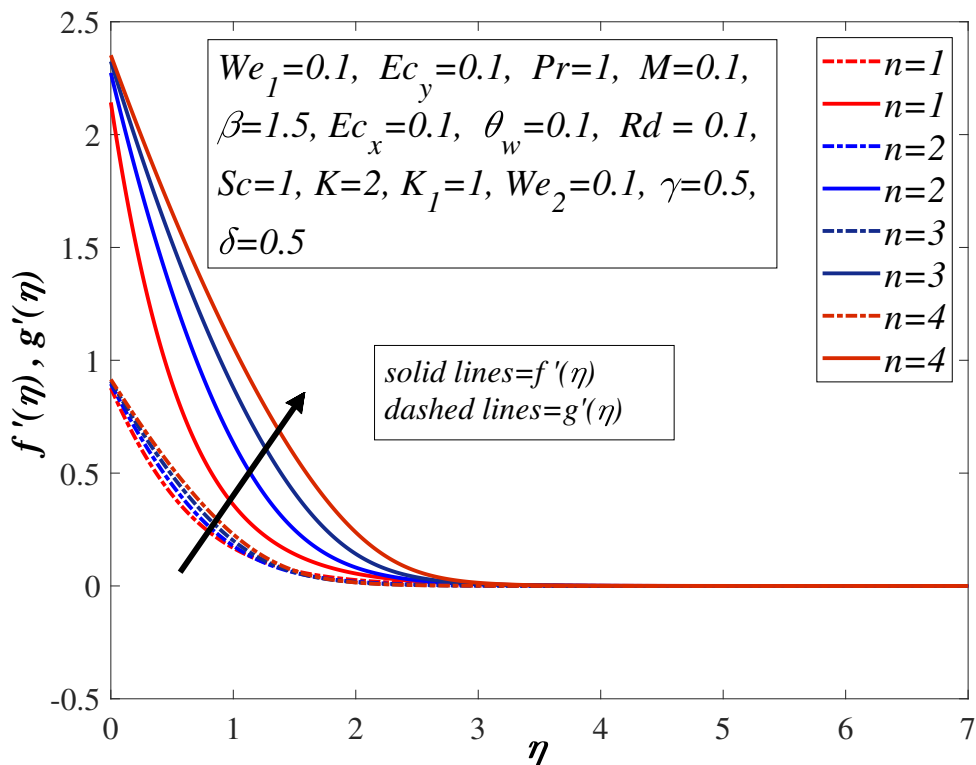


FIGURE 6.3: Effect of n on f' and g' .

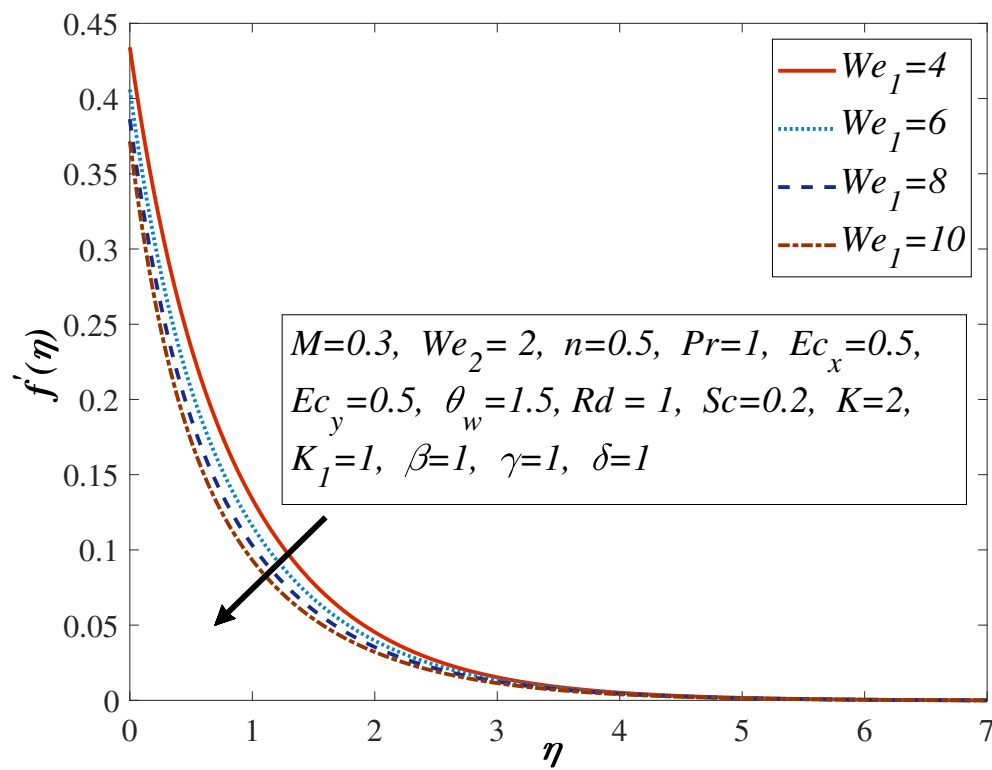


FIGURE 6.4: Impact of We_1 on f' .

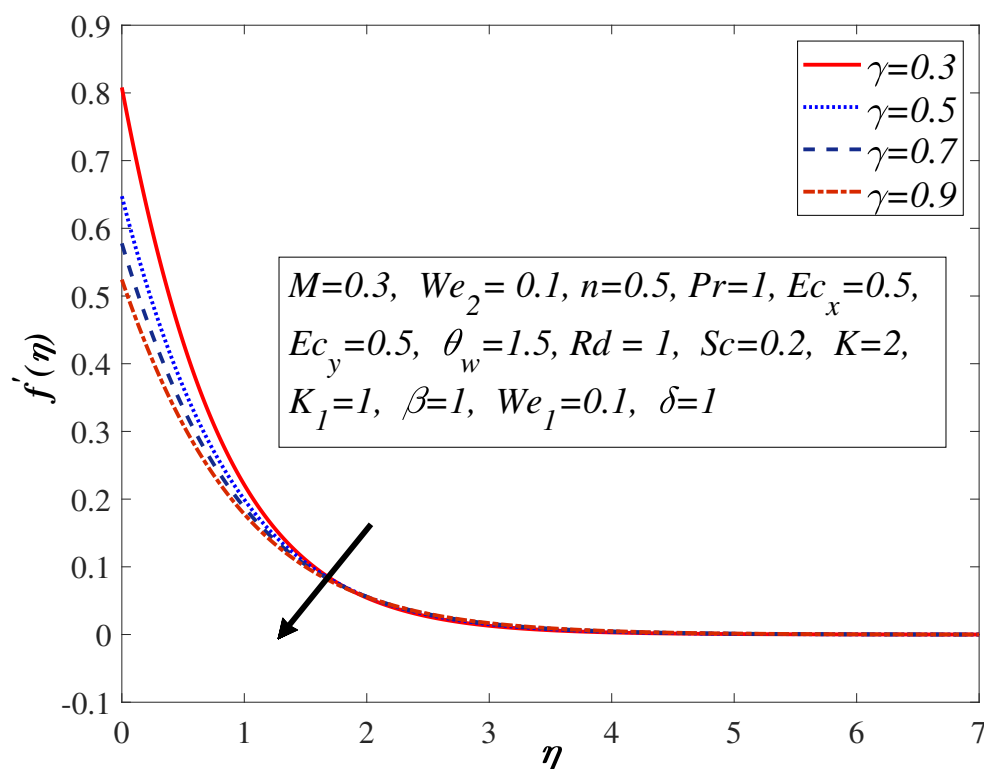


FIGURE 6.5: Effect of γ_3 on f' .

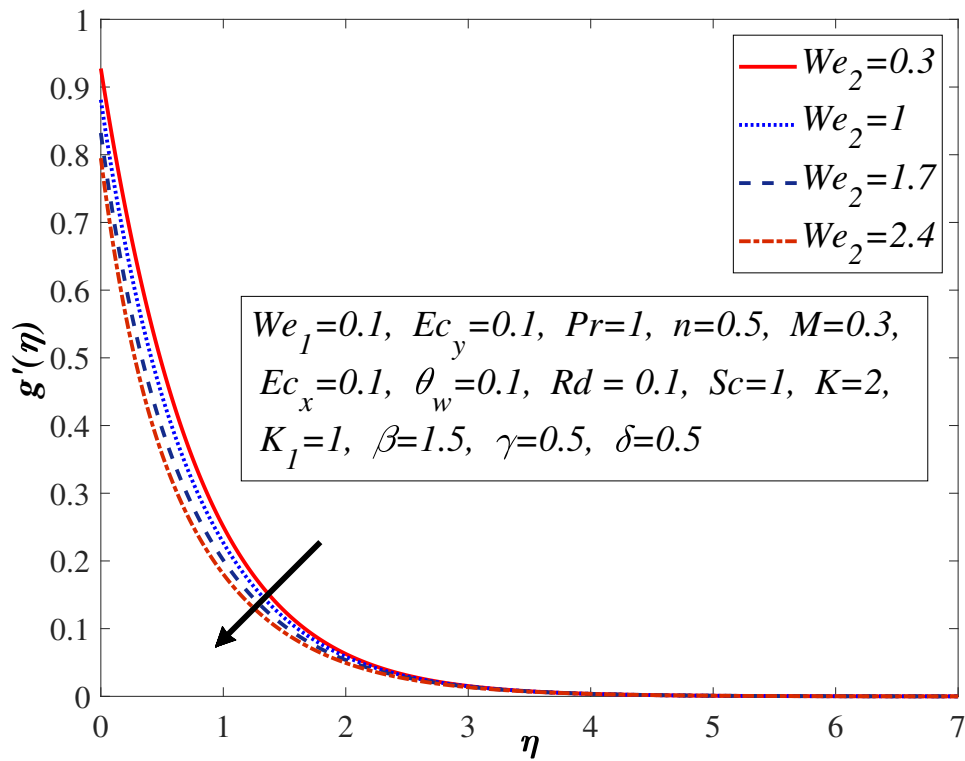


FIGURE 6.6: Impact of We_2 on g' .

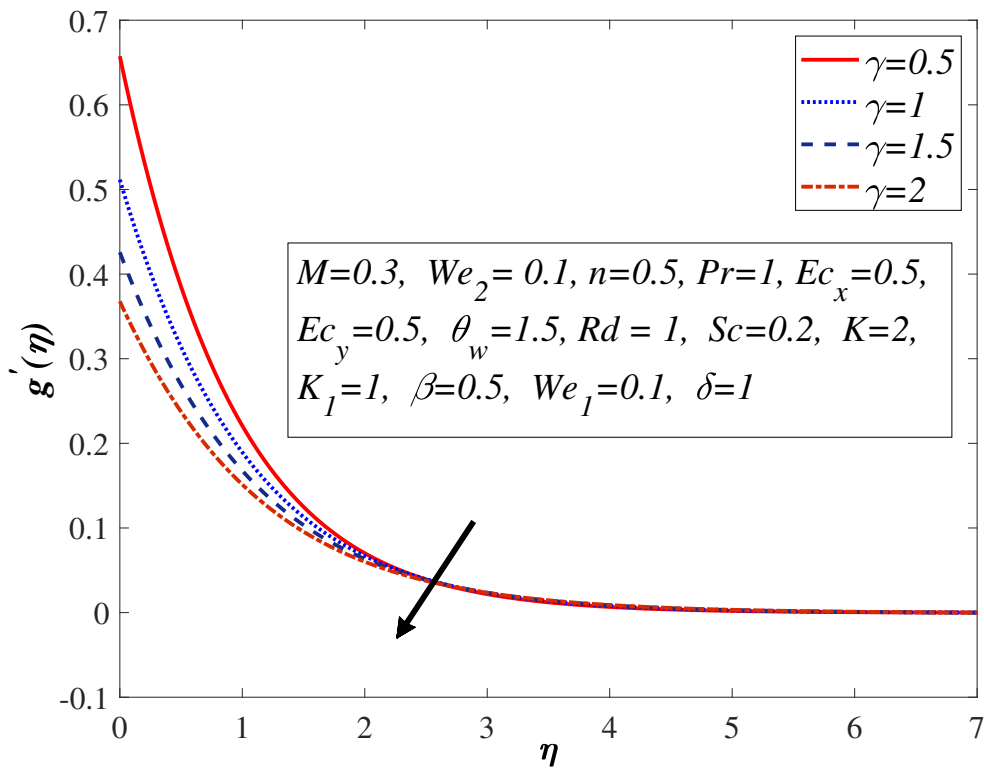
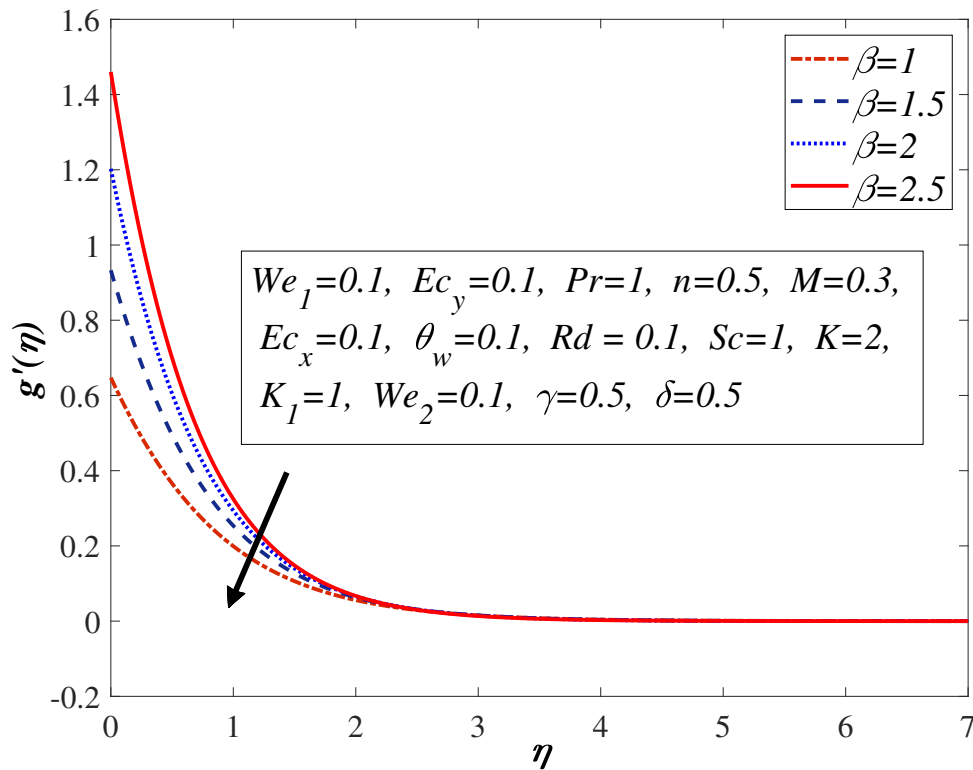


FIGURE 6.7: Influence of γ_3 on g' .


 FIGURE 6.8: Impact of β_3 on g' .

6.3.2 Impact of $Pr, Ec_x, Ec_y, M, Rd, \theta_w$ on $\theta(\eta)$

Figure 6.9 displays the performance of Pr , which is inversely related to the thermal diffusivity. It is well established that Prandtl number reduces the fluid temperature $\theta(\eta)$. Figure 6.10 portrays the behavior of temperature field $\theta(\eta)$ versus the Eckert number Ec_x . By boosting Ec_x , more heat is generated due to the frictional heating which improves $\theta(\eta)$. From Figure 6.11, it is probed that by mounting the Eckert number Ec_y , an additional heat in the liquid is generated on account of the frictional force which amplifies the temperature field. Figure 6.12 portrays the nature of M on $\theta(\eta)$. Lorentz force which is basically a resistive force depreciates the fluid flow and escalates $\theta(\eta)$. The behavior of radiation parameter Rd on $\theta(\eta)$ is deliberated in Figure 6.13. An augmentation in Rd enhances the temperature rise inside the boundary layer, and hence $\theta(\eta)$ escalates. Figure 6.14 determines the impact of the temperature ratio parameter θ_w on $\theta(\eta)$. By ascending θ_w , an enlargement in the wall temperature and temperature profile occurs.

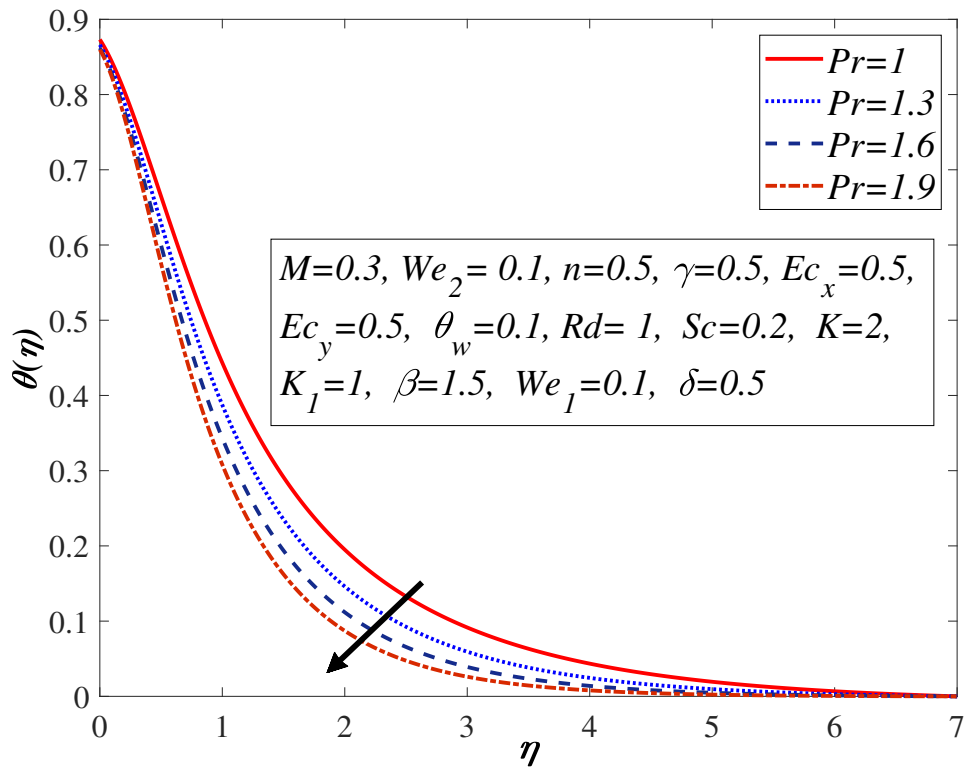


FIGURE 6.9: Impact of Pr on θ .

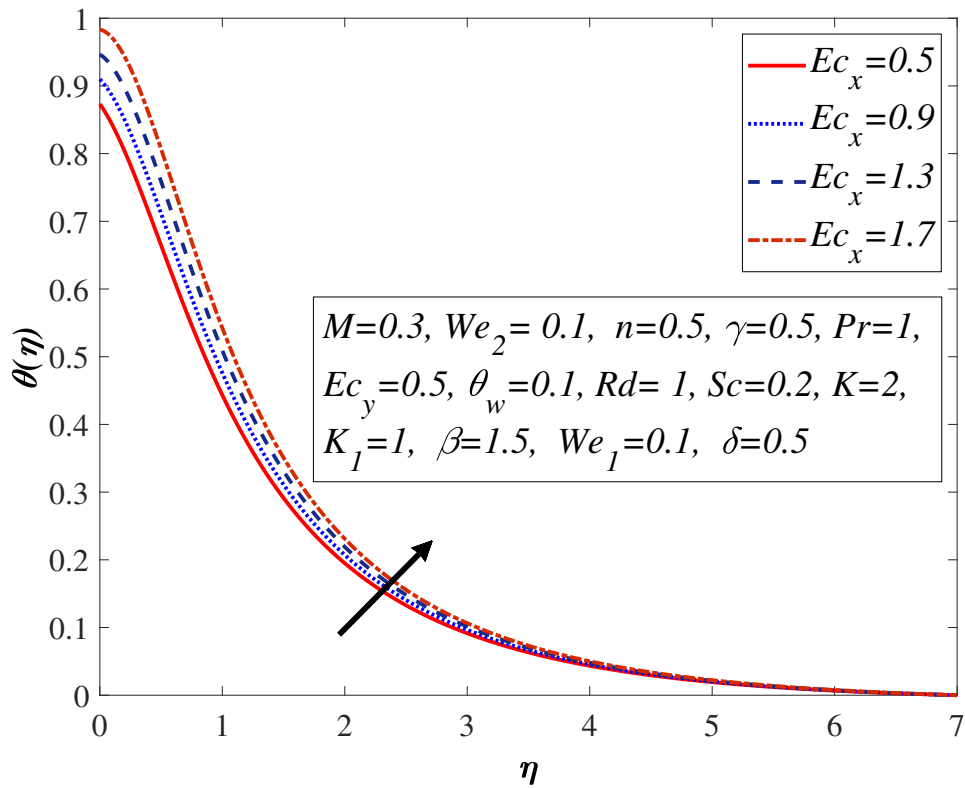


FIGURE 6.10: Effect of Ec_x on θ .

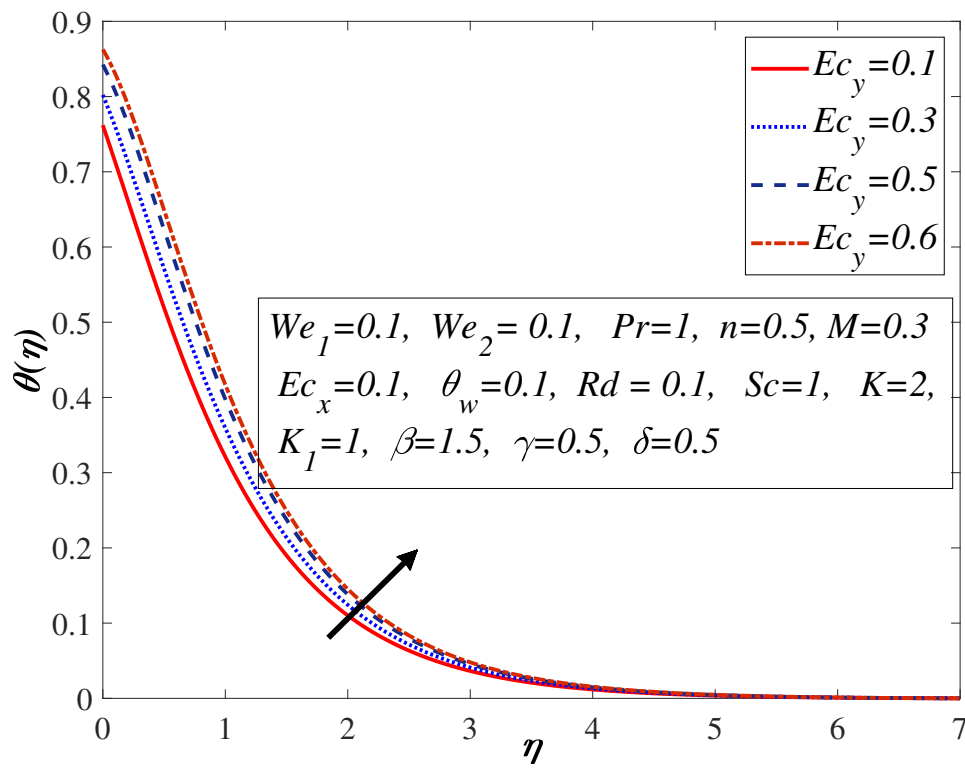


FIGURE 6.11: Effect of Ec_y on θ .

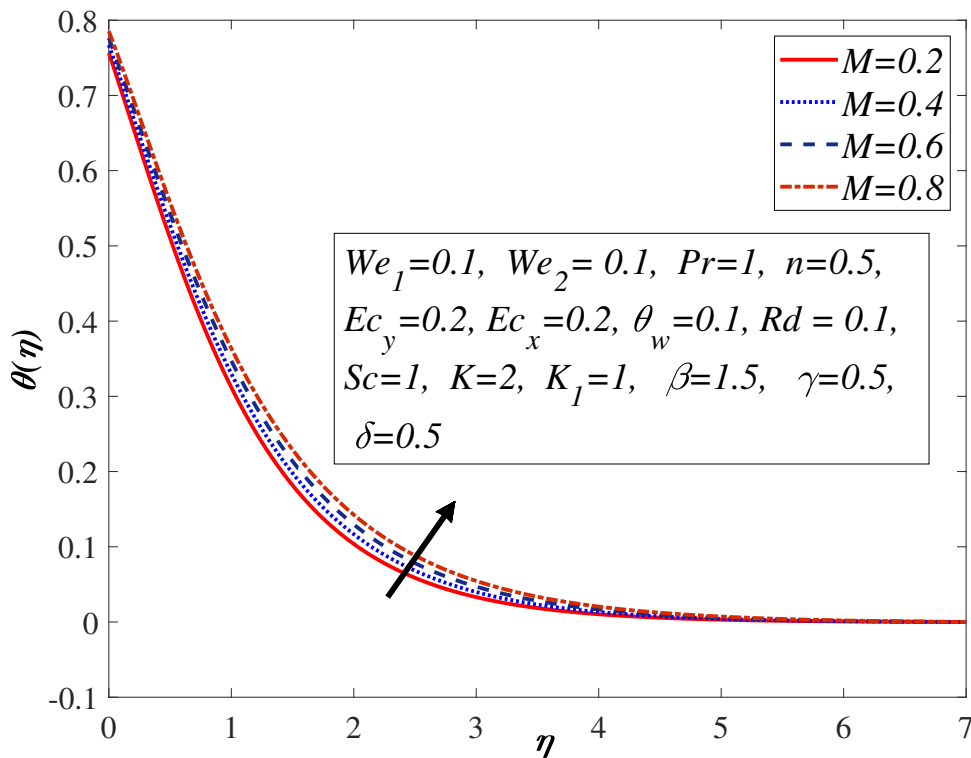


FIGURE 6.12: Impact of M on θ .

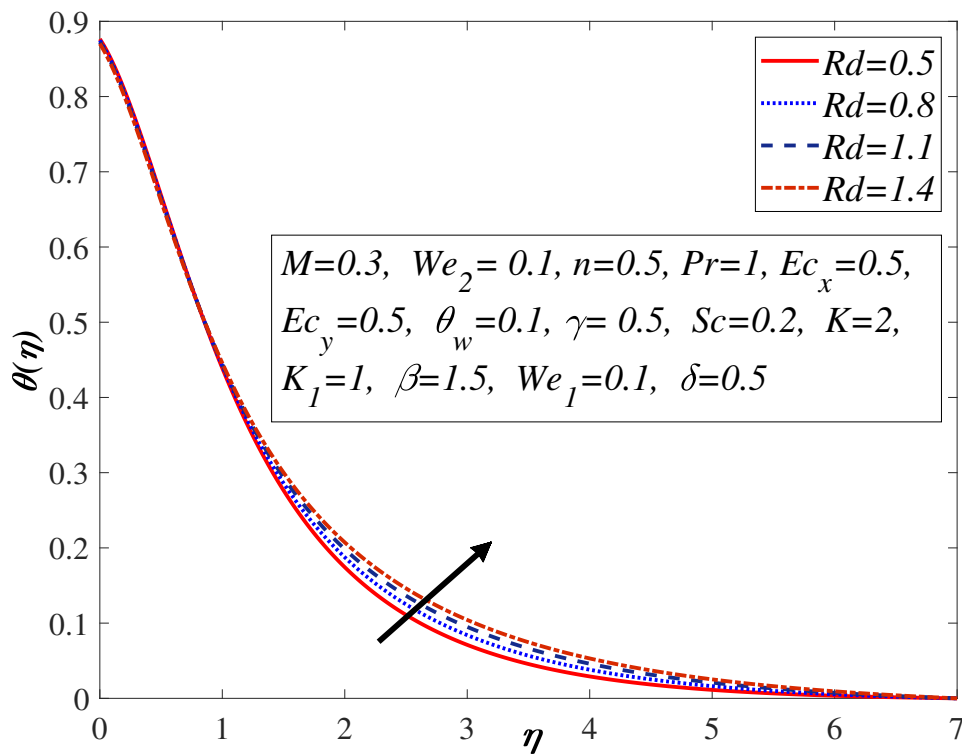


FIGURE 6.13: Influence of Rd on θ .

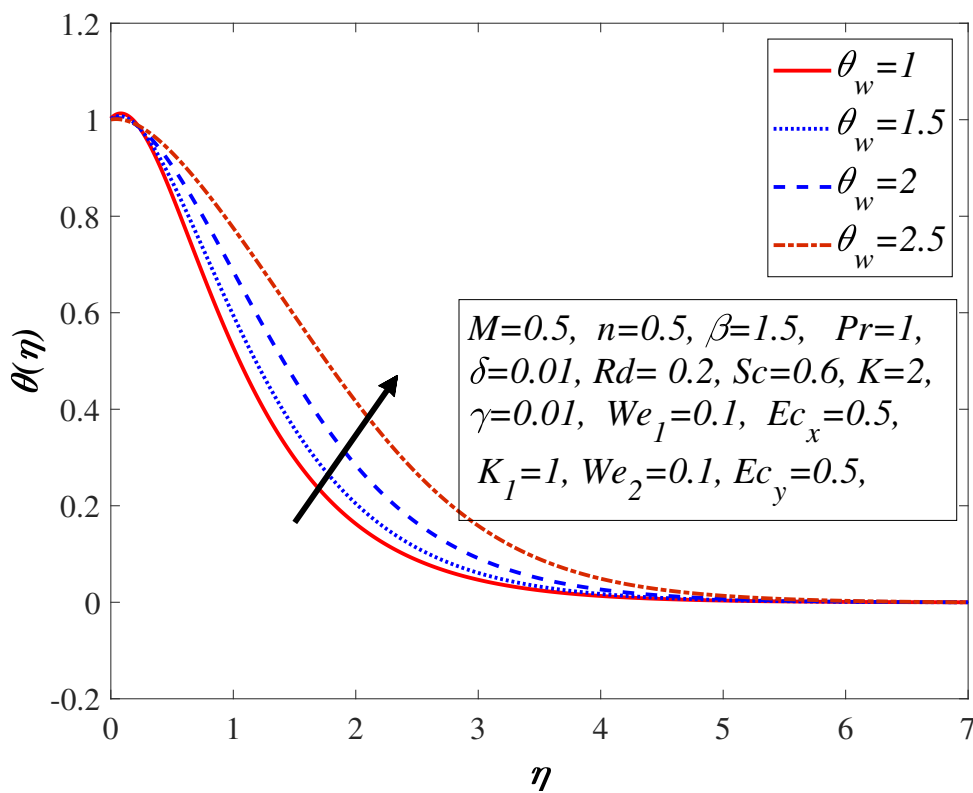


FIGURE 6.14: Impact of θ_w on θ .

6.3.3 Impact of Sc , K , K_1 on $h(\eta)$

In case of the fixed molecular diffusion, when Sc amplifies, the viscous diffusion also amplifies. Schmidt number is directly related to the diffusion phenomenon and perform same role for concentration equation like Prandtl number for the energy equation. Schmidt number is related to the molecular diffusivity. It is quite clear that an incremental change in the molecular diffusivity enhances the concentration of the fluid which guides to a magnification in the concentration profile. The concentration of the fluid increases by the virtue of an amplification in Sc which increases $h(\eta)$ as shown in Figure 6.15. Figure 6.16 and 6.17 displayed the impact of K and K_1 on $h(\eta)$. Diffusivity and the concentration are directly linked with each other. In the case of homogeneous reaction both liquid and catalyst are in the same phase which is also one of the prominent factor for an augmentation in the concentration field. The flow diffusivity also fluctuates by rising the value of the homogeneous reaction, which lessens $h(\eta)$.

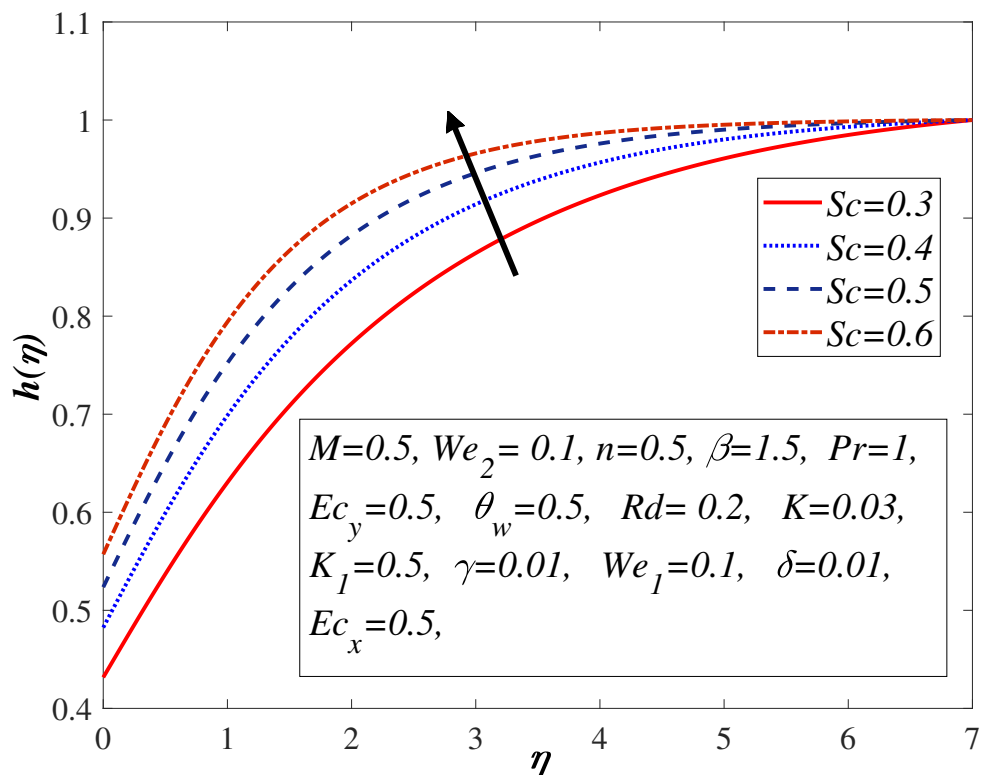


FIGURE 6.15: Impact of Sc on h .

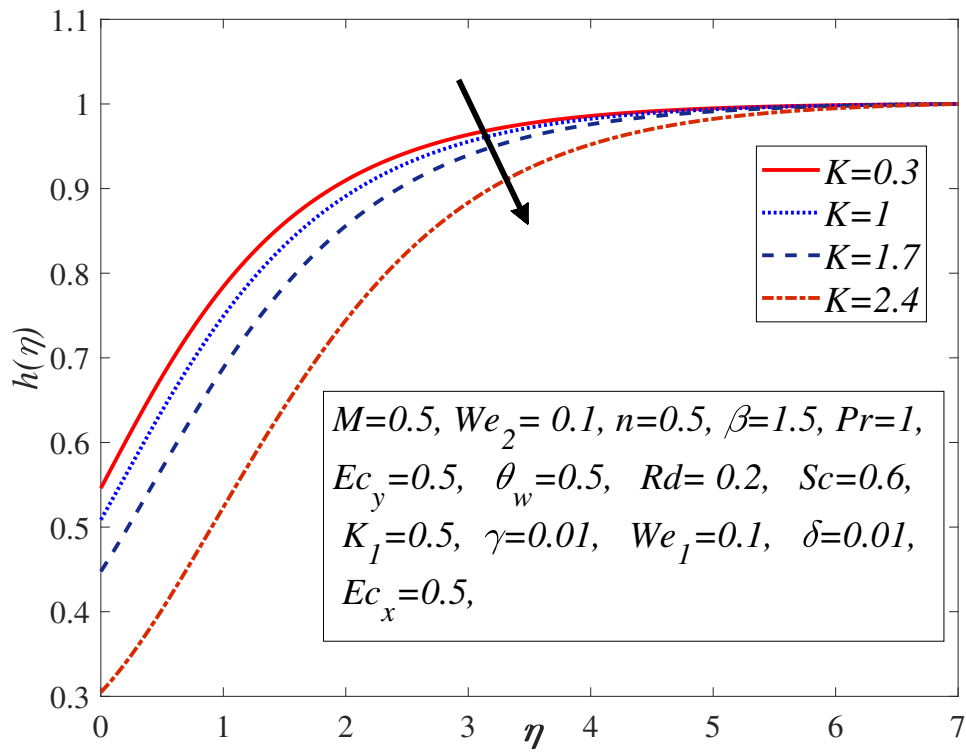


FIGURE 6.16: Effect of K on h .

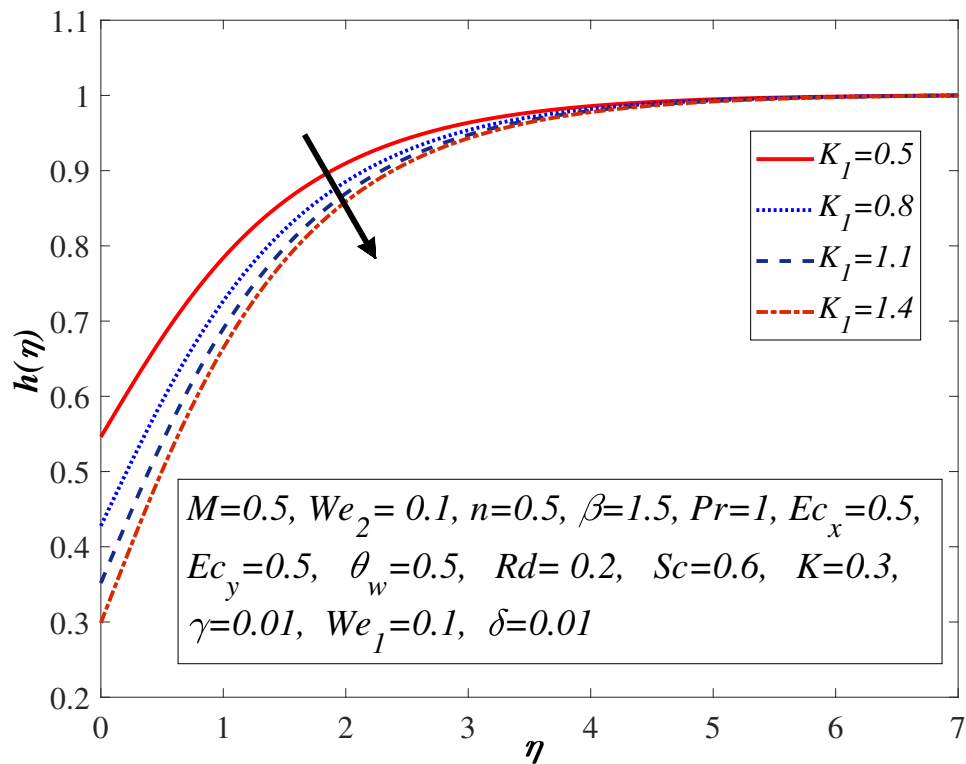


FIGURE 6.17: Effect of K_1 on h .

The skin friction coefficient and $h'(0)$ against various parameters is delineated in Table 6.4 by keeping $Rd = 1$, $\theta_w = 1.5$, $Ec_x = 0.5$, $Ec_y = 0.5$, $Pr = 1$, $\delta_3 = 1$ as fixed. According to Table 4, an enrichment in magnetic parameter M and the stretching rate β_3 prompts a decrease in the skin friction coefficient. Incremental change in M produces a resistive force termed as Lorentz force which reduces the fluid motion and skin friction coefficient. The viscosity of fluid increases as a result of a magnification in stretching parameter β_3 which reduces the skin friction coefficient. An amplification in power-law index n (shear thickening) and the slip parameter γ_3 depreciates the skin friction coefficient along x -axis. Slip phenomenon occurs when the surface is rough and not perfectly smooth. Due to this reason the velocity of the liquid moving across the expandable medium and the velocity of expandable medium is not same which depreciates the liquid velocity and surface drag coefficient. An improved behavior is seen in the surface drag coefficient along y -axis for M and β_3 . However for n and γ_3 a reverse behavior is experienced for skin friction coefficient.

Table 6.5 demonstrates the behaviour of the heat transfer rate against different parameters, for fixed values of $We_1 = 0.1$, $We_2 = 0.1$, $Sc = 0.2$, $K = 2, K_1 = 1$. It is quite clear that boosting the values of n (shear thickening), the radiation parameters Rd , the ratio of wall temperature and ambient temperature θ_w and Pr brings about an enlargement in the Nusselt number. The parameter n describes how much viscous the liquid is. In the case of $n < 1$ the fluid behaviour is shear thinning but the behaviour is shear thickening in the case of an incremental change in n which depreciates the fluid velocity and amplifies the heat transfer rate. Temperature inside the fluid escales by the virtue of a magnification in the nonlinear thermal radiation parameter Rd which amplifies the heat transfer rate. Temperature ratio parameter θ_w is one of the pertinent parameter of the nonlinear thermal radiation term and utilized where large temperature difference is required with remaining two parameters are Pr and Rd . A magnification in θ_w elevates the temperature of the fluid and the heat transfer Nusselt number. It is quite clear that an amplification in M , Eckert number Ec , stretching rate β , slip parameters γ_3 and δ_3 brings about a reduction in the temperature field.

TABLE 6.4: Impact of momentum and concentration equations parameters on surface drag coefficient and concentration profile.

M	n	β_3	γ_3	We_1	We_2	K	K_1	Sc	$\frac{1}{2}C_f Re_x^{\frac{1}{2}}$	$\frac{1}{2}C_f \frac{U_w}{V_w} Re_x^{\frac{1}{2}}$	$h'(0)$
0.3	1.5	0.5	0.3	0.1	0.1	2	1	0.2	-0.82451	-0.37790	-0.05860
	0.5								-0.86909	-0.40432	-0.05484
	0.7								-0.89921	-0.52581	-0.01194
	0.9								-0.94024	-0.44931	-0.52558
	0.5								-0.82311	-0.37773	-0.05856
	1								-0.82382	-0.37782	-0.05858
	1.7								-0.82479	-0.37794	-0.05861
		0.7							-0.83707	-0.55927	-0.06339
		0.9							-0.84888	-0.75331	-0.06805
		1.1							-0.86005	-0.95834	-0.07263
			0.5						-0.68525	-0.31865	-0.05415
			0.7						-0.58884	-0.27663	-0.05094
			0.9						-0.51764	-0.24505	-0.04846
				0.3					-0.82987	-0.37808	-0.05873
				0.5					-0.83969	-0.37839	-0.05858
				0.7					-0.85270	-0.37879	-0.05931
					0.3				-0.82454	-0.37840	-0.05861
					0.5				-0.82461	-0.37938	-0.05865
					0.7				-0.82470	-0.38079	-0.05870
						2.2			-0.82451	-0.37791	-0.04947
						2.4			-0.82451	-0.37791	-0.04171
						2.6			-0.82451	-0.37791	-0.03519
							1.2		-0.82451	-0.37791	-0.06197
							1.4		-0.82451	-0.37791	-0.06466
							1.6		-0.82451	-0.37791	-0.06686
								0.4	-0.82451	-0.37791	-0.03171
								0.6	-0.82451	-0.37791	-0.02326
								0.7	-0.82451	-0.37791	-0.02259

TABLE 6.5: Impact of various embedded parameters on Nu_x .

M	n	Rd	θ_w	Ec_x	Ec_y	Pr	β_3	γ_3	δ_3	$Nu_x Re_x^{-\frac{1}{2}}$
0.3	1	1	1.5	0.5	0.5	1	0.5	0.3	1	0.5305
										0.5041
										0.4808
										0.4048
	0.5									0.5303
	1									0.5304
	1.7									0.5305
		1.2								0.5757
		1.4								0.6209
		1.6								0.6664
			1.7							0.5983
			1.9							0.6748
			2.1							0.7634
				0.7						0.4732
				0.9						0.4156
				1.1						0.3578
					0.7					0.5161
					0.9					0.5016
					1.1					0.4872
						1.2				0.5697
						1.4				0.6077
						1.6				0.6436
							0.7			0.5279
							0.9			0.5112
							1.1			0.4809
								0.5		0.5434
								0.7		0.5471
								0.9		0.5467
									1.2	0.5077
									1.4	0.4865
									1.6	0.4665

6.4 Concluding Remarks

Three dimensional Carreau fluid accompanied with viscous-Ohmic dissipation, homogenous/heterogenous reaction, velocity slips nonlinear thermal radiation moving along a stretchable surface is analyzed. The numerical scheme termed as shooting method is utilized in order to solve ODEs. Some decisive comments from the concluding work are as below:

- Rising the values of Eckert number along $x - axis$ and $y - axis$ termed as Ec_x and Ec_y brings about an augmentation in the temperature profile.
- The velocity profile is quite opposite in the case of Weissenberg numbers We_1 and We_2 . By enhancing We_1 and We_2 , a decrement in the velocity profiles is prompted.
- The temperature profile escalates as a result of a magnification in M and Schmidt parameter Sc .
- In case of boosting the velocity slip parameter γ_3 , a diminishment of both $f'(\eta)$ and $g'(\eta)$ is observed.
- Homogenous and heterogenous reactions are inversely related to the concentration profile.

Chapter 7

Conclusion and Future Work

The purpose of this dissertation was to develop various mathematical models regarding fluid moving across a stretchable surface accompanied with various effects for the purpose of heat and mass transfer analysis. The important results achieved in this thesis have been presented underneath.

7.1 Main Findings

1. The heat as well as the mass transfer analysis is carried out regarding Reiner-Philippoff fluid accompanied with nonlinear thermal radiation, variable species diffusivity, heat source and sink. No literature is available regarding the mass transfer analysis of the Reiner-Philippoff fluid. Heat transfer analysis with the inclusion of nonlinear based thermal radiation, temperature varying conductivity and heat source/sink is studied extensively. It is observed that an amplification in Rd , θ_w , ϵ_1 and A^* amplifies the fluid's temperature and moreover amplifies the heat transfer rate. A magnification in variable molecular diffusivity ϵ_2 enhances the mass transfer rate of the Reiner-Philippoff fluid.
2. The novel idea regarding the influence of double diffusion convection along with motile gyrotactic microorganisms on tangent hyperbolic tangent nanofluid

has not been studied yet in the literature. The impact of double diffusion convection and microorganisms species diffusivity on tangent hyperbolic nanofluid is investigated. It is noted that an augmentation in regular Lewis number Le and Dufour Lewis number Ld lessens the solute profile. A positive variation in Peclet number Pe , bio convective Lewis number Lb , microorganisms concentration difference parameters σ guides to a reduction in the density of the motile microorganism profile.

3. The mathematical model regarding Maxwell nanofluid past a convectively heated expandable sheet accompanied with nonlinear thermal radiation, variable thermal conductivity and activation energy is also analyzed. The heat transfer rate of the fluid improves by the virtue of an amplification in the thermal conductivity ϵ_1 , thermal radiation Rd , inertia coefficient Fr and Biot number γ . The mass transfer rate and concentration of the fluid amplifies by the virtue of an enhancement in the activation energy E , porosity parameter λ_2 , reaction rate constant σ parameters respectively.
4. An attempt is made to study the influence of Maxwell velocity and Smoluchowski temperature slip boundary conditions on 3D Carreau fluid which is never studied yet. The heat and mass transfer aspect of Carreau fluid with the inclusion of various effects like homogeneous/heterogenous reactions, viscous dissipation, Joule heating and nonlinear thermal radiation is debated in detail. It is observed that the fluid velocity depreciates owing an improvement in the velocity slip parameter γ_3 and furthermore heat transfer rate of the fluid diminishes owing to an increment in the temperature slip parameter slip parameter δ_3 . Both homogenous/heterogenous reactions depreciate the mass transfer rate.

7.2 Future Work

The work presented in this thesis can be extended in many directions. Few of this open problem have been listed below.

1. The work presented in Chapter 3 can be extended in terms of Reiner-Philippoff fluid flow over different geometries like wedge, cylinder, sphere, cone etc.
2. The literature mentioned in Chapter 4 can be extended in the direction of hyperbolic tangent fluid flow through parallel stretching disks, converging/-diverging channels, inclined stretching sheet with the inclusion of effects like hybrid nanoparticles, carbon nanotubes, activation energy etc.
3. This study presented in Chapter 5 can be extended in the direction of Maxwell nanofluid past an oscillatory stretching sheet, needle, peristaltic flow, sensor surface, nonlinear stretching sheet etc with the inclusion of effects like gyrotactic microorganisms, melting surface, convective heat and mass transfers, variable molecular diffusivity etc.
4. The momentum and temperature slip boundary conditions presented in Chapter 6 for the case of Carreau fluid can be further utilized in other viscoelastic type non-Newtonian fluids flow over different geometries like channel, sphere, cone, wedge, pipe etc.
5. The non-Newtonian fluid problems mentioned in this thesis can be extended in the field of fractional calculus and furthermore, studied the impact of Reimann-Liouville, Caputo-Erdelyi-Kober fractional derivative and Caputo-Fabrizio types fractional derivatives on momentum and energy equation for the case of fluid flow over various geometries like stretching sheet, stretching wedge, circular cylinder and microchannels.

Bibliography

- [1] J. N. Kapur and R. C. Gupta, “Two dimensional flow of Reiner-Philippoff fluids in the inlet length of a straight channel,” *Appl. Sci. Res.*, vol. 14, pp. 13–24, 1965.
- [2] S. Ghoshal, “Dispersion of solutes in non-Newtonian flows through a circular tube,” *Chem. Engg. Sci.*, vol. 26, no. 2, pp. 185–188, 1971.
- [3] T. Y. Na, “Boundary layer flow of Reiner-Philippoff fluids,” *Int. J. Non-Linear Mech.*, vol. 29, no. 6, pp. 871–877, 1994.
- [4] K. S. Yam, S. D. Harris, D. B. Ingham, and I. Pop, “Boundary-layer flow of Reiner–Philippoff fluids past a stretching wedge,” *Int. J. Non-Linear Mech.*, vol. 44, no. 10, pp. 1056–1062, 2009.
- [5] A. Ahmad, “Flow control of non-newtonain fluid using riga plate:Reiner-Phillipoff and powell-eyring viscosity models,” *J. Appl. Fluid Mech.*, vol. 39, no. 11, pp. 127–133, 2019.
- [6] M. G. Reddy, S. Rani, K. G. Kumar, A. H. Seikh, M. R. Gorji, , and E. M. Sherif, “Transverse magnetic flow over a Reiner–Philippoff nanofluid by considering solar radiation,” *Mod. Phys. Lett. B.*, vol. 33, no. 36, p. 1950449, 2019.
- [7] K. G. Kumar, M. G. Reddy, M. Sudharani, S. A. Shehzad, and A. J. Chamkha, “Cattaneo–Christov heat diffusion phenomenon in Reiner–Philippoff fluid through a transverse magnetic field,” *Phy. A*, vol. 6, p. 123330, 2019.

- [8] M. G. Reddy, M. V. V. N. L. Sudharani, G. Kumar, A. J. Chamkha, and G. Lorenzini, “Physical aspects of Darcy–Forchheimer flow and dissipative heat transfer of Reiner–Philippoff fluid,” *J. Therm. Anal. Calorim.*, pp. 1–10, 2019.
- [9] A. Ullah, E. O. Alzahrani, Z. Shah, M. Ayaz, and S. Islam, “Nanofluids thin film flow of Reiner-Philippoff fluid over an unstable stretching surface with Brownian motion and thermophoresis effects,” *Coatings*, vol. 9, p. 21, 2019.
- [10] A. Ishaq, E. A. Algehyne, A. Ahmad, and F. Mallawi, “Magneto-hydrodynamic flow of Reiner-Philippoff fluid: Stability analysis,” *Phys. Scr.*, vol. 96, no. 3, p. 035203, 2020.
- [11] M. Tahir and A. Ahmad, “Impact of pseudoplasticity and dilatancy of fluid on peristaltic flow and heat transfer: Reiner-Philippoff fluid model,” *Adv. Mech. Engg.*, vol. 12, no. 12, pp. 1–10, 2020.
- [12] P. Y. Xiong, Y. M. Chu, M. I. Khan, S. A. Khan, and Z. Abbas, “Entropy optimized darcy-forchheimer flow of Reiner-Philippoff fluid with chemical reaction,” *Comput. Theor. Chem.*, vol. 1200, p. 113222, 2021.
- [13] M. I. Khan, Usman, A. Ghaffari, S. U. Khan, Y. M. Chu, and S. Qayyum, “Optimized frame work for Reiner–Philippoff nanofluid with improved thermal sources and Cattaneo–Christov modifications: A numerical thermal analysis,” *Int. J. Modern Phys. B*, vol. 35, no. 6, p. 2150083, 2021.
- [14] A. M. Megahed, “Flow and heat transfer of Powell–Eyring fluid due to an exponential stretching sheet with heat flux and variable thermal conductivity,” *Zeitschrift fur Naturforschung*, vol. 70, no. 3, pp. 163–169, 2015.
- [15] S. Reddy, K. Naikoti, and M. M. Rashidi, “MHD flow and heat transfer characteristics of Williamson nanofluid over a stretching sheet with variable thickness and variable thermal conductivity,” *Trans. A. Razmadze Math. Inst.*, vol. 171, no. 2, pp. 195–211, 2017.

- [16] M. Ramzan, M. Bilal, S. Kanwal, and J. D. Chung, “Effects of variable thermal conductivity and nonlinear thermal radiation past an Eyring-Powell nanofluid flow with chemical reaction,” *Commun. Theor. Phys.*, vol. 67, no. 6, pp. 723–731, 2017.
- [17] R. A. Shah, T. Abbas, M. Idrees, and M. Ullah, “MHD Carreau fluid slip flow over a porous stretching sheet with viscous dissipation and variable thermal conductivity,” *Bound. Value Probl.*, vol. 2017, p. 94, 2017.
- [18] H. Shokouhmand, A. Sattari, S. E. H. Doost, and A. Maghooli, “Analysis of two-dimensional porous fins with variable thermal conductivity,” *Heat Transf—Asian Res.*, vol. 47, no. 2, pp. 404–419, 2018.
- [19] R. V. M. S. S. K. Kumar and S. V. K. Varma, “MHD boundary layer flow of nanofluid through a porous medium over a stretching sheet with variable wall thickness using Cattaneo-Christov heat flux model,” *J. Theor. Appl. Mech.*, vol. 48, no. 2, pp. 72–92, 2018.
- [20] B. Marinca and V. Marinca, “Some exact solutions for MHD flow and heat transfer to modified second grade fluid with variable thermal conductivity in the presence of thermal radiation and heat generation/absorption,” *Comput. Math. Appl.*, vol. 76, no. 6, pp. 1515–1524, 2018.
- [21] M. Ferdows and M. Z. I. Bangalee, “Electrically conducting flow through exponential power law fluid with variable thermal conductivity,” *Int. J. Appl. Mech. Eng.*, vol. 24, no. 3, pp. 539–548, 2019.
- [22] S. Lahmar, M. Kezzar, M. R. Eid, and M. R. Sari, “Heat transfer of squeezing unsteady nanofluid flow under the effects of an inclined magnetic field and variable thermal conductivity,” *Phy. A*, vol. 540, p. 123138, 2020.
- [23] I. Pop and D. B. Ingham, “Convective heat transfer: mathematical and computational modelling of viscous fluids and porous media,” *Pergamon*, vol. Amsterdam, 2001.

- [24] S. Nadeem and S. Akram, “Peristaltic transport of a hyperbolic tangent fluid model in an asymmetric channel,” *Zeitschrift fur Naturforschung A*, vol. 64, pp. 559–567, 2009.
- [25] N. S. Akbar, S. Nadeem, R. U. Haq, and Z. H. Khan, “Numerical solutions of magnetohydrodynamic boundary layer flow of tangent hyperbolic fluid towards a stretching shee,” *Indian. J. Phys.*, vol. 87, pp. 1121–1124, 2013.
- [26] S. Akram and S. Nadeem, “Consequence of nanofluid on peristaltic transport of a hyperbolic tangent fluid model in the occurrence of apt (tending) magnetic field,” *J. Magnetism. Magnetic. Mater*, vol. 358, pp. 183–191, 2014.
- [27] B. Prabhakar, S. Bandari, and R. U. Rizwan, “Impact of inclined Lorentz forces on tangent hyperbolic nanofluid flow with zero normal flux of nanoparticles at the stretching sheet,” *Neur. Comp. Appl.*, vol. 29, no. 10, pp. 805–814, 2018.
- [28] N. Saidulu, T. Gangaiah, and A. V. Lakshmi, “Radiation effect on mhd flow of a tangent hyperbolic nanofluid over an inclined exponentially stretching sheet,” *Int. J. Fluid Mech. Res.*, vol. 46, no. 3, pp. 277–293, 2019.
- [29] K. Al-Khaled, S. U. Khan, and I. Khan, “Chemically reactive bioconvection flow of tangent hyperbolic nanoliquid with gyrotactic microorganisms and nonlinear thermal radiation,” *Heliyon*, vol. 6, p. e03117, 2020.
- [30] S. N. Gaikwad, M. S. Malashetty, and P. K. R., “An analytical study of linear and non-linear double diffusive convection with soret and dufour effects in couple stress fluid,” *Int. J. Non-Linear Mech.*, vol. 42, pp. 903–913, 2007.
- [31] D. A. Nield and A. V. Kuznetsov, “The cheng-minkowycz problem for the double-diffusive natural convective boundary layer flow in a porous medium saturated by a nanofluid,” *Int. J. Heat Mass Transf.*, vol. 54, pp. 374–378, 2011.

- [32] R. Mahapatra, D. Pal, and S. Mondal, "Effects of buoyancy ratio on double-diffusive natural convection in a lid-driven cavity," *Int. J. Heat Mass Transf.*, vol. 57, pp. 771–785, 2013.
- [33] G. C. Rana and R. Chand, "Stability analysis of double-diffusive convection of rivlin-ericksen elastico-viscous nanofluid saturating a porous medium: a revised model," *Forschung im Ingenieurwesen*, vol. 79, pp. 1–2, 2015.
- [34] G. K. Kumar, B. J. Gireesha, S. Manjunatha, and N. G. Rudraswamy, "Effect of nonlinear thermal radiation on double-diffusive mixed convection boundary layer flow of viscoelastic nanofluid over a stretching sheet," *Int. J. of Mech. and Materials Engg.*, vol. 12, p. 18, 2017.
- [35] B. Gireesha, M. Archana, B. C. Prasannakumara, R. S. R. Gorla, and O. D. Makinde, "MHD three dimensional double diffusive flow of Casson nanofluid with buoyancy forces and nonlinear thermal radiation over a stretching surface," vol. 125, pp. 290–309, 2018.
- [36] B. Mahanthesh, P. B. S. Kumar, B. J. Gireesha, S. Manjunatha, R. S. Gorla, and E. R. Johnson, "Nonlinear convective and radiated flow of tangent hyperbolic liquid due to stretched surface with convective condition," *Results Phys.*, vol. 7, pp. 2404–2410, 2017.
- [37] M. Khan, A. Hussain, M. Y. Malik, T. Salahuddin, and F. Khan, "Boundary layer flow of MHD tangent hyperbolic nanofluid over a stretching sheet: A numerical investigation," *Results Phys.*, vol. 7, pp. 2837–2844, 2017.
- [38] S. Qayyum, T. Hayat, S. A. Shehzad, and A. Alsaedi, "Mixed convection and heat generation/absorption aspects in MHD flow of tangent hyperbolic nanoliquid with Newtonian heat/mass transfer," *Rad. Phys. Chem.*, vol. 144, pp. 396–404, 2018.
- [39] V. Nagendramma, A. Leelarathnam, C. S. K. Raju, S. A. Shehzad, and T. Hussain, "Doubly stratified MHD tangent hyperbolic nanofluid flow due to permeable stretched cylinder," *Result Phys.*, vol. 9, pp. 23–32, 2018.

- [40] M. I. Khan, S. Qayyum, T. Hayat, M. I. Khan, A. Alsaedi, and T. A. Khan, “Entropy generation in radiative motion of tangent hyperbolic nanofluid in presence of activation energy and nonlinear mixed convection,” *Phys. Lett. A*, vol. 382, no. 31, pp. 2017–2026, 2018.
- [41] A. Ali, R. Hussain, and M. Maroof, “Inclined hydromagnetic impact on tangent hyperbolic fluid flow over a vertical stretched sheet,” *AIP Adv.*, vol. 9, p. 125022, 2019.
- [42] Z. Ullah, G. Zaman, and A. Ishak, “Magnetohydrodynamic tangent hyperbolic fluid flow past a stretching sheet,” *Chin. J. Phys.*, vol. 66, pp. 258–268, 2020.
- [43] D. A. Nield and A. V. Kuznetsov, “The onset of bio-thermal convection in a suspension of gyrotactic microorganisms in a fluid layer: oscillatory convection,” *Int. J. Thermal Sci.*, vol. 45, pp. 990–997, 2006.
- [44] Z. Alloui, T. H. Nguyen, and E. Bilgen, “Numerical investigation of thermo-bioconvection in a suspension of gravitactic microorganisms,” *Int. J. Heat Mass Transf.*, vol. 50, pp. 1435–1441, 2007.
- [45] S. P. Oyelakin I. S., Mondal S. and S. D., “Bioconvection in Casson nanofluid flow with gyrotactic microorganisms and variable surface heat flux,” *Int. J. Biomath.*, vol. 12, p. 1950041, 2019.
- [46] Y. Wang, H. Waqas, M. Tahir, M. Imran, and C. Y. Jung, “Effective Prandtl aspects on bio-convective thermally developed magnetized tangent hyperbolic nanofluid with gyrotactic microorganisms and second order velocity slip,” *IEEE Access*, vol. 7, pp. 130 008–130 023, 2019.
- [47] K. Al-Khaled, S. U. Khan, and I. Khan, “Chemically reactive bioconvection flow of tangent hyperbolic nanofluid with gyrotactic microorganisms and nonlinear thermal radiation,” *Heliyon*, vol. 6, no. 1, p. e03117, 2020.

- [48] A. Shafiq, T. N. Sindhu, and C. M. Khalique, “Numerical investigation and sensitivity analysis on bioconvective tangent hyperbolic nanofluid flow towards stretching surface by response surface methodology,” *Alex. Engg. J.*, vol. 59, no. 6, pp. 4533–4548, 2020.
- [49] H. Alfven, “Existence of electromagnetic-hydrodynamic waves,” *Nature*, vol. 150, no. 3850, pp. 405–406, 1942.
- [50] X. Y. Tian, B. W. Li, and Z. M. Hu, “Convective stagnation point flow of a MHD non-Newtonian nanofluid towards a stretching plate,” *Int. J. Heat Mass Transf.*, vol. 127, pp. 768–780, 2018.
- [51] A. I. Fagbade, B. O. Falodu, and A. J. Omowaye, “MHD natural convection flow of viscoelastic fluid over an accelerating permeable surface with thermal radiation and heat source or sink: spectral homotopy analysis approach,” *Ain Shams Eng. J.*, vol. 9, no. 4, pp. 1029–1041, 2018.
- [52] A. Jafarimoghaddam, “On the homotopy analysis method (HAM) and homotopy perturbation method (HPM) for a nonlinear stretching sheet flow of Eyring-Powell fluids,” *Propuls. Power Res.*, vol. 22, pp. 439–451, 2019.
- [53] A. B. Jafar, S. Shafie, and I. Imran Ullah, “Magnetohydrodynamic boundary layer flow of a viscoelastic fluid past a nonlinear stretching sheet in the presence of viscous dissipation effect,” *Coatings*, vol. 9, p. 490, 2019.
- [54] R. E. Rabbi, S. M. Arifuzzaman, T. Sarkar, M. S. Khan, and S. F. Ahmed, “Explicit finite difference analysis of an unsteady MHD flow of a chemically reacting Casson fluid past a stretching sheet with Brownian motion and thermophoresis effects,” *J. King Saud Univ. Sci.*, vol. 32, no. 1, pp. 690–701, 2020.
- [55] T. Muhammad, A. Alsaedi, S. A. Shehzad, and T. Hayat, “A revised model for Darcy-Forchheimer flow of Maxwell nanofluid subject to convective boundary condition,” *Chinese J. Phys.*, vol. 55, no. 3, pp. 963–976, 2017.

- [56] T. Hayat, S. Naz, M. Waqas, and A. Alsaedi, “Effectiveness of Darcy–Forchheimer and nonlinear mixed convection aspects in stratified Maxwell nanomaterial flow induced by convectively heated surface,” *Appl. Math. Mech. Engl. Ed.*, vol. 39, pp. 1374–1384, 2018.
- [57] M. Waqas, M. M. Gulzar, W. A. Khan, M. I. Khan, and N. B. Khan, “Newtonian heat and mass conditions impact in thermally radiated Maxwell nanofluid Darcy–Forchheimer flow with heat generation,” *Int. J. Num. Meth. Heat and Fluid Flow*, vol. 29, pp. 2809–2821, 2019.
- [58] M. A. Sadiq, M. Waqas, T. Hayat, and A. Alsaedi, “Modeling and analysis of Maxwell nanofluid considering mixed convection and Darcy–Forchheimer relation,” *Appl. Nanosci.*, vol. 9, pp. 1155–1162, 2019.
- [59] K. L. Hsiao, “Combined electrical MHD heat transfer thermal extrusion system using Maxwell fluid with radiative and viscous dissipation effects,” *Appl. Therm. Eng.*, vol. 112, pp. 1281–1288, 2017.
- [60] W. Ibrahim and M. Negera, “MHD slip flow of upper-convected Maxwell nanofluid over a stretching sheet with chemical reaction,” *J. Egypt. Math. Soc.*, vol. 28, p. 7, 2020.
- [61] A. Ghaffari, T. Javed, and I. Mustafa, “Non-linear radiation influence on oblique stagnation point flow of Maxwell fluid,” *Rev. Mex. Fis.*, vol. 64, no. 4, pp. 420–428, 2018.
- [62] S. U. S. Choi, “Enhancing thermal conductivity of fluids with nanoparticles,” *American Soc. Mech. Eng.*, vol. 231, pp. 99–105, 1995.
- [63] J. Buongiorno, “Convective transport in nanofluids,” *J. Heat Transf.*, vol. 128, no. 3, pp. 240–250, 2006.
- [64] S. M. S. Murshed, K. C. Leong, and C. Yang, “Investigations of thermal conductivity and viscosity of nanofluids,” *Int. J. Therm. Sci.*, vol. 47, no. 5, pp. 560–568, 2008.

- [65] N. A. Usri, W. H. Azmi, R. Mamat, K. A. Hamid, and G. Najafi, "Thermal conductivity enhancement of Al_2O_3 nanofluid in ethylene glycol and water mixture," *Energy Proc.*, vol. 79, pp. 397–402, 2015.
- [66] A. A. Afify and N. S. Elgazery, "Effect of a chemical reaction on magnetohydrodynamic boundary layer flow of a Maxwell fluid over a stretching sheet with nanoparticles," *Particuology*, vol. 29, pp. 154–161, 2016.
- [67] M. Macha and N. Kishan, "Boundary layer flow of viscoelastic nanofluid over a wedge in the presence of buoyancy force effects," *Comput. Therm. Sci.*, vol. 9, no. 3, pp. 257–267, 2017.
- [68] M. R. Eid and K. L. Mahny, "Flow and heat transfer in a porous medium saturated with a Sisko nanofluid over a nonlinearly stretching sheet with heat generation/absorption," *Heat Transfer-Asian Res.*, vol. 47, no. 1, pp. 54–71, 2018.
- [69] O. K. Koriko, I. L. Animasaun, B. Mahanthesh, S. Saleem, G. Sarojamma, and R. Sivaraj, "Heat transfer in the flow of blood-gold Carreau nanofluid induced by partial slip and buoyancy," *Heat Transfer-Asian Res.*, vol. 47, no. 6, pp. 806–823, 2018.
- [70] S. Shaw, S. S. Sen, M. K. Nayak, and O. D. Makinde, "Boundary layer non-linear convection flow of Sisko nanofluid with melting heat transfer over an inclined permeable electromagnetic sheet," *J. Nanofluids*, vol. 8, no. 5, pp. 917–928, 2019.
- [71] Z. Shafique, M. Mustafa, and A. Mushtaq, "Boundary layer flow of Maxwell fluid in rotating frame with binary chemical reaction and activation energy," *Int. J. Chem. React. Eng.*, vol. 6, pp. 627–633, 2016.
- [72] T. H. M. Mustafa, A. Mushtaq and A. Alsaedi, "Numerical study of MHD viscoelastic fluid flow with binary chemical reaction and arrhenius activation energy," *Int. J. Chem. React. Eng.*, vol. 15, no. 1, pp. 127–135, 2017.

- [73] M. M. Gulzar, S. Jabeen, M. Waqas, S. A. Shehzad, T. Hayat, and A. Alsaedi, "OHAM analysis for dissipative viscoelastic nanofluid considering entropy generation and activation energy," *Int. J. Num. Meth. Heat and Fluid Flow*, vol. 29, no. 12, pp. 4807–4825, 2019.
- [74] K. D. Ramaiah, P. Surekha, G. Kotha, and K. Thangavelu, "MHD rotating flow of a Maxwell fluid with Arrhenius activation energy and non-Fourier heat flux model," *Heat Transf.*, vol. 49, no. 4, pp. 2209–2227, 2020.
- [75] K. Rafiq, M. Irfan, M. Khan, M. S. Anwar, and W. A. Khan, "Arrhenius activation energy theory in radiative flow of Maxwell nanofluid," *Phys. Scr.*, vol. 96, no. 4, p. 045002, 2020.
- [76] B. C. Sakiadis, "Boundary-layer behaviour on continuous solid surfaces: The boundary layer on a continuous flat surface," *American Inst. Chem. Eng. J.*, vol. 7, no. 2, pp. 221–225, 1961.
- [77] L. J. Crane, "Flow past a stretching plate," *J. Appl. Math. Phys.*, vol. 21, no. 4, pp. 645–647, 1970.
- [78] C. Y. Wang, "Liquid film on an unsteady stretching surface," *Quart. Appl. Math.*, vol. 48, no. 4, pp. 601–610, 1990.
- [79] R. Cortell, "A note on magnetohydrodynamic flow of a power law fluid over a stretching sheet," *Appl. Math. Comput.*, vol. 168, pp. 557–566, 2005.
- [80] M. Shaker, E. Birgersson, and A. S. Mujumdar, "Extended Maxwell model for the thermal conductivity of nanofluids that accounts for nonlocal heat transfer," *Int. J. Thermal Sci.*, vol. 84, pp. 260–266, 2014.
- [81] Y. Bai, X. Liu, Y. Zhang, and M. Min Zhang, "Stagnation-point heat and mass transfer of MHD Maxwell nanofluids over a stretching surface in the presence of thermophoresis," *J. Mol. Liq.*, vol. 224, pp. 1172–1180, 2016.
- [82] L. Liu and F. Liu, "Boundary layer flow of fractional Maxwell fluid over a stretching sheet with variable thickness," *Appl. Math. Lett.*, vol. 79, pp. 92–99, 2018.

- [83] N. L. Xu and H. Xu, "Homogeneous–heterogeneous reactions in boundary-layer flow of a Maxwell nanofluid over a stretching surface," *J. Thermal Sci. Eng. Appl.*, vol. 11, no. 4, p. 041011, 2019.
- [84] M. Azam, M. Khan, and A. S. Alshomrani, "Effects of magnetic field and partial slip on unsteady axisymmetric flow of Carreau nanofluid over a radially stretching surface," *Results Phys.*, vol. 7, pp. 2671–2682, 2017.
- [85] K. Masood and Hashim, "Effects of multiple slip on flow of magneto-Carreau fluid along wedge with chemically reactive species," *Neural. Comput. Appl.*, vol. 30, no. 2, pp. 2291–2203, 2018.
- [86] C. S. K. Raju, M. M. Hoque, N. A. Khan, M. Islam, and S. Kumar, "Multiple slip effects on magnetic-Carreau fluid in a suspension of gyrotactic microorganisms over a slendering sheet," *Appl. Math. Mech.*, vol. 233, no. 2, pp. 1–13, 2018.
- [87] K. G. Kumar, G. K. Ramesh, B. J. Gireesha, and A. M. Rashad, "On stretched magnetic flow of Carreau nanofluid with slip effects and nonlinear thermal radiation," *Nonlinear Eng.*, vol. 8, no. 1, pp. 340–349, 2018.
- [88] P. D. Prasad, S. V. K. Varma, C. S. K. Raju, S. A. Shehzad, and M. A. Meraj, "3D flow of Carreau polymer fluid over variable thickness sheet in a suspension of microorganisms with Cattaneo-Christov heat flux," *Rev. Mex. de Fis.*, vol. 64, pp. 519–529, 2018.
- [89] M. I. Khan, F. Alzahrani, A. Hobiny, and Z. Ali, "Estimation of entropy generation in Carreau-Yasuda fluid flow using chemical reaction with activation energy," *J. Mater. Res. Technol.*, vol. 9, no. 5, pp. 9951–9964, 2020.
- [90] T. Muhammad, S. Z. Alamri, H. Waqas, D. Habib, and R. Ellahi, "Bioconvection flow of magnetized Carreau nanofluid under the influence of slip over a wedge with motile microorganisms," *J. Therm. Anal. Calorim.*, vol. 143, pp. 945–957, 2021.

- [91] E. Magyari and A. Pantokratoras, “Note on the effect of thermal radiation in the linearized Rosseland approximation on the heat transfer characteristics of various boundary layer flows,” *Int. Commun. Heat. Mass Transf.*, vol. 38, pp. 554–556, 2011.
- [92] A. Pantokratoras, “Natural convection along a vertical isothermal plate with linear and nonlinear Rosseland thermal radiation,” *Int. J. Therm. Sci.*, vol. 84, pp. 151–157, 2014.
- [93] M. J. Babu, N. Sandeep, C. S. K. Raju, J. V. R. Reddy, and V. Sugunamma, “Nonlinear thermal radiation and induced magnetic field effects on stagnation-point flow of ferro fluids,” *J. Adv. Phys.*, vol. 5, p. 1, 2015.
- [94] B. Mahanthesha, B. J. Gireesha, and R. S. R. Gorla, “Nonlinear radiative heat transfer in MHD three-dimensional flow of water based nanofluid over a non-linearly stretching sheet with convective boundary condition,” *J. Nigerian Math. Soc.*, vol. 35, pp. 178–198, 2016.
- [95] Y. B. Kho, A. Hussanan, M. K. Mohamed, N. M. Sarif, Z. Ismail, and M. Z. Salleh, “Thermal radiation effect on MHD flow and heat transfer analysis of Williamson nanofluid past over a stretching sheet with constant wall temperature,” *J. Phys. : Conf. Ser.*, vol. 890, p. 012034, 2017.
- [96] A. Zaib, M. Rashidi, A. Chamkha, and N. Mohammad, “Impact of nonlinear thermal radiation on stagnation-point flow of a Carreau nanofluid past a nonlinear stretching sheet with binary chemical reaction and activation energy,” *Proc. Inst. of Mech. Eng. C. J. Mech. Eng. Sci.*, vol. 232, no. 6, pp. 962–972, 2017.
- [97] O. K. Koriko, I. L. Animasaun, M. G. Reddy, and N. Sandeep, “Scrutinization of thermal stratification, nonlinear thermal radiation and quartic autocatalytic chemical reaction effects on the flow of three-dimensional Eyring-Powell alumina-water nanofluid,” *Multidiscip. Model. Mater. Struct.*, vol. 14, no. 2, pp. 261–283, 2018.

- [98] K. Hosseinzadeh, M. Gholinia, B. Jafari, A. Ghanbarpour, H. Olfian, and D. D. Ganji, “Nonlinear thermal radiation and chemical reaction effects on Maxwell fluid flow with convectively heated plate in a porous medium,” *Heat transf-Asian Res.*, vol. 48, no. 2, pp. 744–759, 2019.
- [99] H. Mondal, P. De, S. Goqo, and P. Sibanda, “A numerical study of nanofluid flow over a porous vertical plate with internal heat generation and nonlinear thermal radiation,” *J. Por. Med.*, vol. 23, no. 6, pp. 517–529, 2020.
- [100] D. Pal and G. Mondal, “Double diffusive magnetohydrodynamic heat and mass transfer of nanofluids over a nonlinear stretching/shrinking sheet with viscous-ohmic dissipation and thermal radiation,” *Propuls. Power Res.*, vol. 6, no. 1, pp. 58–69, 2017.
- [101] Y. S. Daniel, Z. A. Aziz, Z. Ismail, and F. Salah, “Effects of thermal radiation, viscous and Joule heating on electrical MHD nanofluid with double stratification,” *Chinese J. Phys.*, vol. 55, no. 3, pp. 630–651, 2017.
- [102] S. P. Anjali and D. V. Kumari, “Thermal radiation, viscous dissipation, Ohmic dissipation and mass transfer effects on unsteady hydromagnetic flow over a stretching surface,” *Ain Shams. Eng. J.*, vol. 9, no. 4, pp. 1161–1168, 2018.
- [103] H. Upreti, A. K. Pandey, and M. Kumar, “MHD flow of Ag-water nanofluid over a flat porous plate with viscous-Ohmic dissipation, suction/injection and heat generation/absorption,” *Alex. Eng. J.*, vol. 57, no. 3, pp. 1839–1847, 2018.
- [104] D. Pal, “Magnetohydrodynamic viscous–Ohmic dissipation performance on unsteady convective heat transfer over a stretching surface in existence of internal heat generation/absorption,” *Int. J. Comput. Meth. Eng. Sci. Mech.*, vol. 20, no. 4, pp. 308–318, 2019.
- [105] B. J. Giresha, K. G. Kumar, M. R. Krishnamurthy, S. Manjunatha, and N. G. Rudraswamy, “Impact of Ohmic heating on MHD mixed convection

- flow of Casson fluid by considering cross diffusion effect,” *Non-linear Eng.*, vol. 8, pp. 380–388, 2019.
- [106] D. Srinivasacharya and P. Jagadeeshwar, “Effect of Joule heating on the flow over an exponentially stretching sheet with convective thermal condition,” *Math. Sci.*, vol. 13, pp. 201–211, 2019.
- [107] J. P. William, “Matlab for engineering applications,” *McGraw-Hill*, 1998.
- [108] Y. A. Cengel and J. M. Cimbala, “Fluid Mechanics Fundamentals and Applications,” *New York: NY McGraw-Hill*, 2014.
- [109] R. P. Chhabra, “Non-Newtonian Fluids: An Introduction,” *Rheology of Complex Fluids*, pp. 3–34, 2010.
- [110] Y. A. Cengel, “Heat transfer : a practical approach.” *New York : McGraw-Hill*, 2004.
- [111] J. Kunes, “Dimensionless Physical Quantities in Science and Engineering,” *London : Elsevier*, 2012.
- [112] A. Mojtabi and M. C. Charrier-Mojtabi, “Double-diffusive convection in porous media,” *Handbook of Porous Media*, vol. 2, pp. 269–320, 2005.
- [113] A. Oschlies, H. Dietze, and P. Kahler, “Salt-finger driven enhancement of upper ocean nutrient supply,” *Geophys. Res. Lett.*, vol. 30, p. 2204, 2003.
- [114] T. Radko, “Double Diffusive Convection,” https://gfd.who.edu/wp-content/uploads/sites/18/2018/03/lecture10_136325.pdf.
- [115] D. Radha, “The effect of constraints on the concentration gradients in a suspension of chemotactic bacteria,” <http://hdl.handle.net/10603/9218>.
- [116] I. Horkendorff and J. W. Niemantsverdriet, “Concepts of Modern Catalysis and Kinetics,” *John Wiley and Sons: Weinheim*, 2006.
- [117] A. K. Datye and N. J. Long, “The use of nonporous oxide particles for imaging the shape and structure of small crystallites in heterogeneous catalysts,” *Ultramicroscopy*, vol. 25, no. 3, pp. 203–208, 1988.

-
- [118] T. C. Papanastasiou and G. C. Georgiou, “Viscous Fluid Flow,” *CRC Press, Boca Raton*, 2000.
- [119] J. Goedbloed and S. Poedts, “In principles of Magnetohydrodynamics: with applications to laboratory and astrophysical plasmas,” *Cambridge University Press*, pp. 594–605, 2004.
- [120] T. Y. Na, “Computational Methods in Engineering Boundary Value Problems,” *Academic Press, New York*, 1979.
- [121] H. B. Keller, “Numerical Methods for Two-Point Boundary Value Problems,” *Dover publications, New York*, 1992.
- [122] J. C. Maxwell, “On stresses in rarefied gases arising from inequalities of temperature,” *Phil. Trans. Royal Soc. London*, vol. 170, pp. 231–256, 1879.
- [123] M. Smoluchowski, “Ueber warmeleitung in verdunnten gasen,” *Annal. d. Phys.*, vol. 64, pp. 101–130, 1898.
- [124] S. Mansur, A. Ishak, and I. Pop, “MHD homogeneous-heterogeneous reactions in a nanofluid due to a permeable shrinking surface,” *J. Appl. Fluid Mech.*, vol. 9, pp. 1073–1079, 2016.
- [125] I. C. Liu and H. I. Andersson, “Heat transfer over a bidirectional stretching sheet with variable thermal conditions,” *Int. J. Heat Mass Transf.*, vol. 51, pp. 4018–4024, 2008.
- [126] P. D. Ariel, “The three-dimensional flow past a stretching sheet and the homotopy perturbation method,” *Comput. Math. Appl.*, vol. 54, pp. 920–925, 2007.